MECHANISMS OF BIOMATERIAL-MEDIATED CARDIAC AND ESOPHAGEAL REPAIR

by

Ricardo Londono

Bachelor of Science in Electrical and Computer Engineering, Florida International University,

2006

Submitted to the Graduate Faculty of

The School of Medicine in partial fulfillment

of the requirements for the degree of

Doctor of Philosophy

University of Pittsburgh

2015

UNIVERSITY OF PITTSBURGH

SCHOOL OF MEDICINE

This dissertation was presented

by

Ricardo Londono

It was defended on

July 6th, 2015

and approved by

Jon D. Piganelli, PhD, Assistant Professor, Department of Immunology

Bryan N. Brown, PhD, Assistant Professor, Department of Bioengineering

Patricia A. Hebda, PhD, Adjunct Professor, School of Medicine

Kacey G. Marra, PhD, Associate Professor, Department of Bioengineering

Sanjeev G. Shroff, Professor and Chair, Department of Bioengineering

Dissertation Advisor: Stephen F. Badylak, DVM, PhD, MD, Professor, Department of Surgery

MECHANISMS OF BIOMATERIAL-MEDIATED CARDIAC AND ESOPHAGEAL REPAIR

Ricardo Londono, PhD

University of Pittsburgh, 2015

Biologic scaffolds derived from mammalian extracellular matrix (ECM) have been extensively used in pre-clinical and clinical applications to promote constructive tissue remodeling in a number of anatomic locations. The clinical success of these technologies depends on a number of factors including the species and tissues from which they are derived, the efficacy of the decellularization process, and post-processing modifications such as crosslinking and solubilization, among others.

The ECM is produced by the resident cells of every tissue and hence, it is thought to constitute the ideal substrate for each unique cell population. It is therefore logical to assume that a substrate composed of site-specific ECM would be favorable for clinical use in homologous anatomic locations. However, the advantages of using site-specific (homologous) ECM scaffolds in clinical applications is still a matter of debate. Part of the difficulty in addressing this issue arises from the fact that most studies have investigated the application of ECM-derived scaffolds in either homologous or non-homologous locations independently, but they have rarely been directly compared in properly designed studies.

The present dissertation shows the development of ECM-based biomaterials derived from cardiac and esophageal tissues. The decellularized scaffolds are compliant with decellularization standards and are then used to evaluate the tissue specific effects of homologous ECM *in vitro* and in a preclinical models of cardiac and esophageal repair.

TABLE OF CONTENTS

LIST OF TABLES

LIST OF FIGURES

PREFACE

This dissertation is dedicated to my parents, Ricardo Londono and Adriana Escobar, to my sister Sofia Londono, and to my late grandparents. Any success I have achieved and will achieve is a direct result of their love, support, inspiration, and sacrifice. My accomplishments are the fruits of our combined effort.

I would like to thank my first mentor Dr. Scott VanEpps for sharing with me his passion for science and discovery. With patience and kindness he introduced me to the scientific method and gave me an ideal to strive towards. You inspired me to become a physician scientist and you will always be my gold standard.

I would like to thank Dr. Richard Steinman, Dr. Manjit Singh, Dr. Clayton Wiley, Dr. Paul Monga, and Dr. Harvey Borovetz for believing in me and giving me the chance to be part of the Medical Scientist Training Program at the University of Pittsburgh. Your mentorship throughout the years has been invaluable to me. My success is yours as well; I hope to make you proud one day.

I would like to thank Dr. Badylak for receiving me in his laboratory and providing me with all the necessary tools a student needs to succeed in graduate school. Thank you for your mentorship, motivation, and inspiration. You lead by example and it has truly been an honor and a privilege working with you. The multidisciplinary environment and structure you have created

in your laboratory through decades of hard work and dedication provide your students with unique and valuable opportunities. I will be forever grateful to you and your team.

I would like to thank my colleagues: Dr. Alejandro Nieponice, Dr. Antonio D'Amore, Dr. Neill Turner, Dr. Steve Tottey, Dr. Chris Dearth, Dr. Jeremy Kelly, Dr. Alessandra Costa, Dr. Luai Huleihel, Dr. Chris Medberry, Dr. Matt Wolf, Dr. Chris Carruthers, Dr. Brian Sicari, Dr. Denver Faulk, Dr. Hongbin Jiang, Dr. Li Zhang , Dr. Peter Slivka, Dr. Fan Wei Meng, Dr. Beth Kollar, Scott Johnson, Janet Reing, Li Zhang, John Freund, Lisa Carey, Tim Keane, Linsey Saldin, Jenna Dziki, and Catalina Pineda.

Special thanks to Jocelyn Runyon, Eve Simpson, Allyson Lacovey, and Rachel Thomas for all of your help and support.

I would like to thank the students that have been part of our team and I have had the pleasure to mentor throughout the years. Dr. David Hirsch, Ryan Carey, Adam Attaar, Eric Haljasmaa, Marshall Steele, Jeremy Gale, and Mike Pezzone. This work is the result of your hard work and dedication. I can only wish to I have been a better mentor to you all.

I would like to thank DLAR personnel, especially Dr. Michael Winnen, Robin Frederick, Stacy Cashman, Renee Ruderman, Mark Petts, and Mike Nakon for their help and hard work.

Special thanks to my committee members: Dr. Jon Piganelli, Dr. Bryan Brown, Dr. Patricia Hebda, Dr. Kacey Marra, and Dr. Sanjeev Shroff. Your mentoring and influence has been central to my education and the success of this project.

I would also like to thank the National Institutes of Health for funding this body of work through the University of Pittsburgh MSTP program, the Cellular Approaches to Tissue Engineering and Regeneration CATER Award, and the Cardiovascular Bioengineering Training Program CBTP Award.

1.0 INTRODUCTION AND SPECIFIC AIMS

This section will introduce the mechanism of biomaterial mediated tissue repair and discuss current limitations in tissue engineering. The clinical need for cardiac and esophageal tissue repair as well as currently available regenerative medicine technologies for these applications will be discussed as well. Finally, the central hypothesis and specific aims of the present dissertation will be introduced

1.1 FACTORS WHICH AFFECT THE CLINICAL OUTCOME OF BIOMATERIAL-BASED THERAPIES

1.1.1 Overview of the Biomaterial-Host Interaction.

The host response to an implanted material begins immediately upon implantation and consists of both the response to the inevitable iatrogenic tissue injury during implantation and the response to the material itself. In most cases, the implantation-induced component resolves quickly as part of the normal wound healing process. However, the response to the material will last for the length of time the material is present in the host. Materials which elicit a persistent proinflammatory response are likely to be associated with abundant fibrous connective tissue

deposition and the consequences of effector molecules secreted by recruited inflammatory cells. Materials which either rapidly degrade or reach a steady state of tolerance with adjacent host tissue are typically associated with minimal scarring, a quiescent population of resident inflammatory cells, and adjacent tissue types appropriate for the anatomic location. The host response to an implanted material can be affected by the aforementioned factors. (Table 1).

Table 1. Factors that Affect the Host Response to Biomaterials

The biomaterial-host interaction is a complex process that depends upon many different factors. These factors can be conceptually categorized in four different groups: Host-related and biomaterial-related factors which affect the host response and chapters in which they are discussed.

Biomaterial-Related Factors	Host-Related Factors	Application-Related Factors	Microenvironmental Factors
Composition (material)	Age	Complexity of tissue/organ to be repaired	Contamination of the treatment site
Degradability	Nutritional status	Performance expectations	Presence of scar tissue
Mechanical properties	Immunocompetence	Adjuvant therapy	Previous interventions
Sterility	Co-morbidities	Surgical placement	Availability of healthy and vascularized adjacent tissue
Antigenicity	Medications	Exposure to appropriate physiologic and mechanical stimuli	
Active ingredients (drugs)	Wound healing ability		

1.1.2 Biomaterial-Related Factors

Biomaterial-related factors have been the focus of studies for many years. Such factors include the base composition of the material (e.g. Titanium alloy versus Poly(etherurethane urea) versus Extracellular Matrix, etc.), surface texture, surface ligand landscape, degradability, and device design parameters such as pore and fiber size among others. At the very best, it can be assured

that no biomaterial is inert and the functional success of any implanted biomaterial is ultimately determined by the interplay between material and other factors.

The primary determinant of success or failure of an implanted biomaterial is the host response to the material itself over time (Figure 1). Although the physical and mechanical properties of a material at the time of implantation are obviously important, the integrity of the properties at one month, one year, five years and beyond is just as important for those materials intended to remain for the lifespan of the patient. The host response can mitigate or destroy, encapsulate, or otherwise alter the composition of the biomaterial over time resulting in changes to the form and mechanical properties of the material itself [25]. Hence, it is not the degree to which the physical characteristics of the material resemble the targeted anatomic location before implantation that determines the performance of a biomaterial, but rather the host response over time.

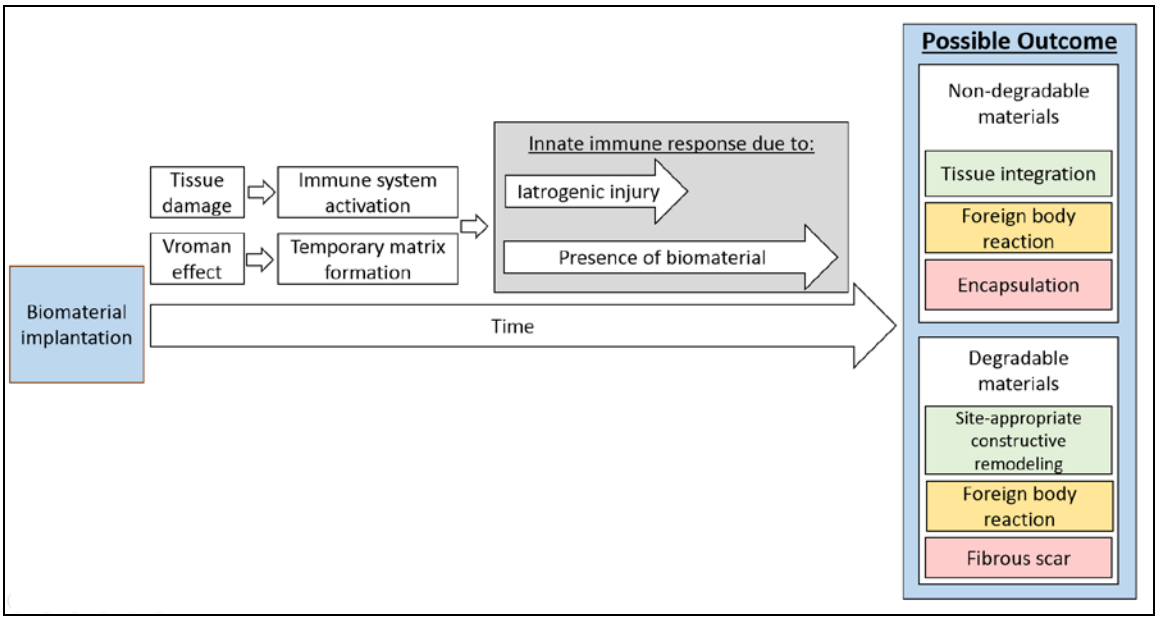

Figure 1. Host response to biomaterial implantation

The host response to implanted biomaterials depends upon many factors. Although the initial stages of the biomaterial-host interaction are shared among all materials and include tissue damage during implantation and protein adsorption to the surface of the material, the host response quickly transitions into complex phases that depend directly upon the type of material being implanted, implantation location, and the conditions of the microenvironment. These phases involve cellular and molecular components of the innate immune system and the wound healing response, and will ultimately determine the clinical outcome (i.e. encapsulation Vs. scar formation Vs. constructive remodeling).

The host response is initiated with the activation of the immune system as a result of cell and tissue damage during biomaterial implantation. Upon contact with the host tissues, the surface of the biomaterial is coated with blood and plasma proteins through a process known as the Vroman effect [415]. Depending on the type of biomaterial and surface topography (i.e. type I collagen vs. heparin coated polytetrafluoroethylene vs titanium), the type and amount of adsorbed molecules will vary, and as a result, so will the composition and arrangement of the interface between the host tissues and the implant.

As a result of the Vroman effect, host cells typically do not interact directly with the surface of the biomaterial, but rather with the adsorbed protein layer. This protein layer – sometimes in conjunction with clot formation during hemostasis, forms a temporary yet fibrin-rich matrix that bridges and mediates the interaction between the host tissues and the biomaterial. With degradable materials (e.g. non-cross linked biologic scaffolds, poly (lactic-co-glycolic acid), polyglactin), this temporary matrix serves as a bridge that facilitates cellular access and promotes infiltration into the material. With non-degradable biomaterials (e.g. permanent titanium alloy implants, polypropylene) the adsorbed protein layer serves as an interface that provides sites for cell attachment and mediates the interaction between the host and the implanted construct [271] .

Within minutes of implantation the cellular response becomes predominated by neutrophils at the host-biomaterial interface. The neutrophil response peaks within 48-72 hours after implantation and it is the hallmark of the acute innate immune response. In addition to eliminating pathogens that may be present at the treatment site, neutrophils play important roles in the immune response such as establishment of signaling gradients that attract and activate other components of the innate immune system[457], initiation of granulation tissue formation, and - in the case of degradable biomaterials, secretion of enzymes such as collagenases and serine proteases [312] that initiate the process of biomaterial degradation and remodeling of the treatment site[271].

As a result of signaling gradients established by neutrophils, the innate immune response transitions to a macrophage dominant infiltrate that slowly replaces the accumulated neutrophils at the host-biomaterial interface. The type and magnitude of the macrophage response will depend primarily on the material and host factors identified in Table 1. Some degradable

biologic materials placed in anatomic locations within healthy, vascularized tissue can degrade within weeks[78, 354] and promote a pro-remodeling M2 macrophage-associated response that leads to functional, site-appropriate tissue deposition[27, 410]. Alternatively, certain types of synthetic biomaterials can promote pro-inflammatory processes that will lead to foreign body reaction, scar tissue formation, and chronic inflammatory processes associated with an M1 macrophage phenotype [13, 240, 261]. Permanent, non-degradable biomaterials, such as metallic plates or screws, typically lead to a foreign body reaction as a result of "frustrated phagocytosis", and can promote inflammation, seroma formation, and eventually encapsulation. The degree to which each type of response is deemed acceptable will depend upon the type and specific performance expectations of the application (e.g. temporary orthopedic support vs. functional organ replacement vs. tissue fillers in reconstructive applications).

1.1.3 Host-Related Factors

Host-related factors have been underappreciated as a determinant of the host response to implanted materials. As a result, host-related factors have not been thoroughly considered in the context of patient outcomes in existent studies. These factors include age, nutritional status, body mass index, co-morbidities such as diabetes, and medications being taken by the patient among others. As stated previously, the initial host response to implanted biomaterials is primarily orchestrated by plasma proteins and the innate immune system and as such, any factors or underlying conditions that may affect these variables will inevitably alter the biomaterial-host interaction.

1.1.3.1 Age

The aging process affects all body systems and associated functions including immunocompetence. In fact, immunosenescence is thought to be one of the major predisposing factors to increased incidence of infection in older individuals [185]. Some of the most important age-related changes in the cellular component of the innate immune system are summarized in (Table 2).

Table 2. Effect of age in cellular component of innate immunity

(Adapted from [185]) Although the absolute and circulating numbers of neutrophils and monocytes/macrophages in the immune system is not typically affected by age, important changes including decrease phagocytosis, decreased chemotaxis, and decreased signaling molecule production are observed with age. In turn, these changes have the potential to negatively affect the host response to implanted biomaterials.

Cell type	Changes in Composition	Changes in Function	References
Monocytes/ Macrophages	No change in absolute number	Decreased phagocytosis	Hearps et al. 2012[186] McLachlan et al. 1995[291]
	No change in circulating frequency	Decreased ROS production	Nguyen et al. 2005[313] Qian et al. 2012[350]
	Increased percentage of CD14+ 16++ non-classical monocytes	Increased TNF-α production via TLR-4	Seidler et al. 2010[393] van Duin et al. 2007[446]
	Reduced percentage of CD14+ 16- classical monocytes	Decreased IL-6 and TNF-α production via TLR1/2	
Neutrophils	No change in circulating numbers	Reduced chemotaxis *in vitro*	Born et al. 1995[54] Butcher et al. 2001[72]
	No change in CD11a, CD11b expression	Reduced phagocytosis	Fulop et al. 2004[151] Tseng et al. 2012[439]
		Impaired NET formation	Wenisch et al. 2000[459]
		Increased/decreased ROS formation	

The cellular component of the innate immune system and its role in responding to the presence of foreign materials is closely examined in Section 1.4.3. Although absolute numbers of neutrophils and macrophages are not typically affected by aging, important cellular changes including the ability to mobilize, establish chemical gradients, and phagocytize pathogens and foreign elements are usually observed with advanced age. These changes can affect the process of biomaterial-associated tissue repair by affecting material degradation, cell migration and proliferation, angiogenesis, neo-matrix deposition, and tissue remodeling.

In addition to affecting the immune system, the aging process alters adult stem cell functionality and behavior [277, 327]. Stem cells are necessary for homeostasis and the wound healing response. These precursor cells maintain organ function and are responsible for tissue repair. In turn, therapeutic approaches that rely on native stem cell populations[410] for the organization of newly formed tissue will inevitably be affected by the aging process. As in the case of age-related changes associated with the innate immune system, aging does not appear to decrease the absolute number of stem cells, but instead, it impairs their capacity to produce progenitor cells and to differentiate [404].

1.1.3.2 Nutritional Status

Malnutrition is a global problem with implications for the host-biomaterial interaction. Malnutrition can result in increased susceptibility to infections and co-morbidities, impaired healing ability, altered metabolic state, and changes to the innate immune system that directly affect the interaction between the host and an implanted biomaterial (Table 3).

Table 3. Nutritional status-related changes to innate immune system

Although malnutrition can increase the number of leukocytes and granulocytes, this phenomenon is attributed to an underlying chronic pro-inflammatory state due in part to increased susceptibility to infections. As with aging, malnutrition causes a decrease in functionality in the cells of the immune system. These changes affect the host-biomaterial interaction and include decreased chemotaxis, phagocytosis, and adherence among others.

Parameter	References
Similar or elevated number of leukocytes	Hughes et al. (2009) [208] Schopfer and Douglas (1976)[387]
Elevated number of granulocytes	Najera et al. (2004)[307] Schopfer and Douglas (1976)[387]
Reduced granulocyte chemotaxis	Vasquez-Garibay et al. (2002)[450] Vasquez-Garibay et al. (2004)[451]
Reduced granulocyte adherence to foreign material	Goyal et al. (1981)[173]
Reduced granulocyte microbicidal activity	Dougals and Schopfer (1974)[120] Chhangani et al (1985)[91] Keusch et al. (1987)[235]
Reduce leukocyte phagocytosis	Carvalho Neves Forte et al. (1984)[80] Shousha and Kamel (1972)[406] Schopfer and Douglas (1976)[387]
Increased markers of apoptosis in leukocytes	Nassar et al. (2007)[309]
Increased signs of DNA damage in leukocytes	Gonzalez et al. (2002)[167]
Reduced levels or activity of complement system components	McFarlane (1971) [290] Ozkan et al. (1993)[334] Sakamoto et al. (1992)[377] Kumar et al. (1984)[253] Sirisinha et al. (1973)[412]

1.1.3.3 Comorbidities

The host response is affected by a number of underlying pathologic conditions, particularly those which affect the immune system, wound healing ability, stem cell viability, and/or the state of the tissues adjacent to the treatment site.

1.1.3.4 Obesity

Data from the National Health and Nutrition Examination Survey, 2009–2010[140, 325] indicates that more than 2 in 3 adults are considered to be overweight or obese in the United States. Obesity is a risk factor for type 2 diabetes and cardiovascular disease, and both obesity and diabetes are now recognized as pro-inflammatory diseases [331]. Although the inflammatory state present in these conditions is distinct from that of acute inflammation [249], there are a number of implications for the field of biomaterial-mediated tissue repair that have been often ignored in preclinical and clinical studies.

Inflammation is a fundamental component of the host response to implanted bio-materials. The innate immune system modulates the wound healing response and is a key mediator and determinant of the clinical outcome of biomaterial implantation[273] (Figure 1). Immune cells, particularly neutrophils and macrophages are the main effectors in most biomaterial applications. As first responders, neutrophils clear pathogens and establish chemical gradients that affect later stages of biomaterial–host inter-action. Macrophages, on the other hand, display phenotypic heterogeneity and are responsible for both positive and negative events during biomaterial-mediated tissue repair. Macrophage phenotype has been shown to be predictive of clinical outcome in the context of biologically derived biomaterials. While the presence of M1 macrophages is associated with pro-inflammatory processes including foreign body reaction, cytotoxicity, and biomaterial encapsulation, M2 macrophages are associated with constructive tissue remodeling and site-appropriate tissue deposition[25, 62, 65, 471]. Obesity has been tightly associated with M1 macrophage accumulation within adipose tissue and other organs [249, 458, 473]. In addition, obesity has also been shown to increase pro-inflammatory molecule production [206]. Hence, obesity and other underlying conditions that may promote

proinflammatory environments should be taken into account when considering biomaterials as possible treatment options.

1.1.3.5 Diabetes

Diabetes mellitus, a condition that affects an estimated 29 million patients in the United States and an additional 86 million pre-diabetic patients[1], is among the most overlooked factors that can affect the host–biomaterial interaction. Diabetes mellitus is considered a pro-inflammatory disease[249] that increases susceptibility to infections and bacteremia in the acute setting and can cause vascular deterioration and diabetic ulcers chronically. Increased susceptibility to infections and bacteremia are risk factors for bacterial engraftment on artificial heart valves and in synthetic vascular grafts, and both conditions are independent risk factors for infective endocarditis [93, 239]. Vascular damage, on the other hand, can promote tissue necrosis and infection, and can prevent the cellular component of the immune system to access the treatment site.

1.1.4 Application-Specific Factors

1.1.4.1 Anatomical Placement

Biomaterials are used in virtually every anatomic location for a wide variety of clinical applications. Each anatomic site (e.g., blood contact, musculotendinous, central nervous system, skin, GI tract, respiratory, pelvic floor reconstruction, bone and cartilage, total joints, etc.) is associated with distinctive conditions such as an air interface, blood contact, and mechanical loading (Figure 2). These environmental conditions affect the host response by providing stimuli

(e.g., cyclic stretching, load bearing, laminar flow, presence of an interface, etc.) that directly affect cellular processes such as migration and differentiation[127, 157, 267, 324, 374].

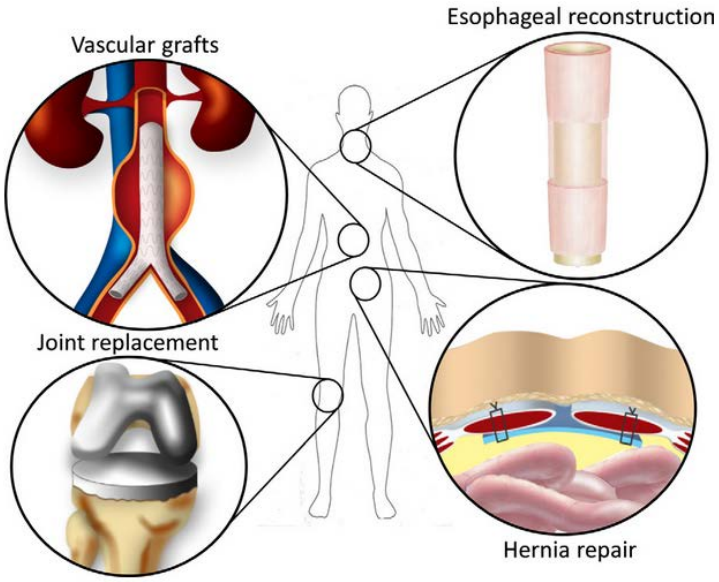

Figure 2. Anatomic placement

Distinctive conditions such as an air interface (esophagus), blood contact (vascular grafts), and mechanical loading (orthopedic applications) play a role in the host response to implanted materials. Anatomic placement and performance expectations (e.g. temporary orthopedic support versus whole organ regeneration) dictate biomaterial design parameters.

1.1.4.2 Performance Expectations

Application-specific requirements such as electrical conductivity, biosensing (e.g., glucose sensors, implantable cardioverter defibrilators), enzyme/hormone production, contractility, and load bearing will exist depending on the target tissue/organ to be repaired. In addition, these conditions necessarily dictate design parameters. For example, joint replacement implants must be strong enough to bear weight without breaking or deformation, heparin-coated vascular

constructs are intended to decrease thrombus formation and improve blood flow, synthetic meshes used in hernia repair must possess sufficient tensile strength to withstand the biomechanical forces exerted by and on the abdominal wall, and semi-permeable membranes in dialysis and extra corporeal membrane oxygenation (ECMO) machines must selectively facilitate molecule traffic.

1.1.5 Microenvironment-Related Factors

1.1.5.1 State of Adjacent Tissue

In addition to the aforementioned factors, the clinical outcome of regenerative strategies for tissue repair also depends on microenvironmental conditions such as the state of adjacent and surrounding tissue (i.e. healthy and vascularized versus hypoxic and necrotic), the presence structural damage due previous interventions and scarring, and bacterial contamination. Vascularized healthy tissue facilitates nutrient traffic and immune system access to the treatment site[273]. Granulation tissue formation and angiogenesis are both important phases of the host response to implanted biomaterials, and they depend on the state of the surrounding tissue and the microenvironment. While healthy and vascularized surrounding tissue is typically associated with clinical success of biomaterial technologies, necrotic and contaminated implantation areas are associated with infection and implant failure[82, 116, 156] . Furthermore, scarred tissue can act as a fibrotic barrier between the host and the implant, affecting the host-biomaterial interaction, and ultimately leading to implant failure.

1.1.5.2 Implant Site Contamination

Bacterial contamination can cause implant failure. For example, once engrafted in biomaterials, bacteria have been shown to cause artificial heart valve dysfunction [252, 258, 320], abscess formation[116, 129] , biofilm formation[15, 19], and sepsis[12, 306, 416]. In the case of degradable materials, bacterial contamination can affect degradation rates and compromise the biomechanical properties of the biomaterial [365, 482] . In fact, when the surgical field is contaminated, biomaterials derived from biologic sources are indicated for use over synthetic biomaterials [238] due in part to their antimicrobial properties and their degradability [56, 378]. If contamination persists, further interventions including revisions and abscess drainage are required. The clinical performance of biomaterials has consistently been suboptimal once these events have occurred

In summary, no biomaterial is biologically inert, and while it might be acceptable for constructs intended for temporary use to be merely biotolerable[68] , biomaterials intended for use in more complex applications—including those requiring functional tissue/organ replacement and/or constructive tissue remodeling—will inevitably have to adhere to more stringent design and biocompatibility criteria. Biomaterial composition, the host, the type of tissue/performance expectations of each specific application, and the microenvironment will ultimately dictate whether or not each response to implanted constructs is deemed acceptable.

1.2 BIOMATERIALS FOR TISSUE REPAIR

As stated previously, the discipline of tissue engineering/regenerative medicine (TE/RM) exists, in part, because traditional methods of approaching some challenging medical problems have yielded only incremental advancements in spite of enormous investment of research time and resources. The treatment of pathologies such as stroke[138, 168, 381, 434, 463], Type I diabetes[287, 310, 478], volumetric muscle loss[175, 441], esophageal cancer[89, 142, 191, 228, 476, 477], and inflammatory bowel disease[165, 376] has improved, but the improvement has been largely the result of advancements in symptomatic care, surgical technique and instrumentation; not as a result of curative discoveries or development of methods for replacing the diseased tissue with functional healthy tissue.

The field of tissue engineering/regenerative medicine is based upon the following fundamental strategies to promote functional tissue replacement: cell-based therapies, scaffold-based approaches, provision of bioactive molecules, or combinations of these strategies. The majority of work to date has focused upon cell-based therapies [52, 55, 86, 122, 215, 236, 248, 286, 348, 352]. Of course, any successful approach for creation of functional tissue will require cells, but one strategic variable is the source of cells; i.e., exogenous delivery of harvested allogeneic or autologous cells to the site of interest vs. recruitment of endogenous cells to the site of interest. Similarly, scaffold-based strategies can include approaches in which an appropriately configured scaffold material is placed in-situ as a guide or inductive template for functional tissue replacement or, alternatively, strategies in which the scaffold is used as a substrate upon which cells are seeded ex-vivo, with or without selected bioactive molecules, prior to surgical implantation of the cell-scaffold construct.

Scaffold materials for TE/RM can be either synthetic or harvested from naturally occurring sources (Figure 3). A wide variety of synthetic materials have been used as scaffolds for tissue repair and such materials have mechanical and material properties which are well characterized [18, 21, 35, 103, 223, 370, 407, 447, 491]. Synthetic materials are manufactured with high precision and generally have an identified and expected tissue response. In contrast, biologic scaffolds consist of either the intact extracellular matrix (ECM) following tissue decellularization or individual components of the ECM such as Collagen Type I, laminin, or hyaluronic acid [14, 28, 44, 194, 282, 346, 418, 452, 479]. Biologic scaffolds tend to elicit a friendlier host response than synthetic materials (i.e., less foreign body reaction and promote constructive tissue remodeling – the deposition of site appropriate, functional tissue) but are subject to biologic variability in their natural composition and mechanical properties. Furthermore, the methods by which naturally occurring bioscaffolds are manufactured can have a marked effect upon their performance. The clinical use of naturally occurring scaffolds and the pros and cons of such biologic materials are discussed in this section.

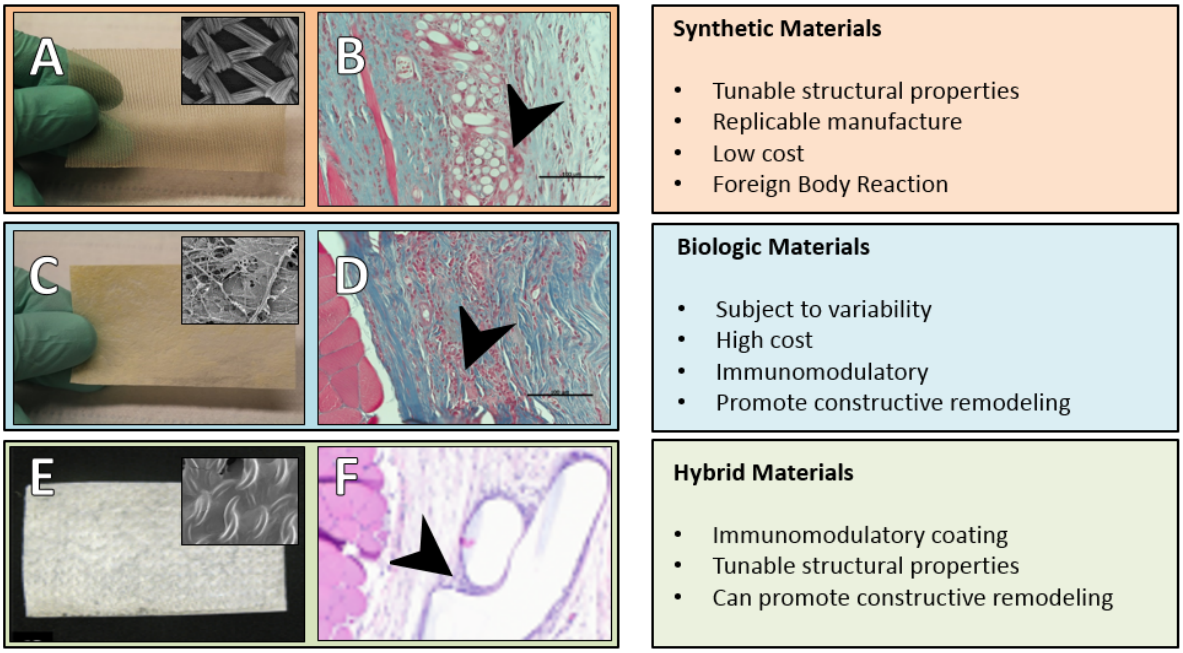

Figure 3. Biomaterials for tissue repair can be classified as synthetic, biologic, or hybrid

1.2.1 Synthetic Biomaterials

A vast array of synthetic biomaterials exists ranging from degradable PLGA or poly(lactic-co-glycolic acid), to permanent titanium allow implants for orthopedic applications. For example, the most commonly used non-degradable synthetic mesh materials for abdominal and inguinal hernia repair are polypropylene (PP), polyethylene, and polyethylene terephthalate (PET)[82, 401], and knitted polypropylene is now the most frequently used material for ventral hernia repair[95, 99, 189, 241]. Polypropylene's robust mechanical properties and beneficial effect upon the repair of ventral hernia and pelvic organ prolapse is well documented, but the host soft tissue

response is characterized by chronic inflammation, dense fibrous connective tissue deposition and complications such as erosion, exposure, and pain for patients [137, 335].

Of particular relevance to this thesis is the synthetic biomaterial poly(ester urethane)urea (PEUU), a biodegradable, cytocompatible elastomer[425], a material that was used to construct the hybrid cardiac patch used in Specific Aim 3. Biomaterials in this class offer interesting characteristics for a variety of soft-tissue remodeling applications. PEEUU enables great control and flexibility in design parameters including the choice of hard and soft segments, and the potential to be utilized as a thermoplastic elastomer[178, 177]. For this study, PEUU was manufactured via electrospinning, a process through which a polymer solution charged with a high voltage generates an electrical force strong enough to overcome surface tension of a pendant drop of the solution and ejecting a polymer jet. The bending and whipping instability of the polymer jet combined with fiber splaying and a rapidly evaporating solvent yields fibers that are collected on a grounded or charged collection surface. Through this process the resulting morphology and size of the fibers can be finely controlled by changing the voltage, feed rate, and collector distance, among others [178].

1.2.2 Biologic Biomaterials

A detailed description of these materials is found in section 1.3. Biologic scaffolds can be composed of intact mammalian extracellular matrix (ECM), or individual components of ECM such as collagen, laminin, or hyaluronan. Such scaffold materials would ideally maintain the native ultrastructure and composition of the ECM. The preparation of an ECM scaffold derived from native mammalian tissue requires a combination of chemical and mechanical processing

steps that result in efficient decellularization of the source tissue. As stated above ECM scaffolds have been prepared from a variety of tissues including dermis, small intestine, urinary bladder, pericardium, liver, skeletal muscle, and adipose tissue among others.

Most source tissue material used for derivation of ECM bioscaffolds are xenogeneic or allogeneic in nature, and therefore require the efficient removal of cellular antigens to prevent foreign body recognition and activation of an antibody-mediated rejection response by the host following in vivo implantation. Depending upon the tissue of interest, mechanical methods such an manual or automated delamination of muscle and mucosal layers is typically followed by a combination of physical, chemical, and enzymatic methods to achieve complete decellularization.

The goal of any decellularization process is the removal of all cellular and nuclear material while maintaining the composition, microstructure, mechanical properties, and biologic activity of the remaining native ECM. A biologic scaffold material is considered efficiently decellularized when it meets the following criteria: (1) Lack of nuclei present within the scaffold material following histologic or chemical nuclear staining; (2) Total scaffold material dsDNA content must be less than 50 ng/mg; (3) Any remaining DNA remnants present in the scaffold material must be less than 200 base pairs in nucleotide length [105]. Physical treatments for decellularization include sonication, scraping and/or shaking, or subjection to freeze-thaw cycles. Such methods facilitate the disruption of cell membranes and removal of cell contents from the native ECM. Enzymatic treatments with detergents or ionic solutions further denature cell membranes and disrupt intercellular bonds. Because the ECM of different tissues varies with regard to composition, structure, and density, the combination of methods used to achieve efficient decellularization varies across tissues.

1.2.3 Hybrid Biomaterials

Hybrid constructs seek to combine the tunable and versatile physical properties of synthetic biomaterials with the immunomodulatory properties and constructive remodeling potential of biologic biomaterials. For example, a method to coat a synthetic polypropylene hernia mesh with ECM has previously been described. [136, 466]. In these studies, the resulting hybrid mesh was shown to alter the default acute host response to the polypropylene mesh by delaying and reducing the accumulation of pro-inflammatory foreign body giant cells. This response was associated with a suppression of the proinflammatory M1 macrophage phenotype at the polypropylene/host tissue interface. The new host tissue deposition was altered after 35 days. The pores in the ECM coated mesh were filled with loose connective tissue rather than the dense, large fiber collagenous tissue noted in the uncoated mesh material pores. These differences in remodeling were associated with no loss of biaxial mechanical strength. Nonetheless, it is unknown whether these favorable outcomes persist in the long term well after the ECM component had fully degraded. In this study a hybrid material composed of PEEU and an acellular matrix derived from cardiac tissue was used to promote constructive remodeling of the myocardium in a preclinical model of myocardial infarction.

1.3 BIOLOGIC SCAFFOLDS COMPOSED OF MAMMALIAN EXTRACELLULAR MATRIX

1.3.1 The Extracellular Matrix: Structure and Function First paragraph.

The ECM is a complex milieu of both structural and functional molecules that are secreted and maintained by the resident cells of every tissue. Originally thought to exist with the singular purpose of providing structural support, it is now recognized that the ECM is a reservoir of information in the form of molecular and mechanical cues that contribute to the maintenance of cellular homeostasis, promotion of optimal tissue/organ function and, if necessary, mediation of wound healing and tissue repair [211]. By providing sites for cell attachment, the ECM can not only facilitate communication between adjacent cells but also participate directly in signal transduction, adapt to mechanical changes in the microenvironment, respond to signaling gradients, and sense and respond to disruption of tissue integrity. In turn, the response of local cell populations to these changes may or may not involve changes in gene expression profiles, cell migration, metabolic and proliferation rates, production of signaling molecules, and neomatrix deposition. In short, in addition to providing structural support, the ECM can modulate cell behavior while in turn, the local cell populations in the microenvironment can respond by modifying the composition and ultrastructure of the ECM. For this reason, the ECM exists in a highly fluidic state of dynamic reciprocity with the local cell populations and the microenvironment [51].

The main components of the ECM are largely conserved across multiple species and include bifunctional proteins such as collagen, fibronectin and laminin, glycosaminoglycans -

and to a lesser extent, growth factors, and cytokines (Figure 4). This principle lays the foundation of biologic scaffold compatibility across multiple species and permits the use of biologic scaffolds derived from xenogeneic sources in clinical applications. The exact distribution and three-dimensional arrangement of these molecules is tissue specific and at least partially responsible for the diverse mechanical, functional, and structural properties observed across different tissues. Not surprisingly, the original in situ composition of the ECM plays an important role in determining composition and structure of the resulting ECM-derived biologic scaffolds, but the main determining factor of these properties are the methods used for processing and manufacture[25].

Both the composition and the structure of ECM-based scaffolds are important aspects of the host-biomaterial interaction. Since the ECM is produced by the resident cells of every tissue, it constitutes the ideal substrate for each cell population and as such, it is logical and plausible that a substrate composed of site-specific ECM would be favorable for clinical use in homologous anatomic locations. However, the advantages and preference of site-specific (homologous) ECM scaffolds is still a matter of debate. Part of the difficulty in addressing this issue arises from the fact that most studies have investigated the application of ECM-derived scaffolds in either homologous or non-homologous locations independently, but they have rarely been directly compared in properly designed studies (Table 4).

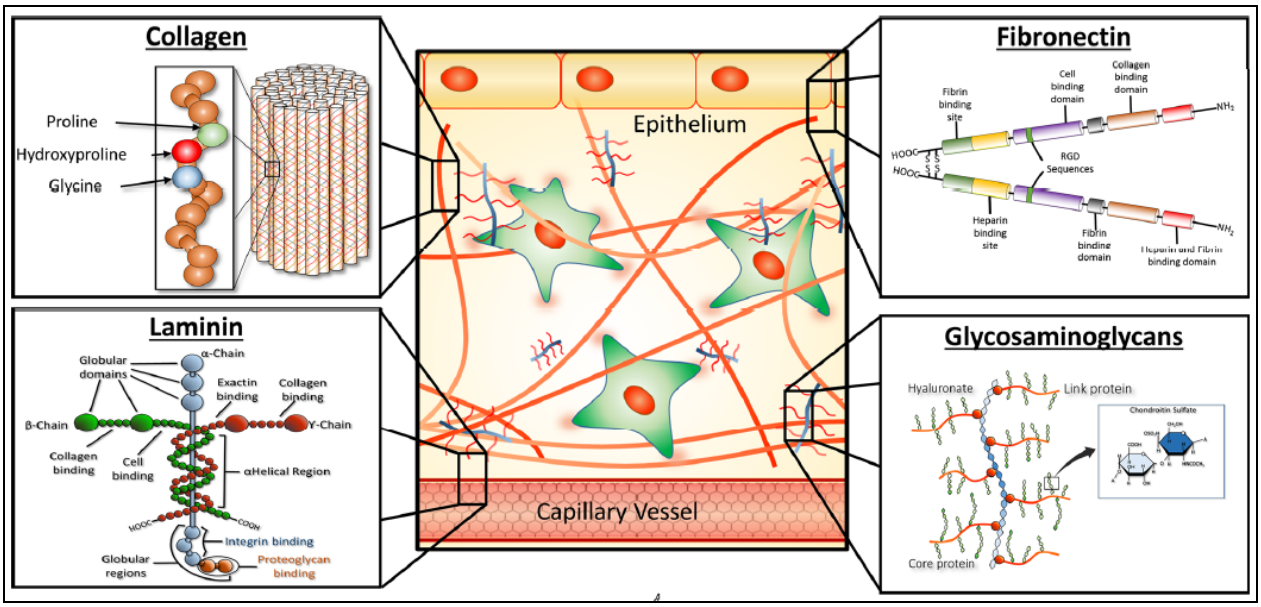

Figure 4. Composition of the Extracellular Matrix:

The extracellular matrix is composed of multiple functional molecules that are shared across multiple tissues and different species. For the most part, the ECM is made up of type I collagen, but other types of collagen are also found throughout the ECM in varying amounts depending on the source tissue. Non-collagenous molecules found in significant amounts include fibronectin, laminin, and glycosaminoglycans. The conformation and structure of these molecules enable the ECM to interact with local cell populations. The specific amount and distribution of these components of the ECM are partially responsible for the mechanical properties and function of the multiple organs and tissues.

Table 4. Site Specificity of ECM-Derived Scaffolds

The final composition and ultrastructure of ECM-derived biomaterials depend on a number of factors including the source tissue from which they are derived and the methods of decellularization. However, it has yet to be determined whether or not differences in composition and structure offer site specific clinical advantages when scaffolds are used in the treatment of homologous anatomic locations. This table shows examples supporting both homologous and heterologous use of ECM-derived biologic scaffolds.

Reports supporting ***homologous*** use of ECM scaffolds		Reports supporting ***heterologous*** use of ECM scaffolds	
Study	**Study details**	**Study**	**Study details**
Sellaro, T.L., et al., *Maintenance of hepatic sinusoidal endothelial cell phenotype in vitro using organ-specific extracellular matrix scaffolds.* Tissue Eng, 2007. **13**(9): p. 2301-10	Liver ECM allows sinusoidal endothelial cells to maintain their differentiated phenotype in culture longer Vs. other ECMs	Badylak, S.F., et al., Esophageal preservation in five male patients after endoscopic inner-layer circumferential resection in the setting of superficial cancer: a regenerative medicine approach with a biologic scaffold. Tissue Eng Part A,	SIS-ECM used to remodel the esophageal mucosa after circumferential, long segment en bloc removal in the setting of adenocarcinoma in 5 male patients
Lin, P., et al., Assessing porcine liver-derived biomatrix for hepatic tissue engineering. Tissue Eng, 2004. **10**(7-8): p. 1046-53	Liver ECM improved maintenance of liver-specific functions of hepatocytes compared to adsorbed collagen cultures	Sicari, B.M., et al., An acellular biologic scaffold promotes skeletal muscle formation in mice and humans with volumetric muscle loss. Sci Transl Med, 2014. **6**(234): p. 234ra58.	UBM-ECM implantation used as surgical treatment for volumetric muscle loss in both a preclinical rodent model and five male patients
Singelyn, J.M., et al., *Catheter-Deliverable Hydrogel Derived from Decellularized Ventricular Extracellular Matrix Increases Endogenous Cardiomyocytes and Preserves Cardiac Function Post-Myocardial Infarction.* J Am Coll Cardiol, 2012. **59**(8): p. 751-63.	Injection of cardiac ECM-derived hydrogel in a myocardial infarction model increases endogenous cardiomyocytes in the infarct area and maintains cardiac function without inducing	Valentin, J.E., et al., *Functional skeletal muscle formation with a biologic scaffold.* Biomaterials, 2010. **31**(29): p. 7475-84	SIS-ECM used to replace abdominal wall muscle showing partial replacement by islands and sheets of skeletal muscle, able to generate maximal contractile force similar to native tissue
Medberry, C.J., et al., Hydrogels derived from central nervous system extracellular matrix. Biomaterials, 2013. **34**(4): p. 1033-40	Brain ECM hydorgels increased neurite length when compared to other ECM-derived hydrogels	Nieponice, A., et al., Patch esophagoplasty: esophageal reconstruction using biologic scaffolds. Ann Thorac Surg, 2014. **97**(1): p. 283-8	Four patients requiring esophageal reconstruction underwent a patch esophagoplasty using an ECM scaffold composed of porcine urinary bladder ECM
Crapo, P.M., et al., Biologic scaffolds composed of central nervous system extracellular matrix. Biomaterials, 2012. **33**(13): p. 3539-47	CNS ECM retains neurosuportive proteins and stimulates proliferation, migration, and differentiation of PC12 cells	Kruper, G.J., et al., Salvage of failed local and regional flaps with porcine urinary bladder extracellular matrix aided tissue regeneration. Case Rep Otolaryngol, 2013. **2013**: p. 917183	UBM-ECM used to salvage flaps with extensive wound breakdown on the face and neck

1.3.1.1 Composition of the ECM

Collagen

Collagen accounts for more than 90% of the protein found in the ECM and although more than 25 different isoforms have been identified, the majority of collagen found within the ECM is type I collagen (Figure 5). Varying amounts of collagen type III, IV, V, VI, and VII are also notably present in the ECM, although not ubiquitously[445]. For example, the collagen composition of ECMs originating from different tissues will vary depending on whether or not a basement membrane is present: While tendons and ligaments rely mostly on type I collagen to provide the tensile strength required to meet the mechanical demands placed upon these structures[50], tissues with a basement membrane will have a more diverse collagen composition with significant amounts of type IV collagen[176] and type VII collagen[88]. Whereas type IV collagen has ligand affinity for endothelial cells and it is therefore found within the basement membrane of vascular structures, type VII collagen is needed to facilitate fibril and epithelial cell anchoring, and as a result it is mostly found protecting overlying keratinocytes from sheer stress forces under epithelial structures.

Collagen-based scaffolds are among the most extensively used scaffolds in clinical applications and are available in multiple formats including native, cross-linked, and solubilized gel forms. Due to its abundance and ubiquity, type I collagen is the most commonly used isoform, although other forms have also been used. Currently available collagen-based products are beyond the scope of the present manuscript, but their composition and applications have been thoroughly reviewed by Chattopadhyay, S and Raines, RT [85].

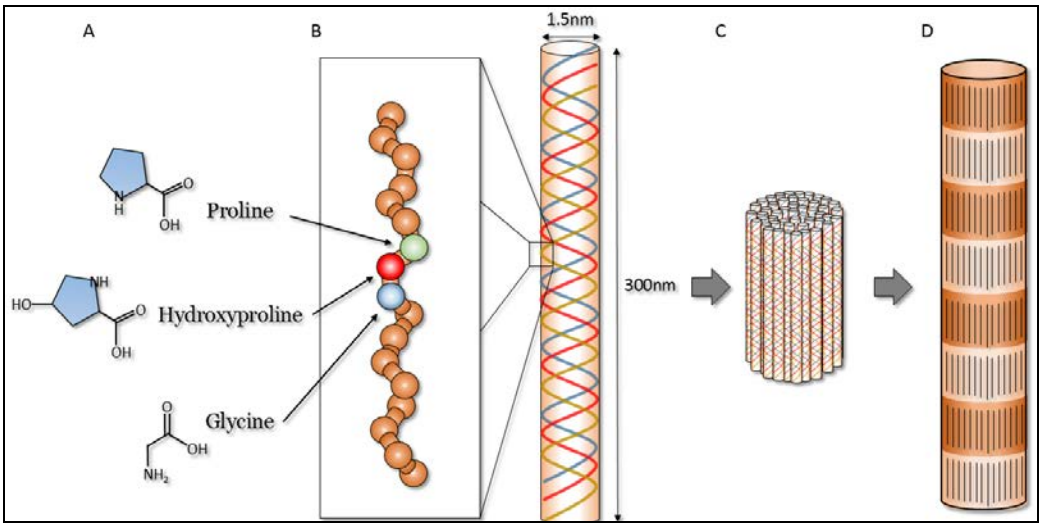

Figure 5. Schematic representation of the assembly of collagen I

A, Individual collagen polypeptide chains. The polypeptides consist of the repeating sequence Gly-X-Y, where X is often proline and Y is often hydroxyproline; B, Collagen is made up of three polypeptide strands which are all left-handed helixes and twist together to form a right handed coiled coil. The strands are synthesized as precursor chains with propeptides on the C and N ends. The propeptides are cleaved into short non-helical telopeptides; C, Collagen molecules self-assemble into collagen fibrils; D, Collagen fibers are formed by end to end and lateral assembly of collagen fibrils, resulting in a regular banding pattern that is characteristic of collagen.

Fibronectin

Fibronectin is the second most abundant molecule in the ECM and it is present in both soluble and tissue isoforms in submucosal, basement membrane, and interstitial tissues. Fibronectin is rich in domains that facilitate adhesion to multiple cell types via integrins, a unique property that makes it suitable for the coating of biomaterials and tissue culture instrumentation [197] (Figure 6).

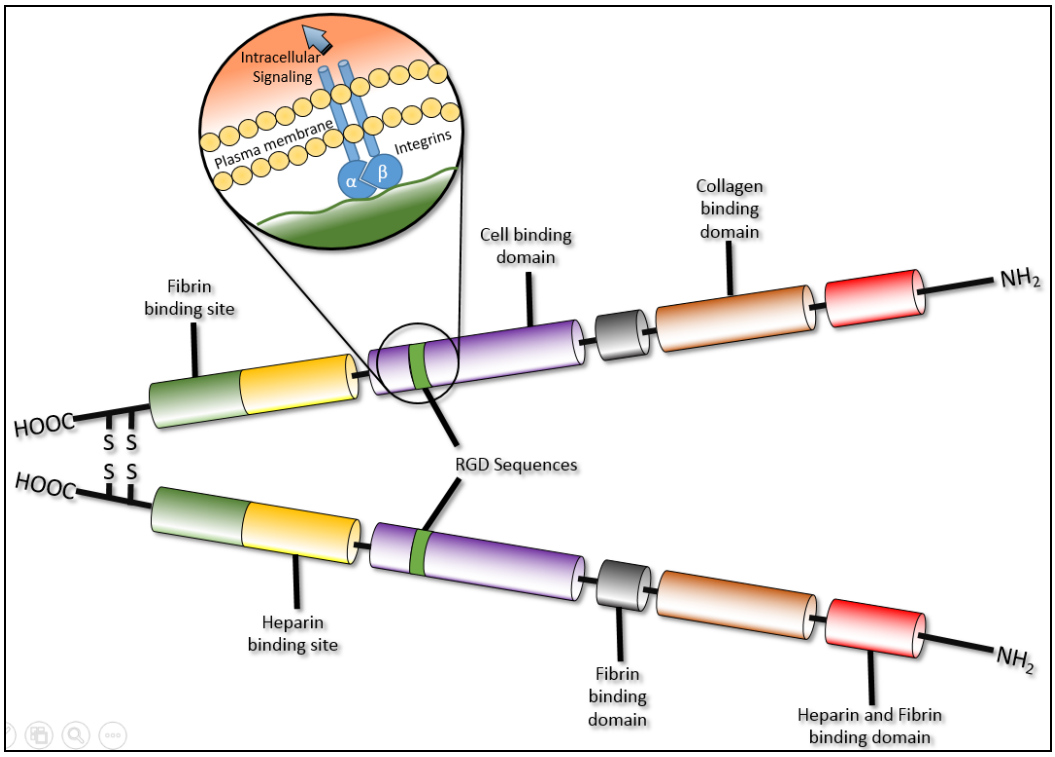

Figure 6. Structural Composition of Fibronectin

Fibronectin is a dimeric molecule joined by two disulfide bonds at the carboxy end. Each domain of the fibronectin molecule has binding sites for cell receptors and ECM molecules

Laminin

Laminin is a trimeric cross-linked polypeptide that exists in multiple configurations depending upon the specific combination of the peptide side chains that make up its main molecule (Figure 7). Laminin can be found throughout the body within basement membranes where it mainly acts as an adhesion molecule for different cell types and other components of the ECM. Laminin is an important molecule for the organization and maintenance of vascular structures and for interactions between the ECM and mesenchymal stem cells [344].

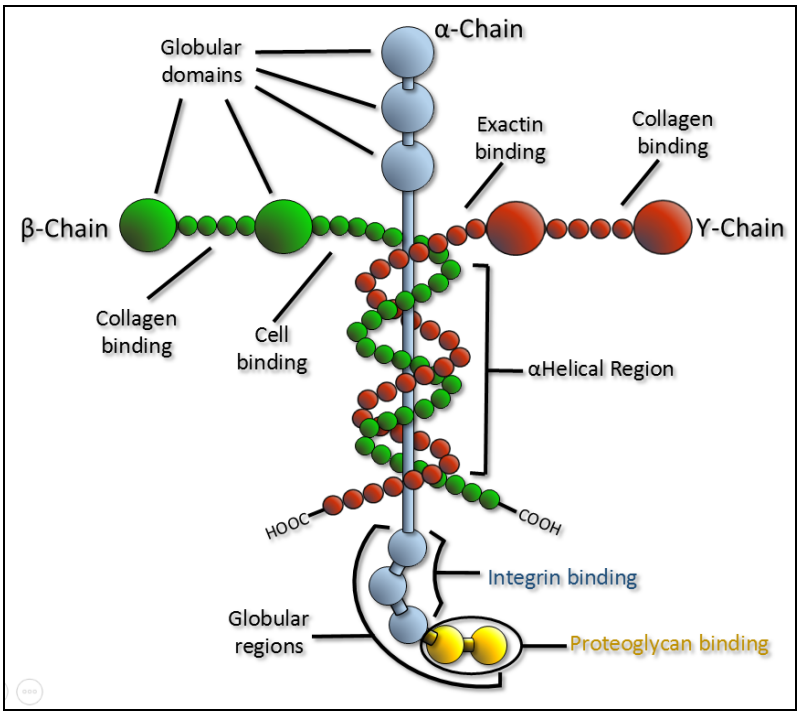

Figure 7. Laminin Structure

Laminin is composed of three polypeptide chains (α, β1, and β2) organized into the shape of a cross. Laminin has binding domains for heparin, collagen IV, heparin sulfate, and cells.

Second paragraph.

Glycosaminoglycans

Glycosaminoglycans (GAGs) present in ECM include heparin, heparan sulfate, chondroitin sulfate A and B, and hyaluronic acid (HA). GAGs are unbranched polysaccharides composed of repeating disaccharide units that possess the ability to retain water and bind growth factors and cytokines (Figure 8). HA possesses significant biologic activity by itself, directly influencing cell proliferation, migration, and differentiation. The concentration of HA within ECM is highest in fetal and newborn tissues and has been associated with the enhanced healing ability of the human body during these early stages of life[198].

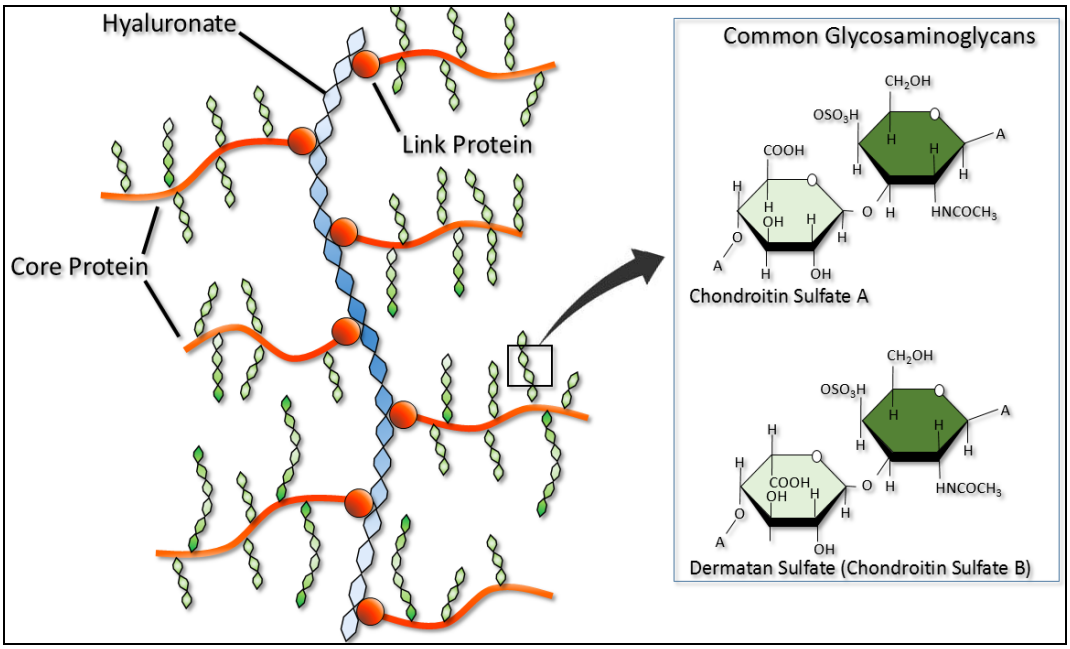

Figure 8. Glycosaminoglycan Structure

Glycomsaminoglycans are long unbranched polysaccharides that are composed of a repeating disaccharide unit. The disaccharide unit is composed of one of two modified sugars, either N-acetylgalactosamine or N-acetylglucosamine.

Matricryptic peptides

Matricryptic peptides are molecular fragments of parent proteins within the ECM that possess important biologic activity [97, 301, 358]. During degradation, the ECM undergoes structural and conformational alterations that result in matricryptic peptide exposure, activation, and release into the microenvironment. The processes responsible for these events include enzymatic cleavage[159], protein multimerization[483], adsorption of molecules to other ECM components[396], cell-mediated mechanical deformation[389], and ECM denaturation[375]. As a whole, the processes that result in matricryptic peptide encryption, activation, and release are thought to have evolved as a mechanism to embed and hide these signals making them available only when necessary (i.e. after tissue injury). To date, several matricryptic peptides have been

identified, and although a thorough examination of matricryptic peptide activity is beyond the scope of this manuscript, comprehensive reviews of matricryptic peptide activation and function have been presented by Davis et al.[110] and Ricard-Blum et al. [361] .

Growth factors and Cytokines

As previously mentioned, some components of the ECM such as GAGs and proteoglycans can bind to and sequester growth factors and cytokines, a process that allows the ECM to serve as a reservoir of signaling molecules [246, 417] - storing them after secretion by resident cells, and releasing them when needed and appropriate stimuli are provided[34]. The mechanisms that mediate the process of growth factor and cytokine release are complex and rely upon a number of strategies including binding affinity, conformational changes, and degradation of the ECM during normal and pathologic processes. For instance, perlecan can function as a low-affinity co-receptor for bFGF, a property that makes it an important component of processes such as bFGF-mediated mitogenesis and angiogenesis. Degradation of either the perlecan protein core or the heparan sulfate chains releases ECM-bound bFGF in its active form and allows it to participate in these processes in a controllable fashion[214].

In addition to regulating storage, availability, and biological activity of these molecules, binding to the ECM also influences cytokine diffusion and adequate presentation to receptors on the cell surface[475]. Other important signaling molecules that bind to and associate with perlecan include G-MCSF, IL-3, INFγ, and hepatocyte growth factor[213]. In addition, there is evidence that the activity of TGF-βs may be controlled through binding to ECM components such as decorin and biglycan[385, 386]. Adequately designed decellularization protocols can preserve growth factors and cytokines during the manufacturing process in such a way that they are still detectable in significant amounts in the resulting scaffolds [460].

1.3.2 The Extracellular Matrix as a Bioscaffold for Tissue Repair.

ECM-derived scaffolds are subject to natural variability in their biologic composition and mechanical properties depending on the species, age, [409], and anatomic location [106, 230, 422, 468] from which they are derived. However, a great degree of variability depends upon the exact methods of manufacture[26], the efficiency of the decellularization process[67, 231], and any post-processing modifications to which the materials might be subjected depending on the specific intended application. Commonly used post-processing modifications include different degrees of chemical cross linking, powdering, and manufacture of multi-laminate constructs [444]. Solubilization into hydrogel forms has recently become increasingly popular [218, 219, 292, 379, 395, 467] (Figure 9).

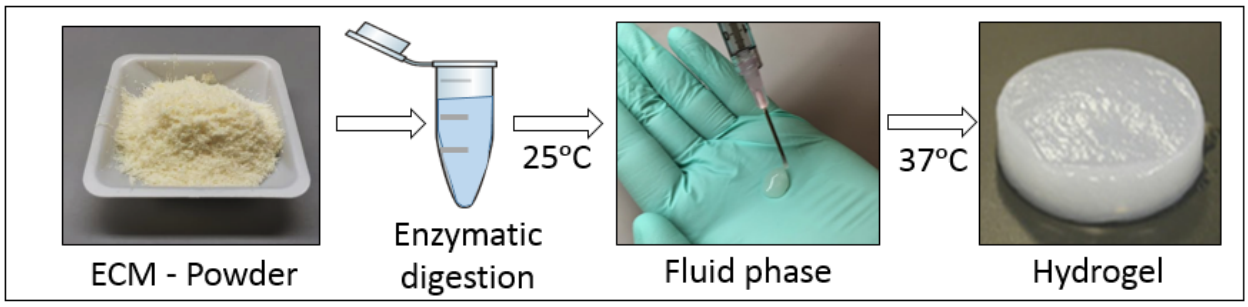

Figure 9. ECM-Derived Hydrogels for Tissue Repair

ECM-derived hydrogels can be prepared by placing lyophilized powdered ECM into a 0.01 N HCl solution of 1mg/mL pepsin and stirring at room temperature for 48hrs. The pre-gel ECM solution is then brought to pH 7.4 using 0.01 N NaOH and diluted to the desired volume/salt concentration using 10× and 1 × PBS. Pepsin is irreversibly inactivated at pH above 7.5ECM at which point the material gels. Hydrogels provide advantages such as injectability, the ability to fill an irregularly shaped space, and possess the inherent bioactivity of native matrix.

The specific composition and three-dimensional architecture of scaffolds composed of decellularized tissues vary significantly depending on the source tissue and the methods used for

decellularization. Scaffolds manufactured from the ECM of small intestinal sub-mucosa (SIS-ECM) and urinary bladder matrix (UBM-ECM) have been most extensively characterized, and will therefore serve as the exemplars. Like the ECM from the tissues they originate from, SIS-ECM and UBM-ECM are composed of more than 90% collagen, the majority of which is type I [26, 282] with varying amounts of collagen type III, IV, V, VI, and VII also present. The ECM derived from the esophageal mucosa (EM-ECM) [230], skeletal muscle (SM-ECM), and dermis (D-ECM) show similar composition [230, 347, 357, 468]. The collagen composition of ECM-derived bioscaffolds originating from different tissues will vary depending on whether or not a basement membrane is present. Tissues with a basement membranes such as UBM-ECM, EM-ECM and SM-ECM contain collagen type IV, type VII and other basement membrane associated adhesion proteins such as laminin and fibronectin, while other ECMs have much less of these collagen types [61, 197, 230, 282]. Originally described as a purely structural biomolecule, evidence has shown that cryptic peptide motifs with important biological activity to the constructive remodeling processes including mitogenesis, chemotaxis, and differentiation of stem cells are still present and active in biologic scaffolds after decellularization [8, 358, 437, 453]. Some matricryptic peptides have been shown to be antimicrobial [56] and antiangiogenic [361]. In the context of biomaterial-mediated tissue repair, these matricryptic peptides are released as a consequence of cleavage and degradation by phagocytic cell populations recruited to the zone of injury and release of matrix metalloproteases (MMPs) and other proteases (See section 1.4.5) [110, 192, 361].

In addition to the various types of collagen and other basement membrane-associated molecules, ECM-derived bioscaffolds contain a mixture of glycosaminoglycans (GAGs)

including heparin, heparan sulfate, chondroitin sulfate and hyaluronic acid [198]. It is now well established that the specific methods of decellularization particularly affect GAG content [161], the details of which will be discussed in the next section.

1.3.3 Tissue and Whole Organ Decellularization

The objective of the decellularization process is to remove cell associated antigens while preserving the ultrastructure and composition of the ECM. When properly manufactured, the resulting scaffold can serve as a cell-guiding template that contains the necessary cues and adequate three-dimensional configuration to facilitate cell infiltration, modulate the immune host response, and mediate tissue repair upon implantation and subsequent degradation[27, 410]. However, even the gentlest methods of tissue decellularization will inevitably alter the composition and ultrastructure of the ECM and remove some of these desirable components. Hence, the decellularization process is better described as a balancing act between thorough decellularization and conservation of biologically active molecules that favorably modulate the host response. In fact, adequate decellularization can only be achieved in some instances at the expense of losing important molecular components of the ECM and dramatically disrupting its original structure. Therefore, a thorough understanding of the properties and application of the various decellularization agents is necessary for the systematic optimization of decellularization protocols.

A number of decellularization methods that are suitable and appropriate for the source tissues have been described [105, 106, 161, 230, 468] (Table 5). The type and amount of bioactive molecules that remain in the scaffolds vary significantly depending on the specific methods of decellularization and other processing steps.

Table 5. Published Protocols for Tissue Decellularization

Source Tissue	Species	Report
Central nervous system	Porcine	Crapo, P.M., et al., Biologic scaffolds composed of central nervous system extracellular matrix. Biomaterials, 2012. **33**(13): p. 3539-47.
Dermis	Human	Wainwright, D.J., Use of an acellular allograft dermal matrix (AlloDerm) in the management of full-thickness burns. Burns, 1995. **21**(4): p. 243-8.
Esophagus	Murine (Rat)	Sjoqvist, S., et al., Experimental orthotopic transplantation of a tissue-engineered oesophagus in rats. Nat Commun, 2014. **5**: p. 3562.
Esophageal mucosa	Porcine	Keane, T.J., et al., Preparation and characterization of a biologic scaffold from esophageal mucosa. Biomaterials, 2013. **34**(28): p. 6729-37.
	Ovine	Ackbar, R., et al., Decellularized ovine esophageal mucosa for esophageal tissue engineering. Technol Health Care, 2012. **20**(3): p. 215-23.
Heart	Porcine	Wainwright, J.M., et al., Preparation of cardiac extracellular matrix from an intact porcine heart. Tissue Eng Part C Methods, 2010. **16**(3): p. 525-32.
	Porcine	French, K.M., et al., A naturally derived cardiac extracellular matrix enhances cardiac progenitor cell behavior in vitro. Acta Biomater, 2012. **8**(12): p. 4357-64.
	Murine (mouse)	de Castro Bras, L.E., et al., Texas 3-step decellularization protocol: looking at the cardiac extracellular matrix. J Proteomics, 2013. **86**: p. 43-52.
Lung	Porcine	Price, A.P., et al., Automated Decellularization of Intact, Human-Sized Lungs for Tissue Engineering. Tissue Eng Part C Methods, 2014.
Skeletal Muscle	Porcine	Wolf, M.T., et al., Biologic scaffold composed of skeletal muscle extracellular matrix. Biomaterials, 2012. **33**(10): p. 2916-25
Trachea	Porcine	Haykal, S., et al., The effect of decellularization of tracheal allografts on leukocyte infiltration and of recellularization on regulatory T cell recruitment. Biomaterials, 2013. **34**(23): p. 5821-32.
	Porcine	Kutten, J.C., et al., Decellularized Tracheal Extracellular Matrix Supports Epithelial Migration, Differentiation and Function. Tissue Eng Part A, 2014.
Small intestinal submucosa	Porcine	Lindberg, K. and S.F. Badylak, Porcine small intestinal submucosa (SIS): a bioscaffold supporting in vitro primary human epidermal cell differentiation and synthesis of basement membrane proteins. Burns, 2001. **27**(3): p. 254-66
Urinary Bladder	Porcine	Lindberg, K. and S.F. Badylak, Porcine small intestinal submucosa (SIS): a bioscaffold supporting in vitro primary human epidermal cell differentiation and synthesis of basement membrane proteins. Burns, 2001. **27**(3): p. 254-66

The use of harsh detergents can thoroughly decellularize tissues and successfully remove undesirable cellular remnants and epitopes, but such methods also disrupt the native ultrastructure and remove or decrease the availability of bioactive molecules that are favorable for the constructive remodeling response in vivo. In turn, milder treatments conserve more bioactive molecules, but may fail to remove all cell remnants and pro-inflammatory epitopes that can cause chronic inflammation leading to scar tissue formation , and dense collagenous non-functional tissue deposition [65, 67, 474, 485]. Consequently, tissue processing methods, including decellularization and terminal sterilization techniques are critical determinants of the clinical performance of these scaffolds [69, 169, 362]. The optimal processing methods represent a balancing act of thorough decellularization vs. maintenance of ECM ultrastructure and favorable bioactive molecules.

The most effective methods for tissue decellularization are determined by multiple factors, including the tissue's cellularity (e.g. muscle vs. tendon), density (e.g. dermis vs. adipose tissue), lipid content (e.g. brain vs. small intestinal submucosa), and thickness (e.g. dermis vs. pericardium) (Figure 10). Inevitably, all methods will alter the composition of the ECM and will cause some degree of ultrastructure disruption. Thus, the objective of every decellularization protocol is to minimize these undesirable effects while meeting the criteria for decellularization. A brief summary of some commonly used decellularization agents (e.g. chemical, enzymatic, and physical) and their effects on cellular and extracellular tissue components is provided below:

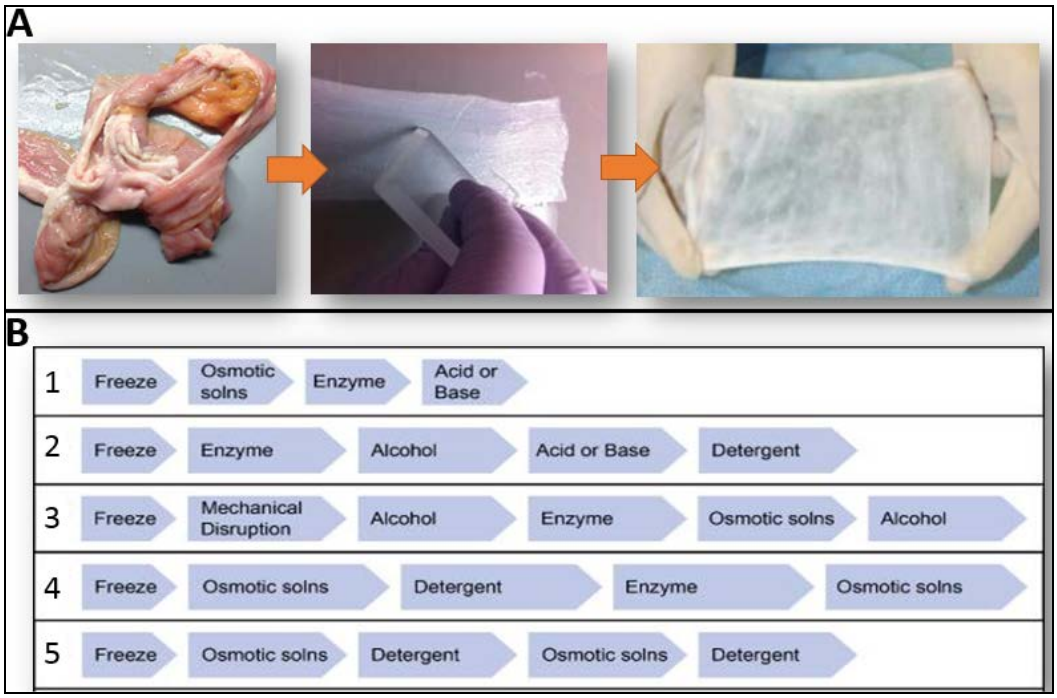

Figure 10. Methods of Decellularization are Determined by the Source Tissue:

A, Small Intestinal Submucosa (SIS) is mechanically decellularized by scarping and chemically decellularized by peracetic acid. The resultant acellular material is white in appearance. B, Example decellularization protocols for (1) thin laminates such as pericardium, (2) thicker laminates such as dermis, (3) fatty, amorphous tissues such as adipose, (4) composite tissues or whole simple organs such as trachea, and (5) whole vital organs such as liver. Arrow lengths represent relative exposure times for each processing step. ((Figure adapted from (Crapo et al., 2011)[105])).

1.3.3.1 Detergents:

Detergents are important decellularization agents because they are very efficient at solubilizing lipid-containing cellular components such as cell walls and nuclear and mitochondrial membranes. In addition, detergents effectively dissociate proteins from DNA[105]. Disruption of nucleic acids facilitates the removal of genetic material from the ECM. However, detergents are non-specific, and therefore also disrupt and dissociate desirable proteins from the ECM, a side effect that can potentially minimize or eliminate the constructive remodeling response in vivo.

Non-ionic detergents such as Triton X-100, can effectively remove cellular material from most tissues and can therefore decrease potentially adverse immune responses following in vivo implantation. However, decellularization of dense tissues requires longer treatments and higher concentrations of such agents, both of which are associated with progressively greater disruption of the ECM ultrastructure and content. In contrast, ionic detergents such as sodium dodecyl sulfate (SDS) can efficiently and thoroughly remove cellular material from dense tissues including solid organs, but have the disadvantage of removing growth factors and significantly altering the ultrastructure of the ECM. Because of its cytotoxicity and ability to penetrate deeper into denser tissues even at low concentrations, multiple washes are necessary to ensure all SDS residues are removed from the scaffolds. Zwitterionic detergents such as 3-[(3-cholamidopropyl)dimethylammonio]-1-propanesulfonate (CHAPS) are preferred when the objective is the preservation of the ECM ultrastructure, but these detergents are only effective in decellularizing less dense tissues such as the lungs. In summary, while non-ionic and zwitterionic detergents are better for ultrastructure preservation, ionic detergents are better cell removal agents[105] .

1.3.3.2 Acids and Bases:

Acids are commonly used agents that catalyze the hydrolytic degradation of multiple biomolecules. For example, peracetic acid is frequently used as a disinfecting agent in the later stages of the decellularization process, but it also doubles as a decellularization agent that removes residual nucleic acids with minimal effect on the ECM composition and structure [163, 193, 195]. Acetic acid can disrupt the structure of collagen within an ECM and therefore affect its biomechanical properties, but it has minimal effect upon sulfated glycosaminoglycan composition (sGAG) [119]. Bases on the other hand, are almost exclusively used to remove hair

from dermis samples during the early stages of decellularization [347, 357]. Bases have been shown to completely eliminate growth factors from the ECM [357], cleave collagen fibrils, and disrupt collagen crosslinks [170].

1.3.3.3 Hypertonic and Hypotonic solutions:

Hypertonic solutions aid in the dissociation of DNA from proteins[104]. Hypotonic solutions have the ability to cause cell swelling and lysis with osmotic pressure without markedly modifying the ultrastructure of the ECM [472]. For optimal results, hyper- and hypotonic solutions are often alternated through several cycles. This process can facilitate removal of cell remnants and chemical residues left from the decellularization process.

1.3.3.4 Alcohols:

Alcohols contribute to the decellularization process by dehydrating and lysing cells [347], and extracting phospholipids [126, 264]. Isopropanol, ethanol, and methanol have been shown to be more effective than lipase in removing lipids from tissue and are therefore widely used in adipose tissue decellularization [64, 141]. Methanol in combination with chloroform has also been used during delipidation of tissues. However, some alcohols such as methanol and ethanol are commonly used as tissue fixatives in histology, and to precipitate proteins in molecular biology [78], and therefore they can potentially damage ECM ultrastructure [170, 171].

1.3.3.5 Enzymes:

The use of enzymes in decellularization protocols provides high specificity for the degradation and removal of specific types of molecules. However, complete decellularization solely via enzymatic treatment is not possible, and enzymatic residues, even at low concentrations, can

impair recellularization and potentially cause an undesirable inflammatory response [105]. DNases and RNases are very useful in the removal of nucleotides, but only after cells have been lysed and lipid membranes have been disrupted with detergents and other agents [342] [128]. Endonucleases [342] may be more suitable for decellularization than exonucleases because they cleave nucleotides mid-sequence and are therefore more effective at fragmenting long strands of nucleic acids in preparation for removal.

1.3.4 Criteria for Tissue Decellularization

The Food and Drug Administration has not established standards for tissue decellularization. As a result, commercially available ECM-derived scaffolds (Table 6) contain different amounts of cell associated antigenic material. Studies have shown that cellular debris within biologic scaffold materials can have a pro-inflammatory effect that has in turn been associated with poor remodeling outcomes[67, 231]. Therefore, establishment of decellularization criteria have been suggested and include the following: 1) No visible nuclei per histologic evaluation via eosin & hematoxylin and 4',6-Diamidino-2-Phenylindole, Dihydrochloride (DAPI) stains, 2) Any remaining DNA content should not exceed 200 base pair in length, and 3) the amount of double stranded DNA should not exceed 50ng per mg of dry weight of the material (Figure 11).

Table 6. Commercially Available Biologic Scaffolds for Tissue Repair

Source Species	Source Tissue	Product	Company	Post-Processing	Form
Bovine	Fetal skin	Durepair™	TEI Biosciences	Natural	Dry scaffold
	Fetal skin	PriMatrix™	TEI Biosciences	Natural	Dry scaffold
	Fetal skin	SurgiMend®	TEI Biosciences	Natural	Dry scaffold
	Fetal skin	TissueMend®	TEI Biosciences	Natural	Dry scaffold
	Fetal skin	Xenform™	TEI Biosciences	Natural	Dry scaffold
	Pericardium	Dura-Guard®	Synovis® Surgical Innovations	Cross-linked	Hydrated scaffold
	Pericardium	Peri-Guard®	Synovis® Surgical Innovations	Cross-linked	Dry scaffold
	Pericardium	Vascu-Guard™	Synovis® Surgical Innovations	Cross-linked	Dry scaffold
	Pericardium	Veritas®	Synovis® Surgical Innovations	Cross-linked	Hydrated scaffold
Equine	Pericardium	DurADAPT™	Pegasus Biologicals	Cross-linked	Dry scaffold
	Pericardium	OrthADAPT™	Pegasus Biologicals	Cross-linked	Dry scaffold
Human	Dermis	Axis™ Dermis	Mentor	Natural	Dry scaffold
	Dermis	Bard Dermal Allograft ®	Bard	Natural	Dry scaffold
	Fascia lata	AlloPatch ®	MTF	Natural	Dry scaffold
	Fascia lata	FasLata®	CR Bard	Natural	Dry scaffold
	Fascia lata	Suspend™	Mentor	Natural	Dry scaffold
	Skin	AlloDerm ®	LifeCell	Natural	Dry scaffold
	Skin	Graft Jacket ®	Wright Medical Tech	Natural	Dry scaffold
Porcine	Dermis	Pelvicol™	CR Bard	Cross-linked	Hydrated scaffold
	Dermis	Zimmer Collagen Patch™	Tissue Science Laboratories	Cross-linked	Hydrated scaffold
	Myocardium	Ventrigel	Ventrix	Gelation	Hydrogel
	Skin	Permacol™	Tissue Science Laboratories	Cross-linked	Hydrated scaffold
	Small intestinal submucosa (SIS)	CuffPatch™	Biomet Sports Medicine	Cross-linked	Hyrdated scaffold
	Small intestinal submucosa (SIS)	Durasis®	SIS Cook	Natural	Dry scaffold
	Small intestinal submucosa (SIS)	Oasis®	Cook Biotech/Healthpoint	Natural	Dry scaffold
	Small intestinal submucosa (SIS)	Restore®	DePuy	Natural	Dry scaffold
	Small intestinal submucosa (SIS)	Stratasis™	Cook Biomedical	Natural	Dry scaffold
	Small intestinal submucosa (SIS)	Surgisis®	Cook Biomedical	Natural	Dry scaffold
	Urinary bladder matrix (UBM)	Matristem™	Acell	Natural	Dry scaffold

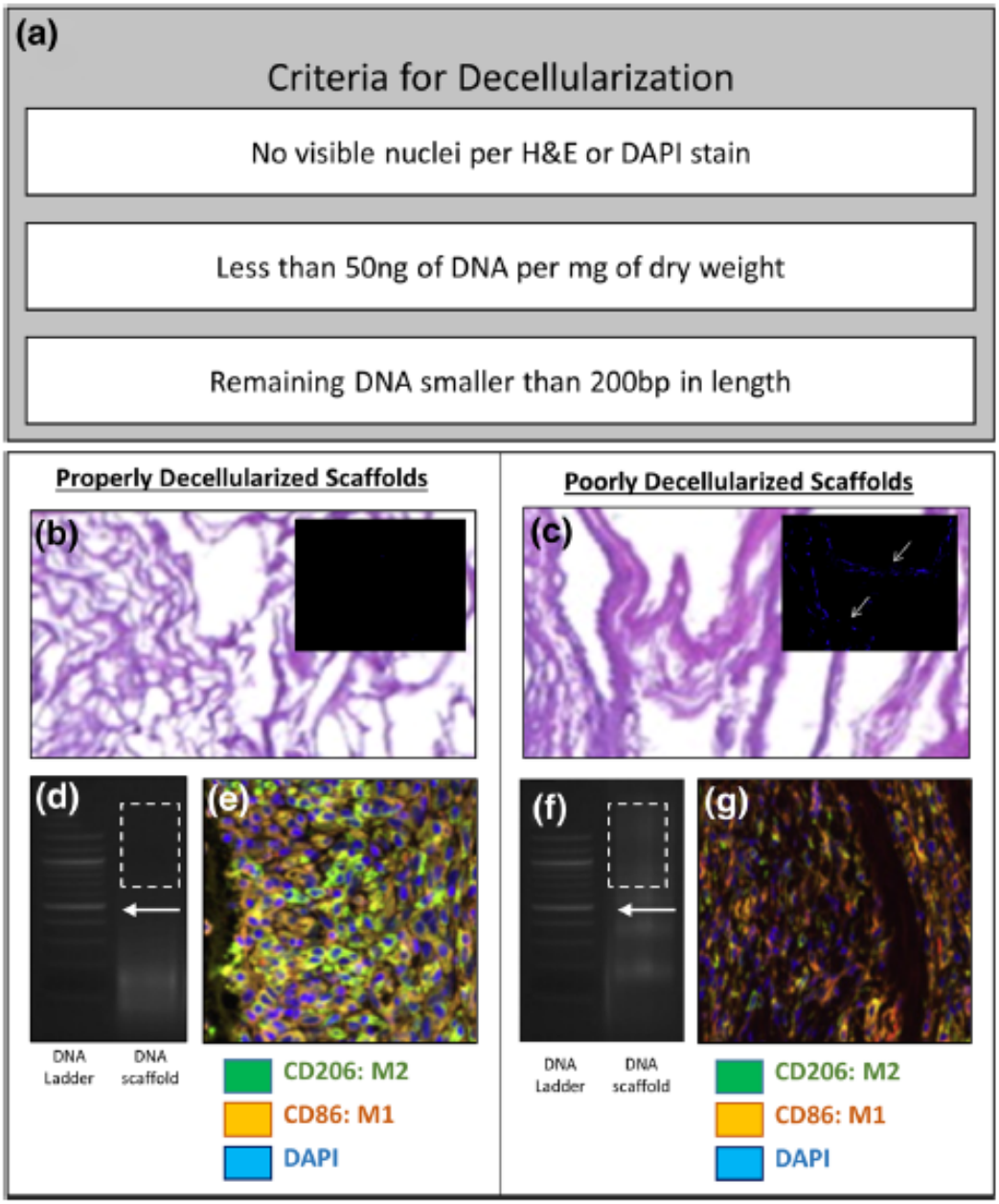

Figure 11. Criteria for Tissue Decellularization

The objective of the decellularization process is to remove all immunogenic cellular material while maintaining components of the ECM that are shared across species. Although official standard criteria for decellularization have not been established, proposed standards in (a) seek to avoid cellular remnants that might initiate or prolong detrimental inflammatory processes and potentially transmit zoonotic and/or prion-based diseases upon implantation. When properly decellularized according to these criteria, ECM-derived biologic scaffolds have consistently shown superior performance in vivo and in vitro. (b) H&E and DAPI stains of properly decellularized

ECM-based scaffolds with no visible nuclei. (c) In contrast, poorly decellularized scaffolds contain visible nuclei per H&E and/or DAPI stains (arrows). (d) Ethidium bromide gel showing that when properly decellularized, scaffolds contain DNA remnants below 200 bp in length (arrow), and (e) promote a quick transition to the favorable M2 pro-remodeling macrophage phenotype upon in vivo implantation (M1 macrophages in orange and M2 macrophages in green). (f) On the other hand, poorly decellularized scaffold contain relatively large fragments of DNA above 200 bp (Arrow) and (g) promote a robust and prolonged M1-proinflamatory macrophage phenotype upon in vivo implantation. Scale bars 100μm.

1.4 BIOMATERIAL-HOST INTERACTION

1.4.1 Default Mammalian Wound Healing Response

The adult mammal has a few privileged tissues such as the epidermis, the intestinal epithelium, and the bone marrow which have the ability to regenerate, at least to a certain extent; however, this regenerative response is the exception rather than the rule in most adult mammals, and it only occurs after mild to moderate injury. In contrast, the more common wound healing response eventually and inevitably leads to fibrotic tissue formation through a process that involves a variety of cell types acting in highly coordinated spatial and temporal processes that eventually organize into dense scar tissue. For example, myocardial fibrosis is the usual sequela following infarction, liver fibrosis is a downstream consequence of chronic hepatic disease, and esophageal scarring with associated clinical stricture is the expected outcome of extensive surgical ablation of the diseased esophageal mucosa. Even though the mechanisms underlying these processes are tissue-specific and not entirely understood, it is generally recognized that wound healing occurs in several complex phases [216, 296, 321, 366, 382, 461].

Similarly, the response to the presence of foreign materials, including those materials of which biological scaffolds are composed, involves some of the same general components of the inflammatory and remodeling phases. However, regenerative medicine strategies seek to modify this default response by shifting the outcome of tissue injury and loss from an evolutionary derived process of hemostasis and scar tissue formation to one of well-orchestrated constructive remodeling and functional tissue restoration. Not surprisingly, such fundamental changes are not trivial, and they necessarily involve the mechanisms by which stem cell recruitment is initiated,

cell growth is controlled, cell fate is determined, and site appropriate parenchymal and non-parenchymal tissue components are organized, vascularized, and innervated when necessary. Interestingly, signals to control most, if not all such processes exist within the naturally occurring ECM ECM [5, 8, 40, 282, 295, 296, 358, 435, 437, 484]

1.4.2 Biomaterial-Host Interaction: Overview

Most tissues in the human body do not have the ability to regenerate and as a result, an insult of sufficient magnitude will invariably lead to scar tissue formation and loss of tissue function. The steps responsible for tissue damage repair are defined as the wound healing response and have been traditionally classified into a number of complex and overlapping phases that include hemostasis, inflammation, cell proliferation, and tissue remodeling[10, 118, 288, 298]. When properly configured, biologic scaffolds have the ability to modify the outcome of the wound healing response from a process of scar tissue formation to one of constructive tissue remodeling, a term that implies the deposition of newly formed, site appropriate, functional tissue.

Depending on a number of factors including the efficacy of decellularization, the use of chemical crosslinking agents, and the age of the source tissue from which ECM scaffolds are harvested, the host response to implanted ECM-derived biomaterials may vary from unacceptable to excellent[25]. Multiple studies have shown that constructive tissue remodeling consistently occurs when the following conditions are met: 1) The scaffold is thoroughly decellularized[67, 231], 2) Cross linking via chemical agents is avoided[444], 3) The scaffold is free of endotoxin and bacterial contamination[109], and 4) The scaffold is placed in contact with healthy surrounding tissue[32] and subjected to appropriate physiologic mechanical loads[11].

When these conditions are met, the host response consists of an initial neutrophil infiltrate followed by a mononuclear cell response that quickly transitions from an early M1 pro-inflammatory phenotype to an M2 immunomodulatory, pro-remodeling phenotype within days of implantation[66]. As the scaffold degrades, endogenous stem/progenitor cells are recruited to the treatment site, neomatrix deposition occurs, and the remodeling process eventually culminates with the deposition of newly formed site-appropriate tissue that is at least partially functional and devoid of chronic inflammatory processes[25] (Figure 12). In contrast, the host response to an ECM-derived scaffold that has not been properly configured is characterized by a process of chronic inflammation and scar tissue formation. Known causes of such a response include the presence of immunogenic cellular debris due to poor decellularization, the use of chemical crosslinking agents that may inhibit or delay scaffold degradation and matricryptic peptide release, and lack of adequate contact with viable, vascularized, innervated tissue upon surgical placement[25].

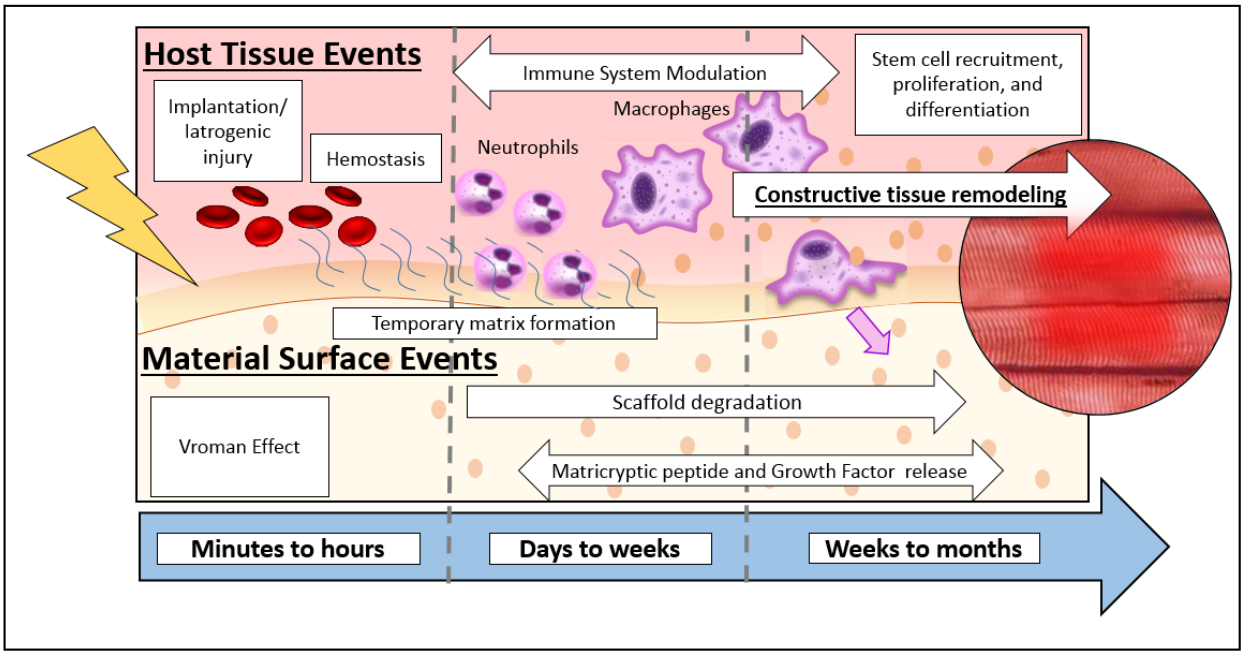

Figure 12. Overview of biomaterial-host Interaction (properly configured biologic scaffolds):

The biomaterial-host interaction is a complex process that is composed of overlapping phases that resemble the traditionally described wound healing response. Within minutes of implantation, hemostasis and the formation of temporary fibrin-rich matrix that facilitates cellular access into the scaffold occurs. When the scaffolds are properly configured, this process is quickly followed by activation of the innate immune response, composed of sequential neutrophil and macrophage infiltrates that remove pathogens, clear cellular debris, and begin the process of scaffold degradation and matricryptic peptide release. As the macrophage infiltrate transitions into the M2 proremodeling phenotype, signaling molecules produced by the innate immune system and scaffold degradation products act synergistically to recruit stem/progenitor cells from adjacent tissues and the bone marrow. This heterogeneous cell population containing immune cells and stem/progenitor cells is referred to as the constructive cell infiltrate, and is responsible for further scaffold degradation, neomatrix deposition, and ultimately constructive functional tissue remodeling.

Although the initial stages of the host response to both properly and poorly configured scaffolds are histologically indistinguishable from one another, the host response to poorly configured scaffolds quickly shows signs of a chronic inflammatory process and foreign body

reaction including the presence of multinucleate giant cells, a persistent M1-proinflammatory macrophage phenotype, and in some cases, serous effusion. The presence of these early signs invariably leads to an outcome of dense scar tissue formation.

1.4.3 Biomaterial- Host Interaction: The Innate Immune Response

As previously stated, the initial stages of the host response to implanted materials are very similar regardless of the quality and exact configuration of the material used. The host response invariably starts with activation of the innate immune system as a result of surgical trauma during implantation. Within seconds of scaffold placement, blood and plasma proteins are adsorbed to the surface of the scaffold - a process known as the Vroman effect [415]. In combination with hemostasis, the Vroman effect results in the formation of a temporary fibrin-rich matrix. This transitional matrix bridges the gap between the host tissue and the implanted material facilitating cellular access into the scaffold. Simultaneously, cellular injury and the presence of a foreign material result in the activation of the innate immune response, a phase that begins with a neutrophil infiltrate within minutes of implantation. The extent and persistence of the neutrophil response depend upon a number of variables including contamination of the surgical field, the type of scaffold used, and the exact anatomic location being treated[20, 25, 272].

As first responders neutrophils are not only important for phagocytosis of cellular debris but are also the first line of defense against invading pathogens that might be present in the surgical field[312]. In addition to phagocytosis, and perhaps more relevant to the process of biomaterial-mediated tissue repair, neutrophils have the ability to secrete digestive enzymes

including collagenases, elastases, and serine proteases[312]. These enzymes allow neutrophils to initiate the processes of scaffold degradation and tissue remodeling, an important step that facilitates angiogenesis, promotes cellular infiltration into the scaffolds, and mediates matricryptic peptide release into the treatment site. An equally important component of the neutrophil response is their ability to secrete a number of inflammatory mediators that include cytokines, chemokines, leukotrienes, and prostaglandins. This array of signaling molecules is controlled in great part by immunoregulatory cytokines such as interferon (INF)-gamma, IL-4, IL-10, and IL-13[440], allowing neutrophils to modulate both acute and chronic inflammatory processes and the process of tissue remodeling. Pro-inflammatory cytokines such as tumor necrosis factor (TNF)-α and IL-1β[363] play an important role in the recruitment of other cell types of the immune system, particularly macrophages, and thus, are necessary for the initiation of the next phases of the innate immune response[457].

The subsequent remodeling events are characterized by a mononuclear cell infiltrate that overlaps with the later stages of the neutrophil response. During this phase, macrophages quickly become the predominant cell type at the treatment site by 7 days post-implantation. The macrophage response is an important determinant of the outcome of the constructive remodeling process and is in fact necessary for a favorable outcome[66, 444]. Studies have shown that in vivo macrophage depletion after scaffold implantation inhibits the process of scaffold degradation and matricryptic peptide release, both of which are necessary steps for constructive remodeling to occur[444]. In addition to scaffold degradation, macrophages are key immunoregulatory mediators and play both positive and negative roles during wound healing and in the response to implanted materials due to their functional plasticity.

Macrophages are a heterogeneous cell population with diverse functional phenotypes ranging from M1 (classically activated, pro-inflammatory) to multiple subtypes of M2 (anti-inflammatory, immunoregulatory, remodeling). M1 pro-inflammatory macrophages can be activated by mediators such as IFN-γ and LPS, and produce traditional pro-inflammatory cytokines including IL-1β, IL-6, IL-12, IL-23 and TNF-α, among others [281]. In addition, M1 macrophages produce reactive oxygen species (ROS), can present antigens, and promote a Th1 pro-inflammatory pathway[303]. In contrast, M2 immunoregulatory macrophages are activated by signals such as IL-4, IL-13, IL-10, and matricryptic peptides released from ECM-derived scaffolds[298]. M2 macrophages show increased expression of scavenger, mannose and galactose receptors, produce ornithine, polyamines, and promote Th2 type reactions [297].

Despite their contrasting differences and heterogeneity, macrophage phenotype is highly plastic and dynamic, and ultimately determined by all factors that affect their microenvironment. In reality, macrophage phenotype exists along a spectrum between the M1 and M2 extremes - where any given cell may express or co-express different components of the M1 or M2 phenotypes, rather than as a discrete functional state with clearly defined boundaries.

In the context of ECM-derived biologic scaffolds, macrophage phenotype has been suggested to be a major determinant factor of the host response and clinical outcome [65-67]. ECM scaffold materials that promote constructive functional remodeling consistently show a higher percentage of M2 macrophages within weeks of implantation than those that promote scar tissue formation and encapsulation. These findings suggest that strategies to promote macrophage phenotype modulation toward a favorable M2 phenotype after implantation of ECM-derived scaffolds might improve clinical outcomes [66] (Figure 13).

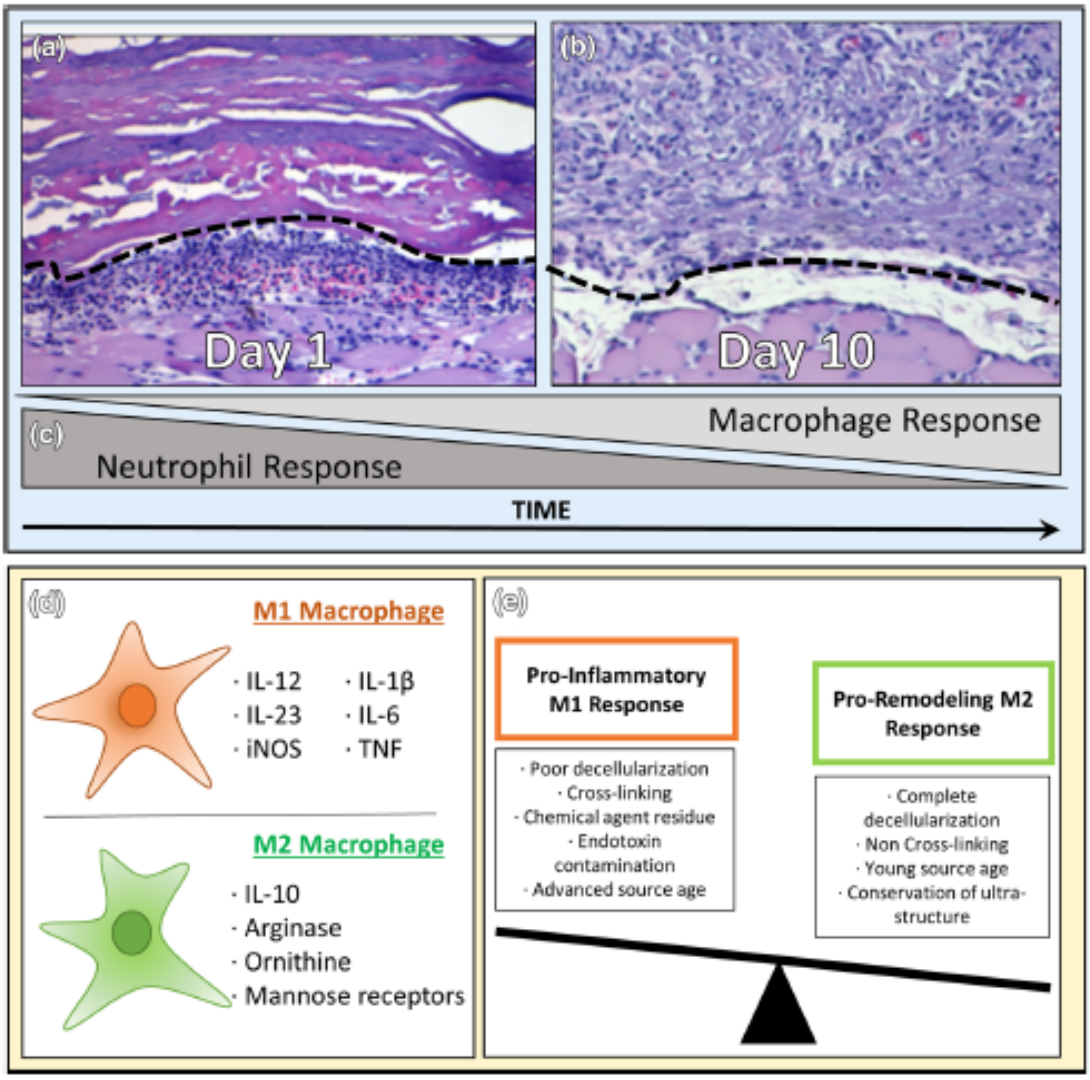

Figure 13. Innate immune response to ECM-derived scaffolds

the innate immune response to ECM-derived scaffolds is characterized by an initial neutrophil infiltrate as a result of tissue injury during the implantation process and the presence of a foreign material. (a) The neutrophil response becomes histologically apparent at the interphase between the scaffold and the native tissue as early as 1 day post implantation. (b) By day ten the constructive cell infiltrate is primarily composed of mononuclear cells that infiltrate deep into the scaffold as the material is degraded and matricryptic peptides are released. (c) By 2 weeks post implantation, the innate immune response is composed primarily of macrophages that have transitioned into the M2 pro-remodeling phenotype. However, transition into the M2 phenotype is not always observed. When scaffolds are

not properly configured, a persistent M1 pro-inflammatory occurs which results in scar tissue formation. (d) M1 macrophages are characterized by expression of CCR7 and CD86 surface cell markers among many others and the expression of pro-inflammatory signaling molecules. In contrast, M2 macrophages have been identified by CD206 surface marker expression and can contribute to the remodeling process by participating in important processes including angiogenesis, immunoregulation, and stem cell recruitment and proliferation. (e) Factors known to contribute to the M1 pro-inflammatory macrophage phenotype, and the M2-proremodeling macrophage phenotype.

1.4.4 Biomaterial- Host Interaction: Degradation of Extracellular Matrix Bioscaffolds

The process of scaffold degradation serves two purposes: 1) As the scaffold degrades it is rapidly infiltrated by host cells and eventually replaced with functional, site-appropriate tissue, and 2) Enzymatic scaffold degradation is one of the most important methods by which matricryptic peptide release occurs in vivo. Both of these steps are necessary for a constructive remodeling process to occur. Inhibition of scaffold degradation either by chemical cross-linking or by methods of in vivo macrophage depletion inhibits the remodeling process [444].

The rate of scaffold degradation varies depending on a number of factors including the source tissue from which the scaffolds are derived, the use of cross-linking agents during manufacturing, and the metabolic and physiologic demands of the treatment site. For example, dermal ECM-scaffolds are characterized by a dense and compact ultrastructure that makes them difficult to fully decellularize and prolongs the in vivo degradation process. In contrast ECM-scaffolds derived from less dense tissues such as the small intestinal submucosa can be easily decellularized and are rapidly degraded in vivo, generally by 10 weeks post-implantation. Degradation rates have been traditionally assessed via histologic examination. However, histologic identification of biologic scaffold ECM versus host tissue can be difficult, particularly

during the later stages of the remodeling process. An alternative to this approach is the use radioactively labeled ECM scaffolds that allow for tracking as they degrade in vivo. The basis of this approach is the integration of benign 14C into the collagen triple helix as a result of 14C-proline weekly injections into the source animals. Over time, all tissues become rich in 14C, and liquid scintillation counting (LSC) can be used to quantitatively measure the in vivo degradation profile of various types of ECM scaffolds derived from these animals. Using this technique, studies have shown that SIS-ECM is completely degraded by 10 weeks post implantation[162, 354], whereas in the case of dermal ECM biologic scaffolds at least 50% of the scaffold material still remains present at 24 weeks post implantation [77].

1.4.5 Biomaterial- Host Interaction: Stem Cell Recruitment

Matricryptic peptide activation and release during scaffold degradation has potent effects on macrophage polarization and stem cell behavior, both important components of the remodeling response. When generated in vitro via enzymatic degradation, matricryptic peptides have been shown to increase migration and proliferation rates of perivascular stem cells and endothelial cells [6, 358, 453], and favorably polarizing naïve macrophages (MØ) into and M2-like, pro-remodeling phenotype.

The in vivo study of matricryptic peptide release is a challenging task, as the effect observed in host tissues is confounded by multiple paracrine effector molecules. In vivo studies have shown that in addition to perivascular stem/progenitor cells originating from adjacent tissues [410], stem cells populations originating from the bone marrow can also contribute to the process of biomaterial-mediated tissue repair [317].

1.4.6 Clinical Applications

Commercially available biologic scaffolds (Table 6) vary widely in their composition and methods of manufacture. As a result, the clinical performance of these scaffolds can vary widely. Some of the clinical applications in which these scaffolds have been successfully used are summarized in (Figure 14). For example, due to their antibacterial properties [56, 378], biologic scaffolds are preferred over synthetic meshes for hernia repair when the operative field is contaminated [238]. In reconstructive surgery, acellular tissue scaffolds have been widely used for breast reconstruction[73], although side effects including increased risk of seroma formation, foreign body reactions, and scarring have been observed [438]. The use of biologic scaffolds in fields such as vascular [255] and cardiothoracic surgery [383] is becoming increasingly popular, and to a lesser degree in applications including facial [383] and esophageal repair[27, 315], among others.

The process of biomaterial-mediated tissue repair is inherently different from true tissue regeneration. However, when appropriately manufactured, an implanted biologic scaffold can lead to constructive tissue remodeling and significant clinical success. The performance of biologic scaffold-based therapies is dependent upon a variety factors that ultimately affect the wound healing response. Although the set of criteria that have been historically identified to describe the ideal biomaterial focus upon the physical characteristics of the material (e.g., uniaxial or multidirectional strength, surface topology, suture retention strength, and compliance), the primary determinant of success of an implanted biomaterial is the host response to the material over time. The ability to understand and control the factors that play a role in modulating the host response will guide the design of the next generation biomaterials.

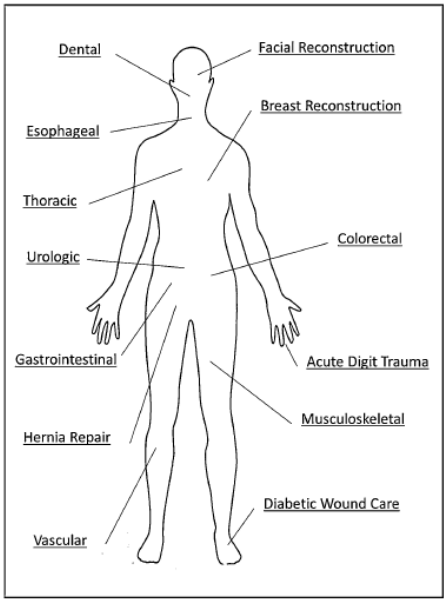

Clinical Application	Report	Scaffold used	Result
Breast Repair	Butterfield, JL. Plast Reconstr Surg. 2013 May;131(5):940-51	Human dermis Vs. fetal bovine dermis	**440 patients:** No significant differences in complication rates between the two scaffolds
Dental	Gholami et al. Dental Res J. 2013 Jul;10(4):506-13	Human dermis	**16 patients**: This scaffold can be considered as a substitute for palatal donor tissue for root coverage procedures in class I or II gingival recessions treated
Diabetic Ulcers	Lecheminant et al. J Wound Care. 2012 Oct;21(10):476, 478-80, 482.	Urinary bladder	**34 patients:** All patients treated with UBM progressed to full healing
Esophagus	Badylak et al. Tissue Eng Part A. 2011 Jun;17(11-12):1643-50	Small intestinal submucosa	**5 patients:** Restoration of normal mature, esophageal epithelium and return to a normal diet without significant dysphagia is reported for all patients
Facial	Leventhal et al. Laryngoscope. 2008 Jan;118(1):20-3	Small intestinal submucosa	**6 patients:** Static facial suspension with the scaffold improved cosmesis and function. One patient was displeased with the esthetic outcome and required a revision procedure
Skeletal Muscle	Sciari et al. Sci Transl Med. 2014 Apr 30;6(234):234ra58	Urinary bladder	**5 patients**. Scaffold implantation was associated with perivascular stem cell mobilization and accumulation within the site of injury, and de novo formation of skeletal muscle cells
Urologic	Alpert et al. J Urol. 2005 Oct;174(4 Pt 2):1687-89	Small intestinal submucosa	**2 patients:** Preliminary results of small intestinal submucosa coverage are encouraging and the scaffold will continue to be evaluated
Ventral Hernia	Kissane et al. Plast Reconstr Surg. 2012 Nov;130:194S-202S	Various	**635 patients:** Use of biologic scaffolds in contaminated fields has allowed for a one-stage repair with no or little subsequent removal. Ventral incisional hernia repair still presents high recurrence rate and complications.
Vascular	Ladowski et al. Ann Vasc Surg. 2011 Jul;25(5):646-50	Bovine pericardium	**845 patients**: The use of bovine pericardium for patch closure in carotid endarterectomy yields excellent freedom from residual or recurrent postoperative stenosis
Colorectal	Cintron et al. Tech Coloproctol. 2013 Apr;17(2):187-91	Small intestinal submucosa	**73 patients:** Use of AFP for treatment of fistula-in-ano is safe and modestly effective in reasonable long-term (15 months) follow-up
Thoracic	Scholl et al. World J Pediatr Congenit Heart Surg. 2010 Apr;1(1):132-6	Small intestinal submucosa	**40 patients:** Repair of congenital heart defects using SIS-ECM is feasible and safe

Figure 14. Clinical applications of ECM-derived scaffolds

To date, ECM-derived biologic scaffolds have been used in multiple clinical applications with various degrees of success. For example, a number of multi-center clinical studies of ventral hernia repair have shown superior performance of ECM-derived biomaterials when applied to contaminated fields. In esophageal repair after mucosal resection in the setting of superficial non-invasive neoplastic disease, ECM-derived biomaterials have proven to be a viable alternative to radical esophagectomy. The use of ECM-derived biomaterials in applications such as neural tissue repair is still in very early stages and as a result, clinical studies have not yet been initiated.

1.5 REGENERATIVE MEDICINE APPROACHES FOR ESOPHAGEAL REPAIR

1.5.1 The Human Esophagus

The human esophagus is a tubular organ that extends from the epiglottis in the pharynx to the stomach. Structurally, it is composed of four concentric layers: the mucosa, the submucosa, the muscularis externa, and the adventitia [414]. The mucosa lines the lumen of the esophagus and is composed of a stratified squamous epithelium that serves as a protective layer for the deeper layers of the esophagus during deglutition. The submucosa consists of vascular, connective, and glandular tissues that provide mucous secretions to facilitate the passage of food. The muscularis externa is composed of two distinct muscular layers organized in circumferential and longitudinal directions that function in tandem to generate esophageal peristalsis. The muscularis externa transitions from skeletal muscle in the proximal end of the esophagus, to smooth muscle in the distal two thirds of the esophagus. The skeletal muscle portion of the esophagus is innervated by lower motor neurons that course through the vagus nerve and allow voluntary initiation of the deglutition process. The distal two thirds of the esophageal muscularis externa is composed of smooth muscle and is innervated by fibers originating from the sympathetic trunk and the vagus nerve. Once the deglutition process is voluntarily initiated, esophageal peristalsis is mediated by the sympathetic and parasympathetic innervation via a series of well-orchestrated muscle contractions, including opening and closing of the lower esophageal sphincter, that allow the process of food intake to occur[3, 205] (Figure 15).

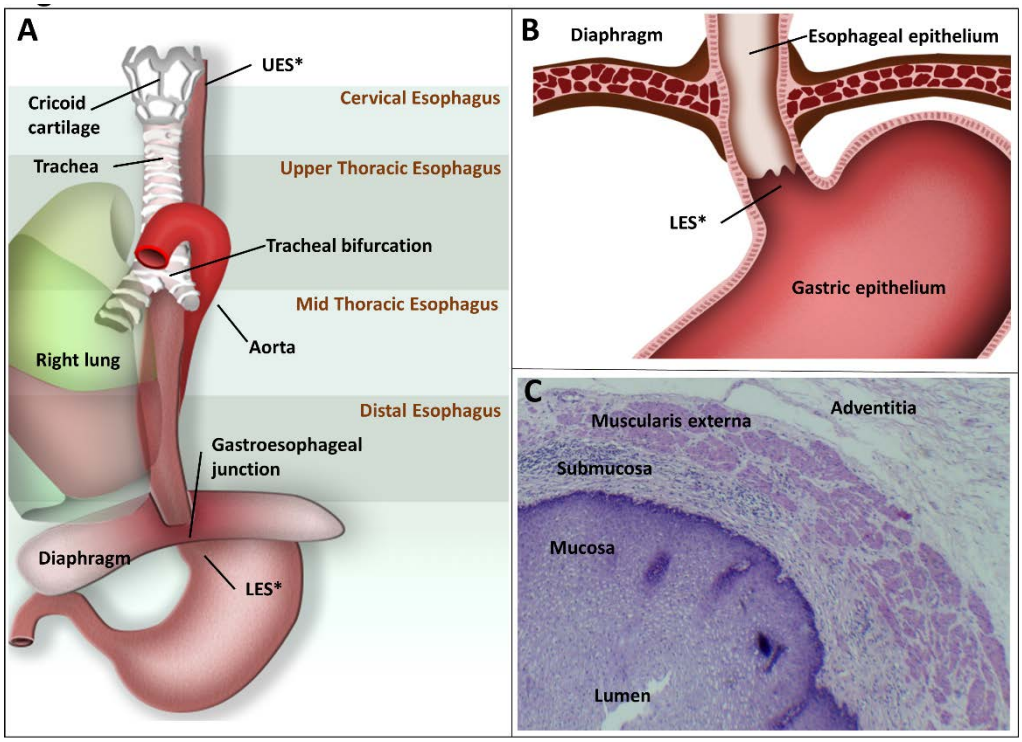

Figure 15. The Human Esophagus

(A) The majority of the esophagus resides in the mediastinum anteriorly to the vertebral column and the descending aorta and posteriorly to the trachea, lungs, and heart. The esophagus has three natural narrowings: at the cricoid cartilage, at the tracheal bifurcation, and as it passes through the diaphragm. (B) The esophagus and the stomach are separated by the gastroesophageal sphincter. While the esophagus is lined by a stratified squamous epithelium, the stomach is lined by a columnar epithelium. (C) The esophagus comprises four concentric layers: starting from the lumen, the mucosa (stratified squamous epithelium), submucosa (glands and connective tissue), muscularis externa (two layers: circumferential and longitudinal), and adventitia (connective tissue). UES, upper esophageal sphincter; LES, lower esophageal sphincter.

1.5.2 Need for Esophageal Repair

Pathologies that involve the structure and/or function of the esophagus are often life threatening. While damage to the mucosa can result in scar tissue formation and clinical stricture, damage to the muscularis externa, or injury to the innervation of the esophagus or lower esophageal

sphincter can compromise peristalsis and result in achalasia [323]. Damage to the lower esophageal sphincter itself can result in gastroesophageal reflux disease (GERD), a condition that can lead to Barrett's esophagus and progress to adenocarcinoma [454]. Trauma, iatrogenic injury, and congenital malformations can have a variety of adverse consequences depending on the anatomic structures that are compromised. The most common of these adverse consequences include fistula and stricture formation [209].

There is currently an unmet clinical need for effective methods of esophageal repair. The esophagus is a complex organ composed of non-redundant tissue that does not have the ability to regenerate. Currently available interventions for esophageal pathology have limited success and are typically associated with significant morbidity. An understanding of the different diseases that affect the esophagus, the anatomic and functional consequences of each pathologic process, and the shortcomings associated with currently available therapies is necessary for the development of successful strategies for esophageal repair (Table 7).

Table 7 Anatomic Involvement of Esophageal Pathologies

		Anatomic Involvement					
Condition	***Incidence***	***Mucosa***	***Submucosa***	***Muscularis***	***Proximal Esophagus***	***Distal Esophagus***	***LES****
Adenocarcinoma	52,000/year [16] (world)	Always	Upon invasion	Upon invasion	Rarely	Mostly	Mostly
Squamous cell carcinoma	398,000/year[16] (world)	Always	Upon invasion	Upon invasion	Mostly	Rarely	Rarely
Caustic injury	5000/year [237] (US)	1st degree	2nd degree	3rd degree	Possible	Possible	Possible
Congenital deformity	1 in 3000 births[112, 172, 232]	Possible	Possible	Possible	Possible	Possible	Possible
Perforations (trauma)	Very rare [102, 154, 421]	Usually	If severe	If severe	Mostly	Rare	Rare

1.5.2.1 Esophageal Cancer

The incidence of esophageal cancer has shown a recent dramatic increase in the US[130, 201] and worldwide[217]. This recent increase in esophageal cancer incidence is associated with a

change in the epidemiology of the two major types of esophageal cancer: adenocarcinoma and squamous cell carcinoma [16, 308] (Table 8). As recently as 30 years ago, squamous cell carcinoma was responsible for more than 90% of esophageal neoplasia in the United States. However, adenocarcinoma is now more prevalent in the United States and accounts for more than 80% of esophageal cancer cases[340]. Squamous cell carcinoma remains the most prevalent form of esophageal cancer in the rest of the world [100]. Despite advances in detection, diagnosis, and treatment, the 5-year survival rate for all patients diagnosed with esophageal cancer ranges from 15% to 20% [340].

Table 8. Esophageal Cancer: Comparative Characteristics of Adenocarcinoma Versus Squamous Cell Carcinoma

	Adenocarcinoma	***Squamous cell carcinoma***
Overall incidence	Increasing	Decreasing
Geography	Predominant in the U.S.	Predominant outside U.S.
Demographics	White males mostly	African American males mostly
Anatomic locations affected	Distal esophagus	Middle esophagus
Risk factors	GERD, Barrett's esophagus	Alcohol and tobacco

Adenocarcinoma

Esophageal adenocarcinoma has one of the highest rates of increased incidence among neoplastic diseases worldwide [217, 338]. Esophageal adenocarcinoma is not only the most common form of esophageal cancer in the United States, but its increase in incidence is only matched by that of obesity [343, 480] (Figure 16).

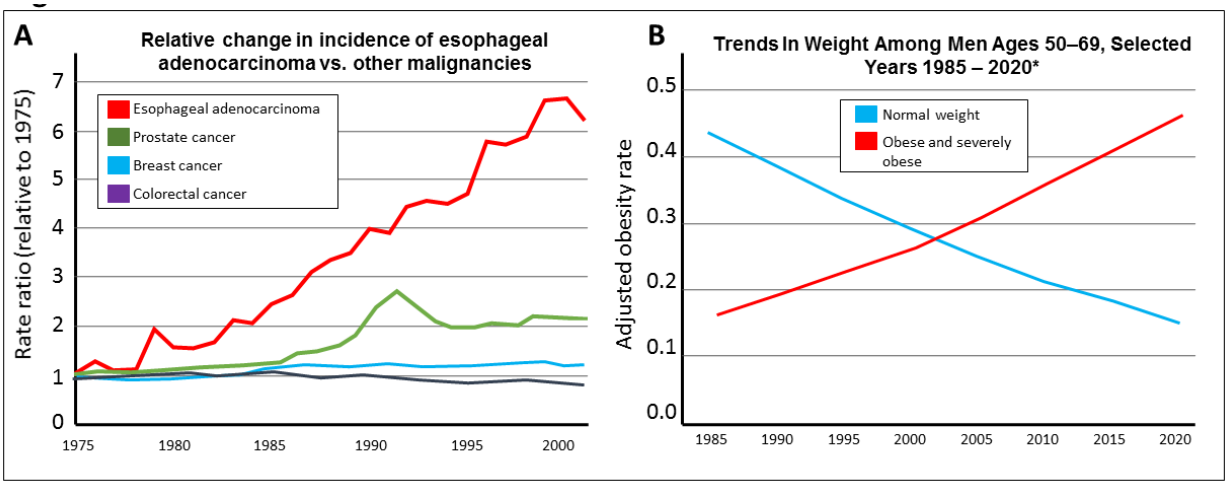

Figure 16. Increase in incidence of esophageal adenocarcinoma and obesity

(A) Esophageal adenocarcinoma has one of the highest rates of increased incidence among neoplastic diseases. (B) The increase in the incidence rate of esophageal adenocarcinoma is only matched by that observed in obesity. *Data for 2005–2020 are extrapolated. Figures adapted from Pohl and Welch 2005[343] and Sturm et al., 2004.[430]

Esophageal adenocarcinoma develops primarily in the distal portion of the esophagus including the gastroesophageal junction as a consequence of Barrett's esophagus, a pathologic process that is a downstream complication of GERD. The most common cause of GERD is lower esophageal sphincter relaxation or insufficiency, a condition that can be caused by mechanical factors such as obesity, pregnancy, or increased gastric volume and by non-mechanical factors such as central nervous system depressants and alcohol and tobacco abuse [340]. Barrett's esophagus develops in approximately 10% of patients with GERD as a result of chronic exposure to the acidic contents of the stomach [454]. Over time, the esophageal epithelium adapts to the new acidic environment by transforming from squamous epithelium to columnar epithelium through a process known as metaplasia. Barrett's esophagus is more common in white males over the age of 40 than in the rest of the population, and once it develops, 10% of those patients will further develop high grade dysplasia and adenocarcinoma[341]. Hence, the increased incidence of

esophageal adenocarcinoma is attributed in great part to obesity-related GERD and Barrett's esophagus [355, 371].

Squamous cell carcinoma

Squamous cell carcinoma is less common than adenocarcinoma in the United States and it typically occurs in patients over 45 years of age. It is four times more frequent in males than in females and it is eight times more frequent in Blacks than in Caucasians[486]. In the rest of the world, however, particularly in rural and underdeveloped areas, squamous cell carcinoma remains the most common cause of esophageal cancer[166]. As with many cancers, the main risk factors associated with squamous cell carcinoma are alcohol and tobacco use. Other factors such as poverty, caustic injury, achalasia, human papilloma virus[423], and consumption of hot beverages and mutagenic compounds (i.e. polycyclic hydrocarbons, nitrosamines) have also been associated with the disease [221].

Squamous cell carcinoma has an insidious onset that typically presents with dysphagia, odynophagia, and/or esophageal obstruction [160, 429]. Although both adenocarcinoma and squamous cell carcinoma begin as superficial lesions in the esophageal mucosa, squamous cell carcinoma tends to localize to the middle third of the thoracic esophagus. Early lesions typically begin as patchy thickenings that slowly develop into polyps or exophytic tumors that eventually obstruct the lumen of the esophagus, or as ulcerated and infiltrative lesions that progressively invade all layers of the esophagus and eventually infiltrate the surrounding organs in the mediastinum (Figure 17). Whereas invasion of the trachea, bronchi, or lungs can lead to pneumonia usually resulting in detection of the disease, invasion of the aorta and pericardium can lead to catastrophic exsanguination [328].

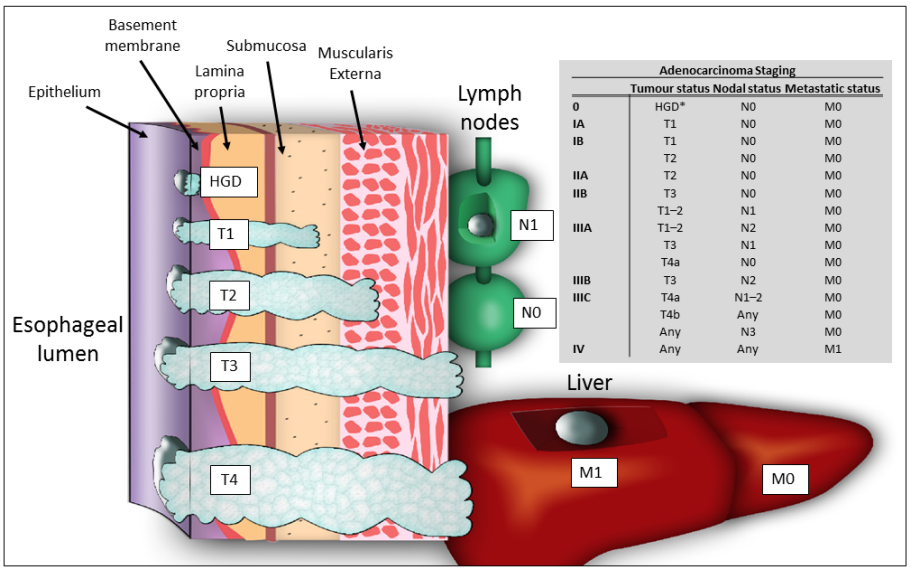

Figure 17. Esophageal Cancer Staging

The TNM (tumor, node, and metastasis) staging system takes into consideration a number of variables, including tumor invasion (T), the presence or absence of metastatic disease (M), and nodal invasion (N). Tumor staging will determine the clinical approach to the disease. Staging for adenocarcinoma of the esophagus is shown as an example. HGD, high-grade dysplasia. Figure adapted from Pennathur et al.[340]

Standard of care

Although recent improvements in screening, staging, surgical technique, adjuvant therapy, and patient selection have reduced morbidity and prolonged postoperative survival[53, 300, 304], significant controversy remains over the optimal management of esophageal carcinoma [38, 302].

As with many neoplastic processes, the primary objective following detection is surgical removal of the neoplastic tissue with or without adjuvant therapy. In the case of advanced disease, an esophagectomy followed by gastric pull up into the mediastinum and anastomosis of the gastric cardia and the proximal esophagus remains the only viable alternative [181].

However, this procedure is associated with high morbidity, decreased quality of life, and high mortality rates [251, 402, 481].

A number of novel alternatives for the treatment of non-invasive early stage disease are under investigation to ultimately replace the traditional watchful wait approach that inevitably leads to esophagectomy. Minimally invasive endoscopic ablation techniques for the treatment of Barrett's esophagus with high grade dysplasia and superficial carcinoma are among the most studied approaches. Radiofrequency ablation is now an accepted treatment for flat Barrett's esophagus. This technique offers significantly lower rates of stricture formation than other ablative techniques [233]. In cases where nodularity exists, endomucosal resection with or without ablation has been shown to be an effective treatment that prevents recurrence [400]. These procedures have shown improved survival rates and quality of life [125, 289]. However, the development of metachronous lesions after these procedures remains a common finding (21.5%). Risk factors for the development of metachronous lesions include piecemeal resection, no ablation therapy following endomucosal resection, multifocal neoplasia, and long segment Barrett's esophagus [476]. Stepwise radical endoscopic resection (SRER), a technique being investigated for the treatment of recurrent Barrett's esophagus after radiofrequency ablation or endomucosal resection, has shown to be effective, although it usually requires a large number of therapeutic sessions and complications such as esophageal stenosis require dilation in 50% of cases [403].

In summary, limitations associated with these techniques include the requirement for numerous interventions, incidence of metachronous lesions, absence of a suitable tissue specimen for histologic assessment, and the unavoidable sampling error that occurs in patients

with long segment disease [275]. Furthermore, even with successful treatment there is need for repeated postsurgical dilation in more than 50% of cases [329, 403].

1.5.2.2 Congenital Abnormalities

Every year, 1 in 3000 births presents with esophageal pathology **(Table 7)**. Congenital abnormalities can compromise all layers of the esophagus and include esophageal atresia, tracheo-esophageal fistulas, and esophageal agenesis **(Figure 18)**. Without exception, these defects are incompatible with life.

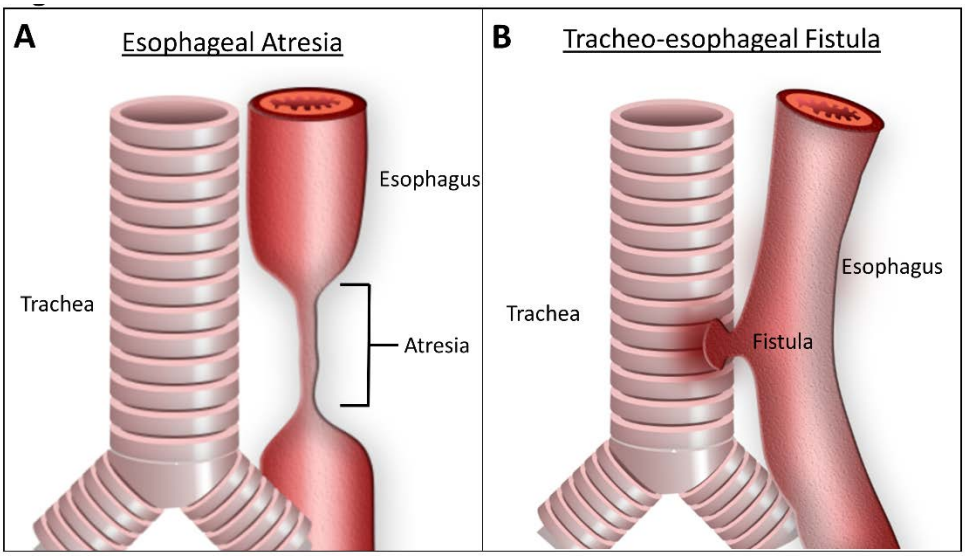

Figure 18. Esophageal Congenital Abnormalities

The most common congenital abnormalities of the esophagus include (A) esophageal atresia and (B) tracheoesophageal fistula. These conditions result in mechanical obstruction of the esophagus and are incompatible with life. Detection occurs shortly after birth

Esophageal atresia is characterized by the replacement of a portion of the esophagus with a non-patent esophageal segment that results in mechanical obstruction. This segment of the esophagus is typically present at or near the carina of the trachea and usually associated with a

fistula connecting either the upper or lower fully developed esophageal segments to the trachea [111]. Agenesis of the esophagus is a very rare condition [74, 399].

The survival rate for patients with esophageal atresia has been approximately 95% in the last ten years [114, 369]. Depending on the specific underlying pathology, congenital abnormalities may be surgically addressed with synthetic prosthetics, flaps, or grafts. One of the major issues with congenital abnormalities is that pediatric patient outgrow prosthetic devices such as stents, and as result often require further intervention.

1.5.2.3 Esophageal Injury

Despite decades of clinical experience, most perforations of the esophagus are iatrogenic and occur during endoscopy. The esophagus is a highly vascularized organ, particularly in the gastro-esophageal junction. Hence, mortality from esophageal perforations is close to 20% [92]. Other important causes of esophageal injury include Mallory Weiss tear, ingestion of foreign body, and acute trauma.

1.5.3 The Esophagus and Regenerative Medicine

The ultimate goal of regenerative medicine is the functional restoration of lost or damaged tissues. To date, strategies for functional tissue repair have included delivery of bioactive molecules, cell-based therapies, biomaterials-based therapies, and combinations thereof [46, 227, 234]. The delivery of these technologies and their effect upon host tissues have been investigated in various anatomic locations and have shown different degrees of success. This section focuses on progress made in the field of regenerative medicine with respect to strategies for esophageal repair, from benchtop to bedside.

In vitro studies and preclinical animal studies are necessary steps toward the development of novel strategies for tissue repair. Well-designed experiments permit the isolation of test variables and the establishment of necessary parameters for optimal pre-clinical study design. In the field of regenerative medicine, important aspects of preliminary studies include the cellular composition and architecture of target tissues and organs, the mechanical properties of biomaterials and scaffolds, the assessment of cytotoxicity and cytocompatibility of new technologies, and the biochemical properties of novel constructs. Pre-clinical studies permit the evaluation of new technologies in-situ including the different components of the host response such as the type and magnitude of the immune response, and important cellular processes such as stem cell migration, proliferation and differentiation. Scar tissue formation, resistance to infection, angiogenesis, and functional tissue remodeling are important processes that are also evaluated during the pre-clinical stage.

1.5.3.1 Esophageal architecture and stem cell populations

Several differences across multiple species have been identified in the microarchitecture of the esophagus including the presence of a keratinized epithelium in mice, rats, pigs, and domesticated animals [188, 294, 353], and a different distribution of striated versus smooth muscle within the muscularis externa. While striated muscle is only present in the proximal one third of the human esophagus, striated muscle can be found in virtually the entire length of the esophagus in other mammalian species. This configuration allows these species to voluntarily regurgitate gastric contents to chew cud and/or to feed the young[427]. The differences in the cellular composition and tissue architecture of the esophagus among different species should be

taken into consideration when choosing an animal model for preclinical study design and when interpreting the results from these studies.

Several groups have further characterized the esophageal epithelium as a high turnover tissue comprised of two layers: a basal layer composed of a single sheet of cells in direct contact with the basement membrane that have self-renewal capacity, and a supra-basal layer that contains progressively more differentiated cell populations and lines the lumen of the esophagus[293]. The basal layer is composed of two distinct zones: the papillary basal layer (PBL) which extends along papillae that invaginate the epithelium, and the interpapillary basal layer (IBL) which is located at the flat interface between papillae [158] (Figure 5a). The IBL cells constitute the stem cell compartment of the esophageal epithelium and proliferate infrequently and asymmetrically [391, 392]. Recent studies in the mouse esophagus have identified these cells to be Itgb4High, CD73+ and having the greatest stem cell potential, whereas CD73- transit-amplifying cells show variation in their degree of maturation. Esophageal stem cells have been used in vitro to show three-dimensional organoid forming capacity (Figure 5b-e) and the participation of Sox2, Wnt, and bone morphogenetic protein signaling pathways in the process of esophageal epithelium self-renewal [115].

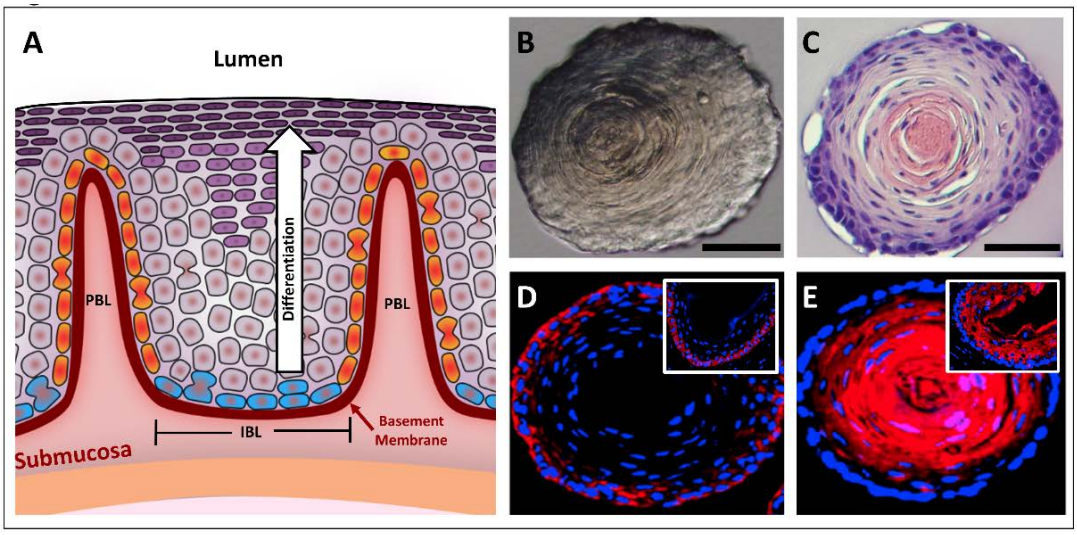

Figure 19. The Esophageal Epithelium

(A) The architecture of the esophageal epithelium includes papillary structures located at regular intervals (PBL) separated by flat interpapillary zones (IBL). The basal cells comprise a heterogeneous population of epithelial cells with cells located in the IBL constituting the stem cell compartment (blue) and transit-amplifying cells residing in the PBL (orange). Epibasal layers (purple) are undergoing differentiation and can no longer divide. The arrow indicates the direction of differentiation. (B) When isolated and cultured, esophageal stem cells have shown organoidforming capacity114 and show similar organization to native tissues through (C) hematoxylin and eosin staining and (D) Cytokeratin 14 and (E) Cytokeratin 13 stains. Native tissue shown in inset for comparison (D, E).

1.5.3.2 Biomaterials for Esophageal Repair

The ideal biomaterial for esophageal repair remains to be determined and it is unlikely that a one size fits all approach will be optimal. A number of synthetic and biologic materials have been proposed for esophageal repair (Table 8). While synthetic scaffolds can be manufactured with precision and their mechanical properties can be fine-tuned for specific applications, these materials tend to cause a well characterized foreign body reaction[13]. In contrast, biologic materials are subject to natural variability and have less tunable properties, but tend to produce a

friendlier host response and promote constructive tissue remodeling, a term that implies the deposition of site-specific, functional tissue[271].

Biologic scaffolds composed of acellular esophageal tissue have been proposed by a number of groups. Work by Bhrany et al. [47] presented an SDS-based method for decellularization of murine esophagi. The resulting scaffold showed ECM protein preservation, the ability to support esophageal cell proliferation in vitro, and neovascularization with minimal inflammation after subcutaneous implantation. Although studies have shown that constructive tissue remodeling consistently occurs when chemical crosslinking of biologic scaffolds is avoided, the same group crosslinked the developed acellular matrix in additional studies with the intent of reducing antigenicity and improving collagen stability to prolong in vivo durability. As expected, results showed increased stability in crosslinked scaffolds, and while minimal inflammatory response was also reported upon in vivo implantation, inflammation was assessed only by quantification of macrophages and multinucleate giant cells at the treatment site, and did not take into consideration macrophage phenotype. Interestingly, while genipin-crosslinked scaffolds supported esophageal epithelial adhesion and proliferation in this study, glutaraldehyde-crosslinked scaffolds did not support epithelial cell adherence or proliferation [48]. Inhibition of biologic scaffold degradation has been shown to prevent matricryptic peptide release and inhibit constructive scaffold remodeling in other studies. [271, 444]

Recognizing the potential benefits of using biologic scaffolds derived from homologous tissues in regenerative medicine applications, a protocol for the decellularization of the porcine esophageal mucosa was developed for the treatment of noninvasive disease by Keane et al.[230]. The protocol developed in this study avoids the use of SDS and other harsh decellularization agents and is compliant with previously established criteria for decellularization [231, 271]. The

resulting scaffold maintained important proteins and ultrastructure consistent with the basement membrane complex including laminin, collagen IV, and fibronectin. Perivascular stem cells remained viable when seeded upon the porcine esophageal ECM scaffold in-vitro, and the in-vivo host response showed an increased number of M2 pro-remodeling macrophages and an associated pattern of constructive remodeling when used to repair striated muscle defects in rats.

Table 9. Biomaterials for Esophageal Repair

Biomaterial	Summary of Results	Reference
Synthetics		
poly(L-lactide-co-caprolactone)	Fibronectin grafted on PLLC scaffold greatly promotes epithelium regeneration	Zhu, 2007 (130)
Poly(3-hydroxybutyrate-co-3-hydroxyvalerate)-based nanofibrous scaffolds (PHBV)	Human esophageal epithelial cells seeded on PHBV present higher proliferation than those seeded in PHBV-gelatin after 7 days of culture	Kuppan, 2014 (63)
Polyvinylidene (PVDF) and absorbable Vicryl surgical meshes	Mucosal regeneration after 3 month. Vicryl treatment group showed leakage	Lynen Jansen, 2004 (70)
poly-ε-caprolactone	Ingrowth of epithelial and smooth muscle cells was observed one month post operatively	Diemer, 2014 (32)
Biologics		
Small intestine submucosa ECM (SIS)	Used in different defect models with different degrees of success	Lopes, 2006 (68) Badylak, 2000 Badylak, 2001
Urinary bladder ECM (UBM)	Used in different defect models with different degrees of success	Badylak, 2000 Badylak, 2005 Nieponice, 2006 Nieponice, 2009 Nieponice, 2013
Esopahgeal ECM	SDS-based decellularization protcol. Supports esophageal cell proliferation *in vitro*and neovascularization upon subcutaneous implantation	Bhrany, 2006 (13)
Gastric ECM	No stenosis or dilatation. Regeneration of keratinized stratified squamous epithelium only, not other layers.	Urita, 2007 (116)
Crosslinked esophageal ECM	Increased stability in genipin-crosslinked vs non-crosslinked scaffolds. Glutaraldehyde crosslinking was detrimental.	Bhrany, 2008 (14)
Esophageal mucosa ECM	Protocl avoids SDS, and is compliant with decellularization criteria. Host response showed increased numbers of M2 macrophages when implanted in striated muscle defects.	Keane, 2013 (54)
Acellular dermal matrix	Superior epithelial organization and stratification compared to synthetic scaffolds.	Beckstead, 2005 (11)
Hybrids		
Collagen-coated Vicryl tubes	Mediastinitis within days of implantation, stenosis and granulation tissue formation	Purushotham, 1991 (94)
Collagen-modified PLGA	Collagen-modified PLGA increases the proliferation of the ESMCs and promotes extended morphology	Zhu, 2005 (129)
Colalgen-coated silicone stents	Segemental defects showed stricture formation and inability to swallow when the stent was removed at 2-3 weeks. When removed at 4 weeks no stricture was observed	Natsume,1993 (80) and Takimoto, 1998 (115)
Complete decellularized esophagus with allogeneic mesenchymal stromal cells	All animals survive the 14-day study period, with patent and functional grafts. Explanted grafts show regeneration of all the major cell and tissue components	Sjöqvist, 2014

Commercially available biologic scaffold materials such as AlloDerm have been evaluated for use in esophageal repair. In a study by Beckstead et al. [41], rat esophageal epithelial cells were isolated and characterized for epithelial identity, adhesion protein preference, and in vitro interaction with both AlloDerm and synthetic scaffolds. Various factors including calcium concentration, scaffold composition, and pore size were evaluated by measuring their influence on epithelial growth and differentiation. Results from this study showed superior epithelial organization and stratification on AlloDerm compared to synthetic scaffolds such as poly(lactic-co-glycolic acid) (PLGA), poly-L-lactic acid (PLLA), and polycaprolactone (PCL)/PLLA. The authors concluded that modification of the synthetic scaffold's surface properties and pore size may be necessary to improve cell behavior in these constructs.

Studies of esophageal epithelial cells have also been performed with other materials including fibronectin grafted poly(L-lactide-co-caprolactone)[489] and Poly(3-hydroxybutyrate-co-3-hydroxyvalerate)-based nanofibrous scaffolds (PHBV) [254]. These studies showed that human esophageal epithelial cells seeded on PHBV present higher proliferation than those seeded in PHBV-gelatin after 7 days of culture. Cells seeded on both scaffolds present epithelial cobblestone morphology after 3 days of culture. However, extracellular matrix proteins including collagen type IV and laminin, and expression of phenotypic markers including cytokeratin-4 and 14 were significantly higher in cells cultured in PHBV-gelatin scaffolds than in cells cultured in PHBV scaffolds without gelatin.

Zhu et. al.[488] studied the effect of covalent immobilization of collagen onto poly(DL-lactideco-glycolide) (PLGA) surfaces on cell behavior by seeding porcine esophageal smooth

muscle cells (ESMC) on collagen-PLGA vs. unmodified PLGA and tissue culture plastic. The authors found that collagen-modified PLGA increases the proliferation of the ESMCs and promotes extended morphology.

The unifying findings of these in-vitro studies is that although a number of materials have been found to be cytocompatible, naturally occurring biomolecules provide superior substrate properties for esophageal cells compared to synthetic materials.

1.5.3.3 Animal models for esophageal repair

A number of animal models are available for the study of regenerative medicine strategies for esophageal repair (Table 10). The use of small animal models - particularly murine species, offers a number of advantages including cost efficiency, the ability to adequately statistically power studies, the availability of genetic modification tools that facilitate mechanistic studies, and the possibility to evaluate multiple innate physiologic variables that cannot be mimicked in-vitro. However, small animal models are technically challenging and a great degree of expertise is required to perform surgical procedures in the murine esophagus. Large animal models, on the other hand, are technically easier to implement and permit the evaluation of technologies at their intended therapeutic physical dimensions. As a result, large animal models are a valuable tool for the optimization of surgical approaches and evaluation of feasibility and delivery of these technologies. However, large animal models are expensive and genetic modification tools are usually not available to the same degree as they are in small animal models.

Esophageal mucosal resection models have been described in the dog [32, 318], pig [135, 339, 384, 464], and in rodents (Figure 20)[317]. These models are particularly important for modeling the treatment of non-invasive neoplastic disease, as a mucosectomy alone can

oftentimes entirely remove early stage neoplastic tissue without compromising the remaining layers of the esophagus. Caustic esophageal burn models [179, 278] also study pathology localized to the mucosa and focus on integrity of the epithelium. Injury or removal of the esophageal mucosa invariably leads to stricture formation, and as a result, regenerative medicine strategies aimed towards mucosal regeneration usually focus on stricture prevention as one of the primary objectives.

Table 10 Animal Models for Esophageal Repair

Animal models for esophageal repair			
Model	*Application*	*Species*	*References*
Mucosal resection	Noninvasive neoplastic disease, superficial trauma	Dog	126
		Pig	129,130
		Mouse	132
Mucosal damage	Caustic injury	Rat	133
Full-thickness defect	Esophagectomy, congenital disease, trauma	Pig	126
		Dog	136
		Rat	137
Anastomosis reinforcement	Anastomosis reinforcement after segmental resection	Dog	127

Full thickness defects including part or the full circumference of the esophagus have been described in the pig[220], dog[23], and rat[413]. Full thickness defect models permit the investigation of treatment options for invasive neoplastic disease, congenital abnormalities involving all layers of the esophagus (e.g.. tracheoesophageal fistulas), and acute trauma. In addition to full thickness defects, anastomosis reinforcement is an important aspect of esophageal repair in these scenarios, particularly after esophagectomy. Anastomosis

reinforcement models focus on leaks and dehiscence, and have been described at different anatomic locations in the esophagus in the dog[316].

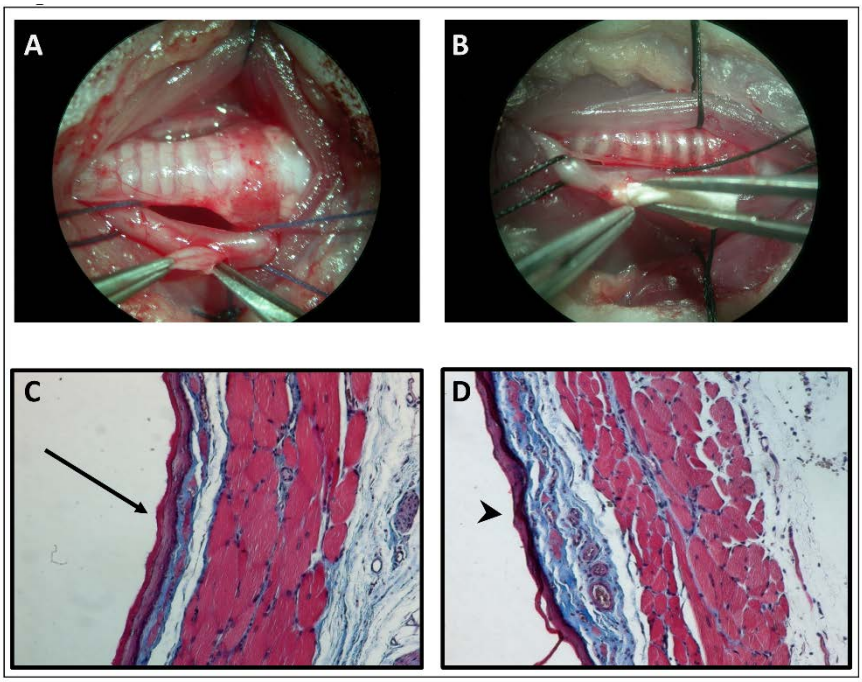

Figure 20. Esophageal Mucosal Resection in the Rat Model

(A) Mucosal resection in the rat is performed by exposing the esophagus around the trachea and performing a mucosectomy through a horizontal incision in the muscularis layer of the esophagus. (B) Once the mucosa is removed, an extracellular matrix (ECM)-derived biomaterial is delivered in situ to facilitate constructive tissue remodeling. (C) Masson's trichrome stain of native esophageal mucosa (arrow) and (D) remodeled esophageal mucosa after biomaterial-mediated repair showing intact keratinized epithelium (arrowhead).

The Levrat procedure is a well-established model involving an esophagojejunostomy, a procedure that produces retrograde flow of gastrointestinal contents into the distal part of the esophagus resulting in Barrett's esophagus and eventually progressing to esophageal adenocarcinoma[71, 90, 247, 268, 299] (Figure 21). The Levrat procedure will be a valuable tool in the study of regenerative medicine strategies for esophageal repair after neoplastic tissue resection with or without adjuvant radiation therapy and chemotherapy.

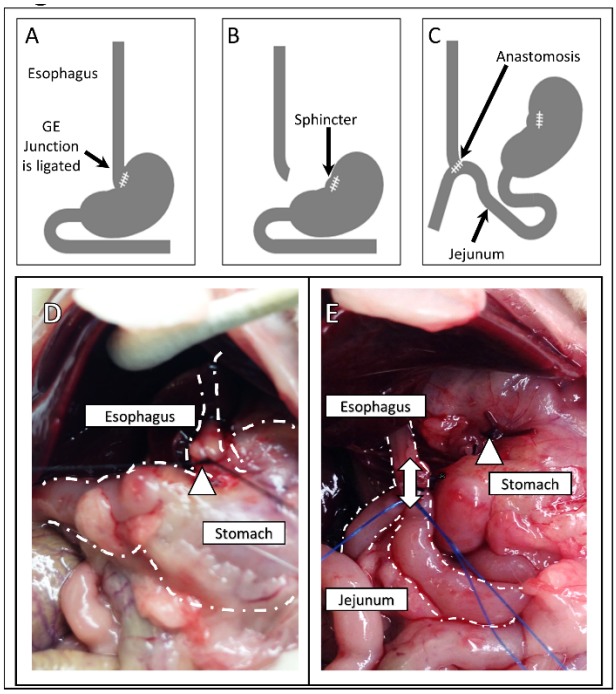

Figure 21. Levrat Model

(A, B) An esophagoduodenal anastomosis is performed by ligating the gastroesophageal junction and (C) anastomosing the distal end of the esophagus to the jejunum, creating a patent conduit that induces gastroduodenojejunal reflux. (D, E) The gastroesophageal sphincter is ligated and remains attached to the stomach (arrow head). The anastomosis between the distal end of the esophagus and the jejunum forms a patent conduit that allows free retrograde flow (double arrow).

1.5.3.4 Pre-clinical Studies

Molecular Therapies

Molecular therapies focus on the delivery of bioactive molecules that aim to modify one or several steps of the wound healing response. Poly(adenosine diphosphate-ribose) polymerase affects the repair of DNA in damaged cells, but its activation can lead to ATP depletion and death in damaged cells[84]. With this in mind, Guven et al. [179] evaluated 3-amino benzamide,

a poly(adenosine diphosphate-ribose) polymerase inhibitor, in the context of caustic esophageal burn and the prevention of stricture-formation in rats. This group reported a decreased stenosis index and histopathologic damage in the treatment group and concluded that 3-amino benzamide has a preventive effect in the scarring of the esophagus and decreases tissue damage by increasing antioxidant enzyme activity.

Growth factors are among the most commonly investigated molecular therapies for tissue repair. In the context of esophageal disease, the effect of basic fibroblast growth factor (bFGF) on vascularization was evaluated in the canine esophagus. In this study, Hori et al. [204] compared an acellular collagen in sponge and gel formats supplemented with bFGF. The scaffolds were implanted in the cervical esophagus and evaluated one month after implantation. Histologic analysis confirmed the presence of blood vessels in significantly higher number in the bFGF-containing collagen gel group compared to the bFGF (-) control group. However, in the collagen sponge groups, no difference was observed between the bFGF (+) group and the bFGF (-) group. This study highlights the fact that structure, in addition to composition, is an important determinant of the host response to implanted biomaterials.

Synthetically-Derived Biomaterials

A number of synthetic materials have been used in preclinical studies for esophageal repair with limited success. In a study by Lynen Jansen et al. [279] ,non-absorbable polyvinylidene (PVDF) and absorbable Vicryl surgical meshes were used to repair 1cm by 2cm semi-circular defects in the rabbit and resulted in mucosal regeneration after 3 months without stricture and initial muscular regeneration in the PVDF group. However, three patch failures with consecutive anastomotic leakage were reported in the Vicryl treatment group.

In a similar study performed in the rabbit by replacing smaller, 0.6cm by 1cm windows, in the abdominal esophagus with poly-ε-caprolactone, ingrowth of epithelial and smooth muscle cells was observed one month post operatively with an almost completely degraded mesh. However, the study had a 75% survival rate, and more than half of the surviving animals developed pseudo-diverticula[117].

The use of hybrid constructs that seek to combine the biomechanical properties of a synthetic material with the biocompatible properties of a biologic material, typically as a coating agent, is becoming increasingly popular in regenerative medicine[136, 465, 469]. This type of construct has been investigated in esophageal repair. Purushotham et al. [349], investigated the replacement of complete esophageal segments in the thoracic esophagus with collagen-coated Vicryl tubes. Preliminary experiments resulted in mediastinitis within days of implantation due to prosthetic leakage secondary to acid reflux and digestion of the construct. The complication was addressed thereafter by crosslinking the constructs with glutaraledehyde, which increased the resistance of the material. The animals, however, developed stenosis at a mean of 11 days post-operatively and considerable granulation tissue and scar formation was found histologically. In addition to coating Vicryl tubes, collagen has been used to coat silicone stents by Natsume et al., and Takimoto et al. [311, 433] In these studies, this group reports the use of collagen-coated silicone tubes to replace 5 cm esophageal segmental defects in dogs followed by endoscopic removal of the inner silicone stent at weekly intervals from 2 to 4 weeks. Results showed stricture formation and inability to swallow when the stent was removed at 2-3 weeks. In the dogs in which the stent was removed at the 4 week time point, a regenerated esophagus with stratified flattened epithelia, striated muscle, and esophageal glands was observed.

In summary, a variety of synthetic materials have been used to attempt to repair esophageal defects with different degrees of success. However, due to the synthetic nature of the materials, recurrent problems include stricture formation, inflammation, foreign body reaction, and leakage.

Biologically-Derived Biomaterials

The advantage of using biologically derived biomaterials for esophageal repair is based on the premise that unlike synthetically derived materials, biologic scaffolds composed of extracellular matrix have the ability to promote constructive tissue remodeling [25, 24]. The mechanisms of in vivo tissue remodeling upon biologic scaffold implantation are reviewed elsewhere[271]. Briefly, appropriately configured biologic scaffolds have the ability to modulate different phases of the wound healing response and induce a shift from a process of inflammation and scar tissue formation to one of constructive tissue remodeling and functional tissue repair.

The factors that facilitate this process during the biomaterial-host interaction are complex and involve both host-related factors (i.e. age, immunocompetence, native stem cell populations, and overall health state of the patient), and biomaterial-related factors (i.e. source and composition[106, 230, 456, 468], efficacy of the decellularization process [67, 231], post-processing modifications such as crosslinking and solubilization [113, 218, 292, 394, 411, 444, 467], source animal age[409],and surface topography [37, 63]).

Biologic scaffolds have been used in multiple large animal models to study the feasibility of biomaterial-mediated esophageal repair. Initial studies by Badylak et.al., [23] utilized porcine-derived acellular small intestinal submucosa (SIS) and urinary bladder matrix (UBM) to repair patch defects in the dog model. The ability of these materials to repair defects measuring 5cm in

length and encompassing either 40% to 50% of the esophageal circumference or the entire circumference of the esophagus was shown as the xenogeneic scaffolds used to repair the patch defects were replaced by appropriately oriented skeletal muscle within 30 to 60 days and showed complete and intact squamous re-epithelialization without signs of clinical dysfunction. However, the scaffolds used to repair full circumference segmental defects showed stricture formation within 45 days of implantation.

Given the results of stricture formation when attempting a full thickness, full circumference defect repair, subsequent experiments by Badylak et. al. [32] addressed the necessity of a native (i.e., host) tissue component for adequate esophageal repair without stricture formation. In these experiments esophageal defects encompassing different portions of the esophageal circumference were repaired with UBM-ECM. Treatment groups included full circumference, full thickness defects; full circumference mucosal resections; and full thickness defects with 30% intact muscularis externa. This study concluded that UBM-ECM scaffolds plus autologous muscle tissue, but not UBM-ECM scaffolds alone or muscle tissue alone, can promote constructive tissue remodeling of segmental defects in the esophagus. Biologic scaffolds have also been shown to be effective in the reinforcement of surgical anastomoses of the esophagus in a dog model[316].

Following these studies, endoscopic-deployment of biologic scaffolds was investigated for mucosal repair after endomucosal resection (EMR) in the dog. EMR is an accepted technique for the treatment of and high-grade dysplasia and early neoplasia, but often leads to stricture formation when used to treat extensive (i.e., long segment) areas. In this study by Badylak et al. [318], endoscopic placement of a biologic scaffold was shown to effectively prevent esophageal stricture formation after EMR. Together, the results from these pre-clinical studies formed the

basis for initial clinical trials of biomaterial-mediated tissue repair after neoplastic tissue resection.

Biologically-derived biomaterials have also been studied in small animal models. In contrast to large animal models, the focus of small animal studies is usually to determine mechanisms of tissue repair, screen large numbers of potential therapies, and optimize treatment options by systematically modifying design parameters. For instance, a murine model of esophageal reconstruction with chimeric mice constitutively expressing green fluorescent protein (GFP) in the bone marrow was used by Nieponice et.al.[317] to study the contribution of bone marrow-derived stem cells to biomaterial mediated esophageal repair. In this study, animals were subjected to partial mucosal resection followed by ECM scaffold implantation. The authors found GFP labeled bone marrow stem cells at the treatment site, and concluded that stem cells originating from the bone marrow participate in ECM remodeling process during tissue repair after esophageal injury. However, the low number of GFP labeled cells argues against the significant involvement of these cells in the constructive remodeling process.

In a different study, Lopes et. al [276] performed semi-circumferential esophageal defects and segmental esophageal defects in a rat model and repaired them with a SIS-patch graft and a SIS-tube interposition graft, respectively. Similarly to results obtained in large animal studies by Badylak et al., all animals in the segmental defect group died within the first post-operative month. Surviving animals in the semi circumferential defect group showed no signs of esophageal dysfunction and returned to normal weight. There was no evidence of fistula, significant stenosis or diverticula. No hematologic or serum biochemistry abnormalities were found. By month 5 the SIS patch had been replaced by esophageal-derived tissues.

A similar study was performed by Urita et al. [442] in the rat model using gastric acellular matrix for the repair of patch esophageal defects created in the abdominal esophagus. In this study, rats were sacrificed 1 week to 18 months after implantation and showed an implant site free of stenosis or dilatation. Keratinized stratified squamous epithelium had regenerated in the entire construct after the 2 week time point. However, regeneration of the muscle layer or lamina muscularis mucosa was not observed.

1.5.3.5 Clinical studies

Properly designed clinical studies for regenerative medicine approaches to esophageal repair are scarce. In 2008, a case study presented by Knorr et. al.[242], reported a 16-year-old female with perforated esophagus after accidental ingestion of a toothbrush. Inspection of the esophagus after retrieval of the brush revealed a near total perforation of the esophageal wall below the upper esophageal sphincter measuring approximately 1.5 × 2 cm which was treated with antibiotics and no oral ingestion. Two days after the primary treatment, an area measuring 1 × 2 cm covered with fibrin was found via endoscopy and the area was treated with factor XIII in all four quadrants of the lesion. Eight weeks after the incident esophagogastroduodenoscopy (EGD) showed a completely healed wound at the site of the rupture. Coagulation factor XIII was first used by Laki and Lóránd in 1948 as fibrin-stabilizing factor [256] and has been used since as therapy for ulceration due to pressure, large burns, sepsis, and acute liver disorders [75].

In 2011, Badylak et. al. [27] reported results of five male patients with adenocarcinoma of the esophagus treated by an entirely endoscopic technique for long segment en bloc resection of the mucosa and submucosa followed by placement of a biologic scaffold. Results from this study reported at 4 to 24-month follow-up showed restoration of normal, mature, K4+/K14+, squamous epithelium, and return to a normal diet. These patients had no significant

complications from the procedure. Two of five patients showed recurrent Barrett's esophagus confined to the gastroesophageal junction after 12 months, while the rest of the reconstituted esophageal mucosa remained intact. This study provided evidence that a biomaterial-based regenerative medicine approach may enable aggressive endoscopic resection of early stage neoplastic disease avoiding the traditional approach of watchful wait followed by radical esophagectomy (Figure 22).

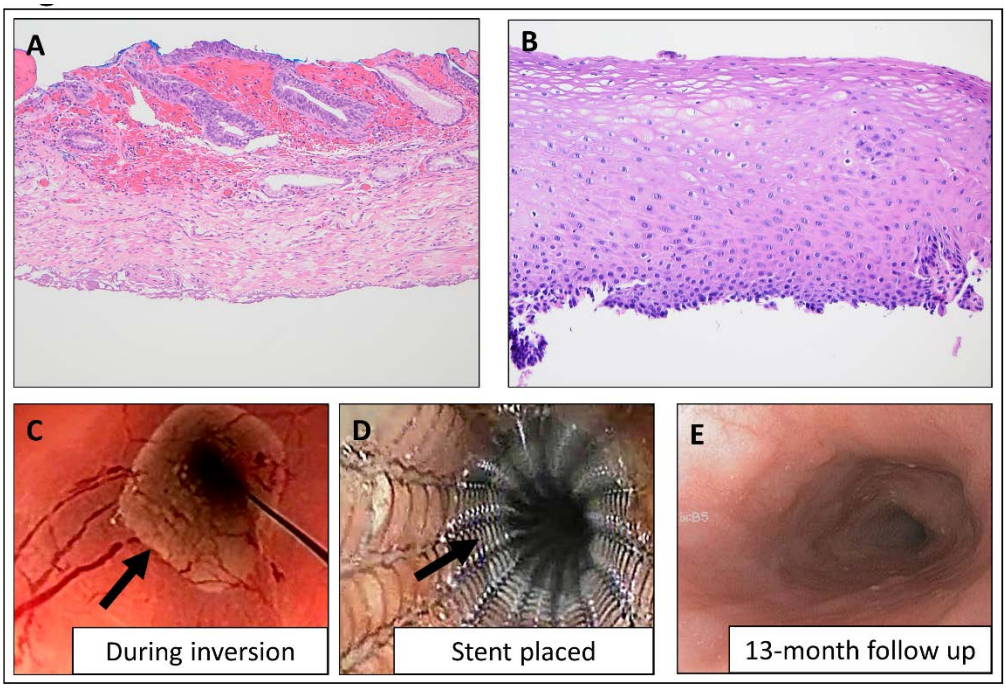

Figure 22. Esophageal preservation in human patients after endomucosal resection in the setting of superficial cancer

The current standard of care for esophageal neoplasia is esophagectomy, a procedure associated with high morbidity and mortality. As an alternative, Badylak et al.174 have implemented an entirely endoscopic method for removal of the mucosa and submucosa with subsequent placement of a biologic scaffold to promote constructive mucosal remodeling and minimize stricture formation in the setting of superficial cancer. To date, the method has been successfully used to treat eight human patients. (A) Diagnostic biopsy showing high-grade dysplasia. (B) Postoperative biopsy showing replacement of the ECM scaffold with mature, differentiated squamous epithelium.

Representative endoscopic views of each stage in the procedure and follow-up: (C) Muscularis externa being exposed during inversion and resection of the entire sleeve of mucosal and submucosal layers (arrow). (D) Stent placed to gently compress the ECM scaffold (arrow) against the exposed muscularis layer. (E) Thirteen-month follow-up showing complete coverage of the resected area by normal esophageal epithelium without stricture formation.

In 2014, Nieponice et al. [315] proposed the use of an ECM scaffold as a reconstructive patch for the augmentation of esophageal diameter during primary repair. In this study, four patients requiring esophageal reconstruction underwent patch esophagoplasty with a UBM-ECM scaffold. The full thickness of the esophagus was replaced by the scaffold by securing it to the edges of the remaining esophagus. All patients had a favorable clinical recovery and resumed normal oral intake after 7 days. One of the patients presented a micro leak that closed spontaneously after drainage. Follow-up studies including barium swallow and EGD showed normal esophageal emptying in all patients. Complete mucosal remodeling was observed at 2 months and was indistinguishable from surrounding healthy tissue. Implant sites presented 20% area contraction and biopsy of the treatment site showed normal esophageal epithelium.

In summary, the esophagus is a complex organ composed of multiple tissues that do not have the ability to regenerate. Esophageal pathologies that effect the esophagus are life threatening and currently available treatment options are very limited. This problem is compounded by the default inflammatory and scarring response of the esophagus following surgical intervention, even in the case of minimally invasive endoscopic approaches. Regenerative medicine strategies that utilize cell based, scaffold based, and bioactive molecule based approaches for tissue repair show promise as effective alternatives for the treatment of esophageal disease. However, esophageal pathologies are diverse, and a single regenerative

medicine approach is unlikely to prove effective in all settings of esophageal pathology. A thorough understanding of different pathologies that affect the esophagus, the anatomic and functional consequences of each disease, and the shortcomings associated with currently available therapies is necessary for the development of successful regenerative medicine strategies for esophageal repair.

1.6 REGENERATIVE MEDICINE APPROACHES FOR CARDIAC REPAIR

1.6.1 The Human Cardiovascular System

The cardiovascular system provides the vital function of pumping and distributing blood throughout the body to provide oxygen, vital nutrients, and to facilitate waste removal from tissues and organs. At the core of the cardiovascular system is the heart, a muscular pump composed of four structurally and functionally distinct chambers. The two atria receive blood from the peripheral and pulmonary circulation through the pulmonary vein and vena cava, respectively. Blood is then pumped it into the ventricles through the mitral and tricuspid valves, respectively. Once the blood is in the ventricles, coordinated myocardial contractions pump it out of the heart into the peripheral and pulmonary circulations through the aortic and pulmonary valves that serve to prevent retrograde blood flow back into the heart. The coronary vessels originate from the base of the aorta above the cusps of the aortic valve and supply the myocardium itself with oxygen and nutrients. The pumping action of the heart is achieved through coordinated myocardial contractions that are generated and distributed by a highly specialized conduction system composed of the sinoventricular node, the atrio-ventricular node, and purkinje fibers. The pericardium is an epithelial tissue that encloses all components of the heart and separates them from the rest of the mediastinal organs. The endocardium is continuous with the vascular endothelium [364].

The cardiomyocytes in the left ventricle are arranged circumferentially in a spiral orientation. This organization helps generate a highly coordinated contraction wave that starts at the apex in the bottom of the heart and spreads upwards to squeeze blood in that direction out of the aortic valve into the aorta and the peripheral tissues. Cardiomyocytes in the right ventricle are less organized, and as a result, less powerful contractions are generated. The coordinated beating of cardiac myocytes depends on intercalated discs —specialized intercellular junctions that facilitate cell-to-cell mechanical and electrical (ionic) coupling [262, 390, 428]. In addition with total muscular ventricular mass, this arrangement serves to pump the same amount of blood through different circuits having different resistance and pressure.

Atrial myocytes, on the other hand, are randomly organized, and as a result, contractions generated by the atria are very weak comparted to ventricular contractions[364]. A subset of atrial cells possess storage granules containing atrial natriuretic peptide [419, 420]. In addition to contributing to arterial vasodilation, this hormone stimulates salt and water elimination through the kidneys. This is one of the many mechanisms by which blood pressure is regulated [83, 448].

1.6.2 Cardiovascular Disease

Cardiovascular disease is the leading cause of death in the United States with about 80% of the worldwide burden occurring in third world[145, 155, 164, 225, 432]. In the United States alone, a third of all deaths are caused by cardiovascular disease, totaling about 800,000 patients—or roughly 1.5 times the number of deaths caused by all types of cancer combined [134]. A non-functional cardiovascular system is incompatible with life. Cardiac function is so imperative for human body that under normal circumstances, tissue and organ death will occur within minutes if the heart stops.

Most occurrences of cardiovascular disease manifests as structural or functional damage in one or more anatomic cardiac components. This set of conditions includes congenital heart abnormalities such as tetralogy of Fallot [81, 337, 345] and septal defects[36, 42, 123, 283, 285], arterial hypertension [2, 79, 132, 326, 388], diseases of the valvular disease [76, 96, 184, 280], and ischemic or coronary heart disease[45, 70, 98, 265, 373]. Of these, coronary heart disease is a major cause of death and disability in developed countries.

1.6.3 Coronary Artery Disease and Myocardial Infarction

Although mortality rates for coronary artery disease (CAD) have declined worldwide over the past four decades, CAD it remains responsible for more than one-third of all mortality in individuals over 35 years of age[269, 314, 372]. Furthermore, recent estimates suggest that as much as one-half of all middle-aged males and nearly one-third of middle-aged females in the United States will develop at some point a form of coronary artery disease [270].

The two main risk factors that contribute to coronary artery disease are hypertension, cigarette smoking, and diabetes mellitus, of which hypertension and diabetes mellitus are also associated with an increased tendency toward unrecognized myocardial infarction (MI)[405]. Hypertension is the most important risk factor for cardiovascular disease, scoring even above diabetes, cigarette smoking and dyslipidemia. In fact, hypertension is responsible for more than half of all cerebral ischemic events, and about 50% of all ischemic heart disease [260]. On the

other hand, diabetes mellitus has been confirmed as a risk factor for silent infarction, but only in males [224].

Interestingly, even though the incidence of CAD has decreased steadily in the United States [87, 131, 152, 368], studies indicated the incidence of myocardial infarction in has not deacrease d[131, 152, 367, 368]. These findings are attributed, at least in part, to the use of the more sensitive tests that allow for better detection and diagnosis of MIs, even when a smaller region of the myocardium is infarcted [336].

1.6.4 Cardiac Regenerative Medicine

The main objective or regenerative medicine approaches to cardiac repair is the replacement or regeneration of damaged myocardial tissue with functional, site appropriate cell types that can synchronize and act together to generate myocardial contraction and maintain the heart's ability to adequately perfuse peripheral tissues.

Early approaches to cardiac tissue repair included the localized delivery of stem cell and progenitor cell populations directly into affected myocardial tissue [305]. Although such an approach was reported to be partially successful in increasing cardiac function [59, 380], additional studies suggested that the actual number of surviving cells is in fact dramatically low. The high percentage of nonviable cells is attributed to a number of factors, including the lack of adequate substrate for cell delivery, and the lack of an appropriate microvasculature within the transplanted mass of cells to support cellular metabolism and function [200, 351]. As a result, the benefits of this approach have not been thoroughly exploited.

The use of biomaterials in cardiac repair has been motivated by a number of observations including the lack of cell survival in cardiac stem cell delivery applications, and the ability of

some biologic materials to promote constructive tissue remodeling. Synthetic biomaterials have been used in cardiac repair applications in the form of overlaying patches aimed to prevent ventricular remodeling following myocardial infarction. These materials include collagen [490], alginate [263], and [178, 182, 183].

An approach that is becoming increasingly popular is the use of biomaterial-derived hydrogels. These materials offer a number of advantages over solid scaffolds including the possibility of non-invasive delivery in a liquid phase that polymerizes in situ. This property allows hydrogels gives hydrogels flexible geometry and permits them to conform to the shape of multiple defects. In addition, biomaterial-derived hydrogels can be used as injectable substrates for drug and/or cell delivery. For instance, myoblast have been delivered to the myocardium using an injectable scaffold composed of fibrin that can increase cell survival after 5 weeks [94]. Synthetic constructs offer additional advantages, such as the ability to finely control polymerization and degradation rates as in the case of hybrid constructs composed of fibrinogen conjugated with poly-ethylene glycol [462].

Finally, whole organ decellularization offers great potential for the development of novel biologic scaffolds for organ repair. Cardiac perfusion decellularization as a method for the preparation of such scaffolds has been described by a number of groups [333, 360, 456]. As with traditional sheet scaffolds derived from natural tissue sources, the objective of this method is to remove the cellular compartment while maintaining the structure and components of the extracellular matrix. Once decellularized, these scaffolds can be repopulated with cells from different sources, including perfusion seeding of endothelial cells and transmural seeding cardiomyocytes. Using this technique constructs have recovered 2% of normal cardiac function [333].

1.7 CENTRAL HYPOTHESIS

The central hypothesis of the present dissertation states: biologic scaffolds composed of extracellular matrix from derived homologous anatomic structures have the ability to modulate cell processes associated with constructive remodeling and the host response in preclinical models of cardiac and esophageal injury.

1.8 SPECIFIC AIMS

Aim 1: To develop and characterize extracellular matrix based bioscaffolds from the mucosal layer and muscularis externa of the porcine esophagus.

Sub-Aim: To characterize the host response to implanted esophageal ECM-derived bioscaffolds in a preclinical murine model of abdominal wall defect.

Aim 2: To evaluate the tissue specific effects of biologic scaffolds derived from esophageal tissues in vitro and in a preclinical murine model of esophageal mucosal resection.

Aim3: To evaluate the ability of cardiac-ECM to modify the host response to an implanted cardiac patch in a preclinical murine model of myocardial infarction.

2.0 DEVELOPMENT AND CHARACTERIZATION OF ECM-DERIVED BIOMATERIALS FROM ESOPHAGEAL TISSUES

Aim 1: To develop and characterize extracellular matrix based bioscaffolds from the mucosal layer and muscularis externa of the porcine esophagus.

Sub-Aim: To characterize the host response to implanted esophageal ECM-derived bioscaffolds in a preclinical murine model of abdominal wall defect.

2.1 BACKGROUND

The default mechanism of mammalian tissue repair typically results in scar tissue deposition, a protective and favorable response in most tissues. However, this scar tissue formation is associated with adverse clinical consequences including stricture in select anatomic locations such as the esophagus. Preclinical studies have shown that placement of an extracellular matrix (ECM) scaffold derived from heterologous tissue is capable of restoring a functional esophagus with minimal stricture and normal esophageal motility following circumferential mucosal resection [32]. A clinical report involving patients with stage 1 esophageal adenocarcinoma corroborated this finding and provided proof-of-concept in the clinical setting[27] and [203]. While heterologous ECM was successful in reducing stricture formation, the remodeled tissue did not fully reconstitute all components of normal esophageal tissue; for example, glandular tissue was absent. Delivery of the scaffold also required temporary placement of an intraluminal stent to allow integration of the scaffold with the subjacent tissue. A possible advantage of a site-specific, homologous ECM could be more rapid integration and faithful remodeling of the esophageal mucosa.

Recent work has described potential benefits of ECM scaffold materials derived from homologous tissue versus heterologous tissue when used in selected anatomic locations [9, 39, 58, 101, 106, 143, 292, 397, 398, 487]. While tissue specificity is not necessary for all therapeutic applications [27, 30, 468], some studies have shown that site-specific ECM can preferentially maintain tissue-specific cell phenotypes [9, 143, 397, 398], promote cell proliferation [9] and [487], induce tissue-specific differentiation [101], and enhance the

chemotaxis of lineage-directed progenitor cells [58, 106, 180]. It is plausible therefore that a site-specific esophageal mucosal ECM may promote similar effects and further improve clinical outcomes in esophageal mucosa repair. The harvesting and preparation of an ECM scaffold requires tissue-specific methodologies for optimal outcomes [149, 174, 180, 195, 196].

Biologic scaffolds composed of ECM, when prepared by methods designed to preserve structure and composition of the native source tissue, contain bioactive molecules including growth factors (e.g., vascular endothelial growth factor (VEGF) [199][21], basic fibroblast growth factor (bFGF) [455]) and glycosaminoglycans (GAGs) [198][23]. The composition, ultrastructure, and mechanical properties of an ECM construct are affected by the methods used to decellularize the source tissue as well as the methods of sterilization and storage of such bioscaffolds [105, 146, 149]. Therefore, the methods of preparing ECM scaffolds intended for use in the repair and reconstruction of the esophageal mucosa must be carefully considered as regenerative medicine strategies are developed for this intended therapeutic application.

The objective of Specific Aim 1 was to prepare, characterize, and determine the in-vitro cytocompatibility of two ECM bioscaffolds derived from 1) the esophageal mucosa and 2) the esophageal muscularis externa. Porcine esophagi were collected and the mucosa and muscularis layers were independently decellularized by methods sufficient to meet stringent decellularization criteria: specifically no visible intact nuclei by hematoxylin and eosin staining, remnant DNA concentration less than 50 ng/mg dry weight, and DNA fragment length less than 200 basepairs [105]. Biochemical and mechanical properties of the ECM were then characterized by quantitative and qualitative measures, and the in vivo host response to the mucosal ECM bioscaffold was evaluated in a murine model of abdominal wall defect.

2.2 MATERIALS AND METHODS

2.2.1 Harvest and preparation of ECM bioscaffolds from porcine esophagus

Esophageal mucosal decellularization: Esophagi were harvested from market weight (240–260 lbs) pigs. The mucosa and submucosa were isolated by mechanical separation from the muscularis propria. The luminal of the mucosa surface was gently abraded to remove squamous epithelium. The tissue that remained was composed primarily of the basement membrane, lamina propria, muscularis mucosa, and submucosa. The mucosa was then subjected to a series of immersion treatments as follows: 1% trypsin/0.05% EDTA (Invitrogen, Carlsbad, CA) for 1 h at 37 °C on a rocker plate, deionized water for 15 min, 1.0 m sucrose (Fisher Scientific, Pittsburgh, PA) for 30 min, deionized water for 30 min, 3.0% Triton X-100 (Sigma Aldrich, St. Louis, MO) for 48 h, deionized water for 15 min, PBS (Fisher Scientific) for 15 min, 10% deoxycholate (Sigma Aldrich) for 4 h, deionized water for 30 min, 0.1% peracetic acid (Rochester Midland Corp., Rochester, NY) in 4.0% ethanol for 4 h, 100 U/mL DNAse (Invitrogen) for 2 h on a rocker plate, followed by 15 min washes with PBS, deionized water, PBS, and deionized water. All treatments were performed at room temperature with agitation on a shaker plate at 300 RPM unless otherwise stated. For cytocompatibility evaluation and in-vivo remodeling evaluation, chemically cross-linked emECM (XL-emECM) scaffolds were used as negative controls. Chemically cross-linked bioscaffolds have been shown to consistently inhibit a constructive remodeling response [443] and [31]. Cross-linking was achieved by immersion in 0.01 m carbodiimide for 24 h with multiple subsequent washes in PBS over 48 h. The esophageal mucosa ECM (emECM) was lyophilized and sterilized using ethylene oxide.

Muscularis Externa decellularization: In contrast to the esophageal mucosa, the esophageal muscularis externa was decellularized via perfusion decellularization in an attempt to conserve the ECM ultrastructure of its two layers. Each esophagus was placed in a 2 L container with 1 L of hypotonic type 1 water and connected in a close circuit to a peristaltic pump (L/S® Drive EW-07550-30; Cole-Parmer, Vernon Hills, IL) for 15 min at 800 mL/min. The type 1 water was replaced with fresh solutions 3 times and then with 2 × phosphate-buffered saline (PBS) at for 15 min and two fresh solution washes. Two liters of 0.02% trypsin/0.05% ethylenediaminetetraacetic acid/0.05% NaN3 solution was warmed to 37°C using a digital hotplate and then perfused through the esophageal muscularis at 800 L/min for 3 h. Two DI water washes followed by two-2 x PBS washed were used before a 6 h, 2% Triton X-100/0.05% ethylenediaminetetraacetic acid/0.05% NaN3 solution was followed by washes of DI water and PBS and a 4% deoxycholic acid solution at for 6 h at room temperature. Disinfection was accomplished by perfusion of 0.1% peracetic acid/4% ethanol for 2 h. The acid was neutralized and removed from the ECM by perfusing the intact matrix with PBS (pH 7.4) two times and type 1 water three times for 15 min each at 800mL/min. The resulting muscularis externa ECM (meECM) was then lyophilized until dry for characterization and analysis.

2.2.2 Assessment of DNA content

DNA was extracted from representative samples (n = 6) of emECM and (n = 3) of meECM. For DNA extraction, lyophilized ECM scaffolds were powdered using a Wiley Mill and filtered through a 60-mesh screen. One hundred milligrams of lyophilized, powdered emECM was digested with proteinase K digestion buffer (100 mm NaCl, 10 mm Tris–HCl (pH = 8), 25 mm EDTA (pH = 8), 0.5% SDS, 0.1 mg/mL proteinase K) at 50 °C for 24 h. The digest was

extracted twice using 25:24:1 (v/v/v) phenol/chloroform/isoamyl alcohol. DNA was precipitated from the aqueous phase at −20 °C with the addition of 2 volumes of ethanol and 0.1 volume of 3 m sodium acetate (pH = 5.2). The DNA was then centrifuged at 10,000 g for 10 min and resuspended in 1 mL of TE buffer (10 mm Tris (pH = 8), 1 mm EDTA).

The concentration of each extracted DNA sample was determined using Quant-iT PicoGreen dsDNA Assay Kit (Invitrogen) following the manufacturer's recommended protocol. A standard curve was constructed by preparing samples of known DNA concentrations from 0 to 1000 ng/mL and concentration of DNA was found by linear interpolation of the standard curve. Samples were read using SpectraMax M2 Plate Reader (Molecular Devices, Sunnyvale, CA). DNA samples were diluted to ensure their absorbance properties fell within the linear region of the standard curve.

To determine the fragment size of remnant DNA, equal concentrations of extracted DNA from each sample were separated on a 2% agarose gel containing 0.5% ethidium bromide and visualized with ultraviolet transillumination using a reference 100-bp ladder (New England BioLabs, Ipswich, MA). All assays were performed in quadruplicate.

2.2.3 Immunolabeling and histochemistry

Slides (n = 6 for each bioscaffold) were stained to visualize the extent of cell removal with a hematoxylin and eosin (H&E) protocol. Antigen retrieval was performed for immunolabeling studies using a 0.01 m citrate buffer (pH = 6) heated to 95–100 °C. Slides were placed in hot buffer for 20 min and rinsed in PBS (3 × 5 min). Sections were placed in pepsin solution (0.05% pepsin/0.01 m HCl) at 37 °C for 15 min. After rinsing in PBS (3 × 5 min), the samples were

blocked in blocking buffer (2% goat serum/1% bovine serum albumin/0.1% Triton X-100/0.1% Tween) for 1 h at room temperature. The sections were incubated in blocking buffer with rabbit polyclonal collagen IV antibody (1:500 dilution, Abcam, Cambridge, UK), rabbit polyclonal laminin antibody (1:200 dilution, Abcam), or mouse monoclonal fibronectin (1:200 dilution, Abcam) overnight at 4 °C in a humidified chamber. Sections were subsequently rinsed in PBS (3 × 5 min). Peroxidase activity was quenched by rinsing sections in a 3% hydrogen peroxide in methanol solution for 30 min followed by rinsing in PBS (3 × 5 min). Biotinylated goat anti-rabbit or goat anti-mouse secondary antibodies (Vector Laboratories, Burlingame, CA) were diluted 1:200 in blocking buffer and added to the sections for 30 min at 25 °C and sections were rinsed in PBS (3 × 5 min). The slides were incubated in detection solution (VectaStain® Elite ABC Reagent, Vector Laboratories) for 30 min at 37 °C. Peroxidase substrate, 3,3′-diaminobenzadine (ImmPACT™ DAB, Vector Laboratories) was prepared and sections were incubated while being visualized under a microscope to time the color change for subsequent section staining intensities. Tissues were rinsed in water (3 × 5 min). Sections were dipped in hematoxylin (Thermo Shandon, Pittsburgh, PA) for 1 min for a nuclear counterstain and subsequently rinsed in PBS (3 × 5 min).

2.2.4 Sulfated glycosaminoglycan assay

Sulfated glycosaminoglycan (sGAGs) concentration in emECM samples was determined using the Blyscan Sulfated Glycosaminoglycan Assay Kit (Biocolor Ltd, Belfast, Northern Ireland). For extraction of sGAGs, lyophilized ECM scaffolds were powdered using a Wiley Mill and filtered through a 60-mesh screen. Samples were prepared by digestion of 50 mg/mL dry weight of each sample with 0.1 mg/mL proteinase K in buffer (10 mm Tris–HCl, pH 8, 100 mm NaCl,

25 mm EDTA) for 48 h at 50 °C. Digested samples were assayed following the manufacturer's protocol, and the assay was performed in duplicate on three different emECM sample.

2.2.5 Growth factor assay

The concentration of basic fibroblast growth factor (bFGF) and vascular endothelial growth factor (VEGF) in urea-heparin extracts of emECM samples was determined with the Quantikine Human FGF basic Immunoassay, Human VEGF Immunoassay (R&D Systems, Minneapolis, MN). Each assay for bFGF and VEGF was performed in quadruplicate. The ELISA assays are cross-reactive with porcine growth factors and do not measure activity.

2.2.6 Scanning electron microscopy

Scanning electron micrographs were taken to examine the surface topology of emECM. Prior to final lyophilization, samples were fixed in cold 2.5% (v/v) glutaraldehyde (Electron Microscopy Sciences, Hatfield, PA) in PBS for at least 24 h, followed by three washes in PBS. Fixed samples were then dehydrated using a graded series of alcohol (30, 50, 70, 90, 100%) for 15 min each, followed by 15 min in hexamethylenediamine (Fisher) and subsequent air-drying. The dried samples were sputter coated with a 3.5 nm layer of gold/palladium alloy using a Sputter Coater 108 Auto (Cressington Scientific Instruments, Watford, UK) and imaged with a JEOL JSM6330f scanning electron microscope (JEOL, Peabody, MA) at 100× and 500× magnifications.

2.2.7 Perivascular stem cell (PVSC) culture

Perivascular stem cells isolated by flow cytometry from fetal muscle [107] and [108] were used in all experiments. These cells (CD146+/NG2+/CD34−/CD144−/CD56−) have been previously shown to represent a distinct population of perivascular cells obtained after positive selection and stringent exclusion of hematopoietic, endothelial, and myogenic cells, and which are able to differentiate into mesodermal lineages [108] and [437]. Isolated cells were cultured in high-glucose Dulbecco's modified Eagle's medium (Invitrogen) containing 20% fetal bovine serum (Thermo), 100 U/mL penicillin, and 100 μg/mL streptomycin (Sigma Aldrich) at 37 °C in 5% CO2.

In-vitro cell viability assays were performed using single layer sheets of ECM. PVSCs (0.5 × 106) were cultured for 48 h on 2 cm diameter circular sheets of emECM or XL-emECM. Cell viability was compared to growth on tissue culture plastic (TCP) using LIVE/DEAD® Viability/Cytotoxicity Kit (Invitrogen) following manufacturer's guidelines. Capturing 4 random fields across the emECM scaffold, the live and dead cells were imaged with green fluorescent calcein-AM (cAM) and red fluorescent ethidium homodimer-1 (EtH1), respectively. Quantification of live and dead cells was achieved using a custom image analysis algorithm developed using the cell profiler image analysis package [222] and [257]. This custom algorithm identified and quantified the number of cAM+ (live) and EtH1+ (dead) cells present on the emECM scaffolds. These results were then expressed as a percentage of total cells.

2.2.8 In-vivo Biocompatibility

All procedures were performed in accordance with the National Institute of Health (NIH) guidelines for care and use of laboratory animals and with approval of the Institutional Animal Care and Use Committee (IACUC) at the University of Pittsburgh. Sprague Dawley rats (female; 250–350 g) were anesthetized with 1.5–3% isoflurane and maintained at a surgical plane of anesthesia. The surgical site was shaved, disinfected with a betadine solution, and an incision was made into the ventrolateral abdominal wall. Bilateral partial thickness abdominal body wall defects [109] were created by excision of a 1 cm2 piece of tissue comprising the internal and external oblique muscles but leaving the transversalis muscle intact [443]. Size matched emECM or XL-emECM scaffolds were then sutured into the defect site using nonresorbable 4-0 proline sutures at each of the 4 corners of the device. The skin was closed using 3-0 resorbable vicryl sutures. Rats were euthanized at 14 or 35 days post-implantation and implant sites were identified by nonresorbable sutures. The implant site containing emECM devices and adjacent tissue site were isolated and placed in 10% neutral buffered formalin. Fixed samples were paraffin embedded and cut into 6 μm sections.

The sections obtained at 14 and 35 days post-op were stained with H&E for a qualitative and semiquantitative histomorphologic analysis that evaluated cell infiltration, multinucleated giant cells, vascularity, connective tissue, encapsulation, and scaffold degradation. Two blinded investigators scored the sections according to a previously established and validated semiquantitative scoring method [443] and [65]. Using quantitative scoring criteria (Table 11), biologic scaffolds can be grouped according to chronic inflammation and foreign body response (quantitative score < 5), early inflammatory cell infiltration with decreased cellularity and little evidence of constructive remodeling at later time points (5 < quantitative score < 10), and early

infiltration by inflammatory cells and signs of constructive remodeling at a later time point (quantitative score >10).

Table 11. Semiquantitative scoring criteria for day 14 and day 35 explants.

	3	2	1	0
Day 14 scoring criteria				
Cellular infiltration (per 40× field)	>150 cells	75–150 cells	1–75 cells	0 cells
Connective tissue organization	Highly organized connective tissue present	Moderately organized connective tissue present	Unorganized connective tissue throughout disrupted original scaffold	Original scaffold intact
Degradation	No scaffold present	Some scaffold present	Mostly present	No degradation
Encapsulation	No encapsulation	Minimal encapsulation	Moderate encapsulation	Dense encapsulation
Multinucleated giant cells (per 40× field)	0 cells	1 cell	2–5 cells	>5 cells
Vascularity (per 40× field)	>10 vessels	6–10 vessels	2–5 vessels	0–1 vessel
Day 35 scoring criteria				
Connective tissue organization	Highly organized connective tissue present	Moderately organized connective tissue present	Unorganized connective tissue throughout disrupted original scaffold	Original scaffold intact
Degradation	No scaffold present	Some scaffold present	Mostly present	No degradation
Encapsulation	No encapsulation	Minimal encapsulation	Moderate encapsulation	Dense encapsulation
Multinucleated giant cells (per 40× field)	0 cells	1 cell	2–5 cells	>5 cells
Muscle ingrowth	Organized muscle throughout scaffold	Muscle cells present in scaffold center	Muscle cells present at scaffold periphery	No muscle ingrowth

Immunolabeling of macrophages was performed on tissue sections from day 14 explants. Paraffin embedded sections were deparaffinized with xylene and rehydrated through a graded ethanol series. Heat-mediated antigen retrieval was performed with 0.01 m citrate buffer (pH = 6) at 95–100 °C for 25 min. The tissue sections were subjected to Tris-Buffered Saline Tween-20 (TBST) for 15 min, followed by incubation in blocking buffer (2% horse serum albumin/1% bovine serum albumin/0.05% Tween-20/0.05% Triton X-100) for 1 h. The primary antibodies, diluted in blocking buffer, were added to the slides for 16 h at 4 °C in a humidified chamber. The slides were then washed three times in PBS prior to the addition of the secondary antibody for 1 h in a humidified chamber at room temperature. DAPI was used as a nuclear counterstain. The primary antibodies used in this study were mouse anti-rat CD68 (1:150, AbD Serotec, Raleigh, NC), goat polyclonal CD206 (Santa Cruz Biotech, Santa Cruz, CA), rabbit anti-rat CD86 (1:150, Abcam) and mouse anti-rat CD68 (1:50, Serotec, Raleigh NC). The secondary antibodies used were Alexa Fluor® donkey anti-mouse 594 (1:200, Invitrogen), Alexa Fluor® donkey anti-goat 488 (1:200, Invitrogen) and donkey anti-rabbit IgG-PerCP-Cy5.5 (1:300, Santa Cruz). CD68 is a pan-macrophage marker. CD86 is an M1 marker. CD206 is an M2 marker. All primary antibodies were confirmed to cross-react with rat epitopes. The sections were imaged at random fields along the interface of the native tissue and ECM scaffold. Quantification of M1/M2 polarization was achieved using a custom image analysis algorithm developed using the cell profiler image analysis package[222, 257]. This algorithm identified and quantified the number of CD68+CD86+ (M1 phenotype) and CD68+CD206+ (M2 phenotype) cells present within the tissue sections. Any cells that co-expressed these markers were not counted. These numbers were then expressed as a ratio of M2/M1.

2.2.9 Biomechanical testing

The passive biaxial mechanical properties were characterized for the native esophageal mucosa and emECM (n = 8). A detailed description of the testing device and methods used for planar biaxial testing has been reported previously [49]. Briefly, samples were affixed to 250 g load cells (Model 31, Honeywell, Columbus, OH) with two loops of suture attached to each side with four hooks, and deformation was measured from a four-marker array. Samples were tested in PBS at room temperature under an equibiaxial stress protocol from a 0.5 g tare load to 250 kPa after 10 cycles of preconditioning with a cycle time of 30 s. All data was referenced to the post-preconditioned free-float state. The maximum strain for each sample was then defined as the strain at the maximum tested stress of 250 kPa.

The suture retention analysis we performed according to a previously described protocol[148]. Briefly, a 2-0 prolene suture with a taper needle was passed through the specimen with a 2 mm bite depth, and tied with a square knot and the loop attached to an Instron machine, and pulled at a constant rate of 10 cm/min[148]. Two locations were tested per sample and eight samples were tested per group. Samples were thoroughly rehydrated prior to testing.

2.2.10 Statistical analysis

An independent samples t-test was used to determine whether the DNA, growth factor, and GAG content, and mechanics of the emECM were different than that of native esophagus ($p < 0.05$). A one-way analysis of variance (ANOVA) was used to determine differences in the percentage of viable cells in culture. Macrophage phenotype ratio between XL-emECM and emECM was compared using an independent samples t-test. A two-way ANOVA with post-hoc Tukey test was performed to determine differences in biomechanical properties with the two independent variables being axIs and material. All data are reported as mean ± standard error.

2.3 RESULTS

2.3.1 Decellularization efficacy

The degree of decellularization following the described method was assessed using previously established guidelines for decellularization [105]. No intact nuclei were visible by H&E or DAPI staining following decellularization (Fig. 1C). The concentration of remnant DNA in emECM and was (48 ± 6.4 ng/mg) and (43.3 ± 4.1ng/mg) in meECM. Both markedly less ($p < 0.001$) than that in native esophageal tissue (855 ± 24 ng/mg) (Fig. 23A). Residual DNA was present only in fragments less than 200 bp in length (Fig. 23B and 23C).

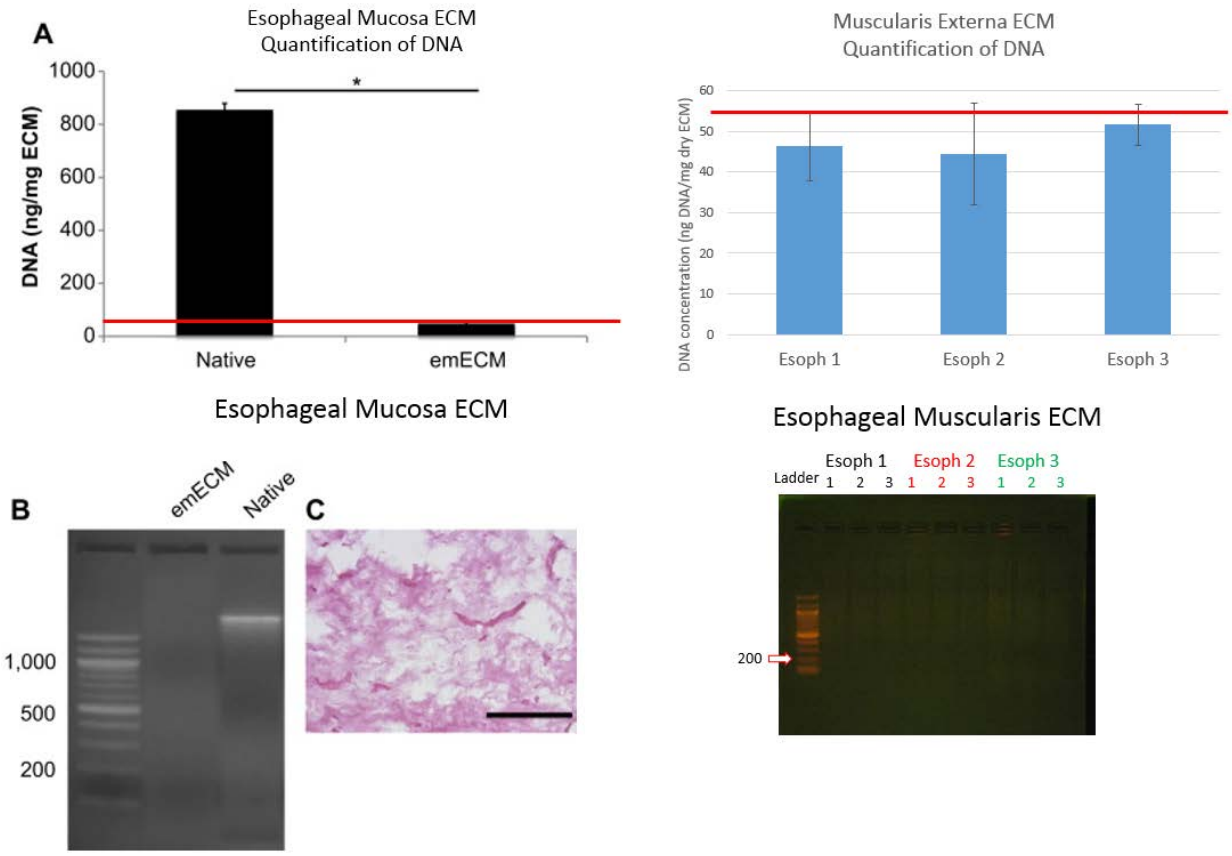

Figure 23. Decellularization Efficacy

Decellularization of emECM and meECM was assessed by the amount and size of remaining DNA and histologically by hematoxylin and eosin (H&E). The amount dsDNA in emECM was less than 50 ng/mg, which was significantly less (asterisk; $p < 0.001$) than native tissue (A). DNA fragment length was assessed by gel electrophoresis using a reference 100 bp ladder (B). No intact nuclei were visible after decellularization by H&E staining (C). Data represented as mean ± standard error. Scale bar = 100 µm.

2.3.2 Ultrastructural characteristics of esophageal ECM

SEM images of the luminal and abluminal surface of emECM showed a smooth surface on the luminal surface of the emECM (Figure. 24A,C). The abluminal surface, however, had a more textured and fibrous structure (Figure. 24B,D). Cross sectional images of meECM show that

perfusion decellularization maintains the ultrastructure of the muscularis layer and preserves the orientation of the two different layers (Figure 25).

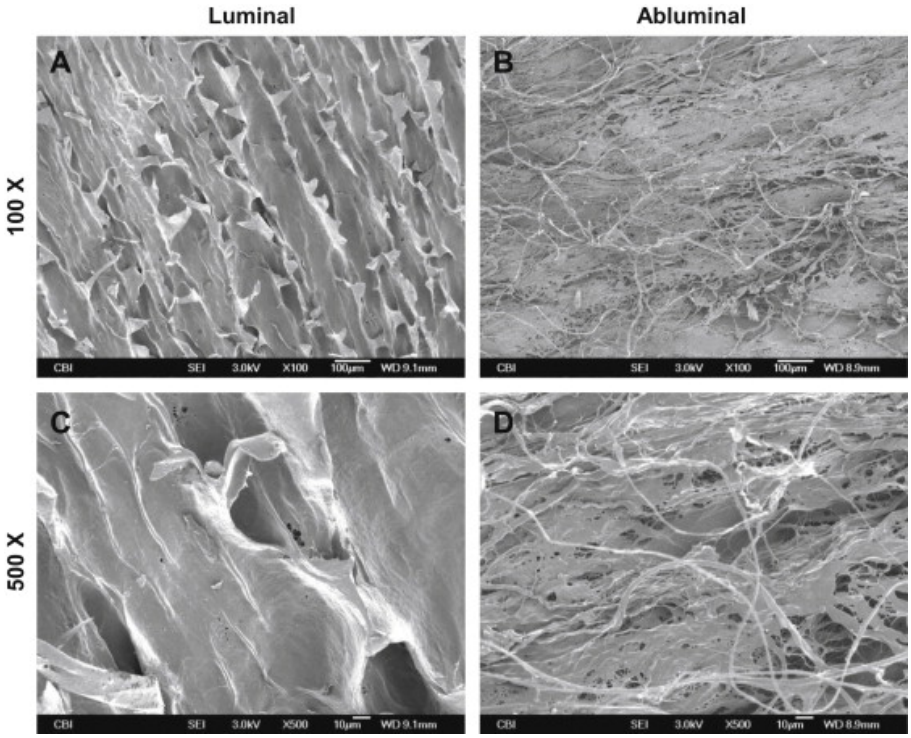

Figure 24. Scanning electron micrographs (SEM) of emECM surface.

The luminal surface of the emECM scaffold was characterized by a smoother surface (A, C) Compared to the abluminal surface which was more textured and fibrous (B, D).

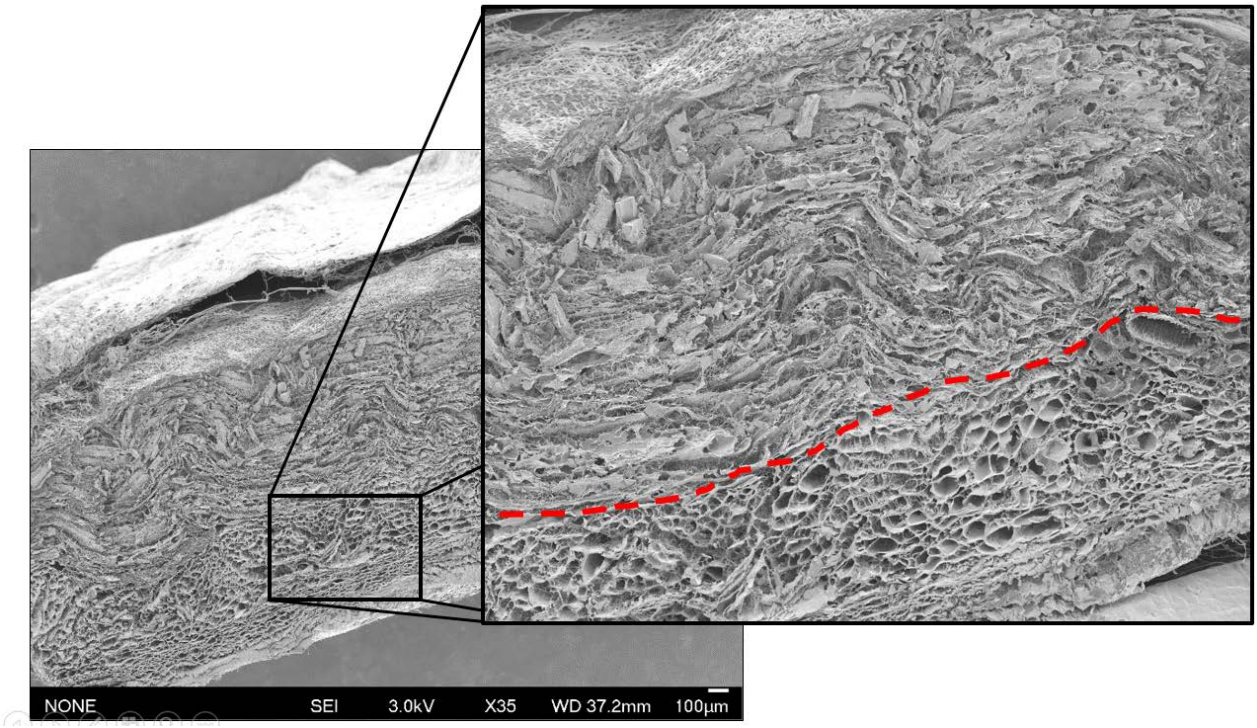

Figure 25. Scanning electron micrographs (SEM) of meECM surface.

The cross sectional surface of the meECM scaffold was characterized by a distinct transition between longitudinally oriented, and circumferentially oriented layers of the muscularis externa that was preserved with perfusion decellularization (red dotted line).

2.3.3 Biomechanical Properties

The equibiaxial stress response of the native esophageal mucosa showed anisotropic behavior with a maximum strain of 83% and 18% in the circumferential and longitudinal direction, respectively (Figure. 26A,B). The emECM showed similar anisotropy, but had a lower compliance along both axes, with the circumferential strain reaching only 10.5% (Figure. 26A,B). The decellularized tissue had 30% lower suture retention strength than the native esophagus. Results for meECM ae shown in (Figure 27)

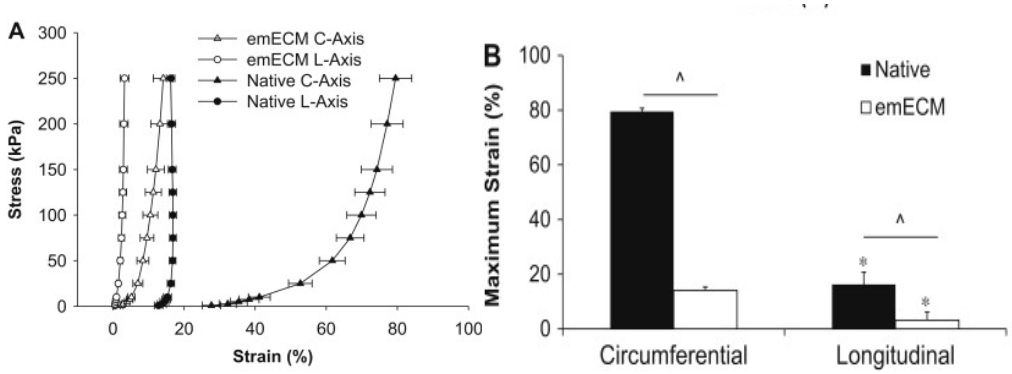

Figure 26. Native and decellularized esophageal mucosa mechanical characterization.

The equibiaxial stress response was characterized along the circumferential and longitudinal axes (A). The maximum strain defined at a stress of 250 kPa for both circumferential (C) and longitudinal (L) axes (B). Significant differences ($p < 0.05$) between the circumferential and longitudinal axes of the same sample are denoted as the following: (*) as different from circumferential. Significant differences between samples in each axis are denoted as the following: (ˆ) as different from native. Data represented as mean ± standard error.

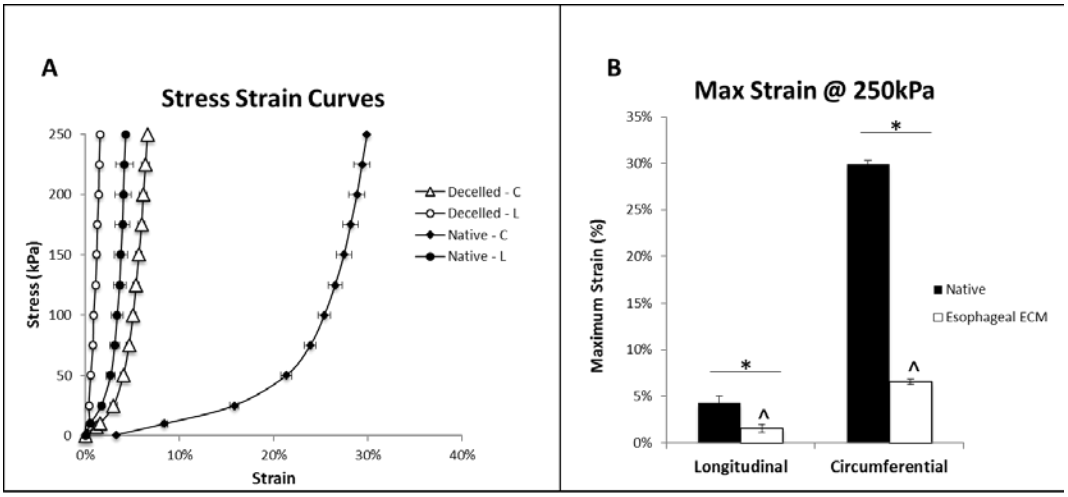

Figure 27. Native and decellularized esophageal muscularis mechanical characterization.

The equibiaxial stress response was characterized along the circumferential and longitudinal axes (A). The maximum strain defined at a stress of 250 kPa for both circumferential (C) and longitudinal (L) axes (B). Significant differences ($p < 0.05$) between the circumferential and longitudinal axes of the same sample are denoted as the following: (*) as different from circumferential. Significant differences between samples in each axis are denoted as the following: (^) as different from native. Data represented as mean standard error.

2.3.4 Cytocompatibility and Immunomodulation in vitro

When cultured on emECM, XL-emECM, and meECM quantification of PVSC cell viability in-vitro showed no difference when compared to tissue culture plastic ($p = 0.67$). All conditions resulted in over 98% viability following 48 h in culture (Figure. 28A,B, and C). Results for meECM are shown in (Figure 29A and B).

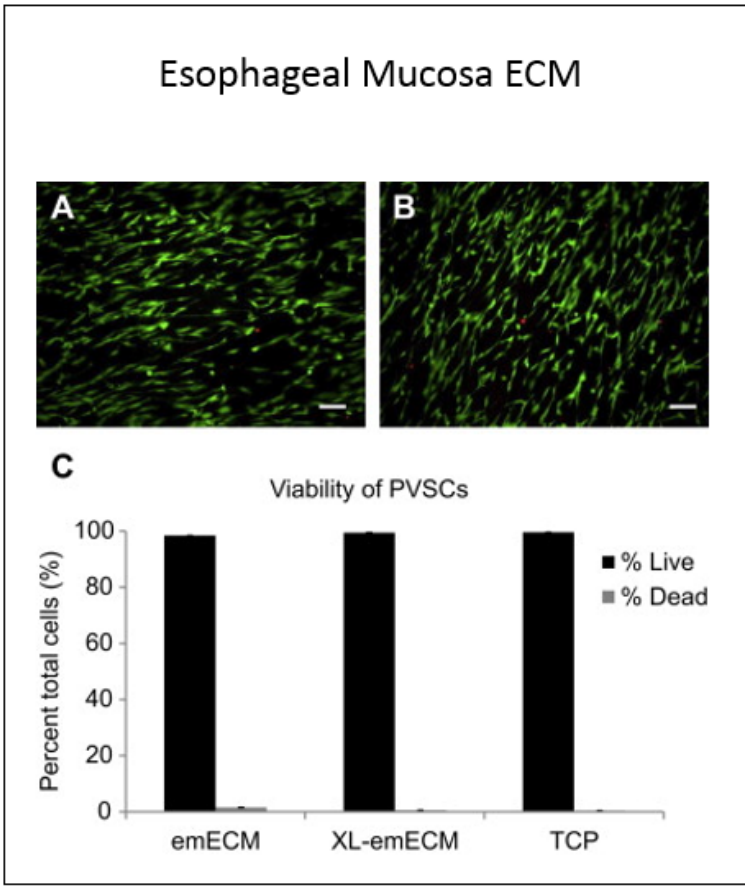

Figure 28. Cytocompatibility of emECM and XL-emECM.

The viability of perivascular stem cells (PVSCs) after 48 h culture on emECM (A), XL-emECM (B), and tissue culture plastic (TCP) was assessed. Percentage of live cells was quantified and compared across groups (C). Data represented as mean ± standard error. Scale bar = 50 μm.

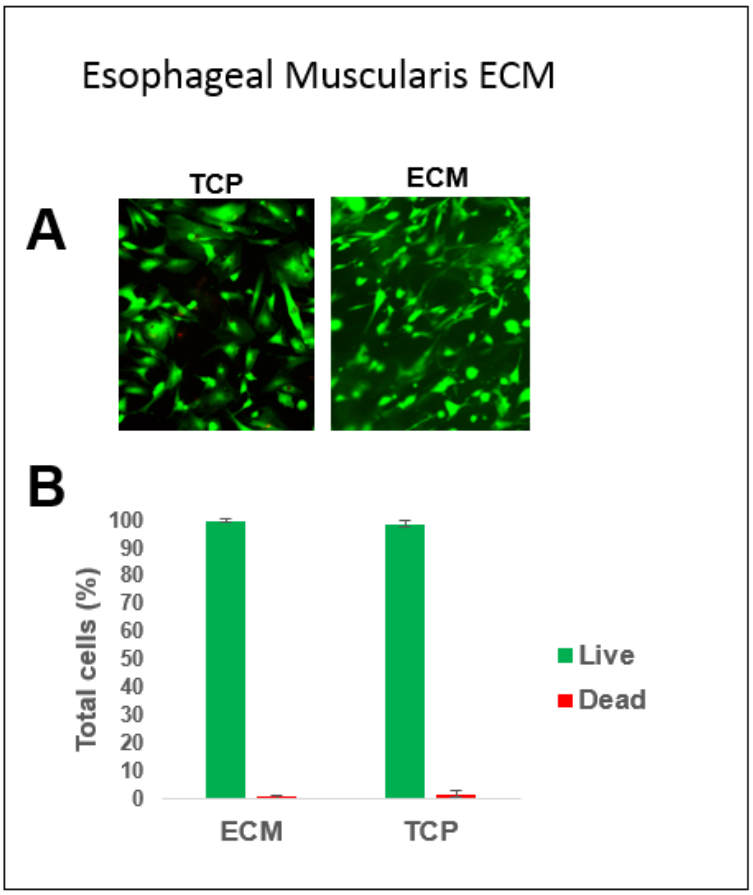

Figure 29. Cytocompatibility of meECM

The viability of perivascular stem cells (PVSCs) after 48 h culture on TCP and meECM (A) was assessed. Percentage of live cells was quantified and compared across groups (B). Data represented as mean ± standard error. Scale bar = 50 μm.

Primary monocytes isolated from murine bone marrow and matured into macrophages showed expression of M2 macrophage phenotype-associated marker Fizz1 after exposure to esophageal mucosa ECM and esophageal muscularis ECM digests. The same populations did not show expression of M1 macrophage phenotype-associated marker iNOS (Figure 30)

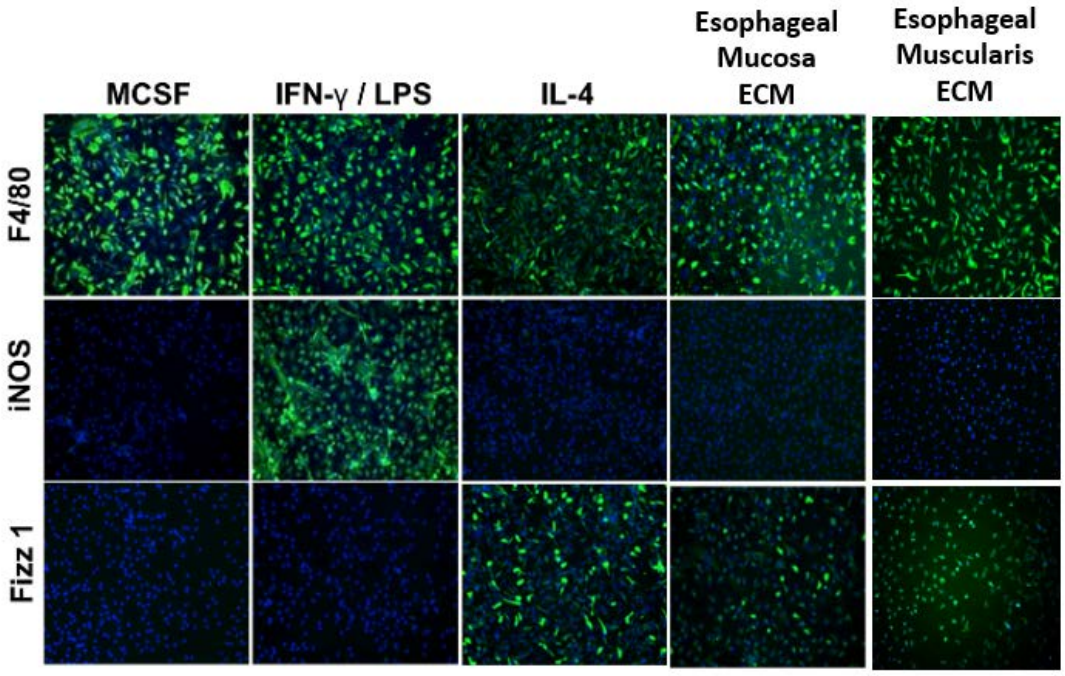

Figure 30. Immunomodulatory effects of esophageal ECM in vitro

Esophageal mucosal ECM and esophageal muscularis ECM pepsin digests promote an immunomodulatory macrophage phenotype when exposed to murine macrophages in vitro. iNOS: M1 macrophage marker, Fizz1: M2 macrophage marker. Both biomaterials derived from esophageal tissues promote an M2 pro-remodeling macrophage phenotype.

2.3.5 Host Response and In vivo Cytocompatibility

In-vivo host response to emECM was examined at both 14 and 35 days post-implantation in a rat abdominal body wall model. The host response to emECM scaffolds showed a robust mononuclear cell response throughout the partially degraded scaffold at 14 days (Figure 31A) and yielded a histologic score of 11.4. Along the interface between the emECM scaffold and native tissue, the macrophage response was predominantly of the M2 phenotype (Figure 32A) with a ratio of M2/M1 macrophages of 1.29 ± 0.21 (Figure 32C). By 35 days post-implantation,

the original material was not identifiable by histologic evaluation and the remodeling site was composed of organized host connective tissue and islands of skeletal muscle at the periphery that extended into the center of the remodeling site (Figure 31B). Semiquantitative histomorphologic analysis of emECM at day 35 resulted in a total score of 12. In contrast, the host response to XL-emECM was characterized by little to no cellular infiltration or vasculature within the chemically cross-linked bioscaffold, a dense population of mononuclear macrophages at the host–scaffold interface, the deposition of disorganized connective tissues surrounding the implanted test article, and little to no degradation of the material at 14 days (Figure 31C). The cellular response along the scaffold and native tissue interface was shown to be predominantly macrophages of the M1 phenotype (Figure 32B) with an M2/M1 ratio of 0.19 ± 0.03, which was less than ($p < 0.001$) the M2/M1 ratio in emECM. By 35 days, the XL-emECM was still largely intact and showed no infiltration of skeletal muscle (Figure 31D).

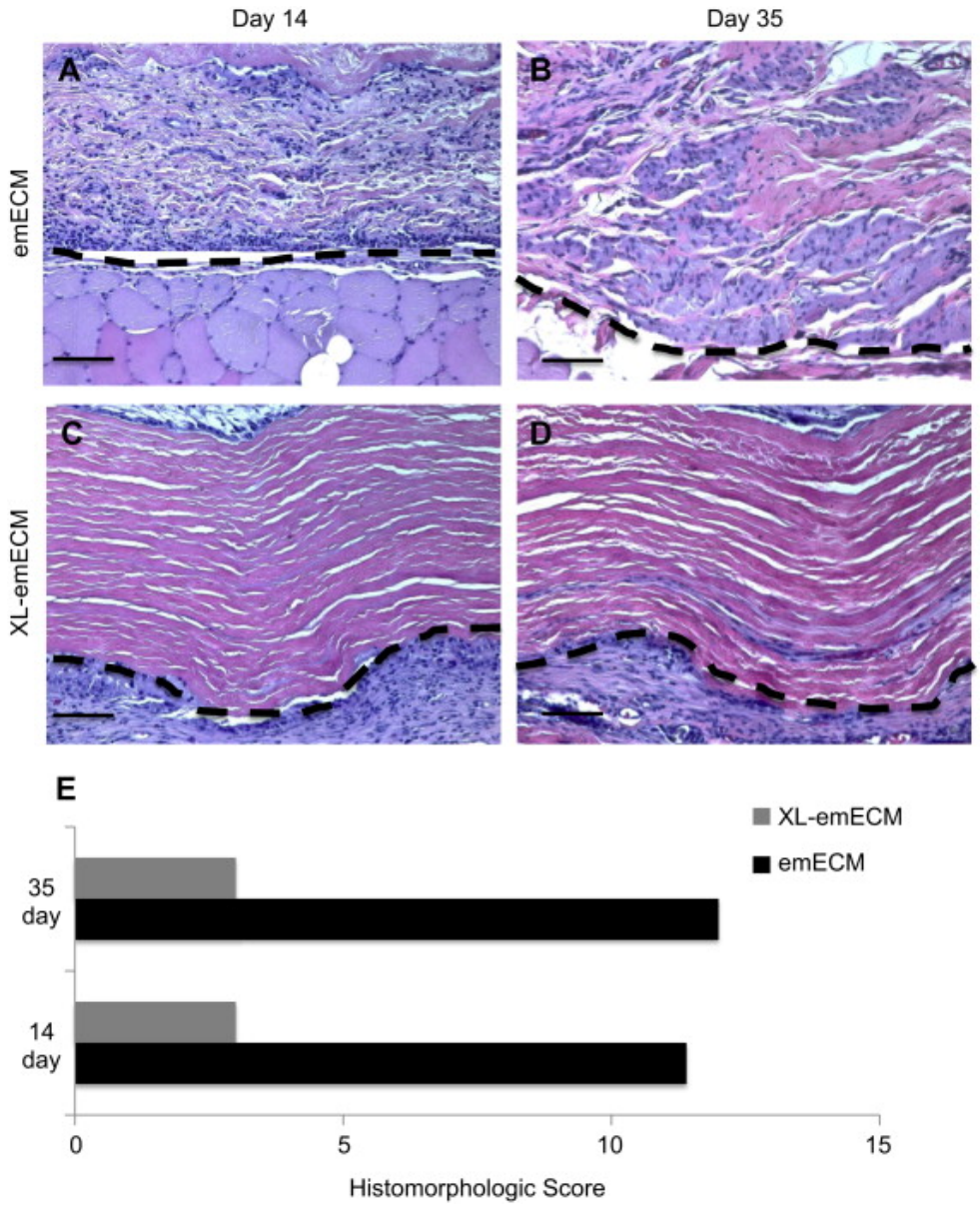

Figure 31. In-vivo Cytocompatibility

Tissue sections were stained with H&E at 14 and 35 days after implantation of emECM (A,B) and XL-emECM (C,D). Histomorphologic sections were evaluated and scored according to previously established criteria (E). Scale bar = 100 μm.

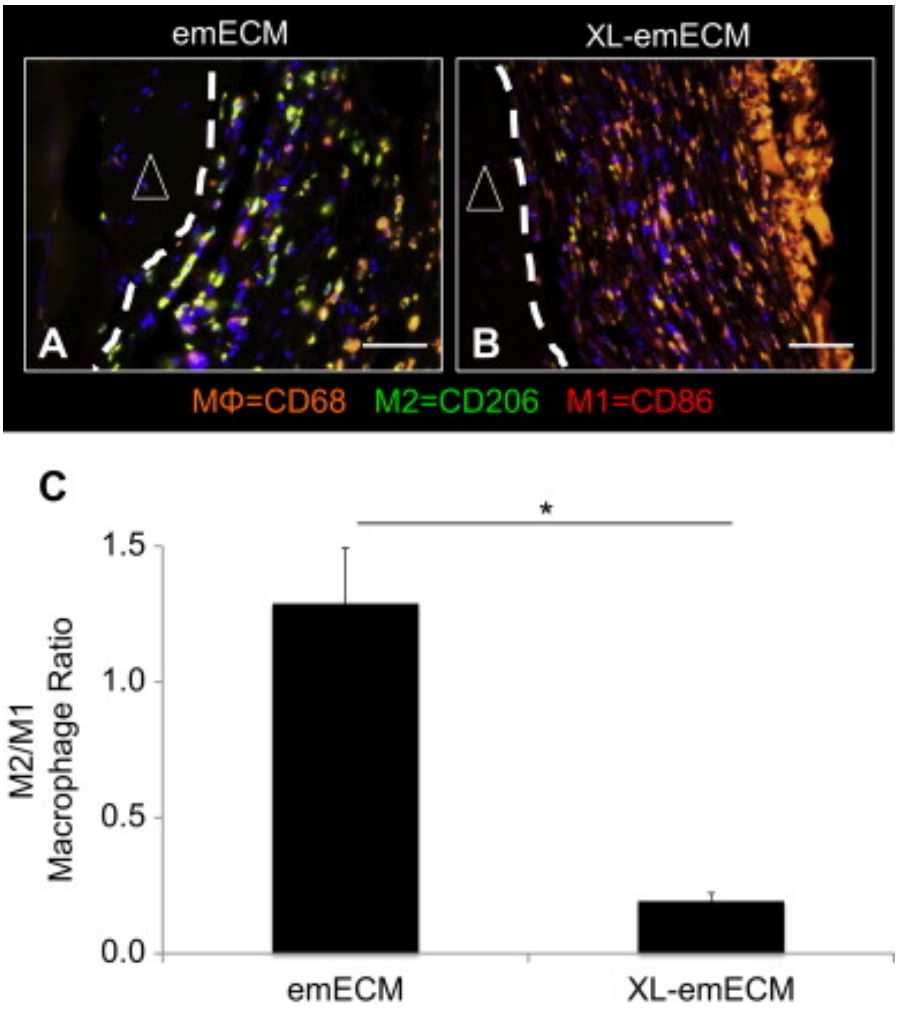

Figure 32. In-vivo macrophage response

Macrophage immunolabeling in emECM (A) and XL-emECM (B) in explants 14 d after implantation was quantified and represented as a ratio of M2/M1 phenotype (C). Dashed line indicates the interface of native tissue (marked by a triangle) and the surgical site. Data represented as mean ± standard error. Scale bar = 50 μm.

2.4 DISCUSSION AND CONCLUSIONS

2.4.1 Discussion

While ECM-derived materials were manufactured and characterized from both the muscularis layer and the mucosa layer of the esophagus, due to the clinical higher relevance of mucosal repair in the setting of neoplastic tissue resection, only the biocompatibility of ECM-derived scaffolds from the esophageal mucosa was assessed in vivo using the abdominal wall defect model, and subsequently in aim 2.

Although current clinical applications of ECM-based biologic scaffolds have included the use of devices originating from heterologous tissue sources, recent studies have suggested there may be an advantage to using ECM derived from homologous tissue (i.e., site-specific) [9, 58, 397, 398]. This concept is based upon the fact that ECM from different tissue sources have distinct and specific properties, including the ultrastructure and composition; i.e., a tissue-specific microenvironmental niche.

The necessity or preference for site-specific ECM remains unknown for many therapeutic applications. Zhang et al. have shown that ECM derived from liver, skin, and skeletal muscle increases the proliferation and differentiation potential for site-matched cell types [487]. Sellaro and colleagues have shown that ECM derived from liver improves the maintenance of sinusoidal endothelial cell phenotype [398] and the function of hepatocytes in-vitro [397]. More recently, porcine myocardial ECM has been shown to improve cardiac progenitor cell function in-vitro [143]. Seif-Naraghi et al. have shown that injection of a hydrogel form of cardiac ECM after myocardial infarct improves cardiac function and results in increased cardiac muscle mass [395]. Although the present study showed that the emECM facilitates a constructive remodeling

response in a heterologous location and excellent in-vitro cytocompatibility, any site-specific benefit in the esophageal mucosa (homologous) location has not yet been tested.

The importance of effective decellularization is well recognized [105, 231]. While protocols for decellularizing the esophagus have been reported, little has been described with focus on the esophageal mucosa. Bhrany et al. developed a rat full thickness esophageal scaffold that was able to support epithelial cell growth [47]. Marzaro et al. decellularized intact porcine esophagus and seeded with autologous smooth muscle cells for repair of an esophageal muscularis defect [284]. Using a similar protocol, Totonelli et al. decellularized intact esophagus using luminal perfusion [436]. These groups reported decellularization of the entire esophagus, including both muscularis externa and mucosa. However, the efficacy of these decellularization protocols, characterization, and cytocompatibility of the scaffold were not investigated in a comprehensive manner.

Protocols for esophageal decellularization have been reported but have been conducted using non-porcine species and/or have used harsh detergents such as sodium dodecyl sulfate (SDS) [41, 243]. SDS, as an ionic detergent, destroys the cell membrane and denatures protein—altering the collagen structure in ECM [105]. Thus, SDS has the associated drawback of ultrastructure disruption [124, 226, 332] and growth factor elimination [357]. A loss of ECM structure is also associated with variability in biomechanical properties [322]. Therefore, the use of SDS was avoided in the present study.

Studies have shown the requirement for retention of at least a portion of the submucosal tissue to promote constructive remodeling of the esophagus over stricture and scarring [4]. The

use of emECM would therefore appear a more logical strategy for clinical translation. The methods of the current study thoroughly decellularized esophageal mucosa with the use of mild detergents while preserving the anisotropic mechanical properties and bioactive molecules. The described method effectively removed cellular components while maintaining ECM constituents and basement membrane proteins, collagen IV and laminin, in a contiguous pattern at the surface of the emECM material. Scanning electron micrographs of the luminal surface of emECM showed a smooth contour that was also consistent with an intact basement membrane surface. The basement membrane complex may be of importance to esophageal mucosal remodeling because of its natural function of supporting the growth of epithelial cell populations [60, 330, 431]. The emECM scaffold was cytocompatible with perivascular stem cells, which were shown to survive and proliferate when cultured on the scaffold.

The role of the host response to biologic ECM scaffolds is a topic of interest and has been reviewed in detail elsewhere [62]. Briefly, the successful therapeutic efficacy of biologic scaffolds is attributed largely to the ability of these ECM-derived materials to modulate the innate immune response in favor of a constructive remodeling outcome over scarring/encapsulation. Key mediators of the innate immune response are macrophages—a highly plastic and heterogeneous cell population [65, 426]. Appropriately prepared biologic scaffolds have been shown to elicit a macrophage response that is predominantly of an anti-inflammatory (M2) phenotype which has been associated with a downstream constructive remodeling response (i.e., formation of functional, site-appropriate tissue) [31, 65, 67]. However, when biologic scaffolds are prepared using harsh decellularization methods, are chemically cross-linked, or are inadequately decellularized, a robust proinflammatory (M1) macrophage

phenotype is observed at the in-situ interface of host tissue and ECM scaffold and ultimately results in chronic inflammation, encapsulation, and fibrosis [65, 243]. In the present study, implantation of emECM scaffolds in an established rodent model was associated with a predominant M2 macrophage response after 14 days and was shown to remodel in a constructive fashion with a histomorphologic score comparable to urinary bladder matrix (UBM-ECM) and small intestinal submucosa ECM (SIS-ECM) [65, 410, 443]. These findings are consistent with the predictive association of the M2 phenotype with constructive remodeling outcomes [65].

The objective of the present specific aim was to develop and characterize two distinct esophageal ECM scaffolds originating from the different layers of the esophagus, but was limited by a number of factors. The effects of the resulting ECM scaffolds on esophageal cells were not studied. Instead, perivascular stem cells were used because they are well-characterized [108] and have been used in a number of studies to evaluate the cytocompatibility of a variety ECM scaffolds [437]. In addition, while retention of growth factor proteins was used as an indicator of the relative mildness of the decellularization protocol, the activity of the growth factors was not determined and the effect of the presence of these growth factors in the overall remodeling process is unknown. While the M2/M1 macrophage phenotype ratio has been shown to be strongly associated with a constructive remodeling response in several anatomic locations, a direct cause–effect relationship has yet to be established. Finally, the present study observed the in-vivo compatibility and constructive remodeling response of the emECM scaffold in a well-characterized abdominal wall defect model, a heterologous anatomic site. Thus, the potential benefits of ECM derived from homologous tissue (i.e., the use of emECM in an esophageal mucosal resection model) remain unknown.

2.4.2 Conclusions

Porcine esophageal mucosa was effectively decellularized with the use of a relatively mild detergent-based protocol. The emECM scaffold maintained structural proteins and an ultrastructure consistent with a basement membrane complex. Likewise, retention of sGAGs and bFGF was shown. Compared to native esophageal mucosal tissue biomechanics, the emECM scaffold was expectedly less compliant but retained similar anisotropy. The emECM biologic scaffold was conducive to stem cell viability in-vitro and was associated with a host innate immune response consisting predominantly of M2 macrophages and a more robust constructive remodeling response when compared to XL-emECM biologic scaffolds in-vivo. Future studies aimed at investigating the specific physical and/or biochemical factors responsible for the constructive remodeling outcome and the utility of an emECM biologic scaffold in an esophageal location are warranted.

3.0 TISSUE SPECIFIC EFFECTS OF BIOLOGIC SCAFFOLDS DERIVED FROM ESOPHAGEAL TISSUES

Aim 2: To evaluate the tissue specific effects of biologic scaffolds derived from esophageal tissues in vitro and in a preclinical murine model of esophageal mucosal resection.

3.1 BACKGROUND

ECM-derived scaffolds have been extensively used in multiple clinical applications for their ability to promote constructive tissue remodeling in several organ systems including the gastrointestinal tract [27, 274, 275, 315]. Furthermore, ECM-derived bioscaffolds have been produced via tissue decellularization[105] from virtually every tissue and organ [22, 106, 147, 272]. Once implanted, the host response is initiated with the Vroman effect followed by a series of complex and overlapling phases that involve the cellular component of the innate immune system and the exposure and release of matricryptic peptide fragments. Matricryptic peptides have been shown to modulate cell behavior and tissue remodeling events[4, 6, 7, 97, 110, 159, 361, 396], and ultimately lead to constructive tissue remodeling.

The ECM represents the structural and functional molecules secreted by the resident cells of every tissue and organ. Hence, the biochemical composition and mechanical properties of an ECM bioscaffold vary according to the tissue source from which the ECM is isolated and the methods of processing and manufacture [105, 271]. It stands to reason that the ideal substrate for cell survival, proliferation, differentiation, and functional tissue remodeling is the native ECM of the homologous tissue or organ. Recent work has described potential benefits of ECM scaffold materials derived from homologous tissue versus heterologous tissue when used in selected anatomic locations [9, 57, 101, 106, 144, 292, 397, 398, 487]. ECM bioscaffolds derived from homologous tissues can preferentially maintain tissue-specific cell phenotypes [9, 144, 397, 398], promote cell proliferation [9, 487], induce tissue-specific differentiation [101], and enhance the chemotaxis of stem cells [40, 57, 106]. However, these preferences have only been

shown in the context of in vitro experiments, and the role of tissue-specificity remains to be determined in vivo and in all ECM all therapeutic applications [27, 29, 468].

The objective of this Specific Aim was to study the cellular behavior and tissue remodeling events in response to esophageal mucosa ECM (emECM) versus small intestinal submucosa (SIS-ECM) and urinary bladder matrix (UBM) in vitro and in vivo. Previous studies have demonstrated that when cultured in a emECM-derived hydrogel, esophageal stem cells[115] have an increased capacity for organoid formation in comparison to other matrices[274] (Figure 33). Hence, in this aim, the chemoatractive and mitogenic properties of emECM were studied and compared to SIS-ECM and UBM-ECM, as well as their ability to promote constructive tissue remodeling in a murine model of esophageal mucosal resection.

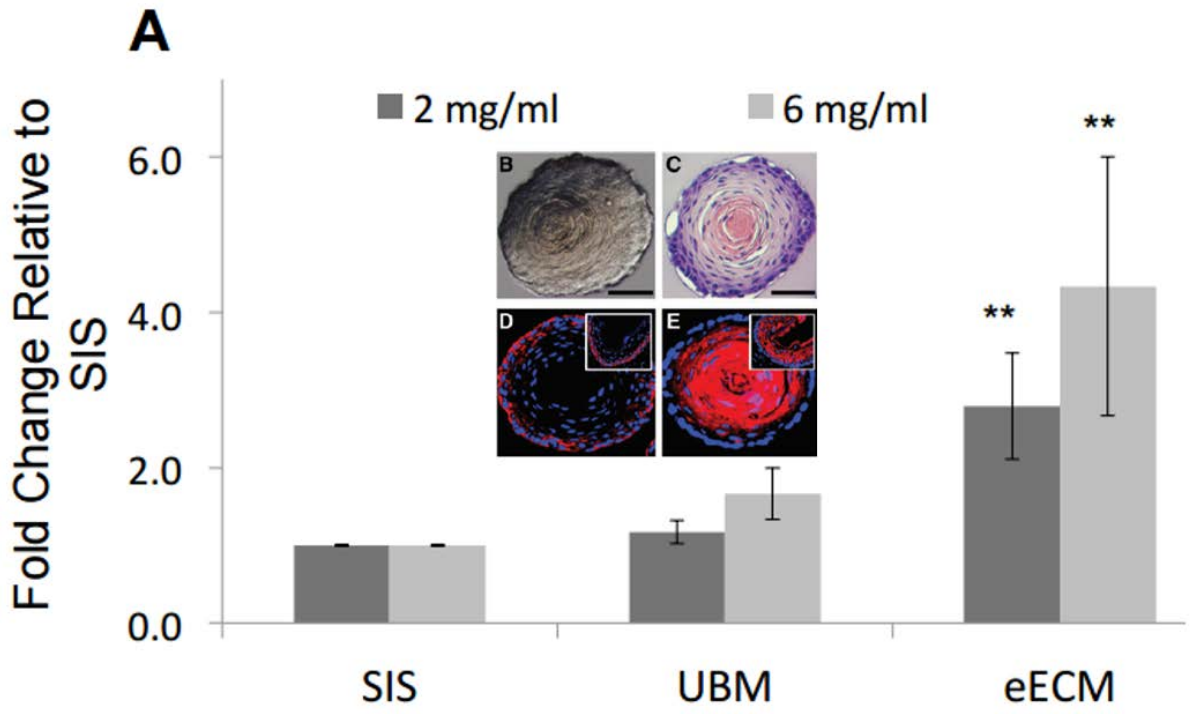

Figure 33. Organoid Forming Capacity

Esophageal stem cells show greater organoid-forming capacity when cultured in ECM hydrogels derived from esophageal tissues when compared to hydrogels derived from SIS-ECM and UBM-ECM

3.2 MATERIALS AND METHODS

3.2.1 Overview of experimental design

Porcine esophageal mucosa was decellularized to produce emECM. Using a population of heterogeneous esophageal primary cells, the ability for emECM to promote migration and proliferation was evaluated and compared to two benchmark ECM scaffolds; specifically urinary bladder matrix (UBM) and small intestinal submucosa (SIS). To assess the role of site specificity of ECM bioscafolds in esophageal repair applications, emECM and UBM scaffolds were subsequently implanted into a rat model of esophageal mucosa resection and the remodeling response was evaluated at 14 days post-surgery.

3.2.2 Animals

Female Sprague Dawley rats (350 – 400 g at implantation) were purchased from Harlan Laboratories and housed in the Division of Laboratory Animal Resources facility at the University of Pittsburgh McGowan Institute for Regenerative Medicine. Experimental protocols followed NIH guidelines for animal care and were approved by the Institutional Animal Care and Use Committee at the University of Pittsburgh.

3.2.3 Harvest and Preparation of ECM scaffolds and hydrogels

The esophagus, urinary bladder, and small intestine were isolated from market weight pigs and frozen at -20 °C until use. All ECM scaffolds were prepared according to established

decellularization protocols (Fig 1). Briefly, esophageal mucosal ECM (eECM) was prepared by mechanically separating the mucosa and submucosa from the muscularis externa and subjecting the mucosal layers to 1% trypsin/0.05% EDTA (Invitrogen, Carlsbad, CA) for 1 h at 37 °C on a rocker plate, deionized water for 15 min, 1 M sucrose (Fisher Scientific, Pittsburgh, PA) for 30 min, deionized water for 30 min, 3.0% Triton X-100 (Sigma Aldrich, St. Louis, MO) for 48 h, deionized water for 15 min, PBS (Fisher Scientific) for 15 min, 10% deoxycholate (Sigma Aldrich) for 4 h, deionized water for 30 min, 0.1% peracetic acid (Rochester Midland Corp., Rochester, NY) in 4.0% ethanol for 4 h, 100 U/mL DNAse (Invitrogen) for 2 h on a rocker plate, followed by 15 min washes with PBS, deionized water, PBS, and deionized water [230]. All washes were at 300 rpm unless otherwise specified.

Small intestinal submucosa (SIS) was prepared by mechanically removing the superficial layers of the tunica mucosa, tunica serosa, and tunica muscularis externa from the intact small intestine, leaving the submucosa, muscularis mucosa, and basilar stratum compactum intact. Urinary bladder matrix (UBM) was prepared by mechanically removing the tunica serosa, tunica muscularis externa, the tunica submucosa, and majority of the tunica muscularis mucosa from the intact bladder, leaving the lamina propria and basement membrane intact. The SIS and UBM were then subjected to 0.1% peracetic acid in 4.0% ethanol for 4 h, followed by 15 min washes with PBS, deionized water, PBS, and deionized water as described above. All treatments were performed at room temperature with agitation on a shaker plate at 300 RPM unless otherwise stated.

For implantation studies, the ECM scaffolds were lyophilized using an FTS Systems Bulk Freeze Dryer (Model 8-54) and sterilized with ethylene oxide. For studies using a hydrogel form of the ECM, the decellularized ECM sheets were lyophilized and comminuted to a particulate form using a Wiley Mini Mill. One gram of lyophilized ECM powder and 100 mg of pepsin (Sigma) were mixed in 100 ml of 0.01 M HCl and kept at a constant stir for 48 h at room temperature.

3.2.4 Isolation and Culture of Esophageal Primary Cells

The esophagus was removed from Sprague Dawly rats followed by physical separation of the mucosa using forceps. The muscularis was minced into small pieces and digested with 1mg/ml Collagenase and 1mg/ml Dispase for 1 h each and remaining tissue were passed through a 70 µm filter to obtain a single cell suspension. The heterogeneous cell population was then placed in tissue culture flasks and cultured in high glucose DMEM media containing 10% fetal bovine serume (FBS) and 1% penicillin streptomicin. The cells were then expanded in culture and passaged for use in the experiments. Cells used for the experiments consisted of pasages 1 and 2.

3.2.5 Preparation of ECM Digestion Products

ECM from different groups (esophageal, UBM, and SIS) was harvested from porcine tissues as previously described. Decellularized material was digested at 10 mg/mL dry weight with 1 mg/mL pepsin (Sigma) in 0.01N HCl for 48 h at 20°C before dialysis at 4°C into phosphate-buffered saline (PBS). Protein concentration was quantified using the BCA protein assay

(Thermo) against bovine serum albumin. The resultant material was referred to as ECM degradation products.

3.2.6 Migration Assay

Migration assays were performed using a 48 well chemotaxis chamber with polycarbonate filters containing 8 μm pores (Neuro Probe, Gaithersburg, MD). The filters were coated with 20 μg/ml collagen (Sigma) and dried prior to use. The bottom wells of the chamber were loaded with 30 μl containing 25 or 100 μg/ml of emECM digest and the top wells were loaded with 50 μl containing 7×104 esophageal cells. Control wells consisted of serum free media and media containing 10% FBS. Following a 3 h incubation, the top filter surface (non-migratory) was scraped and the bottom of the filter was fixed in 95% methanol for 5 min and then mounted on a glass slide with mounting media containing DAPI (Vector Laboratories Inc, Burlingame, CA) and imaged. Migrated cells were quantified using ImageJ (NIH) to set the threshold and count cells, with binning to resolve cell clusters of various counts. The same ImageJ macro was used to analyze all images. Experiments were performed using 4 technical replicates with 3 separate biologic replicates (n=3).

3.2.7 Proliferation assay

Cells isolated from esophageal tissues were inoculated at a concentration of 1 × 104 cells per well in standard 12-well plate (well area 3.8 cm2) at 6% or 21% oxygen. Cell growth was monitored every 24 h using manual counts. Cell proliferation was also monitored via immunohistochemical methods using the thymidine analog 5-bromo-2′-deoxyuridine (BrdU) ELISA (Roche). BrdU incorporation was detected using the supplied anti-BrdU antibody. Cells were plated at 5 × 104 cells per well in a standard 96-well plate with emECM, SIS or UBM at 15 μg/mL digest material and labeled with BrdU for 18 h. Relative proliferation was quantified at 370 and 492 nm in a plate reader (Molecular Devices). Each assay was performed in triplicate on three separate occasions. Statistical significance was evaluated by the Student's t-test and a p-value of 0.05 was considered significant.

3.2.8 Surgical Procedure and ECM Implantation

All surgical procedures were approved by the Institutional Animal Care and Use Committee at the University of Pittsburgh and the animal care complied with the National Institutes of Health Guidelines for the Care and Use of Laboratory Animals. Induction and surgical plane of anesthesia were achieved with 2% inhaled isoflurane and the animals were placed on a warming pad in supine position. The cervical skin was shaved and aseptically prepared with ethanol and betadine. A midline cervical incision was performed above the clavicle and the esophagus exposed via blunt dissection. A transverse incision of the muscularis externa layer was performed, and a window of full thickness mucosa extending 5-10 mm length including 70% of the circumference was resected. Animals treated with ECM received a single layer sheet that was

placed over the denuded area and secured in place with interrupted 10.0 prolene sutures (Ethicon, Somerville, NJ). The denuded mucosa was left exposed in non-treated control animals. Skin was closed with 4.0 Vicryl (Ethicon) and buprenorphine (0.5 mg/kg, Benckiser Healthcare (UK) Ltd, Hull, England) was administered intramuscularly immediately postoperatively and twice a day for 3 days. Animals were placed on a soft diet for 5 days post operatively.

3.2.9 Histology and Immunolabeling

Two histology and immunolabeling studies were performed on the explanted esophageal tissue sections. Explanted esophageal tissue sections were fixed in 10% neutral buffered formalin and paraffin embedded.

Serial sections (8 μm) of the samples were stained with hematoxylin and eosin or immunolabeled. Antigen retrieval was performed by heating a citrate antigen retrieval buffer (10 mM citric acid with 0.05% Tween 20, pH 6) until boiling, and incubating the slides in the solution until returning to room temperature. Three washes in phosphate buffered saline (PBS) for five minutes at room temperature were performed. Tissue sections were permeabilized with 1x Tris-Buffered Saline with Tween 20 (TBST) for 10 minutes at room temperature. The slides were incubated in a blocking solution (5% BSA in 1x PBS) at room temperature to prevent non-specific binding. The slides were incubated in primary antibody blocking solution at 4°C overnight. Five washes in PBS were performed for 5 minutes at room temperature. Slides were incubated in secondary antibody in blocking buffer at room temperature for 1 hour. Five washes in PBS were performed for 5 minutes at room temperature. The primary antibodies used for the immunolabeling studies cytokeratin 14 (1:200; NBP1-67606, Novus Biologicals, Littleton, CO) for tissue sections. The secondary antibodies used were Alexa Fluor 488 (1:200; A-11034,

Invitrogen) and Alexa Fluor 594 (1:200; A21203, Invitrogen). Sections were counterstained with 4',6-diamidino-2-phenylindole (DAPI) and mounted in fluorescence mounting medium (Dako). Stained sections were visualized on Nikon E600 fluorescence microscope with Cri Nuance FX multispectral imaging system.

3.2.10 Statistical Analysis

Data sets were analyzed with a one-way analysis of variance (ANOVA) using SPSS Statistical Analysis Software (SPSS Inc., IBM, Chicago, IL). A student t-test was used to identify the differences between means when the observed F ratio was statistically significant ($p < 0.05$). Data are reported as mean ± standard error.

3.3 RESULTS

3.3.1 Degradation Products from ECM Bioscaffolds Promote Cell Migration

The chemotaxis of primarily isolated heterogeneous esophageal cell populations was evaluated using a Boyden chamber assay. Two concentrations of ECM were chosen to determine whether a migration dose response existed. The esophageal cells did not migrate toward serum free media or 10% FBS. However, the cells showed an increased migration response towards all the ECM groups and the positive control. Quantification of migrating cells (Figure 34) showed no statistical significance among groups.

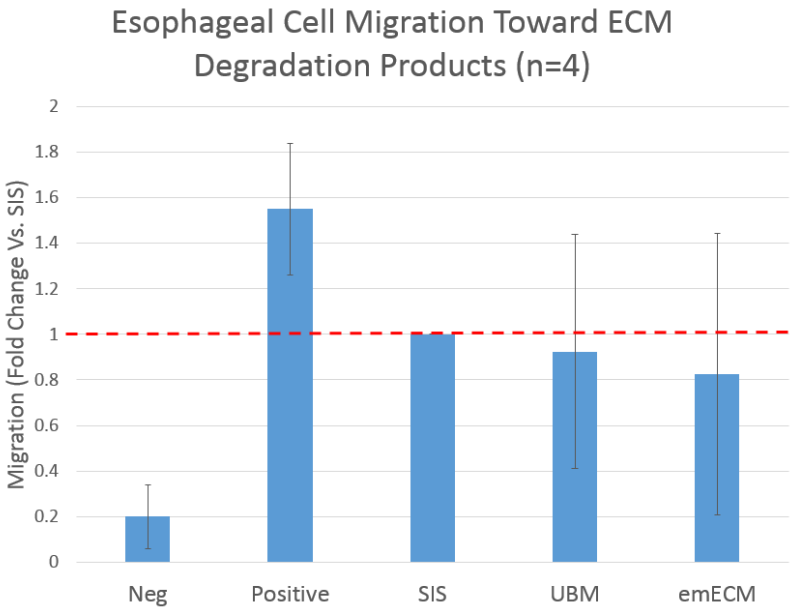

Figure 34. Esophageal cell migration towards ECM degradation products

Primary heterogeneous esophageal cell populations were exposed to degradation products of emECM, UBM, and SIS in a Boyden Chamber assay at concentrations of 25ug/ml and 100ug/ml. No differences were observed between the groups. Equivalent trends have been observed in other studies [359]

3.3.2 Degradation Products from ECM Bioscaffolds Promote Cell Proliferation

Proliferation of cell was assessed via manual counts and by incorporation of EdU. Degradation products of ECM were shown to promote cell proliferation when compared to negative controls. However, there was no difference among the values for proliferating cells culture in eECM, SIS and UBM (Figure 35).

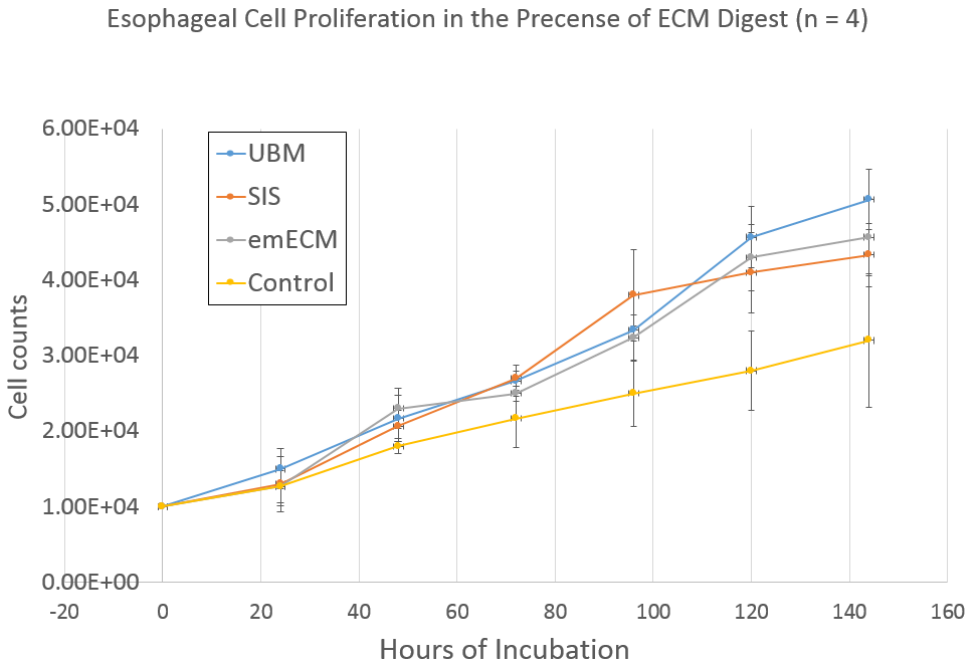

Figure 35. Degradation products of ECM bioscaffolds promote esophageal cell proliferation

Esophageal cell populations exhibit increased growth media containing ECM degradation products compared to controls. Growth of Cells were plated at an initial seeding density of 1 × 104 per well and triplicate wells harvested every 24 h with total cells per well counted. Data presented as means of triplicate determinations with standard deviations. Equivalent trends have been observed in other studies [359, 437]

3.3.3 ECM-Mediated Esophageal Mucosal Remodeling

The ability of ECM to mediate tissue repair in the esophageal mucosa was tested in a rat model of mucosal resection. Following resection of approximately 7 mm length of esophageal mucosa consisting of 70% of the circumference, a size-matched ECM scaffold was placed at the site of tissue resection (Figure 36). Rats weighed 228 ± 2.5g prior to operation, and all animals lost weight following mucosal resection. The ECM treated rats gradually gained weight over time. Eighty-three percent (5 out of 6) of the untreated control animals showed anorexia and complications secondary to anastomotic leaks and stricture formation that required removal from the study prior to the predetermined experimental endpoint. The remaining control rat showed no signs of mucosal coverage of the implant site (Figure 38A). The emECM treated rats lost -7.4 ± 1.3% vs. -11.9 ± 2.5% for the UBM treated rats by 3 days post surgery compared to the UBM treated rats although the difference was not significant ($p=0.243$). By 14 days post surgery both groups had recovered from the weight loss and exceeded their initial weight (emECM +2.4 ± 2.7% vs UBM +1.4 ± 2.6%) (Figure 37). All of the ECM treated rats recovered from surgery and survived to the experimental endpoint (14 days) without complications. Representative images show that remodeling of the esophageal mucosa was indistinguishable in rats treated with UBM (Figure 40B) vs. emECM (Figure 38C). Positive staining for CK14, a marker of basal esophageal epithelium, was absent in the control animals (Figure 38D) but was shown in cells lining the basement membrane of the esophageal mucosa in rats treated with both UBM (Figure 40E) and emECM (Figure 38F).

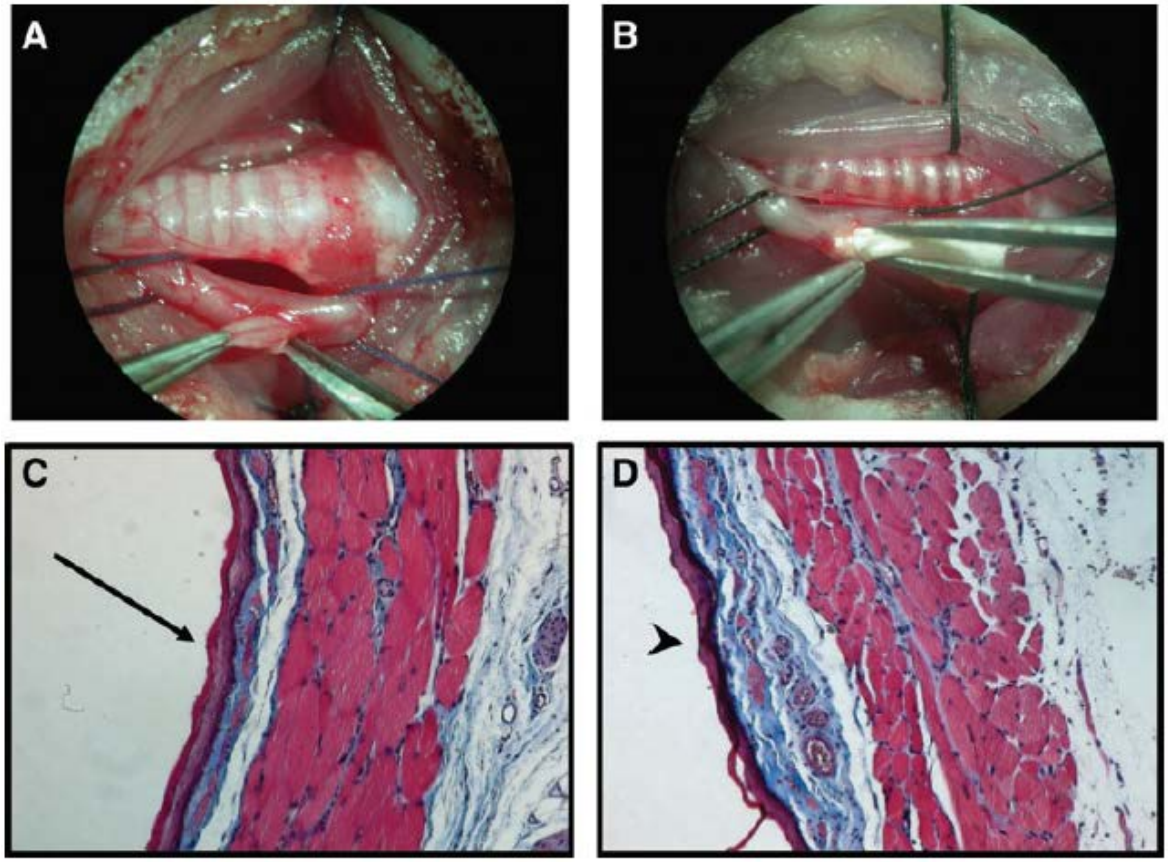

Figure 36. Esophageal mucosal resection in the rat model

(A) Mucosal resection in the rat is performed by exposing the esophagus around the trachea and performing a mucosectomy through a horizontal incision in the muscularis layer of the esophagus. (B) Once the mucosa is removed, an extracellular matrix (ECM)-derived biomaterial is delivered in situ to facilitate constructive tissue remodeling. (C) Masson's trichrome stain of native esophageal mucosa (arrow) and (D) remodeled esophageal mucosa after biomaterial-mediated repair showing intact keratinized epithelium (arrowhead).

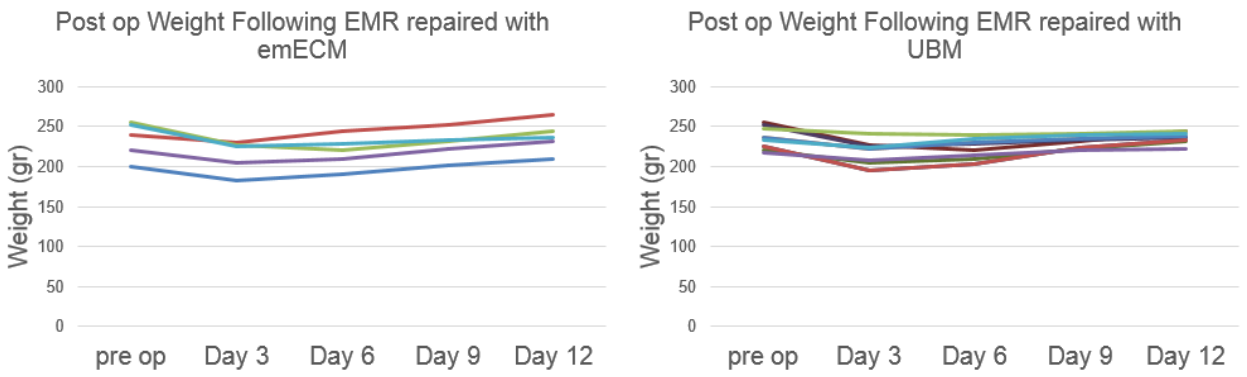

Figure 37. Post-Operative weight of animals undergoing ECM-mediated mucosal repair.

Animals in the no treatment control group present clinical stricture formation and fall below 20% pre-op weight or expire within 4 days and are therefore excluded from the study.

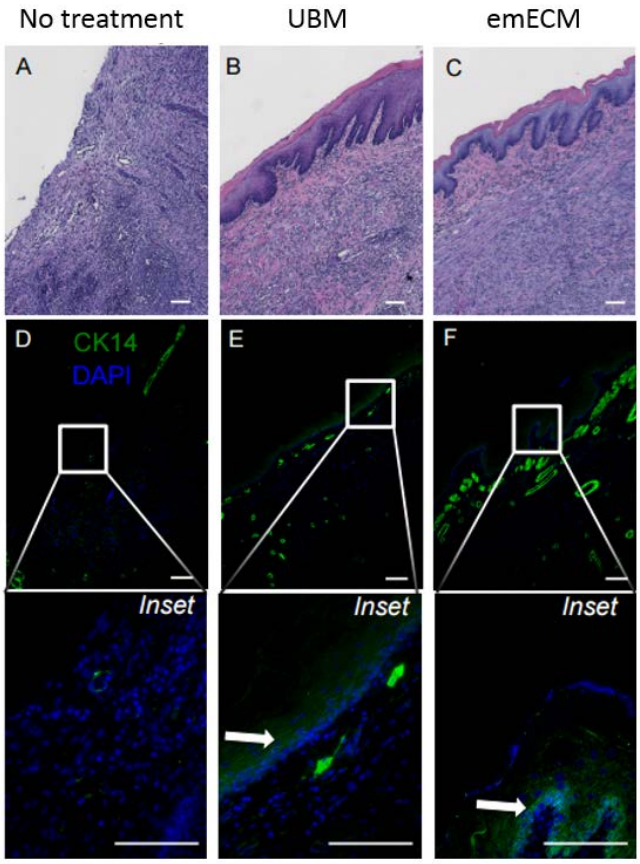

Figure 38. ECM mediated esophageal mucosal repair

Histologic images showin ECM mediated esophageal mucosa repair at 14 days post implantation. A) No treatment control shows an inflammatory cell infiltrate in the esophageal lumen devoid of a normal esophageal mucosa and consistent early stages of collagen deposition and scar tissue formation. B) and C) show a histologically unremarkable neo-mucosa in the groups treated with UBM and emECM respectively. Immunolabeling with cytokeratin 14 stain show no site appropriate differentiated cells in the no treatment control group and positive cells in both UBM and emECM treatment groups.

3.4 CONCLUSION AND DISCUSSION

The clinical translation of successful regenerative medicine strategies for tissue repair is contingent on the implementation of adequate and relevant animal models that permit both the investigation of the mechanisms of tissue repair and the evaluation of the safety and efficacy of these therapies.

Animal models are important tools to predict in vivo human behavior [133]. However, the term has often been used inappropriately to imply that only work with species that closely duplicate human physiology can be useful. Instead, it is important to recognize that there is both a unity and a diversity within animal models [187] and that both differences and similarities can and should be exploited in the development of regenerative medicine strategies for tissue repair.

Results of the present aim indicate that while a homologous emECM preferentially enhances the migration of esophageal stem cells and supports the formation of 3D organoids in culture - as shown in previous studies by Keane et al[275], there seems to be no difference in the ability to attract heterogeneous esophageal cell populations, or in the ability to promote non-stem cell proliferation in vitro. In line with these findings, in-vivo remodeling events of the esophageal mucosa were found to be similar with the use of heterologous (UBM) vs. homologous (emECM) scaffolds. These collective results suggest that although the mucosa of the esophagus might contain favorable tissue-specific properties that are retained following the decellularization process, the contribution of these properties may only be relevant under specific circumstances involving stem cell activity. In contrast, in vitro work with heterogeneous stem cell populations and the overall in-vivo remodeling process are either not identifiable with these experiments or not necessary for the process of constructive remodeling to occur. These findings are in line with other published studies that suggest that tissue specificity of ECM-derived

biomaterials is particularly relevant in specific in vitro experiments involving isolated stem cell and fully differentiated cell types[9, 106, 397, 398].

Furthermore, while the cells that contribute to esophageal remodeling following mucosal resection in the present study are not completely identified, the resident esophageal stem cell population represents a plausible and logical candidate [121]. These cells are present in the basal layer of the esophageal mucosa and following tissue resection must migrate the length of the mucosal resection to aid in tissue repair. Results of the present study show that ECM constituents facilitate the migration and proliferation of esophageal cells

A key indicator of the success or failure of an ECM scaffold to facilitate constructive and functional tissue repair is the host response to the material following implantation. While a distinct and tissue-specific ECM-dependent stem cell response has been observed in-vitro in, the in-vivo remodeling outcome at 14 days post surgery yielded an indistinguishable constructive outcome regardless of which ECM scaffold was used. The fate of the control animals clearly indicated that the mucosal defect was critically sized and both ECM scaffolds promoted a constructive remodeling response compared to the healing response of the untreated control animals. Whether the temporal remodeling response differed between UBM and emECM is unknown since only a single post-operative time point was studied.

Previous studies in the esophageal location suggest constructive tissue remodeling occurs with the use of UBM and SIS [27, 33, 316], incidentally, both heterologous forms of ECM. The use of heterologous ECMs has been well documented in other anatomic locations. In these

studies, all ECMs were successful in reducing stricture formation but the remodeled tissue did not fully reconstitute all components of normal esophageal tissue; for example, glandular tissue was absent . The present study showed that heterologous source ECM scaffolds were inferior to site-specific ECM in-vitro but in-vivo differences in outcomes in eECM vs. UBM at 14 days post mucosectomy were not identified. Species differences in the rat and human esophageal histology, namely the lack of submucosal glands in the rat esophagus, would require testing in a large animal model to determine whether eECM may have clinical benefits.

A variable in the present study that should be noted is that the ECM materials were derived from xenogeneic tissues. However, this is quite representative of the clinical scenario, where a large majority of commercial scaffolds composed of ECM are from a porcine source [229]. Practical considerations favor the use of xenogeneic tissues as they are in abundant supply through the agricultural supply chain. More importantly, the constituent molecules of ECM are some of the most highly evolutionarily conserved proteins across species [210, 212, 250]. The present study shows that porcine eECM regulates murine esophageal stem cell behavior and also mediates esophageal remodeling in the rat, consistent with known species homology of ECM constituents.

There were limitations to the present study. First, the response of only one cell type was evaluated. Esophageal stem cells are not the only cell population that may contribute to remodeling of the esophageal mucosa. Another potential contributing cell population is the multipotent perivascular stem cell [5, 108]. Perivascular stem cells are found surrounding endothelium of normal tissue and are likely to be present in the vasculature within the esophagus.

A number of studies have reported the chemotactic and mitogenic potential of ECM for the perivascular stem cell population [5, 437]. Another limitation of the present study was the use of different decellularization protocols for preparing the ECM scaffolds. Decellularization protocols are typically dictated by tissue-specific characteristics, which almost always differ to achieve effective decellularization. Use of a single decellularization protocol for all tissues in the present study would have resulted in ECM scaffolds with a different content of cell remnants and thus would have added a major variable [231]. The effects of the different decellularization protocols upon the results in the present study are unknown, but protocols similar or identical to those in the present study would likely be used in the clinical setting and therefore have potential clinical relevance.

In conclusion, the present study showed a superior in-vitro response of esophageal stem cells to homologous ECM vs. heterologous ECM. Surgical placement of the scaffold into a rodent mucosal defect, however, showed no differences in remodeling response for homologous vs. heterologous ECM. A single time point limited conclusions from the in-vivo portion of the present study and the preference of homologous ECM in the esophageal location is worthy of further investigation considering the unmet clinical need for therapeutic options for esophageal pathology.

4.0 A CARIDAC-ECM COATING TO MODULATE THE HOST RESPONSE TO A SYNTHETIC CARDIAC PATCH ON A MURINE MODEL OF MYOCARDIAL INFARCTION

Aim3: To evaluate the ability of cardiac-ECM to modify the host response to an implanted cardiac patch in a preclinical murine model of myocardial infarction.

4.1 BACKGROUND

The human heart is a complex organ that unlike the dermis, bone marrow, and the epithelium from the gut, does not have the ability to significantly regenerate. However, recent studies have reported the existence of stem cell populations in the heart, and have suggested that the possibility of recovery in fact exists [43, 259]. Despite these findings, the regenerative capacity of the heart has not yet been deciphered. Nonetheless, different regenerative medicine approaches are currently being developed for cardiac repair, and of these, the manipulation of host cell populations and modulation of the wound healing response are the most promising strategies[319].

Mortality rates from myocardial infarction have decreased significantly in the last few decades due to advancements in quick detection, the establishment of rapid emergency triage and treatment algorithms [356], and better management/medications for risk factors associated with CAD, including hypertension and dyslipidemia[449] (Figure 39).

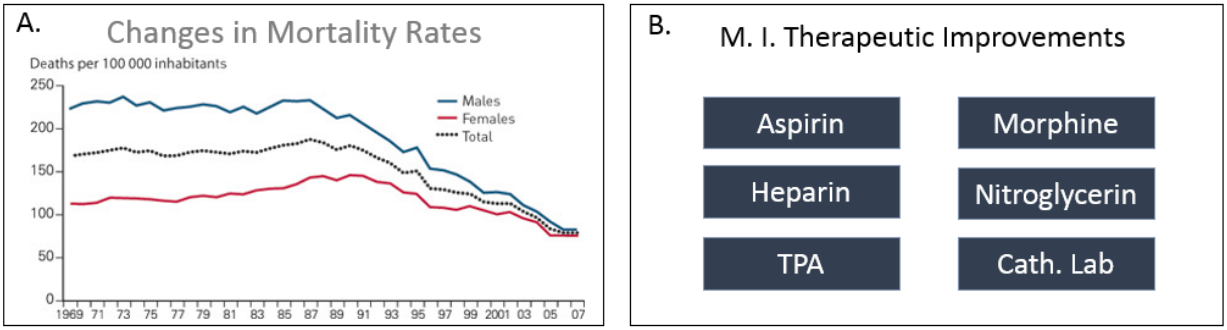

Figure 39. Decrease in MI Mortality. Adapted from [356]

A) The decrease in mortality associated with MI has steadily decreased due to B) therapeutic improvements.

However, due to unprecedented MI survival rates, more and more patients are now living with a partially dysfunctional myocardium with different degrees of severity often times leading to ventricular remodeling and heart failure[245]. In an attempt to prevent these events, several attempts to create cardiac patches to physically restrain the ventricular remodeling by providing additional support to the infarcted region [17, 153].

Our group has reported the implantation of an elastic and biodegradable polyester urethane urea (PEUU) cardiac patch onto a region of myocardial infarct can prevent adverse ventricular remodeling, altered LV wall thickness, and can promote compliance toward normal levels at the site of implantation.[178] The PEUU patch prevents myocardial encapsulation and provides temporary elastic support that mechanically alters the wall stress experienced by the infarcted region resulting in changes in the remodeling course pursued by the tissue towards a more desirable end. In addition, the degradable patch also avoids the existence of a permanent foreign body on the myocardial surface.

However, the host immune response to synthetic biomaterials is well described[13] and these materials lack the bioactivity present in natural ECM[271]. ECM-derived scaffolds contain bioactive molecules that exert in vivo mimicking effects as applied for soft tissue engineering, yet do not possess the same flexibility in mechanical property control as some synthetics[424]. Furthermore, studies have found that an ECM coating can mitigate the chronic inflammatory response and associated scar tissue deposition associated with synthetic meshes[136, 466](Figure 43) and therefore, we hypothesize that a biohybrid patch of PEUU-cardiac ECM is able to modify the host response to an implanted cardiac patch in a murine model of MI.

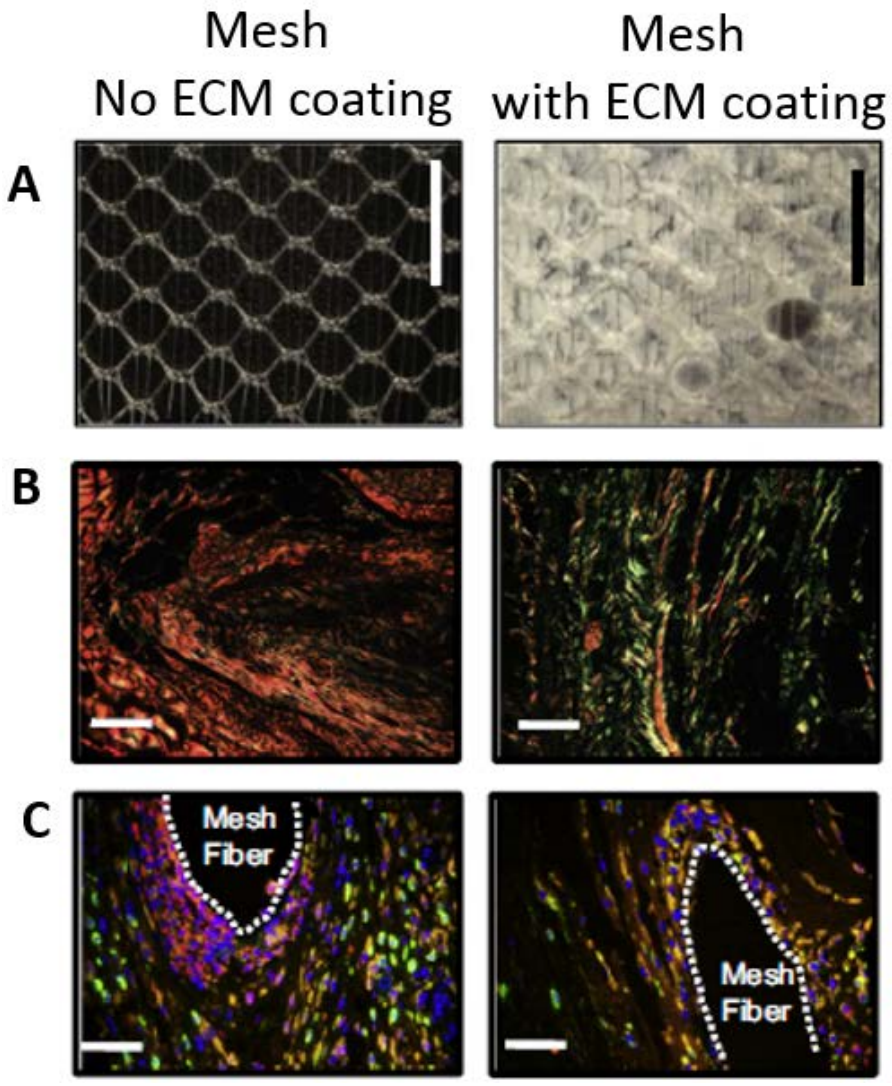

Figure 40. ECM coating of synthetic devices modulates the host response[136]

A) Gross morphology images of non-coated and ECM-coated polypropylene mesh. B)Six months after implantation, the constructs present different size and orientation of collagen fibers. C) ECM coating decreases the M1 macrophage (orange) – response typically associated with synthetic material fibers and promotes a pro-remodeling M2 phenotype (green). Nuclei – blue, DAPI stain.

4.2 MATERIALS AND METHODS

4.2.1 Overview of Experimental Design

A myocardial infarction (MI) was induced in Sprague Dawly rats via coronary artery ligation. Two weeks post MI the size of the infarction was assessed and any animals with smaller infarcts were removed from the study. Those with large infarcts were divided in three groups and implanted with patch composed of either PEUU alone, a biohybrid of PEUU and Cardiac ECM, or received no treatment. Eight weeks post implantation the animals were sacrificed and the tissue was processed for histology.

4.2.2 Cardiac Decellularization

This protocol for decellularization is available at[360]

4.2.2.1 Tissue Preparation and Experiment Setup

Porcine whole hearts were harvested immediately after euthanasia from an abattoir excess blood was rinsed off. Excess fat and tissue were trimmed off keeping the atria and aorta intact. The tissue was then frozen in a -80 °C freezer for at least 24 hr to ensure complete freezing.

When ready for decellularization, the tissue was thawed in Type 1 water overnight submerged in a 4 L beaker at 4 °C, patted dry, and its weigh was recorded. The heart of a market weight pig should weigh approximately 375-450 g. The heart was then connected to a size 18

Masterflex tubing to the ¼" end of a barbed reducer remaining above the aortic valve, so the coronary arteries can be perfused.

The tubing was filled with Type I water and inserted within the cartridge of a Masterflex roller pump at its approximate midpoint. The inflow end of the tubing was submerged in the bottom of a 4 L beaker filled with 2.5 L of water and secure the tubing.

The heart was placed in the beaker filled with water, and prime the pump to remove air bubbles. If bubbles were observed coming from the aorta where the tubing is inserted, the aorta may need to be repositioned or secured with additional ties. An airtight seal is important to maintain adequate pressure during the decellularization process. The 4 L beaker containing 3 L of a 0.2% Trypsin/0.05% EDTA/0.05% NaN3 solution was placed on a stir plate and warmed to 37 °C in preparation of the decellularization process.

4.2.2.2 Tissue Rinses

The pump was set to a flow rate of 400 ml/min, ensuring that the correct tubing size is selected. The heart was flushed with Type I water for 15-25 min. As the pump is started, the heart should swell and effuse blood from the ventricles. Fresh solution should be substituted every 5-10 min, or as needed based on the amount of blood removed from the heart. If blood is not effused from the heart, adjust the tubing and clamps as necessary.

The pump was stopped and the heart was transferred to a separate beaker filled with 2X Phosphate Buffered Saline (PBS). After the tubing was submerged in solution, the pump was started and increased the flow rate to 700 ml/min. The heart should remain in solution for 15 min, changing the solution every 5 min. Each solution change requires the pump to be stopped temporarily while the tissue and tubing is moved to the new beaker.

The heart was then transferred to Type I water for 10 min and increase the flow rate to 750 ml/min.

4.2.2.3 Decellularization and Solution Perfusion

The heart was transferred to the beaker containing 0.2% Trypsin/0.05% EDTA/0.05% NaN3 at 37 °C. The pump speed was increased to 1,200 ml/min and the pump stared using a stir bar placed at the bottom of the beaker to circulate solution in the beaker. The heart should remain in the 0.2% Trypsin/0.05% EDTA/0.05% NaN3 solution at 37 °C for a total of three hours. After 1 hr, the pump speed was increased to 1,500 ml/min. After an additional hour, the pump speed was increased to 1,800 ml/min. The tissue was slowly subjected to increased perfusion speeds to condition the tissue and prevent rupture of the vessels. The heart swells and nearly doubles in size during this step of the protocol. The tissue loses its natural color, progressing from the atria to the apex throughout the protocol.

After each solution perfusion, a two step rinse was performed to remove cellular debris, chemical residue, and aid cell lysis. Each rinse consisted of a 10 min rinse in Type I water followed by a 10 min rinse with 2X PBS solution at room temperature. Each wash consisted of removal of solution from the original beaker, adding rinse solutions, and circulating the perfusate within the beaker containing the submerged heart. After the 0.2% Trypsin/0.05% EDTA/0.05% NaN3 solution, water was perfused at 1,900 ml/min and then 2X PBS at 1950 ml/min.

The heart was transferred to a solution of 3% Triton X-100/0.05% EDTA/0.05% NaN3 at room temperature. Increase the pump speed to 2,000 ml/min and perfuse solution for one hour. The solution was removed from the beaker and replaced with fresh solution, the pump speed was increased to 2100 ml/min, and the fresh solution was perfused for an additional hour and a half, bringing the total time in 3% Triton X-100/0.05% EDTA/0.05% NaN3 to 2.5 hr.

The tissue was rinsed in Type I water at 2150 ml/min and 2X PBS at 2180 ml/min for 10 min each and transferred to a 4% Sodium Deoxycholate solution at room temperature. The pump speed was increased to 2,200 ml/min and perfuse solution for 3 hr. The tissue was rinsed in Type I water at and 2X PBS at 2,200 ml/min for 15 min each, changing the solutions after 5-10 min for each solution. The described perfusion steps may be split over multiple days by performing the rinse step twice and storing the heart with attached tubing overnight at 4 °C and submerged in Type I water.

The following day, a 5 min rinse with Type I water at 750 ml/min was performed, followed by a 5 min rinse in 1X PBS at 1,500 ml/min. The protocol may then be continued at the described flow rate in the proper solution.

4.2.2.4 Disinfection and Final Processing

The heart was transeferred to a 0.1% peracetic acid/4% ethanol solution and perfused in solution for 1.5 hr at 2,200 ml/min. The final rinses for the tissue were all performed at 2,200 ml/min. The tissue was perfused with 1X PBS for 15 min, followed by two 5 min washes in Type I water. This series of rinses is repeated once more in order to complete the solution perfusion procedure. After most of the water is removed, the weight of the cardiac extracellular matrix (C-ECM) was recorded. The heart can be expected to lose approximately 20-25% of its initial weight during the decellularization process (Figure 41).

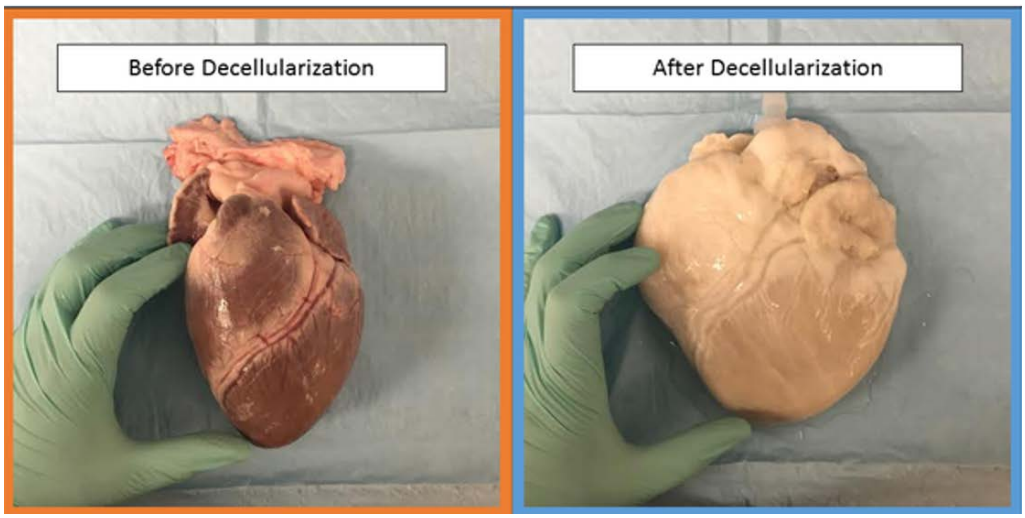

Figure 41. Porcine heart before and after decellularization

4.2.3 Preparation of Cardiac Patch

Polymer patches were were synthesized from soft segments of polycaprolactone (PCL, MW = 2000, Sigma) and diisocynantobutane (BDI, Sigma) hard segment with chain extension by putrescine (Sigma) according to a previous report. The soft segment:hard segment:chain extender molar ratio was set as 1:2:1. For scaffold fabrication, polymer samples were completely dissolved in hexafluoroisopropanol (HFIP) to obtain a 40% (w/v) solution. This solution (1 mL) was blended uniformly with 5 g salt particles (NaCl, Sigma), which had particle sizes of 75–100 μm obtained by serial treatment with American standard sieves. The polymer/salt mixture was poured into a 1 cm diameter cylindrical glass mold. After complete solvent evaporation, the mixture was immersed in an excess of 30% ethanol solution to remove the salt particles from the scaffold with frequent solution changes over 2 d of immersion. The scaffold was then placed in

pure deionized water to exchange the ethanol solution for 3 h, and then frozen at −80 °C, followed by lyophilization for 2 d to obtain a porous scaffold for implantation[202]. The material was sized to circular patches 6 mm in diameter and 300 μm in thickness. The patches were immersed in 70% ethanol for 30 min, followed by washing in phosphate-buffered saline and exposure to the ultraviolet light source for 1 h before implantation. [202]. Hybrid bioscaffolds were manufacter through electrospinning polymer and cardiac-ECM using a proprietary process.

4.2.4 Surgical Procedure

Adult female syngeneic Lewis rats (Harlan Sprague Dawley Inc.) 10–12 wk old, weighing 160–210 g were used for this study. The research protocol followed the National Institutes of Health guidelines for animal care and was approved by the Institutional Animal Care and Use Committee of the University of Pittsburgh (#0903312A-3).

4.2.4.1 Myocardial Infarction Model

The detailed procedure for creating the rat MI model has been described previously [150]. Briefly, rats were anesthetized with 3.0% isoflurane inhalation with 100% oxygen followed by intubation and respiratory support with a rodent volume-controlled mechanical ventilator (683 Ventilator, Harvard Apparatus, Holliston, MA) at a tidal volume of 3 mL and 80 breaths/min. Rats were placed in the right decubitus position, and the chest was shaved and prepared with povidone-iodine solution. Procedures were performed in a sterile environment on a heating blanket. The heart was exposed through a 4th left thoracotomy, monitoring electrocardiogram. The proximal left anterior descending (LAD) coronary artery was ligated with 7-0

polypropylene. Myocardial ischemia was confirmed by decreased movement in the left ventricle (LV) free wall, regional cyanosis and ST-segment elevation. The incision was closed in layers with 5-0 polypropylene continuous sutures. The animals were allowed to recover from anesthesia and returned to their cages. For prophylaxis of lethal ventricular arrhythmia, 10 mg/kg of lidocaine was administered intramuscularly once prior to surgery. For postoperative analgesic treatment, 0.1 mg/kg of buprenorphine was administered subcutaneously 3 times daily for 3 d after surgery. For prophylaxis of surgical site infection, 100 mg/kg of cefuroxime was administered intramuscularly twice daily for 3 d after surgery [183].

4.2.4.2 Patch implantation

Two weeks after coronary artery ligation, animals were anesthetized and examined echocardiographically for infarct size as estimated by the percentage of scar area (akinetic or dyskinetic regions) to LV free wall area. Animals with infarcts greater than 25% of the LV free wall were randomly divided into 3 groups: 1) PEUU patch orthogonal repair, 2) PEUU patch longitudinal repair, and 3) PEUU-Cardiac ECM patch repair (Figure 42). Through a 5th left thoracotomy, the infarcted anterior wall was exposed. Before affixing the patch, the surface of the infarcted area (less than 0.1 mm thickness), including the remnant epicardium and some of the integrated fibrous tissue, was scraped and removed at the patch implant site. Subsequently, the anterior infarcted myocardium was covered with a patch, using 7-0 polypropylene with over-and-over peripheral continuous sutures. For the infarction control group, a thoracotomy was performed 2 weeks after coronary ligation, but no scraping or patch placement was performed.

4.2.4.3 Determination of infarction size, scar area, and LV anterior wall thickening

The cross-sectional surface during sectioning was digitally photographed at the level of the center of patches. Infarction size was defined as a percentage of the sum of the epicardial and endocardial infarct circumference divided by the sum of the total LV epicardial and endocardial circumferences[266]. Scar area was measured as an infarction scar area using computer-based planimetry. LV anterior wall thickness was expressed as follows: scar area/[(epicardial circumference + endocardial circumference)/2]. Measurement of each parameter (n = 6 per each group) was performed using ImageJ analysis software on Masson's trichrome stained sections.

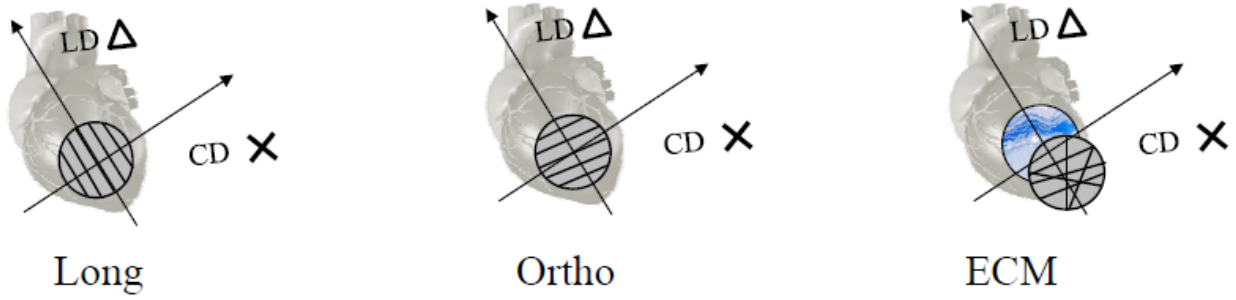

Figure 42. Experimental Groups

Implantation orientation according the orientation of the polymer fibers. 3 groups were used in this study: 1) PEUU patch orthogonal repair, 2) PEUU patch longitudinal repair, and 3) PEUU-Cardiac ECM patch repair.

4.2.5 Specimen Harvest and Histology

The heart (n = 6 per each group) was explanted and fixed in 2% paraformaldehyde for 2 h at 4 °C and then embedded with optimal cutting temperature compound (Tissue-Tek, Torrance, CA) followed by freezing at −80 °C. Embedded, frozen LV tissues were serially sectioned at 8 μm in the LV transverse direction at the center of patched area and mounted on microscopic glass slides and stained with Masson's trichrome.

4.2.5 Sample Analysis

Slides were examined with an Olympus IX51 microscope and images captured using DP2-BSW software (Olympus America Inc.). For each retrieved sample, 10 different microscopic fields at 200× magnification were photographed for αSMA or CD163 positive structures. To determine quantity of vessels or arterioles, the number of αSMA-positive structures was measured using a digital image analyzer (ImageJ v.1.41, National Institutes of Health, Bethesda, Maryland) at 200× magnification. Vessels were identified as tubular structures positively stained for αSMA. Arterioles were defined as αSMA-positive structures, having visible lumen, and more than 10 μm in diameter. All measurements and assessments were performed using a digital image analyzer (ImageJ). Values are reported as the area (μm2) per 200× magnification of high-powered filed (HPF, approximately 0.581mm2) for non-vascular αSMA and as numbers per HPF for αSMA-positive vessels and arterioles, and CD68- and CD163-positive structures. The number of structures positive for a specific antibody was counted for vessel, arteriole, and CD163 evaluation, while the area expressed in pixels was measured for the evaluation of non-vascular αSMA, CD68, elastin, collagen type I, and collagen type III.

4.2.6 Statistical Analysis

Statistical evaluations were performed using Prism version 4.0c (GraphPad Software Inc.). Results are listed as mean ± standard error of the mean. The Komolgorov–Smirnov test for normality was performed for each data set to determine the appropriate statistical testing. One-way ANOVA followed by Bonferroni multiple comparison testing was applied where multiple

comparisons were made at the same time point. For the temporal analysis of echocardiography including EDA and %FAC, two-way repeated measures analysis of variance (ANOVA) was performed using the Bonferroni correction. Differences were considered to be statistically significant at $p < 0.05$.

4.3 RESULTS

4.3.1 Cardiac Decellularization

The left ventricular wall was effectively decellularized via perfusion decellularization. H&E stains show no visible nuclei.

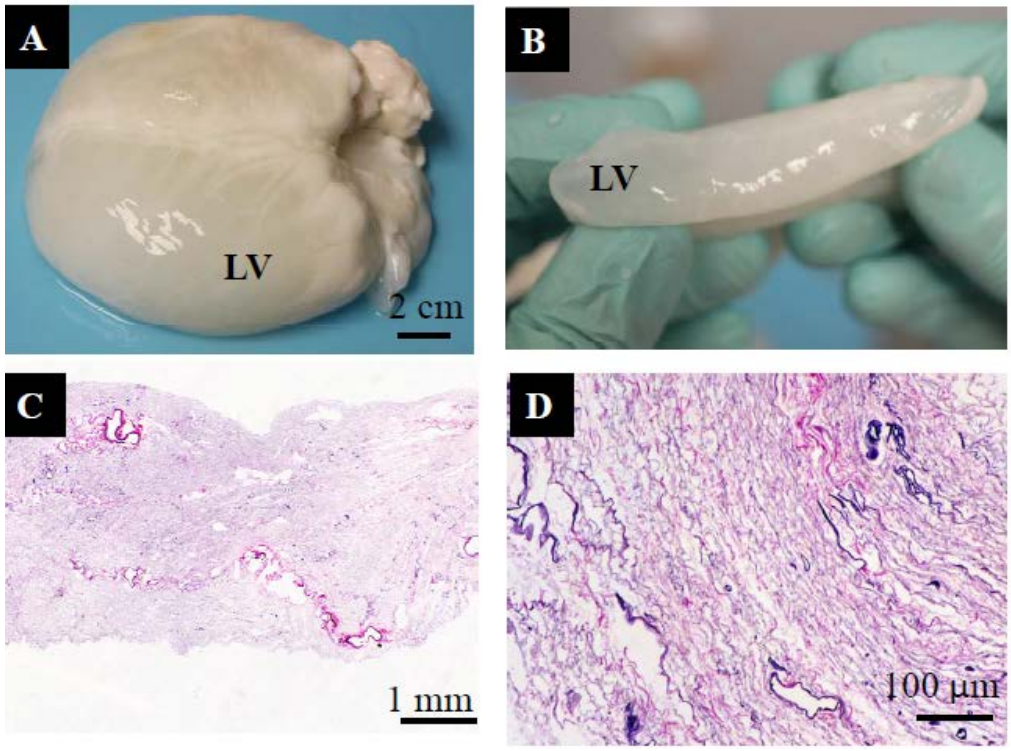

Figure 43. Cardiac Decellularization

A) Whole heart post decellularization. B) Gross image of cross section of the left ventricular wall. H&E cross sectional images show no visible nuclei at C) 100x and D) 400x magnification.

4.3.2 Preparation of Cardiac Patch

Cardiac patches for implantation measuring 0.5cm by 0.5cm were manufactured via electrospinning with either one polymer layer composed of PEUU, or with two layers: a polymer side with PEUU, and a cardiac-ECM rich side (Figure 44). Cardiac patch in situ after implantation (Figure 45).

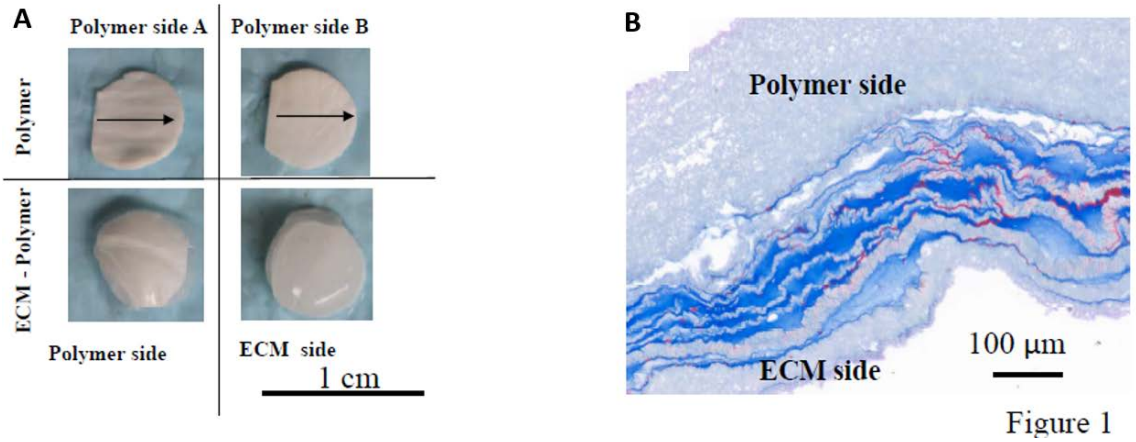

Figure 44. Cardiac Patch for Myocardial Repair

A) Macroscopic image of polymer (top) and hybrid patch (bottom). B) Trichrome stain of hybrid patch containing polymer layer (top) and cardiac ECM-rich layer (bottom).

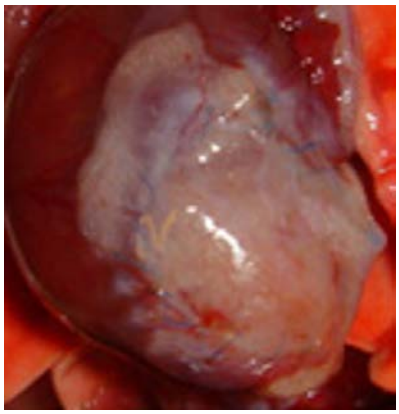

Figure 45. Cardiac patch implanted in situ [183].

4.3.3 Macroscopic Findings

Macroscopic inspection of the ventricular wall showed increased wall thickness in the cardiac ECM-PEUU patch treatment group (2.3cm) compared to PEUU patches implanted in the longitudinal and orthogonal direction (1.2cm and 1.4cm respectively). The left ventricular thickness of the cardiac ECM-PEUU not was statistically different from healthy controls (Figure 46).

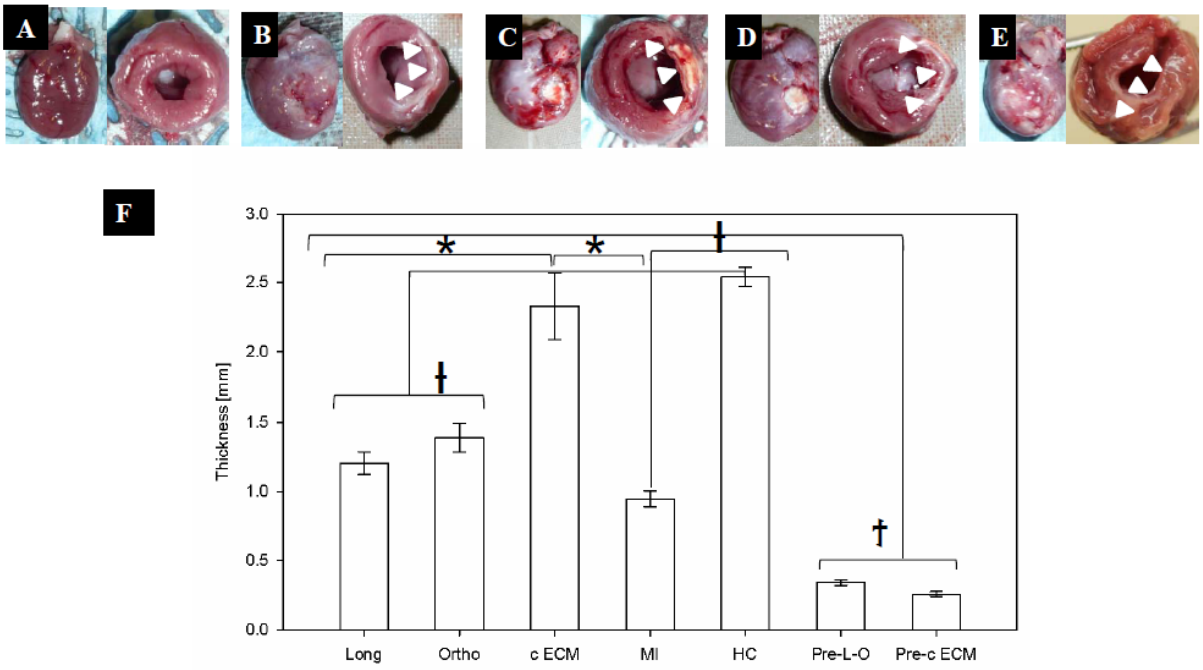

Figure 46. Gross examination of left ventricular wall thickness

Long: patch implanted in the longitudinal direction, Ortho: patch implanted in orthogonal orientation. C-ECM: cardiac ECM-PEUU patch, MI: myocardial infarction, HC: healthy control, pre-L-O: pre longitudinal and orthogonal implantation, Prec-ECM pre cardiac ECM-PEUU patch implantation.

4.3.4 Histomorphology

Microscopic examination of the explanted samples and quantification of the area covered by muscle and scar tissue thickness showed the cardiac ECM-PEUU patch treatment group was able to reduce scar tissue thickness compared to PEUU patches implanted in the orthogonal direction. Thickness of muscle tissue was unchanged among treatment groups. (Figure 47).

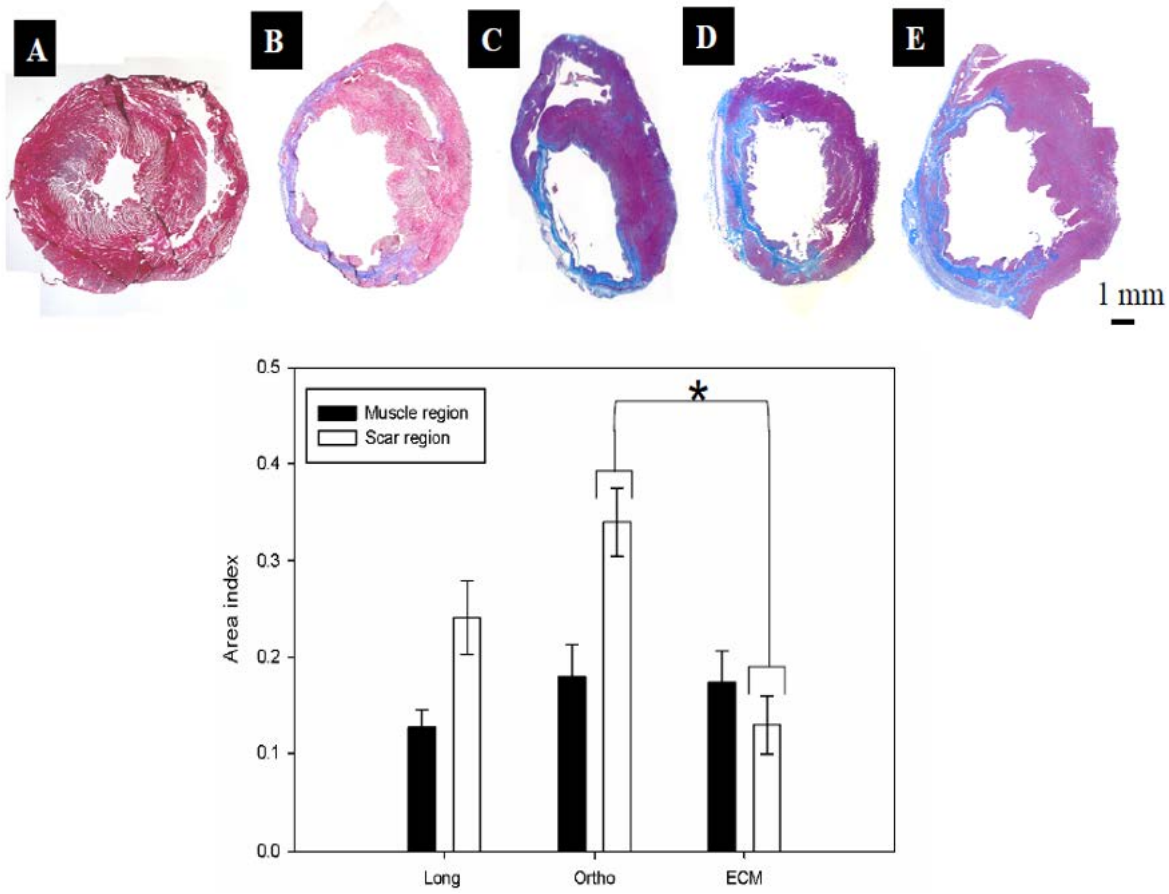

Figure 47. Histologic Examination

Histologic examination of H&E stained tissue sections showed a reduction of scar tissue formation in the cardiac ECM-PEUU patch treatment group.

4.4 DISCUSSION AND CONCLUSIONS

Remodeling events observed in the myocardium following infarction are the result of compensatory mechanism secondary to ischemic cardiomyopathy. These remodeling events are characterized by thining and bulging of the ventricular walls and ultimately lead to heart failure.PREvious studies report that polymer patches composed of PEUU can act as temporary mechanical barrier that can mitigate the amount of ventricular wall remodeling and functional loss following myocardial infarction [139, 182].

However, the host response to synthetic biomaterials is a well described event that in the case of degradable materials, does not lead to constructive tissue remodeling [271, 470]. The data in the current study demonstrated that the addition to of cardiac ECM component to the polymer patch can modify the host response and lead to less scar tissue formation per histologic analysis, and prevention of ventricular wall thining.

Synthetic biodegradable material implantation induces an inflammatory response[13]. However, ECM-derived biomaterials are immunomodulatory [136, 207, 244, 466]. The magnitude of inflammatory response associated with synthetic biomaterials depends upon the specific material chemistry and other physical parameters. As the primary cell type of the post-acute foreign body response, macrophages produce a spectrum of enzymes and cytokines that facilitate tissue remodeling in terms of matrix degradation, cell recruitment, proliferation and extracellular matrix formation for new tissue regeneration. Extracellular matrix-derived biomaterials have been show to modulate these processes both in vivo[408] and in vitro[359].

The addition of a cardiac ECM component to cardiac polymer patches is efficacious in reducing ventricular wall thining and reducing scar tissue formation when compared to polymer patches without an ECM component. These results indicate that a hybrid patch provides a greater benefit in treating ischemic cardiomyopathy than morphologically similar PEUU patches in the rat model. This conclusion was supported gross morphology findings and histological assessment which showed superior performance of the hybrid patch. These results are in line with findings of hybrid bioscaffolds used in other applications [136, 466] and support a tuned biomaterial approach to modulate the remodeling process that occurs in ischemic cardiomyopathy.

5.0 DISSERTATION SYNOPSYS

The work presented in this dissertation focused on the development and characterization of ECM bioscaffolds derived from esophageal tissues and the examination of homologous tissue specificity upon constructive tissue remodeling both in vitro and in vivo models of tissue repair. This work showed that porcine esophageal and cardiac tissues can be decellularized and that the resulting scaffolds are compliant with criteria for decellularization. Furthermore, the resulting scaffolds are able to promote chemotaxis and mitogenesis in vitro, as well as macrophage differentiation into the M2-proremodeling phenotype. Surgically placed ECM-derived bioscaffolds in a model of esophageal mucosal repair are able to promote constructive tissue remodeling. This work also showed that contrary to other studies, homologous site specificity does not play a role in heterogeneous cell population migration and proliferation, or in the host response following in vivo implantation. Modification of existing polymer based scaffolds with the addition of a cardiac-ECM component was able to modify the host response to an implanted cardiac patch following ischemic events in a murine model of myocardial infarction. The major findings for each specific aim are outlined below.

5.1 MAJOR FINDINGS

The major findings of the present work were:

Aim 1: To develop and characterize extracellular matrix based bioscaffolds from the mucosal layer and muscularis externa of the porcine esophagus.

ECM-derived bioscaffolds can be derived from the esophageal mucosa and the muscularis externa, and these bioscaffolds are compliant with proposed decellularization criteria. Perfusion decellularization can maintain the ultrastructure of the original ECM in the muscularis layer of the esophagus. The bioscaffolds are cytocompatible and their degradation products promote and M2-modulatory macrophage phenotype in vitro.

Sub-Aim 1: To characterize the host response to implanted esophageal mucosa ECM-derived bioscaffolds in a preclinical murine model of abdominal wall defect.

When used to repair an abdominal wall defect in the rat, bioscaffolds derived from the extracellular matrix of the esophageal mucosa can modulate the host response and promote a pro-remodeling environment as indicated by M2/M1 macrophage ratios and histologic examination.

Aim 2: To evaluate the tissue specific effects of biologic scaffolds derived from esophageal tissues in vitro and in a preclinical murine model of esophageal mucosal resection

Porcine heterogeneous cell populations isolated from murine esophageal tissue and exposed to degradation products from esophageal ECM show no preference over degradation products from ECMs derived from UBM or SIS. Furthermore, when implanted in a model of esophageal mucosal repair, esophageal ECM, UBM and SIS present the same performance under the evaluated criteria.

Aim3: To evaluate the ability of cardiac-ECM to modify the host response to an implanted cardiac patch in a preclinical murine model of myocardial infarction.

Modification of a PEUU cardiac patch with a cardiac-ECM enriched layer can modify the host response following implantation 2-weeks post MI in a rat model. Findings include increased ventricular wall thickness over infarcted region compared to non-modified PEUU control, and reduce area of scar tissue formation.

APPENDIX A

A.1 PUBLICATIONS

Peer Reviewed Manuscripts

[1] Keane TJ, DeWard A, **Londono R**, Saldin L, Castleton AA, Carey L, et al. Tissue-Specific Effects of Esophageal Extracellular Matrix. Tissue engineering Part A 2015.

[2] Zaidi AH, Saldin LT, Kelly LA, Bergal L, **Londono R**, Kosovec JE, et al. MicroRNA signature characterizes primary tumors that metastasize in an esophageal adenocarcinoma rat model. PloS one 2015;10:e0122375.

[3] **Londono R**, Badylak SF. Regenerative Medicine Strategies for Esophageal Repair. Tissue engineering Part B, Reviews 2015.

[4] **Londono R**, Badylak SF. Biologic Scaffolds for Regenerative Medicine: Mechanisms of In vivo Remodeling. Annals of biomedical engineering 2014.

[5] Faulk DM, **Londono R**, Wolf MT, Ranallo CA, Carruthers CA, Wildemann JD, et al. ECM hydrogel coating mitigates the chronic inflammatory response to polypropylene mesh. Biomaterials 2014;35:8585-95.

[6] Carey LE, Dearth CL, Johnson SA, **Londono R**, Medberry CJ, Daly KA, et al. In vivo degradation of 14C-labeled porcine dermis biologic scaffold. Biomaterials 2014;35:8297-304.

[7] Turner NJ, **Londono R**, Dearth CL, Culiat CT, Badylak SF. Human NELL1 protein augments constructive tissue remodeling with biologic scaffolds. Cells, tissues, organs 2013;198:249-65.

[8] Nieponice A, Ciotola FF, Nachman F, Jobe BA, Hoppo T, **Londono R**, et al. Patch esophagoplasty: esophageal reconstruction using biologic scaffolds. The Annals of thoracic surgery 2014;97:283-8.

[9] Sicari BM, Zhang L, **Londono R**, Badylak SF. An assay to quantify chemotactic properties of degradation products from extracellular matrix. Methods in molecular biology 2014;1202:103-10.

[10] Wolf MT, Carruthers CA, Dearth CL, Crapo PM, Huber A, Burnsed OA, **Londono R** et al. Polypropylene surgical mesh coated with extracellular matrix mitigates the host foreign body response. Journal of biomedical materials research Part A 2013.

[11] Keane TJ, **Londono R**, Carey RM, Carruthers CA, Reing JE, Dearth CL, et al. Preparation and characterization of a biologic scaffold from esophageal mucosa. Biomaterials 2013;34:6729-37.

[12] **Londono R**, Jobe BA, Hoppo T, Badylak SF. Esophagus and regenerative medicine. World Journal of Gastroenterology 2012;18:6894-9.

[13] Brown BN, **Londono R**, Tottey S, Zhang L, Kukla KA, Wolf MT, et al. Macrophage phenotype as a predictor of constructive remodeling following the implantation of biologically derived surgical mesh materials. Acta biomaterialia 2012;8:978-87.

[14] Keane TJ, **Londono R**, Turner NJ, Badylak SF. Consequences of ineffective decellularization of biologic scaffolds on the host response. Biomaterials 2012;33:1771-81.

[15] Tottey S, Corselli M, Jeffries EM, **Londono R**, Peault B, Badylak SF. Extracellular matrix degradation products and low-oxygen conditions enhance the regenerative potential of perivascular stem cells. Tissue engineering Part A 2011;17:37-44.

Book Chapters

[16] **Londono R**, Badylak SF. Factors which Affect the Host Response to Biomaterials. Host Response to Biomaterials. Academic Press; 1 edition (May 21, 2015). ISBN-10: 0128001968 ISBN-13: 978-0128001967

[17] Sicari BM, **Londono R**, Badylak, SF. In Vivo Remodeling of Extracellular Matrix Bioscaffolds. Tissue Engineering. *In press*

[18] **Londono R**, Badylak SF. Biomaterials from Decellularized Tissues. Biomaterials from Nature for Advanced Devices and Therapies Editor(s): Nuno M. Neves and Rui L. Reis. ISBN: 9781118478059. *In press*

BIBLIOGRAPHY

Bibliography

1. Centers for Disease Control and Prevention. National Diabetes Statistics Report: Estimates of Diabetes and Its Burden in the United States, 2014. . Atlanta GA: U.S. Department of Health and Human Services; 2014., 2014.

2. Cost-Effectiveness of Hypertension Therapy According to 2014 Guidelines. N Engl J Med, 2015. 372(17): p. 1677.

3. Achildi, O. and H. Grewal, Congenital Anomalies of the Esophagus. Otolaryngol Clin North Am, 2007. 40(1): p. 219-44, viii.

4. Agrawal, V., B.N. Brown, A.J. Beattie, T.W. Gilbert, and S.F. Badylak, Evidence of Innervation Following Extracellular Matrix Scaffold-Mediated Remodelling of Muscular Tissues. J Tissue Eng Regen Med, 2009. 3(8): p. 590-600.

5. Agrawal, V., et al., Epimorphic Regeneration Approach to Tissue Replacement in Adult Mammals. Proc Natl Acad Sci U S A, 2010. 107(8): p. 3351-5.

6. Agrawal, V., J. Kelly, S. Tottey, K.A. Daly, S.A. Johnson, B.F. Siu, J. Reing, and S.F. Badylak, An Isolated Cryptic Peptide Influences Osteogenesis and Bone Remodeling in an Adult Mammalian Model of Digit Amputation. Tissue Eng Part A, 2011. 17(23-24): p. 3033-44.

7. Agrawal, V., S. Tottey, S.A. Johnson, J.M. Freund, B.F. Siu, and S.F. Badylak, Recruitment of Progenitor Cells by an Extracellular Matrix Cryptic Peptide in a Mouse Model of Digit Amputation. Tissue Engineering - Part A, 2011. 17(19-20): p. 2435-2443.

8. Agrawal, V., S. Tottey, S.A. Johnson, J.M. Freund, B.F. Siu, and S.F. Badylak, Recruitment of Progenitor Cells by an Extracellular Matrix Cryptic Peptide in a Mouse Model of Digit Amputation. Tissue Eng Part A, 2011. 17(19-20): p. 2435-43.

9. Allen, R.A., L.M. Seltz, H. Jiang, R.T. Kasick, T.L. Sellaro, S.F. Badylak, and J.B. Ogilvie, Adrenal Extracellular Matrix Scaffolds Support Adrenocortical Cell Proliferation and Function in Vitro. Tissue Eng Part A, 2010. 16(11): p. 3363-74.

10. Aller, M.A., J.I. Arias, L.A. Arraez-Aybar, C. Gilsanz, and J. Arias, Wound Healing Reaction: A Switch from Gestation to Senescence. World J Exp Med, 2014. 4(2): p. 16-26.

11. Ambrosio, F., S.L. Wolf, A. Delitto, G.K. Fitzgerald, S.F. Badylak, M.L. Boninger, and A.J. Russell, The Emerging Relationship between Regenerative Medicine and Physical Therapeutics. Phys Ther, 2010. 90(12): p. 1807-14.

12. An, Y.H. and R.J. Friedman, Prevention of Sepsis in Total Joint Arthroplasty. J Hosp Infect, 1996. 33(2): p. 93-108.

13. Anderson, J.M., A. Rodriguez, and D.T. Chang, Foreign Body Reaction to Biomaterials. Semin Immunol, 2008. 20(2): p. 86-100.

14. Andree, B., A. Bar, A. Haverich, and A. Hilfiker, Small Intestinal Submucosa Segments as Matrix for Tissue Engineering: Review. Tissue Eng Part B Rev, 2013.

15. Arciola, C.R., D. Campoccia, G.D. Ehrlich, and L. Montanaro, Biofilm-Based Implant Infections in Orthopaedics. Adv Exp Med Biol, 2015. 830: p. 29-46.

16. Arnold, M., I. Soerjomataram, J. Ferlay, and D. Forman, Global Incidence of Oesophageal Cancer by Histological Subtype in 2012. Gut, 2014.

17. Arora, N.D., R. Varghese, S. Pavithran, and S. Kothandam, The Pressures of Surgicel((R)) in Cardiac Surgery. Ann Pediatr Cardiol, 2015. 8(2): p. 167-9.

18. Asefa, T. and Z. Tao, Biocompatibility of Mesoporous Silica Nanoparticles. Chem Res Toxicol, 2012. 25(11): p. 2265-84.

19. Atar-Froyman, L., A. Sharon, E.I. Weiss, Y. Houri-Haddad, D. Kesler-Shvero, A.J. Domb, R. Pilo, and N. Beyth, Anti-Biofilm Properties of Wound Dressing Incorporating Nonrelease Polycationic Antimicrobials. Biomaterials, 2015. 46: p. 141-8.

20. Badylak, S., T. Gilbert, and J. Myers-Irvin, The Extracellular Matrix as a Biologic Scaffold for Tissue Engineering, in Tissue Engineering. 2008. p. 121-143.

21. Badylak, S., K. Kokini, B. Tullius, A. Simmons-Byrd, and R. Morff, Morphologic Study of Small Intestinal Submucosa as a Body Wall Repair Device. J Surg Res, 2002. 103(2): p. 190-202.

22. Badylak, S., A. Liang, R. Record, R. Tullius, and J. Hodde, Endothelial Cell Adherence to Small Intestinal Submucosa: An Acellular Bioscaffold. Biomaterials, 1999. 20(23-24): p. 2257-63.

23. Badylak, S., S. Meurling, M. Chen, A. Spievack, and A. Simmons-Byrd, Resorbable Bioscaffold for Esophageal Repair in a Dog Model. J Pediatr Surg, 2000. 35(7): p. 1097-103.

24. Badylak, S.F., The Extracellular Matrix as a Scaffold for Tissue Reconstruction. Semin Cell Dev Biol, 2002. 13(5): p. 377-83.

25. Badylak, S.F., Decellularized Allogeneic and Xenogeneic Tissue as a Bioscaffold for Regenerative Medicine: Factors That Influence the Host Response. Ann Biomed Eng, 2014. 42(7): p. 1517-27.

26. Badylak, S.F., D.O. Freytes, and T.W. Gilbert, Extracellular Matrix as a Biological Scaffold Material: Structure and Function. Acta Biomater, 2009. 5(1): p. 1-13.

27. Badylak, S.F., T. Hoppo, A. Nieponice, T.W. Gilbert, J.M. Davison, and B.A. Jobe, Esophageal Preservation in Five Male Patients after Endoscopic Inner-Layer Circumferential Resection in the Setting of Superficial Cancer: A Regenerative Medicine Approach with a Biologic Scaffold. Tissue Eng Part A, 2011. 17(11-12): p. 1643-50.

28. Badylak, S.F., D. Taylor, and K. Uygun, Whole-Organ Tissue Engineering: Decellularization and Recellularization of Three-Dimensional Matrix Scaffolds. Annu Rev Biomed Eng, 2011. 13: p. 27-53.

29. Badylak, S.F., R. Tullius, K. Kokini, K.D. Shelbourne, T. Klootwyk, S.L. Voytik, M.R. Kraine, and C. Simmons, The Use of Xenogeneic Small-Intestinal Submucosa as a Biomaterial for Achilles-Tendon Repair in a Dog-Model. Journal of Biomedical Materials Research, 1995. 29(8): p. 977-985.

30. Badylak, S.F., R. Tullius, K. Kokini, K.D. Shelbourne, T. Klootwyk, S.L. Voytik, M.R. Kraine, and C. Simmons, The Use of Xenogeneic Small Intestinal Submucosa as a Biomaterial for Achilles Tendon Repair in a Dog Model. J Biomed Mater Res, 1995. 29(8): p. 977-85.

31. Badylak, S.F., J.E. Valentin, A.K. Ravindra, G.P. McCabe, and A.M. Stewart-Akers, Macrophage Phenotype as a Determinant of Biologic Scaffold Remodeling. Tissue Eng Part A, 2008. 14(11): p. 1835-42.

32. Badylak, S.F., D.A. Vorp, A.R. Spievack, A. Simmons-Byrd, J. Hanke, D.O. Freytes, A. Thapa, T.W. Gilbert, and A. Nieponice, Esophageal Reconstruction with Ecm and Muscle Tissue in a Dog Model. J Surg Res, 2005. 128(1): p. 87-97.

33. Badylak, S.F., D.A. Vorp, A.R. Spievack, A. Simmons-Byrd, J. Hanke, D.O. Freytes, A. Thapa, T.W. Gilbert, and A. Nieponice, Esophageal Reconstruction with Ecm and Muscle Tissue in a Dog Model. Journal of Surgical Research, 2005. 128(1): p. 87-97.

34. Baker, S.M., R.V. Sugars, M. Wendel, A.J. Smith, R.J. Waddington, P.R. Cooper, and A.J. Sloan, Tgf-Beta/Extracellular Matrix Interactions in Dentin Matrix: A Role in Regulating Sequestration and Protection of Bioactivity. Calcif Tissue Int, 2009. 85(1): p. 66-74.

35. Baldwin, A.D. and K.L. Kiick, Polysaccharide-Modified Synthetic Polymeric Biomaterials. Biopolymers, 2010. 94(1): p. 128-40.

36. Baldwin, E.D., L.V. Moore, and R.P. Noble, The Demonstration of Ventricular Septal Defect by Means of Right Heart Catheterization. Am Heart J, 1946. 32: p. 152-62.

37. Barnes, C.A., J. Brison, R. Michel, B.N. Brown, D.G. Castner, S.F. Badylak, and B.D. Ratner, The Surface Molecular Functionality of Decellularized Extracellular Matrices. Biomaterials, 2011. 32(1): p. 137-43.

38. Beasley, W.D., M.T. Jefferies, J. Gilmour, and J.M. Manson, A Single Surgeon's Series of Transthoracic Oesophageal Resections. Ann R Coll Surg Engl, 2014. 96(2): p. 151-6.

39. Beattie, A.J., T.W. Gilbert, J.P. Guyot, A.J. Yates, and S.F. Badylak, Chemoattraction of Progenitor Cells by Remodeling Extracellular Matrix Scaffolds. Tissue Engineering - Part A, 2009. 15(5): p. 1119-1125.

40. Beattie, A.J., T.W. Gilbert, J.P. Guyot, A.J. Yates, and S.F. Badylak, Chemoattraction of Progenitor Cells by Remodeling Extracellular Matrix Scaffolds. Tissue Eng Part A, 2009. 15(5): p. 1119-25.

41. Beckstead, B.L., S. Pan, A.D. Bhrany, A.M. Bratt-Leal, B.D. Ratner, and C.M. Giachelli, Esophageal Epithelial Cell Interaction with Synthetic and Natural Scaffolds for Tissue Engineering. Biomaterials, 2005. 26(31): p. 6217-28.

42. Bedford, D.E., C. Papp, and J. Parkinson, Atrial Septal Defect. Br Heart J, 1941. 3(1): p. 37-68.

43. Beltrami, A.P., et al., Adult Cardiac Stem Cells Are Multipotent and Support Myocardial Regeneration. Cell, 2003. 114(6): p. 763-76.

44. Benders, K.E., P.R. van Weeren, S.F. Badylak, D.B. Saris, W.J. Dhert, and J. Malda, Extracellular Matrix Scaffolds for Cartilage and Bone Regeneration. Trends Biotechnol, 2013. 31(3): p. 169-76.

45. Berman, P. and V.R. Mason, Coronary Artery Disease-an Electrocardiographic Study. Cal West Med, 1928. 28(3): p. 334-41.

46. Berthiaume, F., T.J. Maguire, and M.L. Yarmush, Tissue Engineering and Regenerative Medicine: History, Progress, and Challenges. Annu Rev Chem Biomol Eng, 2011. 2: p. 403-30.

47. Bhrany, A.D., B.L. Beckstead, T.C. Lang, D.G. Farwell, C.M. Giachelli, and B.D. Ratner, Development of an Esophagus Acellular Matrix Tissue Scaffold. Tissue Eng, 2006. 12(2): p. 319-30.

48. Bhrany, A.D., C.J. Lien, B.L. Beckstead, N.D. Futran, N.H. Muni, C.M. Giachelli, and B.D. Ratner, Crosslinking of an Oesophagus Acellular Matrix Tissue Scaffold. J Tissue Eng Regen Med, 2008. 2(6): p. 365-72.

49. Billiar, K.L. and M.S. Sacks, Biaxial Mechanical Properties of the Natural and Glutaraldehyde Treated Aortic Valve Cusp--Part I: Experimental Results. J Biomech Eng, 2000. 122(1): p. 23-30.

50. Birch, H.L., C.T. Thorpe, and A.P. Rumian, Specialisation of Extracellular Matrix for Function in Tendons and Ligaments. Muscles Ligaments Tendons J, 2013. 3(1): p. 12-22.

51. Bissell, M.J. and J. Aggeler, Dynamic Reciprocity: How Do Extracellular Matrix and Hormones Direct Gene Expression? Prog Clin Biol Res, 1987. 249: p. 251-62.

52. Bjorklund, A. and J.H. Kordower, Cell Therapy for Parkinson's Disease: What Next? Mov Disord, 2013. 28(1): p. 110-5.

53. Blackshaw, G., W.G. Lewis, A.N. Hopper, M.A. Morgan, W. Al-Khyatt, P. Edwards, and S.A. Roberts, Prospective Comparison of Endosonography, Computed Tomography, and Histopathological Stage of Junctional Oesophagogastric Cancer. Clin Radiol, 2008. 63(10): p. 1092-8.

54. Born, J., D. Uthgenannt, C. Dodt, D. Nunninghoff, E. Ringvolt, T. Wagner, and H.L. Fehm, Cytokine Production and Lymphocyte Subpopulations in Aged Humans. An Assessment During Nocturnal Sleep. Mech Ageing Dev, 1995. 84(2): p. 113-26.

55. Bovenberg, M.S., M.H. Degeling, and B.A. Tannous, Advances in Stem Cell Therapy against Gliomas. Trends Mol Med, 2013. 19(5): p. 281-91.

56. Brennan, E.P., J. Reing, D. Chew, J.M. Myers-Irvin, E.J. Young, and S.F. Badylak, Antibacterial Activity within Degradation Products of Biological Scaffolds Composed of Extracellular Matrix. Tissue Eng, 2006. 12(10): p. 2949-55.

57. Brennan, E.P., X.H. Tang, A.M. Stewart-Akers, L.J. Gudas, and S.F. Badylak, Chemoattractant Activity of Degradation Products of Fetal and Adult Skin Extracellular Matrix for Keratinocyte Progenitor Cells. J Tissue Eng Regen Med, 2008. 2(8): p. 491-8.

58. Brennan, E.P., X.H. Tang, A.M. Stewart-Akers, L.J. Gudas, and S.F. Badylak, Chemoattractant Activity of Degradation Products of Fetal and Adult Skin Extracellular Matrix for Keratinocyte Progenitor Cells. Journal of Tissue Engineering and Regenerative Medicine, 2008. 2(8): p. 491-498.

59. Britten, M.B., et al., Infarct Remodeling after Intracoronary Progenitor Cell Treatment in Patients with Acute Myocardial Infarction (Topcare-Ami): Mechanistic Insights from Serial Contrast-Enhanced Magnetic Resonance Imaging. Circulation, 2003. 108(18): p. 2212-8.

60. Brown, B., K. Lindberg, J. Reing, D.B. Stolz, and S.F. Badylak, The Basement Membrane Component of Biologic Scaffolds Derived from Extracellular Matrix. Tissue Engineering, 2006. 12(3): p. 519-526.

61. Brown, B., K. Lindberg, J. Reing, D.B. Stolz, and S.F. Badylak, The Basement Membrane Component of Biologic Scaffolds Derived from Extracellular Matrix. Tissue Eng, 2006. 12(3): p. 519-26.

62. Brown, B.N. and S.F. Badylak, Expanded Applications, Shifting Paradigms and an Improved Understanding of Host-Biomaterial Interactions. Acta Biomater, 2013. 9(2): p. 4948-55.

63. Brown, B.N., C.A. Barnes, R.T. Kasick, R. Michel, T.W. Gilbert, D. Beer-Stolz, D.G. Castner, B.D. Ratner, and S.F. Badylak, Surface Characterization of Extracellular Matrix Scaffolds. Biomaterials, 2010. 31(3): p. 428-37.

64. Brown, B.N., et al., Comparison of Three Methods for the Derivation of a Biologic Scaffold Composed of Adipose Tissue Extracellular Matrix. Tissue Eng Part C Methods, 2011. 17(4): p. 411-21.

65. Brown, B.N., R. Londono, S. Tottey, L. Zhang, K.A. Kukla, M.T. Wolf, K.A. Daly, J.E. Reing, and S.F. Badylak, Macrophage Phenotype as a Predictor of Constructive Remodeling Following the Implantation of Biologically Derived Surgical Mesh Materials. Acta Biomater, 2012. 8(3): p. 978-87.

66. Brown, B.N., B.D. Ratner, S.B. Goodman, S. Amar, and S.F. Badylak, Macrophage Polarization: An Opportunity for Improved Outcomes in Biomaterials and Regenerative Medicine. Biomaterials, 2012. 33(15): p. 3792-802.

67. Brown, B.N., J.E. Valentin, A.M. Stewart-Akers, G.P. McCabe, and S.F. Badylak, Macrophage Phenotype and Remodeling Outcomes in Response to Biologic Scaffolds with and without a Cellular Component. Biomaterials, 2009. 30(8): p. 1482-91.

68. Bryers, J.D., C.M. Giachelli, and B.D. Ratner, Engineering Biomaterials to Integrate and Heal: The Biocompatibility Paradigm Shifts. Biotechnol Bioeng, 2012. 109(8): p. 1898-911.

69. Burch, P.T., A.K. Kaza, L.M. Lambert, R. Holubkov, R.E. Shaddy, and J.A. Hawkins, Clinical Performance of Decellularized Cryopreserved Valved Allografts Compared with Standard Allografts in the Right Ventricular Outflow Tract. Ann Thorac Surg, 2010. 90(4): p. 1301-5; discussion 1306.

70. Burgess, A.M., The Clinical Aspects of Acute Coronary Thrombosis. R I Med J, 1945. 28: p. 799.

71. Buskens, C.J., J.B. Hulscher, T.M. van Gulik, F.J. Ten Kate, and J.J. van Lanschot, Histopathologic Evaluation of an Animal Model for Barrett's Esophagus and Adenocarcinoma of the Distal Esophagus. J Surg Res, 2006. 135(2): p. 337-44.

72. Butcher, S.K., H. Chahal, L. Nayak, A. Sinclair, N.V. Henriquez, E. Sapey, D. O'Mahony, and J.M. Lord, Senescence in Innate Immune Responses: Reduced Neutrophil

Phagocytic Capacity and Cd16 Expression in Elderly Humans. J Leukoc Biol, 2001. 70(6): p. 881-6.

73. Butterfield, J.L., 440 Consecutive Immediate, Implant-Based, Single-Surgeon Breast Reconstructions in 281 Patients: A Comparison of Early Outcomes and Costs between Surgimend Fetal Bovine and Alloderm Human Cadaveric Acellular Dermal Matrices. Plast Reconstr Surg, 2013. 131(5): p. 940-51.

74. Byron, F.X., Congenital Stresia of the Esophagus with Hypoplasia or Agenesis of the Lower Segment. Surgery, 1948. 24(5): p. 841-5.

75. Canonico, S., The Use of Human Fibrin Glue in the Surgical Operations. Acta Biomed, 2003. 74 Suppl 2: p. 21-5.

76. Carabello, B., How to Follow Patients with Mitral and Aortic Valve Disease. Med Clin North Am, 2015. 99(4): p. 739-757.

77. Carey, L.E., C.L. Dearth, S.A. Johnson, R. Londono, C.J. Medberry, K.A. Daly, and S.F. Badylak, In Vivo Degradation of 14c-Labeled Porcine Dermis Biologic Scaffold. Biomaterials, 2014.

78. Carey, L.E., C.L. Dearth, S.A. Johnson, R. Londono, C.J. Medberry, K.A. Daly, and S.F. Badylak, In Vivo Degradation of 14c-Labeled Porcine Dermis Biologic Scaffold. Biomaterials, 2014. 35(29): p. 8297-304.

79. Carter, B.D., et al., Smoking and Mortality--Beyond Established Causes. N Engl J Med, 2015. 372(7): p. 631-40.

80. Carvalho Neves Forte, W., J.V. Martins Campos, and R. Carneiro Leao, Non Specific Immunological Response in Moderate Malnutrition. Allergol Immunopathol (Madr), 1984. 12(6): p. 489-96.

81. Cawthorne, D.J. and A.C. Griffith, Tetralogy of Fallot. Univ Durh Med Gaz, 1946. 1: p. 185-92.

82. Cevasco, M. and K.M. Itani, Ventral Hernia Repair with Synthetic, Composite, and Biologic Mesh: Characteristics, Indications, and Infection Profile. Surg Infect (Larchmt), 2012. 13(4): p. 209-15.

83. Chandra, S., D. Saluja, R. Narang, J. Bhatia, and K. Srivastava, Atrial Natriuretic Peptide and Aldosterone Synthase Gene in Essential Hypertension: A Case-Control Study. Gene, 2015. 567(1): p. 92-7.

84. Chatterjee, S., S.J. Berger, and N.A. Berger, Poly(Adp-Ribose) Polymerase: A Guardian of the Genome That Facilitates DNA Repair by Protecting against DNA Recombination. Mol Cell Biochem, 1999. 193(1-2): p. 23-30.

85. Chattopadhyay, S. and R.T. Raines, Review Collagen-Based Biomaterials for Wound Healing. Biopolymers, 2014. 101(8): p. 821-33.

86. Chen, A.K., S. Reuveny, and S.K. Oh, Application of Human Mesenchymal and Pluripotent Stem Cell Microcarrier Cultures in Cellular Therapy: Achievements and Future Direction. Biotechnol Adv, 2013.

87. Chen, J., S.L. Normand, Y. Wang, E.E. Drye, G.C. Schreiner, and H.M. Krumholz, Recent Declines in Hospitalizations for Acute Myocardial Infarction for Medicare Fee-for-Service Beneficiaries: Progress and Continuing Challenges. Circulation, 2010. 121(11): p. 1322-8.

88. Chen, M., M.P. Marinkovich, A. Veis, X. Cai, C.N. Rao, E.A. O'Toole, and D.T. Woodley, Interactions of the Amino-Terminal Noncollagenous (Nc1) Domain of Type Vii Collagen with Extracellular Matrix Components. A Potential Role in Epidermal-Dermal Adherence in Human Skin. J Biol Chem, 1997. 272(23): p. 14516-22.

89. Chen, M.F., Y.H. Yang, C.H. Lai, P.C. Chen, and W.C. Chen, Outcome of Patients with Esophageal Cancer: A Nationwide Analysis. Ann Surg Oncol, 2013.

90. Chen, X., G. Yang, W.Y. Ding, F. Bondoc, S.K. Curtis, and C.S. Yang, An Esophagogastroduodenal Anastomosis Model for Esophageal Adenocarcinogenesis in Rats and Enhancement by Iron Overload. Carcinogenesis, 1999. 20(9): p. 1801-8.

91. Chhangani, L., M.L. Sharma, U.B. Sharma, and N. Joshi, In Vitro Study of Phagocytic and Bactericidal Activity of Neutrophils in Cases of Protein Energy Malnutrition. Indian J Pathol Microbiol, 1985. 28(3): p. 199-203.

92. Chirica, M., A. Champault, X. Dray, L. Sulpice, N. Munoz-Bongrand, E. Sarfati, and P. Cattan, Esophageal Perforations. J Visc Surg, 2010. 147(3): p. e117-28.

93. Chirouze, C., B. Hoen, and X. Duval, Infective Endocarditis Epidemiology and Consequences of Prophylaxis Guidelines Modifications: The Dialectical Evolution. Curr Infect Dis Rep, 2014. 16(11): p. 440.

94. Christman, K.L., A.J. Vardanian, Q. Fang, R.E. Sievers, H.H. Fok, and R.J. Lee, Injectable Fibrin Scaffold Improves Cell Transplant Survival, Reduces Infarct Expansion, and Induces Neovasculature Formation in Ischemic Myocardium. J Am Coll Cardiol, 2004. 44(3): p. 654-60.

95. Chu, C.C. and L. Welch, Characterization of Morphologic and Mechanical Properties of Surgical Mesh Fabrics. J Biomed Mater Res, 1985. 19(8): p. 903-16.

96. Ciolina, F., P. Sedati, F. Zaccagna, N. Galea, V. Noce, F. Miraldi, E. Cavarretta, M. Francone, and I. Carbone, Aortic Valve Stenosis: Non-Invasive Preoperative Evaluation Using 64-Slice Ct Angiography. J Cardiovasc Surg (Torino), 2015. 56(5): p. 799-808.

97. Clark, R.A., N.E. Wikner, D.E. Doherty, and D.A. Norris, Cryptic Chemotactic Activity of Fibronectin for Human Monocytes Resides in the 120-Kda Fibroblastic Cell-Binding Fragment. J Biol Chem, 1988. 263(24): p. 12115-23.

98. Clarke, B.E., The Pathology of Coronary Artery Sclerosis and Thrombosis. R I Med J, 1945. 28: p. 791.

99. Cobb, W.S., K.W. Kercher, and B.T. Heniford, Laparoscopic Repair of Incisional Hernias. Surg Clin North Am, 2005. 85(1): p. 91-103, ix.

100. Cook, M.B., Non-Acid Reflux: The Missing Link between Gastric Atrophy and Esophageal Squamous Cell Carcinoma? Am J Gastroenterol, 2011. 106(11): p. 1930-2.

101. Cortiella, J., et al., Influence of Acellular Natural Lung Matrix on Murine Embryonic Stem Cell Differentiation and Tissue Formation. Tissue Eng Part A, 2010. 16(8): p. 2565-80.

102. Costamagna, G. and M. Marchese, Management of Esophageal Perforation after Therapeutic Endoscopy. Gastroenterol Hepatol (N Y), 2010. 6(6): p. 391-2.

103. Cox, A. and S. Herschorn, Evaluation of Current Biologic Meshes in Pelvic Organ Prolapse Repair. Curr Urol Rep, 2012. 13(3): p. 247-55.

104. Cox, B. and A. Emili, Tissue Subcellular Fractionation and Protein Extraction for Use in Mass-Spectrometry-Based Proteomics. Nat Protoc, 2006. 1(4): p. 1872-8.

105. Crapo, P.M., T.W. Gilbert, and S.F. Badylak, An Overview of Tissue and Whole Organ Decellularization Processes. Biomaterials, 2011. 32(12): p. 3233-43.

106. Crapo, P.M., C.J. Medberry, J.E. Reing, S. Tottey, Y. van der Merwe, K.E. Jones, and S.F. Badylak, Biologic Scaffolds Composed of Central Nervous System Extracellular Matrix. Biomaterials, 2012. 33(13): p. 3539-47.

107. Crisan, M., B. Deasy, M. Gavina, B. Zheng, J. Huard, L. Lazzari, and B. Peault, Purification and Long-Term Culture of Multipotent Progenitor Cells Affiliated with the Walls of Human Blood Vessels: Myoendothelial Cells and Pericytes. Methods Cell Biol, 2008. 86: p. 295-309.

108. Crisan, M., et al., A Perivascular Origin for Mesenchymal Stem Cells in Multiple Human Organs. Cell Stem Cell, 2008. 3(3): p. 301-13.

109. Daly, K.A., et al., The Host Response to Endotoxin-Contaminated Dermal Matrix. Tissue Eng Part A, 2012. 18(11-12): p. 1293-303.

110. Davis, G.E., K.J. Bayless, M.J. Davis, and G.A. Meininger, Regulation of Tissue Injury Responses by the Exposure of Matricryptic Sites within Extracellular Matrix Molecules. Am J Pathol, 2000. 156(5): p. 1489-98.

111. de Jong, E.M., J.F. Felix, A. de Klein, and D. Tibboel, Etiology of Esophageal Atresia and Tracheoesophageal Fistula: "Mind the Gap". Curr Gastroenterol Rep, 2010. 12(3): p. 215-22.

112. Depaepe, A., H. Dolk, and M.F. Lechat, The Epidemiology of Tracheo-Oesophageal Fistula and Oesophageal Atresia in Europe. Eurocat Working Group. Arch Dis Child, 1993. 68(6): p. 743-8.

113. DeQuach, J.A., J.E. Lin, C. Cam, D. Hu, M.A. Salvatore, F. Sheikh, and K.L. Christman, Injectable Skeletal Muscle Matrix Hydrogel Promotes Neovascularization and Muscle Cell Infiltration in a Hindlimb Ischemia Model. Eur Cell Mater, 2012. 23: p. 400-12; discussion 412.

114. Deurloo, J.A., S. Ekkelkamp, M. Schoorl, H.A. Heij, and D.C. Aronson, Esophageal Atresia: Historical Evolution of Management and Results in 371 Patients. Ann Thorac Surg, 2002. 73(1): p. 267-72.

115. DeWard, A.D., J. Cramer, and E. Lagasse, Cellular Heterogeneity in the Mouse Esophagus Implicates the Presence of a Nonquiescent Epithelial Stem Cell Population. Cell Rep, 2014. 9(2): p. 701-11.

116. Diaz, J.J., Jr., J. Guy, M.B. Berkes, O. Guillamondegui, and R.S. Miller, Acellular Dermal Allograft for Ventral Hernia Repair in the Compromised Surgical Field. Am Surg, 2006. 72(12): p. 1181-7; discussion 1187-8.

117. Diemer, P., S. Markoew, D.Q. Le, and N. Qvist, Poly-Epsilon-Caprolactone Mesh as a Scaffold for in Vivo Tissue Engineering in Rabbit Esophagus. Dis Esophagus, 2014.

118. DiPietro, L.A., Angiogenesis and Scar Formation in Healing Wounds. Curr Opin Rheumatol, 2013. 25(1): p. 87-91.

119. Dong, X., X. Wei, W. Yi, C. Gu, X. Kang, Y. Liu, Q. Li, and D. Yi, Rgd-Modified Acellular Bovine Pericardium as a Bioprosthetic Scaffold for Tissue Engineering. J Mater Sci Mater Med, 2009. 20(11): p. 2327-36.

120. Douglas, S.D. and K. Schopfer, Phagocyte Function in Protein-Calorie Malnutrition. Clin Exp Immunol, 1974. 17(1): p. 121-8.

121. Doupe, D.P., M.P. Alcolea, A. Roshan, G. Zhang, A.M. Klein, B.D. Simons, and P.H. Jones, A Single Progenitor Population Switches Behavior to Maintain and Repair Esophageal Epithelium. Science, 2012. 337(6098): p. 1091-3.

122. Drosos, I. and G. Kolios, Stem Cells in Liver Regeneration and Their Potential Clinical Applications. Stem Cell Rev, 2013.

123. Dry, T.J., Atrial Septal Defects. Med Clin North Am, 1948. 32: p. 895-910.

124. Du, L., X. Wu, K. Pang, and Y. Yang, Histological Evaluation and Biomechanical Characterisation of an Acellular Porcine Cornea Scaffold. Br J Ophthalmol, 2011. 95(3): p. 410-4.

125. Dumot, J.A., J.J. Vargo, 2nd, G.W. Falk, L. Frey, R. Lopez, and T.W. Rice, An Open-Label, Prospective Trial of Cryospray Ablation for Barrett's Esophagus High-Grade Dysplasia and Early Esophageal Cancer in High-Risk Patients. Gastrointest Endosc, 2009. 70(4): p. 635-44.

126. Dunmore-Buyze, J., D.R. Boughner, N. Macris, and I. Vesely, A Comparison of Macroscopic Lipid Content within Porcine Pulmonary and Aortic Valves. Implications for Bioprosthetic Valves. J Thorac Cardiovasc Surg, 1995. 110(6): p. 1756-61.

127. Ehnes, D.D., F.D. Price, N.G. Shrive, D.A. Hart, D.E. Rancourt, and N.I. Zur Nieden, Embryonic Stem Cell-Derived Osteocytes Are Capable of Responding to Mechanical Oscillatory Hydrostatic Pressure. J Biomech, 2015.

128. Elder, B.D., D.H. Kim, and K.A. Athanasiou, Developing an Articular Cartilage Decellularization Process toward Facet Joint Cartilage Replacement. Neurosurgery, 2010. 66(4): p. 722-7; discussion 727.

129. Enoch, D.A., N. Phillimore, J.A. Karas, L. Horswill, and D.A. Mlangeni, Relapse of Enterococcal Prosthetic Valve Endocarditis with Aortic Root Abscess Following Treatment with Daptomycin in a Patient Not Fit for Surgery. J Med Microbiol, 2010. 59(Pt 4): p. 482-5.

130. Enzinger, P.C. and R.J. Mayer, Esophageal Cancer. N Engl J Med, 2003. 349(23): p. 2241-52.

131. Ergin, A., P. Muntner, R. Sherwin, and J. He, Secular Trends in Cardiovascular Disease Mortality, Incidence, and Case Fatality Rates in Adults in the United States. Am J Med, 2004. 117(4): p. 219-27.

132. Ernst, M.E. and M. Moser, Use of Diuretics in Patients with Hypertension. N Engl J Med, 2009. 361(22): p. 2153-64.

133. Everitt, J.I., The Future of Preclinical Animal Models in Pharmaceutical Discovery and Development: A Need to Bring in Cerebro to the in Vivo Discussions. Toxicol Pathol, 2014.

134. Ezzati, M., Z. Obermeyer, I. Tzoulaki, B.M. Mayosi, P. Elliott, and D.A. Leon, Contributions of Risk Factors and Medical Care to Cardiovascular Mortality Trends. Nat Rev Cardiol, 2015.

135. Farrell, T.M., S.B. Archer, R.E. Metreveli, C.D. Smith, and J.G. Hunter, Resection and Advancement of Esophageal Mucosa. A Potential Therapy for Barrett's Esophagus. Surg Endosc, 2001. 15(9): p. 937-41.

136. Faulk, D.M., R. Londono, M.T. Wolf, C.A. Ranallo, C.A. Carruthers, J.D. Wildemann, C.L. Dearth, and S.F. Badylak, Ecm Hydrogel Coating Mitigates the Chronic Inflammatory Response to Polypropylene Mesh. Biomaterials, 2014. 35(30): p. 8585-95.

137. Feola, A., W. Barone, P. Moalli, and S. Abramowitch, Characterizing the Ex Vivo Textile and Structural Properties of Synthetic Prolapse Mesh Products. Int Urogynecol J, 2013. 24(4): p. 559-64.

138. Ferrell, A.S. and G.W. Britz, Developments on the Horizon in the Treatment of Neurovascular Problems. Surg Neurol Int, 2013. 4(Suppl 1): p. S31-7.

139. Fleckenstein-Grun, G. and A. Fleckenstein, Calcium--a Neglected Key Factor in Arteriosclerosis. The Pathogenic Role of Arterial Calcium Overload and Its Prevention by Calcium Antagonists. Ann Med, 1991. 23(5): p. 589-99.

140. Flegal, K.M., M.D. Carroll, B.K. Kit, and C.L. Ogden, Prevalence of Obesity and Trends in the Distribution of Body Mass Index among Us Adults, 1999-2010. JAMA, 2012. 307(5): p. 491-7.

141. Flynn, L.E., The Use of Decellularized Adipose Tissue to Provide an Inductive Microenvironment for the Adipogenic Differentiation of Human Adipose-Derived Stem Cells. Biomaterials, 2010. 31(17): p. 4715-24.

142. Forde, P.M. and R.J. Kelly, Chemotherapeutic and Targeted Strategies for Locally Advanced and Metastatic Esophageal Cancer. J Thorac Oncol, 2013.

143. French, K.M., A.V. Boopathy, J.A. DeQuach, L. Chingozha, H. Lu, K.L. Christman, and M.E. Davis, A Naturally Derived Cardiac Extracellular Matrix Enhances Cardiac Progenitor Cell Behavior in Vitro. Acta Biomater, 2012. 8(12): p. 4357-64.

144. French, K.M., A.V. Boopathy, J.A. Dequach, L. Chingozha, H. Lu, K.L. Christman, and M.E. Davis, A Naturally Derived Cardiac Extracellular Matrix Enhances Cardiac Progenitor Cell Behavior in Vitro. Acta Biomater, 2012.

145. Freund, K.M., A.J. Belanger, R.B. D'Agostino, and W.B. Kannel, The Health Risks of Smoking. The Framingham Study: 34 Years of Follow-Up. Ann Epidemiol, 1993. 3(4): p. 417-24.

146. Freytes, D.O., R.M. Stoner, and S.F. Badylak, Uniaxial and Biaxial Properties of Terminally Sterilized Porcine Urinary Bladder Matrix Scaffolds. J Biomed Mater Res B Appl Biomater, 2008. 84(2): p. 408-14.

147. Freytes, D.O., R.M. Stoner, and S.F. Badylak, Uniaxial and Biaxial Properties of Terminally Sterilized Porcine Urinary Bladder Matrix Scaffolds., in J. Biomed. Mater. Res. Part B Appl. Biomater. 2008. p. 408-414.

148. Freytes, D.O., R.S. Tullius, and S.F. Badylak, Effect of Storage Upon Material Properties of Lyophilized Porcine Extracellular Matrix Derived from the Urinary Bladder. Journal

of Biomedical Materials Research - Part B Applied Biomaterials, 2006. 78(2): p. 327-333.

149. Freytes, D.O., R.S. Tullius, J.E. Valentin, A.M. Stewart-Akers, and S.F. Badylak, Hydrated Versus Lyophilized Forms of Porcine Extracellular Matrix Derived from the Urinary Bladder. Journal of Biomedical Materials Research - Part A, 2008. 87(4): p. 862-872.

150. Fujimoto, K.L., Z. Ma, D.M. Nelson, R. Hashizume, J. Guan, K. Tobita, and W.R. Wagner, Synthesis, Characterization and Therapeutic Efficacy of a Biodegradable, Thermoresponsive Hydrogel Designed for Application in Chronic Infarcted Myocardium. Biomaterials, 2009. 30(26): p. 4357-68.

151. Fulop, T., A. Larbi, N. Douziech, C. Fortin, K.P. Guerard, O. Lesur, A. Khalil, and G. Dupuis, Signal Transduction and Functional Changes in Neutrophils with Aging. Aging Cell, 2004. 3(4): p. 217-26.

152. Furman, M.I., H.L. Dauerman, R.J. Goldberg, J. Yarzebski, D. Lessard, and J.M. Gore, Twenty-Two Year (1975 to 1997) Trends in the Incidence, in-Hospital and Long-Term Case Fatality Rates from Initial Q-Wave and Non-Q-Wave Myocardial Infarction: A Multi-Hospital, Community-Wide Perspective. J Am Coll Cardiol, 2001. 37(6): p. 1571-80.

153. Gaetani, R., D.A. Feyen, V. Verhage, R. Slaats, E. Messina, K.L. Christman, A. Giacomello, P.A. Doevendans, and J.P. Sluijter, Epicardial Application of Cardiac Progenitor Cells in a 3d-Printed Gelatin/Hyaluronic Acid Patch Preserves Cardiac Function after Myocardial Infarction. Biomaterials, 2015. 61: p. 339-48.

154. Gander, J.W., W.E. Berdon, and R.A. Cowles, Iatrogenic Esophageal Perforation in Children. Pediatr Surg Int, 2009. 25(5): p. 395-401.

155. Garrison, R.J., M.W. Higgins, and W.B. Kannel, Obesity and Coronary Heart Disease. Curr Opin Lipidol, 1996. 7(4): p. 199-202.

156. Garvey, P.B., R.A. Martinez, D.P. Baumann, J. Liu, and C.E. Butler, Outcomes of Abdominal Wall Reconstruction with Acellular Dermal Matrix Are Not Affected by Wound Contamination. J Am Coll Surg, 2014. 219(5): p. 853-64.

157. Gaut, C. and K. Sugaya, Critical Review on the Physical and Mechanical Factors Involved in Tissue Engineering of Cartilage. Regen Med, 2015: p. 1-15.

158. Geboes, K. and V. Desmet, Histology of the Esophagus. Front Gastrointest Res, 1978. 3: p. 1-17.

159. Giannelli, G., J. Falk-Marzillier, O. Schiraldi, W.G. Stetler-Stevenson, and V. Quaranta, Induction of Cell Migration by Matrix Metalloprotease-2 Cleavage of Laminin-5. Science, 1997. 277(5323): p. 225-8.

160. Gibbs, J.F., A. Rajput, K.S. Chadha, W.G. Douglas, H. Hill, C. Nwogu, H.R. Nava, and M.S. Sabel, The Changing Profile of Esophageal Cancer Presentation and Its Implication for Diagnosis. J Natl Med Assoc, 2007. 99(6): p. 620-6.

161. Gilbert, T.W., T.L. Sellaro, and S.F. Badylak, Decellularization of Tissues and Organs. Biomaterials, 2006. 27(19): p. 3675-83.

162. Gilbert, T.W., A.M. Stewart-Akers, A. Simmons-Byrd, and S.F. Badylak, Degradation and Remodeling of Small Intestinal Submucosa in Canine Achilles Tendon Repair. J Bone Joint Surg Am, 2007. 89(3): p. 621-30.

163. Gilbert, T.W., S. Wognum, E.M. Joyce, D.O. Freytes, M.S. Sacks, and S.F. Badylak, Collagen Fiber Alignment and Biaxial Mechanical Behavior of Porcine Urinary Bladder Derived Extracellular Matrix. Biomaterials, 2008. 29(36): p. 4775-4782.

164. Gillman, M.W., W.B. Kannel, A. Belanger, and R.B. D'Agostino, Influence of Heart Rate on Mortality among Persons with Hypertension: The Framingham Study. Am Heart J, 1993. 125(4): p. 1148-54.

165. Girardin, M., et al., First-Line Therapies in Inflammatory Bowel Disease. Digestion, 2012. 86 Suppl 1: p. 6-10.

166. Giri, S., R. Pathak, M.R. Aryal, P. Karmacharya, V.R. Bhatt, and M.G. Martin, Incidence Trend of Esophageal Squamous Cell Carcinoma: An Analysis of Surveillance Epidemiology, and End Results (Seer) Database. Cancer Causes Control, 2015. 26(1): p. 159-61.

167. Gonzalez, C., O. Najera, E. Cortes, G. Toledo, L. Lopez, M. Betancourt, and R. Ortiz, Hydrogen Peroxide-Induced DNA Damage and DNA Repair in Lymphocytes from Malnourished Children. Environ Mol Mutagen, 2002. 39(1): p. 33-42.

168. Gorelick, P.B. and D. Nyenhuis, Understanding and Treating Vascular Cognitive Impairment. Continuum (Minneap Minn), 2013. 19(2 Dementia): p. 425-37.

169. Gorschewsky, O., A. Klakow, K. Riechert, M. Pitzl, and R. Becker, Clinical Comparison of the Tutoplast Allograft and Autologous Patellar Tendon (Bone-Patellar Tendon-Bone) for the Reconstruction of the Anterior Cruciate Ligament: 2- and 6-Year Results. Am J Sports Med, 2005. 33(8): p. 1202-9.

170. Gorschewsky, O., A. Puetz, K. Riechert, A. Klakow, and R. Becker, Quantitative Analysis of Biochemical Characteristics of Bone-Patellar Tendon-Bone Allografts. Biomed Mater Eng, 2005. 15(6): p. 403-11.

171. Gorschewsky, O., R. Stapf, L. Geiser, U. Geitner, and W. Neumann, Clinical Comparison of Fixation Methods for Patellar Bone Quadriceps Tendon Autografts in Anterior Cruciate Ligament Reconstruction: Absorbable Cross-Pins Versus Absorbable Screws. Am J Sports Med, 2007. 35(12): p. 2118-25.

172. Goyal, A., M.O. Jones, J.M. Couriel, and P.D. Losty, Oesophageal Atresia and Tracheo-Oesophageal Fistula. Arch Dis Child Fetal Neonatal Ed, 2006. 91(5): p. F381-4.

173. Goyal, H.K., S.K. Kaushik, J.P. Dhamieja, R.K. Suman, and K.K. Kumar, A Study of Granulocyte Adherence in Protein Calorie Malnutrition. Indian Pediatr, 1981. 18(5): p. 287-92.

174. Grobe, A.C., D.T. Cheung, H.H. Luo, Y. Shomura, D.C. Marchion, J.C. Pfau, and C.M. Duran, A Study of the Junction between Glutaraldehyde-Treated Allogeneic Aorta and Host Aorta. J Heart Valve Dis, 2000. 9(4): p. 570-5.

175. Grogan, B.F. and J.R. Hsu, Volumetric Muscle Loss. J Am Acad Orthop Surg, 2011. 19 Suppl 1: p. S35-7.

176. Groulx, J.F., D. Gagne, Y.D. Benoit, D. Martel, N. Basora, and J.F. Beaulieu, Collagen Vi Is a Basement Membrane Component That Regulates Epithelial Cell-Fibronectin Interactions. Matrix Biol, 2011. 30(3): p. 195-206.

177. Guan, J., M.S. Sacks, E.J. Beckman, and W.R. Wagner, Synthesis, Characterization, and Cytocompatibility of Elastomeric, Biodegradable Poly(Ester-Urethane)Ureas Based on Poly(Caprolactone) and Putrescine. J Biomed Mater Res, 2002. 61(3): p. 493-503.

178. Guan, J., M.S. Sacks, E.J. Beckman, and W.R. Wagner, Biodegradable Poly(Ether Ester Urethane)Urea Elastomers Based on Poly(Ether Ester) Triblock Copolymers and Putrescine: Synthesis, Characterization and Cytocompatibility. Biomaterials, 2004. 25(1): p. 85-96.

179. Guven, A., S. Demirbag, B. Uysal, T. Topal, E. Erdogan, A. Korkmaz, and H. Ozturk, Effect of 3-Amino Benzamide, a Poly(Adenosine Diphosphate-Ribose) Polymerase Inhibitor, in Experimental Caustic Esophageal Burn. J Pediatr Surg, 2008. 43(8): p. 1474-9.

180. Hafeez, Y.M., A.B. Zuki, N. Yusof, H. Asnah, M.Y. Loqman, M.M. Noordin, and M.Y. Ainul-Yuzairi, Effect of Freeze-Drying and Gamma Irradiation on Biomechanical Properties of Bovine Pericardium. Cell Tissue Bank, 2005. 6(2): p. 85-9.

181. Hanna, G.B., S. Arya, and S.R. Markar, Variation in the Standard of Minimally Invasive Esophagectomy for Cancer--Systematic Review. Semin Thorac Cardiovasc Surg, 2012. 24(3): p. 176-87.

182. Hashizume, R., K.L. Fujimoto, Y. Hong, J. Guan, C. Toma, K. Tobita, and W.R. Wagner, Biodegradable Elastic Patch Plasty Ameliorates Left Ventricular Adverse Remodeling after Ischemia-Reperfusion Injury: A Preclinical Study of a Porous Polyurethane Material in a Porcine Model. J Thorac Cardiovasc Surg, 2013. 146(2): p. 391-9 e1.

183. Hashizume, R., Y. Hong, K. Takanari, K.L. Fujimoto, K. Tobita, and W.R. Wagner, The Effect of Polymer Degradation Time on Functional Outcomes of Temporary Elastic Patch Support in Ischemic Cardiomyopathy. Biomaterials, 2013. 34(30): p. 7353-63.

184. Hayashi, M., W. Shimizu, and C.M. Albert, The Spectrum of Epidemiology Underlying Sudden Cardiac Death. Circ Res, 2015. 116(12): p. 1887-906.

185. Hazeldine, J. and J.M. Lord, Innate Immunesenescence: Underlying Mechanisms and Clinical Relevance. Biogerontology, 2014.

186. Hearps, A.C., G.E. Martin, T.A. Angelovich, W.J. Cheng, A. Maisa, A.L. Landay, A. Jaworowski, and S.M. Crowe, Aging Is Associated with Chronic Innate Immune Activation and Dysregulation of Monocyte Phenotype and Function. Aging Cell, 2012. 11(5): p. 867-75.

187. Hegsted, D.M., Relevance of Animal Studies to Human Disease. Cancer Res, 1975. 35(11 Pt. 2): p. 3537-9.

188. Heimann, R. and R.H. Rice, Rat Esophageal and Epidermal Keratinocytes: Intrinsic Differences in Culture and Derivation of Continuous Lines. J Cell Physiol, 1983. 117(3): p. 362-7.

189. Hernandez-Gascon, B., E. Pena, H. Melero, G. Pascual, M. Doblare, M.P. Ginebra, J.M. Bellon, and B. Calvo, Mechanical Behaviour of Synthetic Surgical Meshes: Finite Element Simulation of the Herniated Abdominal Wall. Acta Biomater, 2011. 7(11): p. 3905-13.

190. Heron, M., Deaths: Leading Causes for 2010. Natl Vital Stat Rep, 2013. 62(6): p. 1-96.

191. Ho, C., D.K. Tong, J.S. Tsang, and S.Y. Law, Post-Esophagectomy Gastric Conduit Cancers: Treatment Experiences and Literature Review. Dis Esophagus, 2013.

192. Hocking, D.C. and K. Kowalski, A Cryptic Fragment from Fibronectin's Iii1 Module Localizes to Lipid Rafts and Stimulates Cell Growth and Contractility. J Cell Biol, 2002. 158(1): p. 175-84.

193. Hodde, J. and M. Hiles, Virus Safety of a Porcine-Derived Medical Device: Evaluation of a Viral Inactivation Method. Biotechnol Bioeng, 2002. 79(2): p. 211-6.

194. Hodde, J. and M. Hiles, Constructive Soft Tissue Remodelling with a Biologic Extracellular Matrix Graft: Overview and Review of the Clinical Literature. Acta Chir Belg, 2007. 107(6): p. 641-7.

195. Hodde, J., A. Janis, D. Ernst, D. Zopf, D. Sherman, and C. Johnson, Effects of Sterilization on an Extracellular Matrix Scaffold: Part I. Composition and Matrix Architecture. J Mater Sci Mater Med, 2007. 18(4): p. 537-43.

196. Hodde, J., A. Janis, and M. Hiles, Effects of Sterilization on an Extracellular Matrix Scaffold: Part Ii. Bioactivity and Matrix Interaction. J Mater Sci Mater Med, 2007. 18(4): p. 545-50.

197. Hodde, J., R. Record, R. Tullius, and S. Badylak, Fibronectin Peptides Mediate Hmec Adhesion to Porcine-Derived Extracellular Matrix. Biomaterials, 2002. 23(8): p. 1841-8.

198. Hodde, J.P., S.F. Badylak, A.O. Brightman, and S.L. Voytik-Harbin, Glycosaminoglycan Content of Small Intestinal Submucosa: A Bioscaffold for Tissue Replacement. Tissue Eng, 1996. 2(3): p. 209-17.

199. Hodde, J.P., R.D. Record, R.S. Tullius, and S.F. Badylak, Retention of Endothelial Cell Adherence to Porcine-Derived Extracellular Matrix after Disinfection and Sterilization. Tissue Eng, 2002. 8(2): p. 225-34.

200. Hofmann, M., K.C. Wollert, G.P. Meyer, A. Menke, L. Arseniev, B. Hertenstein, A. Ganser, W.H. Knapp, and H. Drexler, Monitoring of Bone Marrow Cell Homing into the Infarcted Human Myocardium. Circulation, 2005. 111(17): p. 2198-202.

201. Holmes, R.S. and T.L. Vaughan, Epidemiology and Pathogenesis of Esophageal Cancer. Semin Radiat Oncol, 2007. 17(1): p. 2-9.

202. Hong, Y., J. Guan, K.L. Fujimoto, R. Hashizume, A.L. Pelinescu, and W.R. Wagner, Tailoring the Degradation Kinetics of Poly(Ester Carbonate Urethane)Urea Thermoplastic Elastomers for Tissue Engineering Scaffolds. Biomaterials, 2010. 31(15): p. 4249-58.

203. Hoppo, T., S.D. Rachit, and B.A. Jobe, Esophageal Preservation in Esophageal High-Grade Dysplasia and Intramucosal Adenocarcinoma. Thoracic Surgery Clinics, 2011. 21(4): p. 527-540.

204. Hori, Y., T. Nakamura, D. Kimura, K. Kaino, Y. Kurokawa, S. Satomi, and Y. Shimizu, Effect of Basic Fibroblast Growth Factor on Vascularization in Esophagus Tissue Engineering. Int J Artif Organs, 2003. 26(3): p. 241-4.

205. Hornby, P.J. and T.P. Abrahams, Central Control of Lower Esophageal Sphincter Relaxation. Am J Med, 2000. 108 Suppl 4a: p. 90S-98S.

206. Hotamisligil, G.S., N.S. Shargill, and B.M. Spiegelman, Adipose Expression of Tumor Necrosis Factor-Alpha: Direct Role in Obesity-Linked Insulin Resistance. Science, 1993. 259(5091): p. 87-91.

207. Huber, A. and S.F. Badylak, Biological Scaffolds for Regenerative Medicine, in Principles of Regenerative Medicine. 2011. p. 623-635.

208. Hughes, S.M., B. Amadi, M. Mwiya, H. Nkamba, A. Tomkins, and D. Goldblatt, Dendritic Cell Anergy Results from Endotoxemia in Severe Malnutrition. J Immunol, 2009. 183(4): p. 2818-26.

209. Hurtgen, M. and S.C. Herber, Treatment of Malignant Tracheoesophageal Fistula. Thorac Surg Clin, 2014. 24(1): p. 117-27.

210. Hutter, H., et al., Conservation and Novelty in the Evolution of Cell Adhesion and Extracellular Matrix Genes. Science, 2000. 287(5455): p. 989-94.

211. Hynes, R.O., The Extracellular Matrix: Not Just Pretty Fibrils. Science, 2009. 326(5957): p. 1216-9.

212. Hynes, R.O. and Q. Zhao, The Evolution of Cell Adhesion. J Cell Biol, 2000. 150(2): p. F89-96.

213. Iozzo, R.V., I.R. Cohen, S. Grassel, and A.D. Murdoch, The Biology of Perlecan: The Multifaceted Heparan Sulphate Proteoglycan of Basement Membranes and Pericellular Matrices. Biochem J, 1994. 302 (Pt 3): p. 625-39.

214. Iozzo, R.V. and A.D. Murdoch, Proteoglycans of the Extracellular Environment: Clues from the Gene and Protein Side Offer Novel Perspectives in Molecular Diversity and Function. FASEB J, 1996. 10(5): p. 598-614.

215. Jakob, P. and U. Landmesser, Current Status of Cell-Based Therapy for Heart Failure. Curr Heart Fail Rep, 2013. 10(2): p. 165-76.

216. Janis, J.E., R.K. Kwon, and D.H. Lalonde, A Practical Guide to Wound Healing. Plast Reconstr Surg, 2010. 125(6): p. 230e-44e.

217. Jemal, A., F. Bray, M.M. Center, J. Ferlay, E. Ward, and D. Forman, Global Cancer Statistics. CA Cancer J Clin, 2011. 61(2): p. 69-90.

218. Johnson, T.D. and K.L. Christman, Injectable Hydrogel Therapies and Their Delivery Strategies for Treating Myocardial Infarction. Expert Opin Drug Deliv, 2013. 10(1): p. 59-72.

219. Johnson, T.D., J.A. Dequach, R. Gaetani, J. Ungerleider, D. Elhag, V. Nigam, A. Behfar, and K.L. Christman, Human Versus Porcine Tissue Sourcing for an Injectable Myocardial Matrix Hydrogel. Biomater Sci, 2014. 2014: p. 60283D.

220. Jonsson, L., L.G. Friberg, V. Gatzinsky, E. Jennische, A. Sandin, and K. Abrahamsson, Early Regenerative Response in the Intrathoracic Porcine Esophagus-the Impact of the Inflammation. Artif Organs, 2014. 38(6): p. 439-46.

221. Kamangar, F., W.H. Chow, C.C. Abnet, and S.M. Dawsey, Environmental Causes of Esophageal Cancer. Gastroenterol Clin North Am, 2009. 38(1): p. 27-57, vii.

222. Kamentsky, L., et al., Improved Structure, Function and Compatibility for Cellprofiler: Modular High-Throughput Image Analysis Software. Bioinformatics, 2011. 27(8): p. 1179-80.

223. Kanagarajah, P., R. Ayyathurai, and C. Gomez, Evaluation of Current Synthetic Mesh Materials in Pelvic Organ Prolapse Repair. Curr Urol Rep, 2012. 13(3): p. 240-6.

224. Kannel, W.B., Lipids, Diabetes, and Coronary Heart Disease: Insights from the Framingham Study. Am Heart J, 1985. 110(5): p. 1100-7.

225. Kannel, W.B., R.B. D'Agostino, and H. Silbershatz, Blood Pressure and Cardiovascular Morbidity and Mortality Rates in the Elderly. Am Heart J, 1997. 134(4): p. 758-63.

226. Kasimir, M.T., E. Rieder, G. Seebacher, G. Silberhumer, E. Wolner, G. Weigel, and P. Simon, Comparison of Different Decellularization Procedures of Porcine Heart Valves. Int J Artif Organs, 2003. 26(5): p. 421-7.

227. Katari, R.S., A. Peloso, and G. Orlando, Tissue Engineering. Adv Surg, 2014. 48: p. 137-54.

228. Kato, H. and M. Nakajima, Treatments for Esophageal Cancer: A Review. Gen Thorac Cardiovasc Surg, 2013.

229. Keane, T.J. and S.F. Badylak, The Host Response to Allogeneic and Xenogeneic Biological Scaffold Materials. J Tissue Eng Regen Med, 2014.

230. Keane, T.J., R. Londono, R.M. Carey, C.A. Carruthers, J.E. Reing, C.L. Dearth, A. D'Amore, C.J. Medberry, and S.F. Badylak, Preparation and Characterization of a Biologic Scaffold from Esophageal Mucosa. Biomaterials, 2013. 34(28): p. 6729-37.

231. Keane, T.J., R. Londono, N.J. Turner, and S.F. Badylak, Consequences of Ineffective Decellularization of Biologic Scaffolds on the Host Response. Biomaterials, 2012. 33(6): p. 1771-81.

232. Keckler, S.J., S.D. St Peter, P.A. Valusek, K. Tsao, C.L. Snyder, G.W. Holcomb, 3rd, and D.J. Ostlie, Vacterl Anomalies in Patients with Esophageal Atresia: An Updated Delineation of the Spectrum and Review of the Literature. Pediatr Surg Int, 2007. 23(4): p. 309-13.

233. Keeley, S.B., A. Pennathur, W. Gooding, R.J. Landreneau, N.A. Christie, and J. Luketich, Photodynamic Therapy with Curative Intent for Barrett's Esophagus with High Grade Dysplasia and Superficial Esophageal Cancer. Ann Surg Oncol, 2007. 14(8): p. 2406-10.

234. Kemp, P., History of Regenerative Medicine: Looking Backwards to Move Forwards. Regen Med, 2006. 1(5): p. 653-69.

235. Keusch, G.T., J.R. Cruz, B. Torun, J.J. Urrutia, H. Smith, Jr., and A.L. Goldstein, Immature Circulating Lymphocytes in Severely Malnourished Guatemalan Children. J Pediatr Gastroenterol Nutr, 1987. 6(2): p. 265-70.

236. Khay Leong, W., M.D. Lewis, and S.A. Koblar, Preclinical Studies on Human Cell-Based Therapy in Rodent Ischemic Stroke Models: Where Are We Now after a Decade? Stem Cells, 2013.

237. Kikendall, J.W., Caustic Ingestion Injuries. Gastroenterol Clin North Am, 1991. 20(4): p. 847-57.

238. Kissane, N.A. and K.M. Itani, A Decade of Ventral Incisional Hernia Repairs with Biologic Acellular Dermal Matrix: What Have We Learned? Plast Reconstr Surg, 2012. 130(5 Suppl 2): p. 194S-202S.

239. Klein, M. and A. Wang, Infective Endocarditis. J Intensive Care Med, 2014.

240. Klinge, U., B. Klosterhalfen, M. Muller, and V. Schumpelick, Foreign Body Reaction to Meshes Used for the Repair of Abdominal Wall Hernias. Eur J Surg, 1999. 165(7): p. 665-73.

241. Klosterhalfen, B., K. Junge, and U. Klinge, The Lightweight and Large Porous Mesh Concept for Hernia Repair. Expert Rev Med Devices, 2005. 2(1): p. 103-17.

242. Knorr, C., R.T. Carbon, S. Albrecht, M. Richter, and H. Kohler, Perforation of the Proximal Esophagus Treated with Factor Xiii. Endoscopy, 2008. 40 Suppl 2: p. E197.

243. Koch, H., C. Graneist, F. Emmrich, H. Till, R. Metzger, H. Aupperle, K. Schierle, U. Sack, and A. Boldt, Xenogenic Esophagus Scaffolds Fixed with Several Agents: Comparative in Vivo Study of Rejection and Inflammation. J Biomed Biotechnol, 2012. 2012: p. 948320.

244. Kollar, E.W., C.L. Dearth, and S.F. Badylak, Biologic Scaffolds Composed of Extracellular Matrix as a Natural Material for Wound Healing, in Bio-Inspired Materials for Biomedical Engineering. 2014. p. 111-124.

245. Konstam, M.A., D.G. Kramer, A.R. Patel, M.S. Maron, and J.E. Udelson, Left Ventricular Remodeling in Heart Failure: Current Concepts in Clinical Significance and Assessment. JACC Cardiovasc Imaging, 2011. 4(1): p. 98-108.

246. Korpos, E., C. Wu, J. Song, R. Hallmann, and L. Sorokin, Role of the Extracellular Matrix in Lymphocyte Migration. Cell Tissue Res, 2010. 339(1): p. 47-57.

247. Kosovec, J.E., A.H. Zaidi, Y. Komatsu, P.M. Kasi, K. Cothron, D.V. Thompson, E. Lynch, and B.A. Jobe, Establishing Magnetic Resonance Imaging as an Accurate and Reliable Tool to Diagnose and Monitor Esophageal Cancer in a Rat Model. PLoS One, 2014. 9(4): p. e93694.

248. Koudstaal, S., S.J. Jansen Of Lorkeers, R. Gaetani, J.M. Gho, F.J. van Slochteren, J.P. Sluijter, P.A. Doevendans, G.M. Ellison, and S.A. Chamuleau, Concise Review: Heart Regeneration and the Role of Cardiac Stem Cells. Stem Cells Transl Med, 2013.

249. Kraakman, M.J., A.J. Murphy, K. Jandeleit-Dahm, and H.L. Kammoun, Macrophage Polarization in Obesity and Type 2 Diabetes: Weighing Down Our Understanding of Macrophage Function? Front Immunol, 2014. 5: p. 470.

250. Kramer, J.M., Extracellular Matrix, in C. Elegans Ii, D.L. Riddle, et al., Editors. 1997: Cold Spring Harbor (NY).

251. Kubo, N., et al., The Impact of Combined Thoracoscopic and Laparoscopic Surgery on Pulmonary Complications after Radical Esophagectomy in Patients with Resectable Esophageal Cancer. Anticancer Res, 2014. 34(5): p. 2399-404.

252. Kuehn, C., K. Graf, W. Heuer, A. Hilfiker, I.F. Chaberny, M. Stiesch, and A. Haverich, Economic Implications of Infections of Implantable Cardiac Devices in a Single Institution. Eur J Cardiothorac Surg, 2010. 37(4): p. 875-9.

253. Kumar, R., A. Kumar, R.S. Sethi, R.K. Gupta, A.K. Kaushik, and S. Longia, A Study of Complement Activity in Malnutrition. Indian Pediatr, 1984. 21(7): p. 541-7.

254. Kuppan, P., S. Sethuraman, and U.M. Krishnan, Poly(3-Hydroxybutyrate-Co-3-Hydroxyvalerate)-Based Nanofibrous Scaffolds to Support Functional Esophageal Epithelial Cells Towards Engineering the Esophagus. J Biomater Sci Polym Ed, 2014. 25(6): p. 574-93.

255. Ladowski, J.M. and J.S. Ladowski, Retrospective Analysis of Bovine Pericardium (Vascu-Guard) for Patch Closure in Carotid Endarterectomies. Ann Vasc Surg, 2011. 25(5): p. 646-50.

256. Laki, K. and L. Lorand, On the Solubility of Fibrin Clots. Science, 1948. 108(2802): p. 280.

257. Lamprecht, M.R., D.M. Sabatini, and A.E. Carpenter, Cellprofiler: Free, Versatile Software for Automated Biological Image Analysis. Biotechniques, 2007. 42(1): p. 71-5.

258. Larsson, J., S. Sutherland, A. Soderstrom, C. Roman-Emanuel, A. Jeppsson, E.H. Olofsson, and P.A. Svensson, Bacterial Contamination of Suction Catheter Tips During Aortic Valve Replacement Surgery: A Prospective Observational Cohort Study. Patient Saf Surg, 2015. 9: p. 17.

259. Laugwitz, K.L., et al., Postnatal Isl1+ Cardioblasts Enter Fully Differentiated Cardiomyocyte Lineages. Nature, 2005. 433(7026): p. 647-53.

260. Lawes, C.M., S. Vander Hoorn, A. Rodgers, and H. International Society of, Global Burden of Blood-Pressure-Related Disease, 2001. Lancet, 2008. 371(9623): p. 1513-8.

261. Leber, G.E., J.L. Garb, A.I. Alexander, and W.P. Reed, Long-Term Complications Associated with Prosthetic Repair of Incisional Hernias. Arch Surg, 1998. 133(4): p. 378-82.

262. Lee, M.A., et al., Effects of Long-Term Right Ventricular Apical Pacing on Left Ventricular Perfusion, Innervation, Function and Histology. J Am Coll Cardiol, 1994. 24(1): p. 225-32.

263. Leor, J., S. Aboulafia-Etzion, A. Dar, L. Shapiro, I.M. Barbash, A. Battler, Y. Granot, and S. Cohen, Bioengineered Cardiac Grafts: A New Approach to Repair the Infarcted Myocardium? Circulation, 2000. 102(19 Suppl 3): p. III56-61.

264. Levy, R.J., N. Vyavahare, M. Ogle, P. Ashworth, R. Bianco, and F.J. Schoen, Inhibition of Cusp and Aortic Wall Calcification in Ethanol- and Aluminum-Treated Bioprosthetic Heart Valves in Sheep: Background, Mechanisms, and Synergism. J Heart Valve Dis, 2003. 12(2): p. 209-16; discussion 216.

265. Levy, R.L., H.G. Bruenn, and D. Kurtz, Facts on Coronary Artery Disease, Based on a Survey of the Clinical and Pathological Records of 762 Cases: Abstract. Trans Am Clin Climatol Assoc, 1933. 49: p. 67-76.

266. Li, H., S. Zuo, Z. He, Y. Yang, Z. Pasha, Y. Wang, and M. Xu, Paracrine Factors Released by Gata-4 Overexpressed Mesenchymal Stem Cells Increase Angiogenesis and Cell Survival. Am J Physiol Heart Circ Physiol, 2010. 299(6): p. H1772-81.

267. Li, R., L. Liang, Y. Dou, Z. Huang, H. Mo, Y. Wang, and B. Yu, Mechanical Strain Regulates Osteogenic and Adipogenic Differentiation of Bone Marrow Mesenchymal Stem Cells. Biomed Res Int, 2015. 2015: p. 873251.

268. Li, Y. and R.C. Martin, 2nd, Reflux Injury of Esophageal Mucosa: Experimental Studies in Animal Models of Esophagitis, Barrett's Esophagus and Esophageal Adenocarcinoma. Dis Esophagus, 2007. 20(5): p. 372-8.

269. Lloyd-Jones, D., et al., Executive Summary: Heart Disease and Stroke Statistics--2010 Update: A Report from the American Heart Association. Circulation, 2010. 121(7): p. 948-54.

270. Lloyd-Jones, D.M., M.G. Larson, A. Beiser, and D. Levy, Lifetime Risk of Developing Coronary Heart Disease. Lancet, 1999. 353(9147): p. 89-92.

271. Londono, R. and S.F. Badylak, Biologic Scaffolds for Regenerative Medicine: Mechanisms of in Vivo Remodeling. Ann Biomed Eng, 2014.

272. Londono, R. and S.F. Badylak, Biologic Scaffolds for Regenerative Medicine: Mechanisms of in Vivo Remodeling. Annals of Biomedical Engineering, 2015. 43(3): p. 577-592.

273. Londono, R. and S.F. Badylak, Biologic Scaffolds for Regenerative Medicine: Mechanisms of in Vivo Remodeling. Ann Biomed Eng, 2015. 43(3): p. 577-92.

274. Londono, R. and S.F. Badylak, Regenerative Medicine Strategies for Esophageal Repair. Tissue Eng Part B Rev, 2015.

275. Londono, R., B.A. Jobe, T. Hoppo, and S.F. Badylak, Esophagus and Regenerative Medicine. World J Gastroenterol, 2012. 18(47): p. 6894-9.

276. Lopes, M.F., A. Cabrita, J. Ilharco, P. Pessa, J. Paiva-Carvalho, A. Pires, and J. Patricio, Esophageal Replacement in Rat Using Porcine Intestinal Submucosa as a Patch or a Tube-Shaped Graft. Dis Esophagus, 2006. 19(4): p. 254-9.

277. Ludke, A., R.K. Li, and R.D. Weisel, The Rejuvenation of Aged Stem Cells for Cardiac Repair. Can J Cardiol, 2014.

278. Luostarinen, M. and J. Isolauri, Esophageal Perforation and Caustic Injury: Approach to Instrumental Perforations of the Esophagus. Dis Esophagus, 1997. 10(2): p. 86-9.

279. Lynen Jansen, P., U. Klinge, M. Anurov, S. Titkova, P.R. Mertens, and M. Jansen, Surgical Mesh as a Scaffold for Tissue Regeneration in the Esophagus. Eur Surg Res, 2004. 36(2): p. 104-11.

280. Maganti, K., V.H. Rigolin, M.E. Sarano, and R.O. Bonow, Valvular Heart Disease: Diagnosis and Management. Mayo Clin Proc, 2010. 85(5): p. 483-500.

281. Mantovani, A., A. Sica, S. Sozzani, P. Allavena, A. Vecchi, and M. Locati, The Chemokine System in Diverse Forms of Macrophage Activation and Polarization. Trends Immunol, 2004. 25(12): p. 677-86.

282. Marcal, H., T. Ahmed, S.F. Badylak, S. Tottey, and L.J. Foster, A Comprehensive Protein Expression Profile of Extracellular Matrix Biomaterial Derived from Porcine Urinary Bladder. Regen Med, 2012. 7(2): p. 159-66.

283. Marquis, R.M., Ventricular Septal Defect in Early Childhood. Br Heart J, 1950. 12(3): p. 265-76.

284. Marzaro, M., et al., In Vitro and in Vivo Proposal of an Artificial Esophagus. J Biomed Mater Res A, 2006. 77(4): p. 795-801.

285. Massee, J.C., Atrial Septal Defect Correlation of Autopsy Findings with Data Obtained by Right Heart Catheterization. Am J Med Sci, 1947. 214(3): p. 248-51.

286. Matsuura, K., Y. Haraguchi, T. Shimizu, and T. Okano, Cell Sheet Transplantation for Heart Tissue Repair. J Control Release, 2013.

287. Mavrogiannaki, A.N. and I.N. Migdalis, Long-Acting Basal Insulin Analogs: Latest Developments and Clinical Usefulness. Ther Adv Chronic Dis, 2012. 3(6): p. 249-57.

288. Maxson, S., E.A. Lopez, D. Yoo, A. Danilkovitch-Miagkova, and M.A. Leroux, Concise Review: Role of Mesenchymal Stem Cells in Wound Repair. Stem Cells Transl Med, 2012. 1(2): p. 142-9.

289. May, A., L. Gossner, A. Behrens, R. Kohnen, M. Vieth, M. Stolte, and C. Ell, A Prospective Randomized Trial of Two Different Endoscopic Resection Techniques for Early Stage Cancer of the Esophagus. Gastrointest Endosc, 2003. 58(2): p. 167-75.

290. McFarlane, H., Cell-Mediated Immunity in Protein-Calorie Malnutrition. Lancet, 1971. 2(7734): p. 1146-7.

291. McLachlan, J.A., C.D. Serkin, K.M. Morrey, and O. Bakouche, Antitumoral Properties of Aged Human Monocytes. J Immunol, 1995. 154(2): p. 832-43.

292. Medberry, C.J., et al., Hydrogels Derived from Central Nervous System Extracellular Matrix. Biomaterials, 2013. 34(4): p. 1033-40.

293. Messier, B. and C.P. Leblond, Cell Proliferation and Migration as Revealed by Radioautography after Injection of Thymidine-H3 into Male Rats and Mice. Am J Anat, 1960. 106: p. 247-85.

294. Meyer, W., B. Schoennagel, J. Kacza, R. Busche, I.N. Hornickel, M. Hewicker-Trautwein, and A. Schnapper, Keratinization of the Esophageal Epithelium of Domesticated Mammals. Acta Histochem, 2014. 116(1): p. 235-42.

295. Midwood, K.S., Y. Mao, H.C. Hsia, L.V. Valenick, and J.E. Schwarzbauer, Modulation of Cell-Fibronectin Matrix Interactions During Tissue Repair. J Investig Dermatol Symp Proc, 2006. 11(1): p. 73-8.

296. Midwood, K.S., L.V. Williams, and J.E. Schwarzbauer, Tissue Repair and the Dynamics of the Extracellular Matrix. Int J Biochem Cell Biol, 2004. 36(6): p. 1031-7.

297. Mills, C.D., K. Kincaid, J.M. Alt, M.J. Heilman, and A.M. Hill, M-1/M-2 Macrophages and the Th1/Th2 Paradigm. J Immunol, 2000. 164(12): p. 6166-73.

298. Mills, S.J., A.J. Cowin, and P. Kaur, Pericytes, Mesenchymal Stem Cells and the Wound Healing Process. Cells, 2013. 2(3): p. 621-34.

299. Miwa, K., H. Sahara, M. Segawa, S. Kinami, T. Sato, I. Miyazaki, and T. Hattori, Reflux of Duodenal or Gastro-Duodenal Contents Induces Esophageal Carcinoma in Rats. Int J Cancer, 1996. 67(2): p. 269-74.

300. Moehler, M., et al., International Comparison of the German Evidence-Based S3-Guidelines on the Diagnosis and Multimodal Treatment of Early and Locally Advanced Gastric Cancer, Including Adenocarcinoma of the Lower Esophagus. Gastric Cancer, 2014.

301. Mogford, J.E., G.E. Davis, S.H. Platts, and G.A. Meininger, Vascular Smooth Muscle Alpha V Beta 3 Integrin Mediates Arteriolar Vasodilation in Response to Rgd Peptides. Circ Res, 1996. 79(4): p. 821-6.

302. Mortensen, M.B., Esophageal Cancer: Biology, Natural History, Staging and Therapeutic Options. Minerva Med, 2007. 98(4): p. 299-303.

303. Mosser, D.M., The Many Faces of Macrophage Activation. J Leukoc Biol, 2003. 73(2): p. 209-12.

304. Muller, J.M., H. Erasmi, M. Stelzner, U. Zieren, and H. Pichlmaier, Surgical Therapy of Oesophageal Carcinoma. Br J Surg, 1990. 77(8): p. 845-57.

305. Murry, C.E., L.J. Field, and P. Menasche, Cell-Based Cardiac Repair: Reflections at the 10-Year Point. Circulation, 2005. 112(20): p. 3174-83.

306. Musci, M., Y. Weng, M. Hubler, T. Chavez, N. Qedra, S. Kosky, J. Stein, H. Siniawski, and R. Hetzer, Predictors of Early Mortality in Patients with Active Infective Native or Prosthetic Aortic Root Endocarditis Undergoing Homograft Aortic Root Replacement. Clin Res Cardiol, 2009. 98(7): p. 443-50.

307. Najera, O., C. Gonzalez, G. Toledo, L. Lopez, and R. Ortiz, Flow Cytometry Study of Lymphocyte Subsets in Malnourished and Well-Nourished Children with Bacterial Infections. Clin Diagn Lab Immunol, 2004. 11(3): p. 577-80.

308. Napier, K.J., M. Scheerer, and S. Misra, Esophageal Cancer: A Review of Epidemiology, Pathogenesis, Staging Workup and Treatment Modalities. World J Gastrointest Oncol, 2014. 6(5): p. 112-20.

309. Nassar, M.F., N.T. Younis, A.G. Tohamy, D.M. Dalam, and M.A. El Badawy, T-Lymphocyte Subsets and Thymic Size in Malnourished Infants in Egypt: A Hospital-Based Study. East Mediterr Health J, 2007. 13(5): p. 1031-42.

310. Nathan, D.M. and S. Russell, The Future of Care for Type 1 Diabetes. CMAJ, 2013. 185(4): p. 285-6.

311. Natsume, T., O. Ike, T. Okada, N. Takimoto, Y. Shimizu, and Y. Ikada, Porous Collagen Sponge for Esophageal Replacement. J Biomed Mater Res, 1993. 27(7): p. 867-75.

312. Nauseef, W.M. and N. Borregaard, Neutrophils at Work. Nat Immunol, 2014. 15(7): p. 602-11.

313. Nguyen, M., A.J. Pace, and B.H. Koller, Age-Induced Reprogramming of Mast Cell Degranulation. J Immunol, 2005. 175(9): p. 5701-7.

314. Nichols, M., N. Townsend, P. Scarborough, and M. Rayner, Cardiovascular Disease in Europe 2014: Epidemiological Update. Eur Heart J, 2014. 35(42): p. 2950-9.

315. Nieponice, A., F.F. Ciotola, F. Nachman, B.A. Jobe, T. Hoppo, R. Londono, S. Badylak, and A.E. Badaloni, Patch Esophagoplasty: Esophageal Reconstruction Using Biologic Scaffolds. Ann Thorac Surg, 2014. 97(1): p. 283-8.

316. Nieponice, A., T.W. Gilbert, and S.F. Badylak, Reinforcement of Esophageal Anastomoses with an Extracellular Matrix Scaffold in a Canine Model. Ann Thorac Surg, 2006. 82(6): p. 2050-8.

317. Nieponice, A., T.W. Gilbert, S.A. Johnson, N.J. Turner, and S.F. Badylak, Bone Marrow-Derived Cells Participate in the Long-Term Remodeling in a Mouse Model of Esophageal Reconstruction. J Surg Res, 2013. 182(1): p. e1-7.

318. Nieponice, A., K. McGrath, I. Qureshi, E.J. Beckman, J.D. Luketich, T.W. Gilbert, and S.F. Badylak, An Extracellular Matrix Scaffold for Esophageal Stricture Prevention after Circumferential Emr. Gastrointest Endosc, 2009. 69(2): p. 289-96.

319. Niklason, L.E., J. Gao, W.M. Abbott, K.K. Hirschi, S. Houser, R. Marini, and R. Langer, Functional Arteries Grown in Vitro. Science, 1999. 284(5413): p. 489-93.

320. Nonaka, M., T. Kusuhara, K. An, D. Nakatsuka, Y. Sekine, A. Iwakura, and K. Yamanaka, Comparison between Early and Late Prosthetic Valve Endocarditis: Clinical Characteristics and Outcomes. J Heart Valve Dis, 2013. 22(4): p. 567-74.

321. Novak, M.L. and T.J. Koh, Macrophage Phenotypes During Tissue Repair. J Leukoc Biol, 2013. 93(6): p. 875-81.

322. Nyland, J., N. Larsen, R. Burden, H. Chang, and D.N. Caborn, Biomechanical and Tissue Handling Property Comparison of Decellularized and Cryopreserved Tibialis Anterior Tendons Following Extreme Incubation and Rehydration. Knee Surg Sports Traumatol Arthrosc, 2009. 17(1): p. 83-91.

323. O'Neill, O.M., B.T. Johnston, and H.G. Coleman, Achalasia: A Review of Clinical Diagnosis, Epidemiology, Treatment and Outcomes. World J Gastroenterol, 2013. 19(35): p. 5806-12.

324. Obi, S., K. Yamamoto, and J. Ando, Effects of Shear Stress on Endothelial Progenitor Cells. J Biomed Nanotechnol, 2014. 10(10): p. 2586-97.

325. Ogden, C.L., M.D. Carroll, B.K. Kit, and K.M. Flegal, Prevalence of Obesity and Trends in Body Mass Index among Us Children and Adolescents, 1999-2010. JAMA, 2012. 307(5): p. 483-90.

326. Oh, J., N. Hong, and S.M. Kang, Dietary Therapy in Hypertension. N Engl J Med, 2010. 363(16): p. 1582; author reply 1582-3.

327. Oh, J., Y.D. Lee, and A.J. Wagers, Stem Cell Aging: Mechanisms, Regulators and Therapeutic Opportunities. Nat Med, 2014. 20(8): p. 870-80.

328. Okita, Y., et al., Strategies for the Treatment of Aorto-Oesophageal Fistula. Eur J Cardiothorac Surg, 2014. 46(5): p. 894-900.

329. Orringer, M.B., B. Marshall, and M.D. Iannettoni, Transhiatal Esophagectomy for Treatment of Benign and Malignant Esophageal Disease. World J Surg, 2001. 25(2): p. 196-203.

330. Ortega, N. and Z. Werb, New Functional Roles for Non-Collagenous Domains of Basement Membrane Collagens. J Cell Sci, 2002. 115(Pt 22): p. 4201-14.

331. Osborn, O. and J.M. Olefsky, The Cellular and Signaling Networks Linking the Immune System and Metabolism in Disease. Nat Med, 2012. 18(3): p. 363-74.

332. Ott, H.C., B. Clippinger, C. Conrad, C. Schuetz, I. Pomerantseva, L. Ikonomou, D. Kotton, and J.P. Vacanti, Regeneration and Orthotopic Transplantation of a Bioartificial Lung. Nat Med, 2010. 16(8): p. 927-33.

333. Ott, H.C., T.S. Matthiesen, S.K. Goh, L.D. Black, S.M. Kren, T.I. Netoff, and D.A. Taylor, Perfusion-Decellularized Matrix: Using Nature's Platform to Engineer a Bioartificial Heart. Nat Med, 2008. 14(2): p. 213-21.

334. Ozkan, H., N. Olgun, E. Sasmaz, H. Abacioglu, M. Okuyan, and N. Cevik, Nutrition, Immunity and Infections: T Lymphocyte Subpopulations in Protein--Energy Malnutrition. J Trop Pediatr, 1993. 39(4): p. 257-60.

335. Ozog, Y., M. Konstantinovic, E. Werbrouck, D. De Ridder, E. Mazza, and J. Deprest, Persistence of Polypropylene Mesh Anisotropy after Implantation: An Experimental Study. BJOG, 2011. 118(10): p. 1180-5.

336. Parikh, N.I., P. Gona, M.G. Larson, C.S. Fox, E.J. Benjamin, J.M. Murabito, C.J. O'Donnell, R.S. Vasan, and D. Levy, Long-Term Trends in Myocardial Infarction Incidence and Case Fatality in the National Heart, Lung, and Blood Institute's Framingham Heart Study. Circulation, 2009. 119(9): p. 1203-10.

337. Parker, R.L., Differential Diagnosis of Tetralogy of Fallot. Proc Staff Meet Mayo Clin, 1947. 22(9): p. 177-9.

338. Parkin, D.M., F. Bray, J. Ferlay, and P. Pisani, Global Cancer Statistics, 2002. CA Cancer J Clin, 2005. 55(2): p. 74-108.

339. Pauli, E.M., S.J. Schomisch, J.P. Furlan, A.S. Marks, A. Chak, R.H. Lash, J.L. Ponsky, and J.M. Marks, Biodegradable Esophageal Stent Placement Does Not Prevent High-Grade Stricture Formation after Circumferential Mucosal Resection in a Porcine Model. Surg Endosc, 2012. 26(12): p. 3500-8.

340. Pennathur, A., M.K. Gibson, B.A. Jobe, and J.D. Luketich, Oesophageal Carcinoma. Lancet, 2013. 381(9864): p. 400-12.

341. Pennathur, A., R.J. Landreneau, and J.D. Luketich, Surgical Aspects of the Patient with High-Grade Dysplasia. Semin Thorac Cardiovasc Surg, 2005. 17(4): p. 326-32.

342. Petersen, T.H., et al., Tissue-Engineered Lungs for in Vivo Implantation. Science, 2010. 329(5991): p. 538-41.

343. Pohl, H., B. Sirovich, and H.G. Welch, Esophageal Adenocarcinoma Incidence: Are We Reaching the Peak? Cancer Epidemiol Biomarkers Prev, 2010. 19(6): p. 1468-70.

344. Ponce, M.L., M. Nomizu, M.C. Delgado, Y. Kuratomi, M.P. Hoffman, S. Powell, Y. Yamada, H.K. Kleinman, and K.M. Malinda, Identification of Endothelial Cell Binding Sites on the Laminin Gamma 1 Chain. Circ Res, 1999. 84(6): p. 688-94.

345. Potts, W.J., Tetralogy of Fallot. Am J Nurs, 1947. 47(5): p. 298-300.

346. Pradhan, S. and M.C. Farach-Carson, Mining the Extracellular Matrix for Tissue Engineering Applications. Regen Med, 2010. 5(6): p. 961-70.

347. Prasertsung, I., S. Kanokpanont, T. Bunaprasert, V. Thanakit, and S. Damrongsakkul, Development of Acellular Dermis from Porcine Skin Using Periodic Pressurized Technique. J Biomed Mater Res B Appl Biomater, 2008. 85(1): p. 210-9.

348. Preda, M.B. and G. Valen, Evaluation of Gene and Cell-Based Therapies for Cardiac Regeneration. Curr Stem Cell Res Ther, 2013.

349. Purushotham, A.D., R. Carachi, S.D. Gorham, D.A. French, and A.A. Shivas, Use of a Collagen Coated Vicryl Tube in Reconstruction of the Porcine Esophagus. Eur J Pediatr Surg, 1991. 1(2): p. 80-4.

350. Qian, F., et al., Age-Associated Elevation in Tlr5 Leads to Increased Inflammatory Responses in the Elderly. Aging Cell, 2012. 11(1): p. 104-10.

351. Qian, H., et al., Intracoronary Delivery of Autologous Bone Marrow Mononuclear Cells Radiolabeled by 18f-Fluoro-Deoxy-Glucose: Tissue Distribution and Impact on Post-Infarct Swine Hearts. J Cell Biochem, 2007. 102(1): p. 64-74.

352. Raval, Z. and D.W. Losordo, Cell Therapy of Peripheral Arterial Disease: From Experimental Findings to Clinical Trials. Circ Res, 2013. 112(9): p. 1288-302.

353. Raymond, C., V. Anne, and G. Millane, Development of Esophageal Epithelium in the Fetal and Neonatal Mouse. Anat Rec, 1991. 230(2): p. 225-34.

354. Record, R.D., D. Hillegonds, C. Simmons, R. Tullius, F.A. Rickey, D. Elmore, and S.F. Badylak, In Vivo Degradation of 14c-Labeled Small Intestinal Submucosa (Sis) When Used for Urinary Bladder Repair. Biomaterials, 2001. 22(19): p. 2653-9.

355. Reid, B.J., W.M. Weinstein, K.J. Lewin, R.C. Haggitt, G. VanDeventer, L. DenBesten, and C.E. Rubin, Endoscopic Biopsy Can Detect High-Grade Dysplasia or Early Adenocarcinoma in Barrett's Esophagus without Grossly Recognizable Neoplastic Lesions. Gastroenterology, 1988. 94(1): p. 81-90.

356. Reikvam, A. and T.P. Hagen, Changes in Myocardial Infarction Mortality. Tidsskr Nor Laegeforen, 2011. 131(5): p. 468-70.

357. Reing, J.E., et al., The Effects of Processing Methods Upon Mechanical and Biologic Properties of Porcine Dermal Extracellular Matrix Scaffolds. Biomaterials, 2010. 31(33): p. 8626-33.

358. Reing, J.E., et al., Degradation Products of Extracellular Matrix Affect Cell Migration and Proliferation. Tissue Eng Part A, 2009. 15(3): p. 605-14.

359. Reing, J.E., et al., Degradation Products of Extracellular Matrix Affect Cell Migration and Proliferation. Tissue Engineering - Part A, 2009. 15(3): p. 605-614.

360. Remlinger, N.T., P.D. Wearden, and T.W. Gilbert, Procedure for Decellularization of Porcine Heart by Retrograde Coronary Perfusion. J Vis Exp, 2012(70): p. e50059.

361. Ricard-Blum, S. and L. Ballut, Matricryptins Derived from Collagens and Proteoglycans. Front Biosci (Landmark Ed), 2011. 16: p. 674-97.

362. Rice, R.D., F.S. Ayubi, Z.J. Shaub, D.M. Parker, P.J. Armstrong, and J.W. Tsai, Comparison of Surgisis, Alloderm, and Vicryl Woven Mesh Grafts for Abdominal Wall Defect Repair in an Animal Model. Aesthetic Plast Surg, 2010. 34(3): p. 290-6.

363. Rider, P., Y. Carmi, O. Guttman, A. Braiman, I. Cohen, E. Voronov, M.R. White, C.A. Dinarello, and R.N. Apte, Il-1alpha and Il-1beta Recruit Different Myeloid Cells and Promote Different Stages of Sterile Inflammation. J Immunol, 2011. 187(9): p. 4835-43.

364. Robbins, S.L., V. Kumar, and R.S. Cotran, Robbins and Cotran Pathologic Basis of Disease. 8th ed. 2010, Philadelphia, PA: Saunders/Elsevier. xiv, 1450 p.

365. Roch, T., N. Ma, K. Kratz, and A. Lendlein, Cell-Based Detection of Microbial Biomaterial Contaminations. Clin Hemorheol Microcirc, 2015.

366. Rodero, M.P. and K. Khosrotehrani, Skin Wound Healing Modulation by Macrophages. Int J Clin Exp Pathol, 2010. 3(7): p. 643-53.

367. Roger, V.L., et al., Trends in Incidence, Severity, and Outcome of Hospitalized Myocardial Infarction. Circulation, 2010. 121(7): p. 863-9.

368. Rogers, W.J., et al., Trends in Presenting Characteristics and Hospital Mortality among Patients with St Elevation and Non-St Elevation Myocardial Infarction in the National Registry of Myocardial Infarction from 1990 to 2006. Am Heart J, 2008. 156(6): p. 1026-34.

369. Rokitansky, A.M., et al., Recent Evaluation of Prognostic Risk Factors in Esophageal Atresia--a Multicenter Review of 223 Cases. Eur J Pediatr Surg, 1993. 3(4): p. 196-201.

370. Roll, S., J. Muller-Nordhorn, T. Keil, H. Scholz, D. Eidt, W. Greiner, and S.N. Willich, Dacron Vs. Ptfe as Bypass Materials in Peripheral Vascular Surgery--Systematic Review and Meta-Analysis. BMC Surg, 2008. 8: p. 22.

371. Ronkainen, J., et al., Prevalence of Barrett's Esophagus in the General Population: An Endoscopic Study. Gastroenterology, 2005. 129(6): p. 1825-31.

372. Rosamond, W., et al., Heart Disease and Stroke Statistics--2008 Update: A Report from the American Heart Association Statistics Committee and Stroke Statistics Subcommittee. Circulation, 2008. 117(4): p. e25-146.

373. Ross, P.H. and A.C. Ivy, Tobacco Smoking and Coronary Artery Disease; an Analytical Review of the Literature. Q Bull Northwest Univ Med Sch, 1946. 20(4): p. 424-40.

374. Ruan, J.L., et al., Mechanical Stress Promotes Maturation of Human Myocardium from Pluripotent Stem Cell-Derived Progenitors. Stem Cells, 2015.

375. Ruoslahti, E., E.G. Hayman, M. Pierschbacher, and E. Engvall, Fibronectin: Purification, Immunochemical Properties, and Biological Activities. Methods Enzymol, 1982. 82 Pt A: p. 803-31.

376. Rutgeerts, P., How to Guide Therapeutic Decisions in a Patient-Tailored Approach to Treatment of Ibd? Dig Dis, 2012. 30(4): p. 396-9.

377. Sakamoto, M. and K. Nishioka, Complement System in Nutritional Deficiency. World Rev Nutr Diet, 1992. 67: p. 114-39.

378. Sarikaya, A., R. Record, C.C. Wu, B. Tullius, S. Badylak, and M. Ladisch, Antimicrobial Activity Associated with Extracellular Matrices. Tissue Eng, 2002. 8(1): p. 63-71.

379. Sawkins, M.J., et al., Hydrogels Derived from Demineralized and Decellularized Bone Extracellular Matrix. Acta Biomater, 2013. 9(8): p. 7865-73.

380. Schachinger, V., et al., Transplantation of Progenitor Cells and Regeneration Enhancement in Acute Myocardial Infarction: Final One-Year Results of the Topcare-Ami Trial. J Am Coll Cardiol, 2004. 44(8): p. 1690-9.

381. Schmidt, A., J. Minnerup, and C. Kleinschnitz, Emerging Neuroprotective Drugs for the Treatment of Acute Ischaemic Stroke. Expert Opin Emerg Drugs, 2013.

382. Schober, A. and C. Weber, Mechanisms of Monocyte Recruitment in Vascular Repair after Injury. Antioxid Redox Signal, 2005. 7(9-10): p. 1249-57.

383. Scholl, F.G., M.M. Boucek, K.C. Chan, L. Valdes-Cruz, and R. Perryman, Preliminary Experience with Cardiac Reconstruction Using Decellularized Porcine Extracellular Matrix Scaffold: Human Applications in Congenital Heart Disease. World J Pediatr Congenit Heart Surg, 2010. 1(1): p. 132-6.

384. Schomisch, S.J., L. Yu, Y. Wu, E.M. Pauli, C. Cipriano, A. Chak, R.H. Lash, J.L. Ponsky, and J.M. Marks, Commercially Available Biological Mesh Does Not Prevent Stricture after Esophageal Mucosectomy. Endoscopy, 2014. 46(2): p. 144-8.

385. Schonherr, E., M. Broszat, E. Brandan, P. Bruckner, and H. Kresse, Decorin Core Protein Fragment Leu155-Val260 Interacts with Tgf-Beta but Does Not Compete for Decorin Binding to Type I Collagen. Arch Biochem Biophys, 1998. 355(2): p. 241-8.

386. Schonherr, E., H. Hausser, L. Beavan, and H. Kresse, Decorin-Type I Collagen Interaction. Presence of Separate Core Protein-Binding Domains. J Biol Chem, 1995. 270(15): p. 8877-83.

387. Schopfer, K. and S.D. Douglas, Neutrophil Function in Children with Kwashiorkor. J Lab Clin Med, 1976. 88(3): p. 450-61.

388. Schwarz, U., The Hypertension Paradox. N Engl J Med, 2009. 361(22): p. 2195-6; author reply 2196-7.

389. Schwarzbauer, J.E. and J.L. Sechler, Fibronectin Fibrillogenesis: A Paradigm for Extracellular Matrix Assembly. Curr Opin Cell Biol, 1999. 11(5): p. 622-7.

390. Scollan, D.F., A. Holmes, R. Winslow, and J. Forder, Histological Validation of Myocardial Microstructure Obtained from Diffusion Tensor Magnetic Resonance Imaging. Am J Physiol, 1998. 275(6 Pt 2): p. H2308-18.

391. Seery, J.P., Stem Cells of the Oesophageal Epithelium. J Cell Sci, 2002. 115(Pt 9): p. 1783-9.

392. Seery, J.P. and F.M. Watt, Asymmetric Stem-Cell Divisions Define the Architecture of Human Oesophageal Epithelium. Curr Biol, 2000. 10(22): p. 1447-50.

393. Seidler, S., H.W. Zimmermann, M. Bartneck, C. Trautwein, and F. Tacke, Age-Dependent Alterations of Monocyte Subsets and Monocyte-Related Chemokine Pathways in Healthy Adults. BMC Immunol, 2010. 11: p. 30.

394. Seif-Naraghi, S.B., D. Horn, P.J. Schup-Magoffin, and K.L. Christman, Injectable Extracellular Matrix Derived Hydrogel Provides a Platform for Enhanced Retention and Delivery of a Heparin-Binding Growth Factor. Acta Biomater, 2012. 8(10): p. 3695-703.

395. Seif-Naraghi, S.B., et al., Safety and Efficacy of an Injectable Extracellular Matrix Hydrogel for Treating Myocardial Infarction. Sci Transl Med, 2013. 5(173): p. 173ra25.

396. Seiffert, D. and J.W. Smith, The Cell Adhesion Domain in Plasma Vitronectin Is Cryptic. J Biol Chem, 1997. 272(21): p. 13705-10.

397. Sellaro, T.L., A. Ranade, D.M. Faulk, G.P. McCabe, K. Dorko, S.F. Badylak, and S.C. Strom, Maintenance of Human Hepatocyte Function in Vitro by Liver-Derived Extracellular Matrix Gels. Tissue Eng Part A, 2010. 16(3): p. 1075-82.

398. Sellaro, T.L., A.K. Ravindra, D.B. Stolz, and S.F. Badylak, Maintenance of Hepatic Sinusoidal Endothelial Cell Phenotype in Vitro Using Organ-Specific Extracellular Matrix Scaffolds. Tissue Eng, 2007. 13(9): p. 2301-10.

399. Shaffer, J.O., Treatment of Agenesis of the Diaphragm and Esophageal Crura--an 18-Year Follow-Up. West J Med, 1981. 134(4): p. 361-3.

400. Shaheen, N.J., et al., Radiofrequency Ablation in Barrett's Esophagus with Dysplasia. N Engl J Med, 2009. 360(22): p. 2277-88.

401. Shankaran, V., D.J. Weber, R.L. Reed, 2nd, and F.A. Luchette, A Review of Available Prosthetics for Ventral Hernia Repair. Ann Surg, 2011. 253(1): p. 16-26.

402. Sharma, S., Management of Complications of Radical Esophagectomy. Indian J Surg Oncol, 2013. 4(2): p. 105-11.

403. Sharma, V.K., et al., Balloon-Based, Circumferential, Endoscopic Radiofrequency Ablation of Barrett's Esophagus: 1-Year Follow-up of 100 Patients. Gastrointest Endosc, 2007. 65(2): p. 185-95.

404. Sharpless, N.E. and R.A. DePinho, How Stem Cells Age and Why This Makes Us Grow Old. Nat Rev Mol Cell Biol, 2007. 8(9): p. 703-13.

405. Sheifer, S.E., T.A. Manolio, and B.J. Gersh, Unrecognized Myocardial Infarction. Ann Intern Med, 2001. 135(9): p. 801-11.

406. Shousha, S. and K. Kamel, Nitro Blue Tetrazolium Test in Children with Kwashiorkor with a Comment on the Use of Latex Particles in the Test. J Clin Pathol, 1972. 25(6): p. 494-7.

407. Shue, L., Z. Yufeng, and U. Mony, Biomaterials for Periodontal Regeneration: A Review of Ceramics and Polymers. Biomatter, 2012. 2(4): p. 271-7.

408. Sicari, B.M., C.L. Dearth, and S.F. Badylak, Tissue Engineering and Regenerative Medicine Approaches to Enhance the Functional Response to Skeletal Muscle Injury. Anatomical Record, 2014. 297(1): p. 51-64.

409. Sicari, B.M., et al., The Effect of Source Animal Age Upon the in Vivo Remodeling Characteristics of an Extracellular Matrix Scaffold. Biomaterials, 2012. 33(22): p. 5524-33.

410. Sicari, B.M., et al., An Acellular Biologic Scaffold Promotes Skeletal Muscle Formation in Mice and Humans with Volumetric Muscle Loss. Sci Transl Med, 2014. 6(234): p. 234ra58.

411. Singelyn, J.M., et al., Catheter-Deliverable Hydrogel Derived from Decellularized Ventricular Extracellular Matrix Increases Endogenous Cardiomyocytes and Preserves Cardiac Function Post-Myocardial Infarction. J Am Coll Cardiol, 2012. 59(8): p. 751-63.

412. Sirisinha, S., R. Edelman, R. Suskind, C. Charupatana, and R.E. Olson, Complement and C3-Proactivator Levels in Children with Protein-Calorie Malnutrition and Effect of Dietary Treatment. Lancet, 1973. 1(7811): p. 1016-20.

413. Sjoqvist, S., et al., Experimental Orthotopic Transplantation of a Tissue-Engineered Oesophagus in Rats. Nat Commun, 2014. 5: p. 3562.

414. Skandalakis, J.E. and H. Ellis, Embryologic and Anatomic Basis of Esophageal Surgery. Surg Clin North Am, 2000. 80(1): p. 85-155, x.

415. Slack, S.M., J.L. Bohnert, and T.A. Horbett, The Effects of Surface Chemistry and Coagulation Factors on Fibrinogen Adsorption from Plasma. Ann N Y Acad Sci, 1987. 516: p. 223-43.

416. Slade, D.A. and G.L. Carlson, Takedown of Enterocutaneous Fistula and Complex Abdominal Wall Reconstruction. Surg Clin North Am, 2013. 93(5): p. 1163-83.

417. Smaniotto, S., D.A. Mendes-da-Cruz, C.E. Carvalho-Pinto, L.M. Araujo, M. Dardenne, and W. Savino, Combined Role of Extracellular Matrix and Chemokines on Peripheral Lymphocyte Migration in Growth Hormone Transgenic Mice. Brain Behav Immun, 2010. 24(3): p. 451-61.

418. Song, J.J. and H.C. Ott, Organ Engineering Based on Decellularized Matrix Scaffolds. Trends Mol Med, 2011. 17(8): p. 424-32.

419. Song, W., H. Wang, and Q. Wu, Atrial Natriuretic Peptide in Cardiovascular Biology and Disease (Nppa). Gene, 2015.

420. Sonnenberg, H., C.K. Chong, and A.T. Veress, Cardiac Atrial Factor--an Endogenous Diuretic? Can J Physiol Pharmacol, 1981. 59(12): p. 1278-9.

421. Soreide, J.A. and A. Viste, Esophageal Perforation: Diagnostic Work-up and Clinical Decision-Making in the First 24 Hours. Scand J Trauma Resusc Emerg Med, 2011. 19: p. 66.

422. Soto-Gutierrez, A., et al., A Whole-Organ Regenerative Medicine Approach for Liver Replacement. Tissue Eng Part C Methods, 2011. 17(6): p. 677-86.

423. Souto Damin, A.P., A.P. Guedes Frazzon, D. de Carvalho Damin, H. Beck Biehl, L. Abruzzi de Oliveira, R. Auler, C. Marroni, and C.O. Alexandre, Detection of Human Papillomavirus DNA in Squamous Cell Carcinoma of the Esophagus by Auto-Nested Pcr. Dis Esophagus, 2006. 19(2): p. 64-8.

424. Stankus, J.J., D.O. Freytes, S.F. Badylak, and W.R. Wagner, Hybrid Nanofibrous Scaffolds from Electrospinning of a Synthetic Biodegradable Elastomer and Urinary Bladder Matrix. Journal of Biomaterials Science, Polymer Edition, 2008. 19(5): p. 635-652.

425. Stankus, J.J., J. Guan, and W.R. Wagner, Fabrication of Biodegradable Elastomeric Scaffolds with Sub-Micron Morphologies. J Biomed Mater Res A, 2004. 70(4): p. 603-14.

426. Stansfield, B.K. and D.A. Ingram, Clinical Significance of Monocyte Heterogeneity. Clin Transl Med, 2015. 4: p. 5.

427. Stevens, C.E. and I.D. Hume, Comparative Physiology of the Vertebrate Digestive System. 2nd ed. 1995, Cambridge ; New York: Cambridge University Press. xvi, 400 p.

428. Stinson, E.B. and M.E. Billingham, Correlative Study of Regional Left Ventricular Histology and Contractile Function. Am J Cardiol, 1977. 39(3): p. 378-83.

429. Streitz, J.M., Jr., F.H. Ellis, Jr., S.P. Gibb, and G.M. Heatley, Achalasia and Squamous Cell Carcinoma of the Esophagus: Analysis of 241 Patients. Ann Thorac Surg, 1995. 59(6): p. 1604-9.

430. Sturm, R., J.S. Ringel, and T. Andreyeva, Increasing Obesity Rates and Disability Trends. Health Aff (Millwood), 2004. 23(2): p. 199-205.

431. Sundaramoorthy, M., M. Meiyappan, P. Todd, and B.G. Hudson, Crystal Structure of Nc1 Domains. Structural Basis for Type Iv Collagen Assembly in Basement Membranes. J Biol Chem, 2002. 277(34): p. 31142-53.

432. Sytkowski, P.A., W.B. Kannel, and R.B. D'Agostino, Changes in Risk Factors and the Decline in Mortality from Cardiovascular Disease. The Framingham Heart Study. N Engl J Med, 1990. 322(23): p. 1635-41.

433. Takimoto, Y., T. Nakamura, Y. Yamamoto, T. Kiyotani, M. Teramachi, and Y. Shimizu, The Experimental Replacement of a Cervical Esophageal Segment with an Artificial Prosthesis with the Use of Collagen Matrix and a Silicone Stent. J Thorac Cardiovasc Surg, 1998. 116(1): p. 98-106.

434. Thom, T., et al., Heart Disease and Stroke Statistics--2006 Update: A Report from the American Heart Association Statistics Committee and Stroke Statistics Subcommittee. Circulation, 2006. 113(6): p. e85-151.

435. To, W.S. and K.S. Midwood, Plasma and Cellular Fibronectin: Distinct and Independent Functions During Tissue Repair. Fibrogenesis Tissue Repair, 2011. 4: p. 21.

436. Totonelli, G., et al., Esophageal Tissue Engineering: A New Approach for Esophageal Replacement. World Journal of Gastroenterology, 2012. 18(47): p. 6900-6907.

437. Tottey, S., M. Corselli, E.M. Jeffries, R. Londono, B. Peault, and S.F. Badylak, Extracellular Matrix Degradation Products and Low-Oxygen Conditions Enhance the Regenerative Potential of Perivascular Stem Cells. Tissue Eng Part A, 2011. 17(1-2): p. 37-44.

438. Tran Cao, H.S., C. Tokin, J. Konop, H. Ojeda-Fournier, J. Chao, and S.L. Blair, A Preliminary Report on the Clinical Experience with Alloderm in Breast Reconstruction and Its Radiologic Appearance. Am Surg, 2010. 76(10): p. 1123-6.

439. Tseng, C.W., P.A. Kyme, A. Arruda, V.K. Ramanujan, W. Tawackoli, and G.Y. Liu, Innate Immune Dysfunctions in Aged Mice Facilitate the Systemic Dissemination of Methicillin-Resistant S. Aureus. PLoS One, 2012. 7(7): p. e41454.

440. Turner, M.D., B. Nedjai, T. Hurst, and D.J. Pennington, Cytokines and Chemokines: At the Crossroads of Cell Signalling and Inflammatory Disease. Biochim Biophys Acta, 2014.

441. Turner, N.J. and S.F. Badylak, Regeneration of Skeletal Muscle. Cell Tissue Res, 2012. 347(3): p. 759-74.

442. Urita, Y., H. Komuro, G. Chen, M. Shinya, S. Kaneko, M. Kaneko, and T. Ushida, Regeneration of the Esophagus Using Gastric Acellular Matrix: An Experimental Study in a Rat Model. Pediatr Surg Int, 2007. 23(1): p. 21-6.

443. Valentin, J.E., J.S. Badylak, G.P. McCabe, and S.F. Badylak, Extracellular Matrix Bioscaffolds for Orthopaedic Applications. A Comparative Histologic Study. J Bone Joint Surg Am, 2006. 88(12): p. 2673-86.

444. Valentin, J.E., A.M. Stewart-Akers, T.W. Gilbert, and S.F. Badylak, Macrophage Participation in the Degradation and Remodeling of Extracellular Matrix Scaffolds. Tissue Eng Part A, 2009. 15(7): p. 1687-94.

445. van der Rest, M. and R. Garrone, Collagen Family of Proteins. FASEB J, 1991. 5(13): p. 2814-23.

446. van Duin, D., S. Mohanty, V. Thomas, S. Ginter, R.R. Montgomery, E. Fikrig, H.G. Allore, R. Medzhitov, and A.C. Shaw, Age-Associated Defect in Human Tlr-1/2 Function. J Immunol, 2007. 178(2): p. 970-5.

447. van Tienen, T.G., G. Hannink, and P. Buma, Meniscus Replacement Using Synthetic Materials. Clin Sports Med, 2009. 28(1): p. 143-56.

448. Vardar, S.A., O. Palabiyik, R.D. Topuz, E.E. Gurel, S. Caliskan, S. Topcu Ozen, N. Sut, and C.H. Karadag, Hemodynamic Effects of Atrial Natriuretic Peptide in Ischemia-Repertusion Injury That Occurs after Exercise. Turk J Med Sci, 2015. 45(2): p. 298-305.

449. Vartiainen, E., et al., Thirty-Five-Year Trends in Cardiovascular Risk Factors in Finland. Int J Epidemiol, 2010. 39(2): p. 504-18.

450. Vasquez-Garibay, E., O. Campollo-Rivas, E. Romero-Velarde, C. Mendez-Estrada, T. Garcia-Iglesias, J.G. Alvizo-Mora, and B. Vizmanos-Lamotte, Effect of Renutrition on Natural and Cell-Mediated Immune Response in Infants with Severe Malnutrition. J Pediatr Gastroenterol Nutr, 2002. 34(3): p. 296-301.

451. Vasquez-Garibay, E., C. Mendez-Estrada, E. Romero-Velarde, M.T. Garcia-Iglesias, and O. Campollo-Rivas, Nutritional Support with Nucleotide Addition Favors Immune Response in Severely Malnourished Infants. Arch Med Res, 2004. 35(4): p. 284-8.

452. Volpato, F.Z., T. Fuhrmann, C. Migliaresi, D.W. Hutmacher, and P.D. Dalton, Using Extracellular Matrix for Regenerative Medicine in the Spinal Cord. Biomaterials, 2013. 34(21): p. 4945-55.

453. Vorotnikova, E., et al., Extracellular Matrix-Derived Products Modulate Endothelial and Progenitor Cell Migration and Proliferation in Vitro and Stimulate Regenerative Healing in Vivo. Matrix Biol, 2010. 29(8): p. 690-700.

454. Voutilainen, M., P. Sipponen, J.P. Mecklin, M. Juhola, and M. Farkkila, Gastroesophageal Reflux Disease: Prevalence, Clinical, Endoscopic and Histopathological Findings in 1,128 Consecutive Patients Referred for Endoscopy Due to Dyspeptic and Reflux Symptoms. Digestion, 2000. 61(1): p. 6-13.

455. Voytik-Harbin, S.L., A.O. Brightman, M.R. Kraine, B. Waisner, and S.F. Badylak, Identification of Extractable Growth Factors from Small Intestinal Submucosa. J Cell Biochem, 1997. 67(4): p. 478-91.

456. Wainwright, J.M., C.A. Czajka, U.B. Patel, D.O. Freytes, K. Tobita, T.W. Gilbert, and S.F. Badylak, Preparation of Cardiac Extracellular Matrix from an Intact Porcine Heart. Tissue Eng Part C Methods, 2010. 16(3): p. 525-32.

457. Wang, J. and H. Arase, Regulation of Immune Responses by Neutrophils. Ann N Y Acad Sci, 2014. 1319(1): p. 66-81.

458. Weisberg, S.P., D. McCann, M. Desai, M. Rosenbaum, R.L. Leibel, and A.W. Ferrante, Jr., Obesity Is Associated with Macrophage Accumulation in Adipose Tissue. J Clin Invest, 2003. 112(12): p. 1796-808.

459. Wenisch, C., S. Patruta, F. Daxbock, R. Krause, and W. Horl, Effect of Age on Human Neutrophil Function. J Leukoc Biol, 2000. 67(1): p. 40-5.

460. Whitelock, J.M., A.D. Murdoch, R.V. Iozzo, and P.A. Underwood, The Degradation of Human Endothelial Cell-Derived Perlecan and Release of Bound Basic Fibroblast Growth Factor by Stromelysin, Collagenase, Plasmin, and Heparanases. J Biol Chem, 1996. 271(17): p. 10079-86.

461. Wilgus, T.A., Immune Cells in the Healing Skin Wound: Influential Players at Each Stage of Repair. Pharmacol Res, 2008. 58(2): p. 112-6.

462. Williams, C.G., A.N. Malik, T.K. Kim, P.N. Manson, and J.H. Elisseeff, Variable Cytocompatibility of Six Cell Lines with Photoinitiators Used for Polymerizing Hydrogels and Cell Encapsulation. Biomaterials, 2005. 26(11): p. 1211-8.

463. Witsch, J., H. Neugebauer, K. Zweckberger, and E. Juttler, Primary Cerebellar Haemorrhage: Complications, Treatment and Outcome. Clin Neurol Neurosurg, 2013.

464. Witteman, B.P., et al., Transoral Endoscopic Inner Layer Esophagectomy: Management of High-Grade Dysplasia and Superficial Cancer with Organ Preservation. J Gastrointest Surg, 2009. 13(12): p. 2104-12.

465. Wolf, M.T., et al., Polypropylene Surgical Mesh Coated with Extracellular Matrix Mitigates the Host Foreign Body Response. J Biomed Mater Res A, 2013.

466. Wolf, M.T., et al., Polypropylene Surgical Mesh Coated with Extracellular Matrix Mitigates the Host Foreign Body Response. J Biomed Mater Res A, 2014. 102(1): p. 234-46.

467. Wolf, M.T., K.A. Daly, E.P. Brennan-Pierce, S.A. Johnson, C.A. Carruthers, A. D'Amore, S.P. Nagarkar, S.S. Velankar, and S.F. Badylak, A Hydrogel Derived from Decellularized Dermal Extracellular Matrix. Biomaterials, 2012. 33(29): p. 7028-38.

468. Wolf, M.T., K.A. Daly, J.E. Reing, and S.F. Badylak, Biologic Scaffold Composed of Skeletal Muscle Extracellular Matrix. Biomaterials, 2012. 33(10): p. 2916-25.

469. Wolf, M.T., C.L. Dearth, C.A. Ranallo, S.T. LoPresti, L.E. Carey, K.A. Daly, B.N. Brown, and S.F. Badylak, Macrophage Polarization in Response to Ecm Coated Polypropylene Mesh. Biomaterials, 2014. 35(25): p. 6838-49.

470. Wolf, M.T., C.L. Dearth, S.B. Sonnenberg, E.G. Loboa, and S.F. Badylak, Naturally Derived and Synthetic Scaffolds for Skeletal Muscle Reconstruction. Adv Drug Deliv Rev, 2014.

471. Wolf, M.T., Y. Vodovotz, S. Tottey, B.N. Brown, and S.F. Badylak, Predicting in Vivo Responses to Biomaterials Via Combined in Vitro and in Silico Analysis. Tissue Eng Part C Methods, 2014.

472. Xu, C.C., R.W. Chan, and N. Tirunagari, A Biodegradable, Acellular Xenogeneic Scaffold for Regeneration of the Vocal Fold Lamina Propria. Tissue Eng, 2007. 13(3): p. 551-66.

473. Xu, H., et al., Chronic Inflammation in Fat Plays a Crucial Role in the Development of Obesity-Related Insulin Resistance. J Clin Invest, 2003. 112(12): p. 1821-30.

474. Xu, H., H. Wan, M. Sandor, S. Qi, F. Ervin, J.R. Harper, R.P. Silverman, and D.J. McQuillan, Host Response to Human Acellular Dermal Matrix Transplantation in a Primate Model of Abdominal Wall Repair. Tissue Eng Part A, 2008. 14(12): p. 2009-19.

475. Yamaguchi, Y., D.M. Mann, and E. Ruoslahti, Negative Regulation of Transforming Growth Factor-Beta by the Proteoglycan Decorin. Nature, 1990. 346(6281): p. 281-4.

476. Yamamoto, H., Technology Insight: Endoscopic Submucosal Dissection of Gastrointestinal Neoplasms. Nat Clin Pract Gastroenterol Hepatol, 2007. 4(9): p. 511-20.

477. Yamamoto, M., J.M. Weber, R.C. Karl, and K.L. Meredith, Minimally Invasive Surgery for Esophageal Cancer: Review of the Literature and Institutional Experience. Cancer Control, 2013. 20(2): p. 130-7.

478. Yaturu, S., Insulin Therapies: Current and Future Trends at Dawn. World J Diabetes, 2013. 4(1): p. 1-7.

479. Yildirimer, L., N.T. Thanh, and A.M. Seifalian, Skin Regeneration Scaffolds: A Multimodal Bottom-up Approach. Trends Biotechnol, 2012. 30(12): p. 638-48.

480. Yoon, H.H., M.A. Lewis, Q. Shi, M. Khan, S.D. Cassivi, R.B. Diasio, and F.A. Sinicrope, Prognostic Impact of Body Mass Index Stratified by Smoking Status in Patients with Esophageal Adenocarcinoma. J Clin Oncol, 2011. 29(34): p. 4561-7.

481. Yoshida, N., et al., Risk Factors for Pulmonary Complications after Esophagectomy for Esophageal Cancer. Surg Today, 2014. 44(3): p. 526-32.

482. Yue, C., H.C. van der Mei, R. Kuijer, H.J. Busscher, and E.T. Rochford, Mechanism of Cell Integration on Biomaterial Implant Surfaces in the Presence of Bacterial Contamination. J Biomed Mater Res A, 2015.

483. Zamarron, C., M.H. Ginsberg, and E.F. Plow, Monoclonal Antibodies Specific for a Conformationally Altered State of Fibrinogen. Thromb Haemost, 1990. 64(1): p. 41-6.

484. Zantop, T., T.W. Gilbert, M.C. Yoder, and S.F. Badylak, Extracellular Matrix Scaffolds Are Repopulated by Bone Marrow-Derived Cells in a Mouse Model of Achilles Tendon Reconstruction. J Orthop Res, 2006. 24(6): p. 1299-309.

485. Zhang, Q., M. Raoof, Y. Chen, Y. Sumi, T. Sursal, W. Junger, K. Brohi, K. Itagaki, and C.J. Hauser, Circulating Mitochondrial Damps Cause Inflammatory Responses to Injury. Nature, 2010. 464(7285): p. 104-7.

486. Zhang, Y., Epidemiology of Esophageal Cancer. World J Gastroenterol, 2013. 19(34): p. 5598-606.

487. Zhang, Y., Y. He, S. Bharadwaj, N. Hammam, K. Carnagey, R. Myers, A. Atala, and M. Van Dyke, Tissue-Specific Extracellular Matrix Coatings for the Promotion of Cell Proliferation and Maintenance of Cell Phenotype. Biomaterials, 2009. 30(23-24): p. 4021-8.

488. Zhu, Y., M.B. Chan-Park, and K. Sin Chian, The Growth Improvement of Porcine Esophageal Smooth Muscle Cells on Collagen-Grafted Poly(Dl-Lactide-Co-Glycolide) Membrane. J Biomed Mater Res B Appl Biomater, 2005. 75(1): p. 193-9.

489. Zhu, Y., M.F. Leong, W.F. Ong, M.B. Chan-Park, and K.S. Chian, Esophageal Epithelium Regeneration on Fibronectin Grafted Poly(L-Lactide-Co-Caprolactone) (Pllc) Nanofiber Scaffold. Biomaterials, 2007. 28(5): p. 861-8.

490. Zimmermann, W.H., K. Schneiderbanger, P. Schubert, M. Didie, F. Munzel, J.F. Heubach, S. Kostin, W.L. Neuhuber, and T. Eschenhagen, Tissue Engineering of a Differentiated Cardiac Muscle Construct. Circ Res, 2002. 90(2): p. 223-30.

491. Zippel, N., M. Schulze, and E. Tobiasch, Biomaterials and Mesenchymal Stem Cells for Regenerative Medicine. Recent Pat Biotechnol, 2010. 4(1): p. 1-22.